Aqueous RAFT Polymerisation of Acrylamide Monomers

By

CAROLINE PRISCA BRAY

A thesis submitted in partial fulfilment of the requirements for the degree of Doctor of Philosophy in Chemistry

UNIVERSITY OF WARWICK, DEPARTMENT OF CHEMISTRY

[April 2018]

CONTENTS

ACKNOWLEDGEMENTS

My sincere gratitude goes to my supervisor, Professor Sebatien Perrier, for giving me the opportunity to work and study in his research group. Without his guidance, enthusiasm and *good* humour, this project would not have been anywhere near as enjoyable or successful!

I also would like to thank Hyungsoo Kim and Antonio Mastrangelo, my industrial supervisors, and the whole Lubrizol team for their guidance throughout the years. I would like to extend my gratitude to the following people for their help during my PhD: James Town (MALDI-ToF), Pratik Gurnani (TEM), Junliang Zhang (AFM), Samuel Lawton (AFM), Steven Huband (SAXS), Edward Mansfield (SAXS), Raoul Peltier (Cell Culture), Ivan Prokes (NMR), Daniel Lester (SEC) and Laura McDougall (Rheology).

Many thanks goes to all the members of the Perrier Group, both past and present, for making the group so energetic and enjoyable over the years! It has been a real pleasure to both work and socialise in such a vibrant research group. Particular gratitude goes to the middle office and my colleagues within; some hilarious discussions, fun times and fond memories!

I would especially like to thank my partner, Paul Kerby for his love and support through the completion of this thesis. His devotion and *humour* through the stressful periods of my PhD will always be cherished, and he will now no longer be the only Doctor in the house!

Finally, I would like to thank my family for their continuous support throughout my PhD. I am extremely grateful for their advice, encouragement and love throughout my studies, and for being such a strong pillar in my life.

Caroline Bray, April 2018

DECLARATION

I hereby declare that all of the work described in this thesis is the original work carried out by the author, unless stated otherwise, at the University of Warwick between October 2014 and April 2018. I declare that the material described that is not original has been identified and appropriately referenced. I certify that the material within this thesis has not been submitted for a degree at any other university.

CHAPTER 3:

- MALDI-ToF analysis performed by James Town (University of Warwick).
- TEM microscopy obtained by Pratik Gurnani (University of Warwick).

CHAPTER 4:

- AFM analysis performed by Dr Junliang Zhang and Sam Lawton (University of Warwick).
- SAXS analysis performed by Dr Steven Huband and processed by Dr Edward Mansfield (University of Warwick).

Publications by the author arising from parts of **CHAPTER 2** and **CHAPTER 3**:

- Bray, C.; Peltier, R.; Kim, H.; Mastrangelo, A.; Perrier, S. *Polym. Chem.* 2017, *8*, 5513.

ABSTRACT

The challenge of this project was to control the polymerisation of acrylamide monomers, particularly sodium 2-acrylamido-2-methylpropane sulfonate (Lubrizol trademark, AMPS®2405), via reversible addition-fragmentation chain transfer (RAFT) polymerisation in aqueous solution. AMPS® based polymers are employed in a wide range of applications (e.g. medical, paint, oil recovery and water treatment), and are typically obtained via conventional radical polymerisation. Here, the use of the RAFT process to control the polymerisation of AMPS®2405 was reported, and well-defined polymeric architectures were obtained compared to materials obtained via free radical polymerisation (FRP). The chain transfer agent (CTA) of choice for this project was initially DDMAT (CTA-A, Z-group is $C_{12}H_{25}$), and a water soluble CTA synthesised by the Lubrizol corporation (USA) in tonne-scale. DDMAT is known to form aggregates in water ($[CAC]_{DDMAT}$ =0.005 M) and this is likely to disrupt the RAFT mechanism and consequently diminish the control over the polymerisation. To overcome this problem a chain transfer agent with a shorter alkyl chain (BDMAT, Z-group is C_4H_9) was used for comparison with DDMAT.

The polymerisation of AMPS®2405 monomer was optimised, as discussed in **CHAPTER 2**, in aqueous solution using either DDMAT or BDMAT as a chain transfer agent. These conditions were found to be universal to other water soluble acrylamide monomers (*N*,*N*-dimethylacrylamide, *N*-hydroxyethyl acrylamide and 4-acryloylmorpholine). More complex architectures were designed, as described in **CHAPTER 3**, exploiting the high chain end fidelity and chain extensions. A small library of diblock copolymers using various comonomers (*N*,*N*-dimethylacrylamide, *N*-hydroxyethyl acrylamide, 4-acryloylmorpholine, acrylic acid and acrylamide) were first synthesised. The synthesis of star polymers using the arm first approach was further studied, and well-defined multiblock star copolymers were obtained by RAFT polymerisation. These structures synthesised were characterised, as discussed in **CHAPTER 4**, using diverse techniques (e.g. SAXS, DLS, SEC with triple detection and AFM). While copolymers prepared from AMPS®2405 can be used in numerous applications, the focus of this thesis, as discussed in **CHAPTER 5**, was to study their benefit as heparin-mimicking polymers.

ABBREVIATIONS

^{1}H NMR	Proton nuclear magnetic resonance
AA	Acrylic Acid
ACVA	4,4′-Azobis(4-cyanovaleric acid)
aFGF / FGF1	Acid fibroblast growth factor
AFM	Atomic force microscopy
AHPS	Sodium 1-allyloxy-2 hydroxypropyl sulfonate
AIBN	Azobisisobutyronitrile
AM	Acrylamide
AMBA	Sodium 3-acrylamido-2-methylpropane-sulfonate
AMPS®	2-Acrylamido-2-methyl-1-propanesulfonic acid
AMPS®2405	Sodium 2-acrylamido-2-methyl-1-propanesulfonate
ar.	Aromatic
ATRP	Atom transfer radical polymerisation
BA	Butyl acrylate
BCS	Bovine calf serum
BDMAT	2-(Butylthiocarbonothioylthio)-2-methylpropanoic acid
bFGF / FGF2	Basic fibroblast growth factor
BMA	*n*-Butyl methacrylate
br.	Broad (IR and NMR)
CAC	Critical aggregation concentration
Cat.	Catalyst
CCS	Core cross-linked
CL	Cross-linker

Conv.	Conversion
CRP	Control radical polymerisation
CTA	Chain transfer agent
C_{tr}	Chain transfer constant
C_{tr}^{app}	Apparent chain transfer constant
DDMAT	2-(Dodecylthiocarbonothioylthio)-2-methylpropanoic acid
DLS	Dynamic light scattering
DMA	*N*,*N*-Dimethylacrylamide
DMEM	Dulbecco's modified eagle medium
DMF	*N*,*N*-Dimethylformamide
DMSO	Dimethyl sulfoxide
dn/dc	Refractive index increment
DP	Degree of polymerisation
Đ	Dispersity
EA	Ethyl acrylate
ESI	Electrospray ionisation
F	Star polymer functionality
FBS	Foetal bovine serum
FDA	Federal drug administration
FGF	Fibroblast growth factor
FGFR	Fibroblast growth factor receptor
FRP	Free radical polymerisation
G′	Storage modulus
G″	Loss modulus
GAG	Glycosaminoglycan

HEAm	*N*-Hydroxyethyl acrylamide
HPLC	High performance liquid chromatography
HS	Heparan sulfate
I	Initiator
IL-3	Interleukin 3
IV	Intrinsic viscosity
K_p	Rate constant of polymerisation
k_p^{app}	Apparent rate constant of polymerisation
k_{tr}	Rate constant of transfer
L	Livingness
LS	Light scattering
M	Mol/L
M	Medium (IR)
	Multiplet (NMR)
m.p.	Melting point
MA	Methyl acrylate
MALDI-ToF	Matrix assisted laser desorption / ionisation-time of flight
MALS	Multi-angle light scattering
Me_6-TREN	*N*,*N*,*N*′,*N*′,*N*″,*N*″-Hexamethyl-[tris(aminoethyl)amine]
MMA	Methyl methacrylate
M_n	Number average molar mass
$M_{n,th}$	Theoretical number average molar mass
MRI	Magnetic resonance imaging
NAM	4-Acryloylmorpholine
NAS	*N*-Acryloxysuccinimide

NMP	Nitroxide-mediated polymerisation
PBS	Phosphate-buffered saline
PDI	Polydispersity Index
PEG	Poly(ethylene glycol)
PEGMA	Poly(ethylene glycol) methyl ether methacrylate
PEO	Poly(ethylene oxide)
pI	Isoelectric point
PMS	*N*-Methyl dibenzopyrazine methyl sulfate
RAFT	Reversible Addition-Fragmentation chain-Transfer
Rg	Radius of gyration
R-group	Reinitiating group
RI	Refractive index
RPMI	Roswell park memorial institute medium
S	Styrene
S	Strong (IR)
	Singlet (NMR)
SAXS	Small-angle X-ray scattering
SEC	Size exclusion chromatography
SFRP	Stable free radical polymerisation
SS	Styrene sulfonate
t.	Triplet
TEM	Transmission electron microscopy
UV-vis	Ultraviolet-visible
V-40	1,1′-Azobis(cyclohexane-1-carbonitrile)
V-501	4,4′-Azobis(4-cyanovaleric acid)

VA-086	2,2′-Azobis[2-methyl-*N*-(2-hydroxyethyl)propionamide]
VP	1-Vinyl-2-pyrrolidinone
VS	Viscometer
VS	Vinyl sulfonate
W	Weak
XTT	(Sodium 2,3-bis(2-methoxy-4-nitro-5-sulfophenyl)-5- [(phenyl mino)-carbonyl]-2H-tetrazolium) inner salt
Z-group	Stabilising group
Δ	Chemical shift

LIST OF FIGURES

LIST OF SCHEMES

LIST OF TABLES

CHAPTER 1:
INTRODUCTION

1.1 Radical Polymerisation

1.1.1 Free Radical Polymerisation

Conventional radical polymerisation is the most widely used polymerisation process in industry to synthesise low cost materials.[1] Compared to ionic polymerisation, radical polymerisation requires non-stringent reactions conditions regarding solvent selection and reaction temperature, in addition to exhibiting a high tolerance of impurities (e.g. water, oxygen, and stabilisers). A wide range of commercially available vinyl monomers can be used by FRP to target materials with high molecular weight without the need of extended precursor purifications. While copolymers can easily be synthesised using FRP to obtain different material properties, no control over microstructures, architectures, molecular weights and chain end functionalities are possible compared to controlled polymerisations such as ionic polymerisation.[2]

The mechanism of FRP involves three main steps: initiation, propagation and termination (**Scheme 1-1**). The initiation steps allow the formation of free radicals (I·) from an initiator (I_2) which are usually dissociated by heat or light and characterised by their rate of dissociation (k_d). This newly formed radicals react rapidly with a monomer first forming Pn·, where k_i is the initiation step rate constant. Further monomer units are then added to the growing radical chains; this step being named propagation. The propagation step is usually rapid, and the rate of polymerisation (k_p) is around 10^2-10^4 s^{-1}.[3] Finally, the growth of the chains are stopped due to the high reactivity of radical species; a process named the termination step (rate of termination k_t). The termination can occur either by the combination of two radical species or by disproportionation (i.e. hydrogen abstraction). Unreactive chains called dead chains are formed all along the polymerisation process at a rate constant range of 10^6 to 10^8 L/mol/s.[3] Additionally, the active free-radical can be shifted onto a transfer agent (e.g.

monomer, solvent, polymer or chain transfer agent) which can then reinitiate a new polymer chain. This process usually induces a decrease of the molecular weight of the final materials.[4]

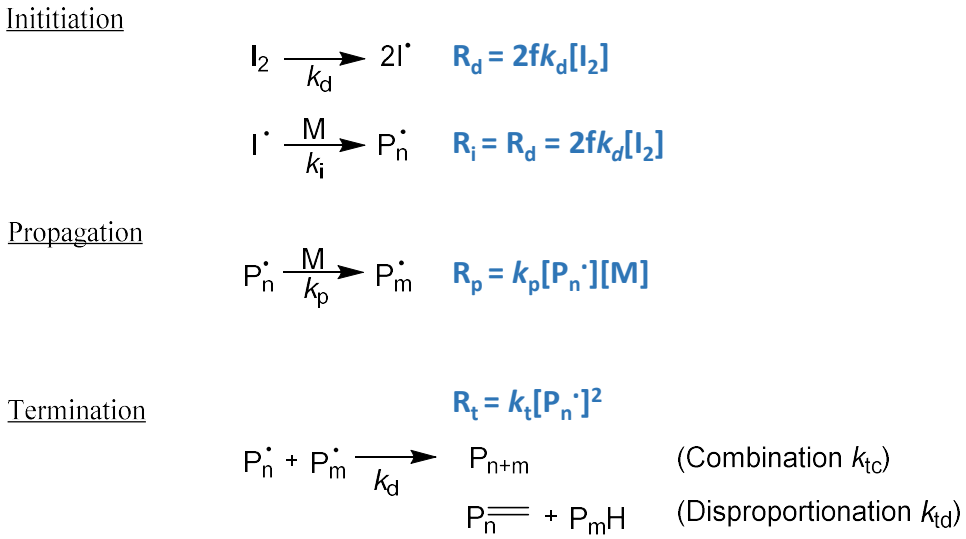

Scheme 1-1: FRP mechanism.

Free radicals are formed by the dissociation of initiators over the course of the polymerisation and is typically the rate determining step, with $R_d = 2fk_d[I_2]$ where f is the efficiency of a given initiator. Monomers are consumed during both the initiation and propagation steps, the consumption during the initiation steps being governed by the rate of initiator decomposition, which is typically negligible. The general rate of monomer consumption is given by the following equation: $Rp = kp[Pn^{\cdot}][M]$. The concentration of radical (10^{-8} M) is very difficult to measure experimentally but can be theoretically calculated using the steady state assumption. During the course of the polymerisation, the concentration of free radicals increases rapidly in the first stage and reaches a constant concentration due to the concurrent radical destruction. Thus, the rate of initiation is equal to the rate of termination.[5] The concentration of radicals can then be estimated by the following equation:

$$[p^{\cdot}] = \sqrt{\frac{2fk_d[I_2]}{k_t}} \quad \textbf{(Eq. 1-1)}$$

1.1.2 Controlled Radical Polymerisation

Control radical polymerisation (CRP) is a "pseudo"-living system consisting of a dynamic equilibrium between dormant and active species allowing the synthesis of more complex materials than previously obtained by FRP.[6] The main equilibrium can be reached by two main mechanisms,[7] noted below:

- Reversible deactivation of propagating radicals to form a dormant species (e.g. NMP and ATRP). The kinetics are then governed by the persistent radical effect.
- Degenerate transfer between propagating radical and dormant species (e.g. RAFT). The kinetics are governed by external source of initiator and is analogous to FRP.

While the termination steps can be reduced, they cannot be completely stopped due to the high reactivity of free radicals formed. However, in order to control the polymerisation process, termination steps are minimised by keeping the concentration of radical species as low as possible (i.e. [dormant species] >> [active species]).[8] The proportion of terminated chains (i.e. dead chains) needs to be controlled as it would drastically affect not only the properties of such materials but also their potential uses for a wide range of applications (e.g. coating, adhesives, dispersant, surfactant, lubricants, electronics and biomedical devices).[9]

In order to qualify a polymerisation process as controlled a few criteria need to be met, including; a) a fast initiation compared to the propagation step; b) a full monomer consumption even in the case of further addition; c) a linear evolution of the molecular weight with the conversion; d) a constant number of polymer chains during the polymerisation which is independent of the conversion; e) a control of the molecular weight by the stoichiometry of the reaction. Overall, polymers with narrow dispersity should be obtained ($Đ < 1.3$) and controlled architectures can then be obtained (i.e. block copolymers, star polymers and brush polymers).[10] [11,12]

Nitroxide-Mediated Polymerisation (NMP)

NMP belongs to the class of stable free radical polymerisation (SFRP) and are based on a reversible termination between a growing polymer chain radical and a nitroxide, forming an alkoxyamine (dormant species). The alkoxyamine, which governs the stoichiometry of the reaction, is activated by heat allowing the homolytic cleavage between the growing polymeric chain and the nitroxide. The control over polymerisation is tuned by carefully choosing an alkoxyamine / monomer couple allowing the activation-deactivation equilibrium to take place (**Scheme 1-2**).[13,14] In order to obtain well-defined materials the equilibrium need to be pushed towards the dormant species ($k_{deac} >> k_{act}$) which is governed by the persistent radical effect.[15,16]

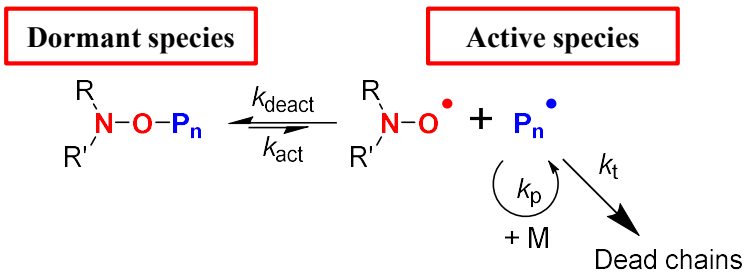

Scheme 1-2: NMP equilibrium.[13]

However, some disadvantages of using NMP include slow kinetics of polymerisation, high reaction times, lower control of methacrylate monomers and synthetic difficulties of making alkoxyamines, where the availability is then limited.[17] NMP allows control over polymerisations for a narrow range of monomers only, and there are only a few reports of NMP using charged monomers, all in organic solvents (**Figure 1-1**).[18,19]

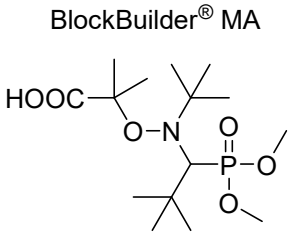

Figure 1-1: Alkoxyamine used by Charleux *et al.* to polymerise styrene sulfonate in DMSO.[18]

Atom Transfer Radical Polymerisation (ATRP)

With ATRP, a similar mechanism to NMP takes place with an equilibrium between dormant species (P_n-X) and active species (propagating radical, P_n·). Dormant species (halides/macromolecular species) react with transition metal complexes in their lower oxidation state at the rate of k_{act}, where a deactivator (metal complex with higher oxidation state) and a growing radical, which can propagate, are then formed. This reaction is reversible and is governed by k_{deact}, with k_{deact} usually higher than k_{act} to reach control over the molecular weight. ATRP is catalysed by redox-active transition metal complexes (Cu, Ru, Fe, Mo, Os), however, copper is the most widely used transition metal linked to its availability, low cost and simplicity of usage.[20,21] Similarly to NMP, the kinetics in ATRP follows the persistent radical effect. The rate of polymerisation in ATRP depends on a few different parameters, such as monomer and growing radical concentration but also the solvent, temperature and the ligand structure and activity.[22]

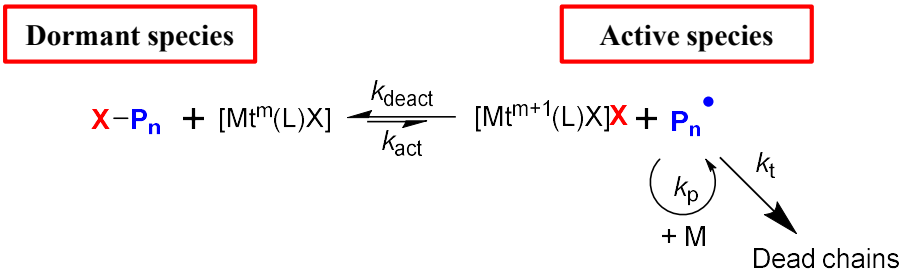

Scheme 1-3: ATRP equilibrium.[23]

While ATRP is effective for a wide range of monomers upon comparison to NMP, the presence of metals requires purification processes of the final materials.[24-26] Other related techniques such as ARGET-ATRP requires only small amount of catalyst (a few ppm) as the catalyst is regenerated in situ by a reducing agent.[23] Furthermore, the choice of the ligand is critical for each monomer, solvent and metal couple and could be costly if specific ligands are required.[27-31] ATRP is very versatile regarding the use of a variety of monomer-solvent pairs, and is extensively reported in aqueous solution.[32-35]

Reversible Addition-Fragmentation Chain-Transfer (RAFT) Polymerisation

Moad *et al.* first reported the reversible addition-fragmentation chain–transfer (RAFT) process in 1998 at the Commonwealth Scientific and Industrial Research Organisation (CSIRO) in Australia, and has since become one of the most powerful techniques for the synthesis of well-defined materials with complex architectures.[36] The RAFT process is a free radical process in which a transfer agent is added to a solution of monomer and initiator. RAFT polymerisation is a reversible, degenerative chain transfer mechanism mediated by a thiocarbonyl-thio (R-SC(Z)=S) compound named the chain transfer agent (CTA) providing control over the polymeric chains (**Scheme 1-4**).[37] CTAs possess two distinctive groups; R- and Z-, which regulate its efficiency.[38] The R group or reinitiating group is a key group in the CTA: it should be able to both fragment efficiently and re-initiate the growth of a polymer chain, but also to stabilise the C=S bond. The Z group, or stabilising group, stabilises the C=S bond and controls the addition rate of the monomer onto the CTA (**Section 1.2.2**).

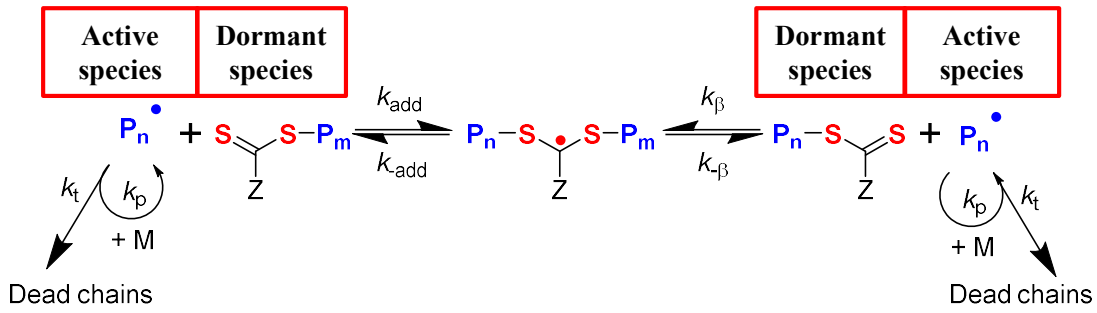

Scheme 1-4: RAFT polymerisation main equilibrium.[37]

The main advantages of this technique are the opportunities to polymerise a large range of vinyl monomers, typically employed in conventional radical polymerisation (e.g. (meth)acrylate, (meth)acrylamide, styrenic monomers) and a wide range of molecular weights can easily be targeted.[39,40] RAFT polymerisation can be easily set-up in aqueous media, or even bulk polymerisation, and be performed at room temperature (via redox or photoinitiation).[41,42] However, some drawbacks prevent this technique from reaching full commercialisation, such as the cost of commercially available RAFT agents and their demanding synthesis. Additionally, the presence of the thiocarbonyl-thio group at the end of the polymer chain typically gives a non-desirable colour and/or odour, unwanted for certain applications. RAFT agents however can easily be removed by post-polymerisation modifications.[43,44]

1.2 RAFT Polymerisation

1.2.1 Mechanism and Kinetic

The RAFT polymerisation mechanism (**Scheme 1-5**) involves five steps, with the kinetics of free radical polymerisation, and thus overall reaction, are described below in **Section 1.1.1**.[45]

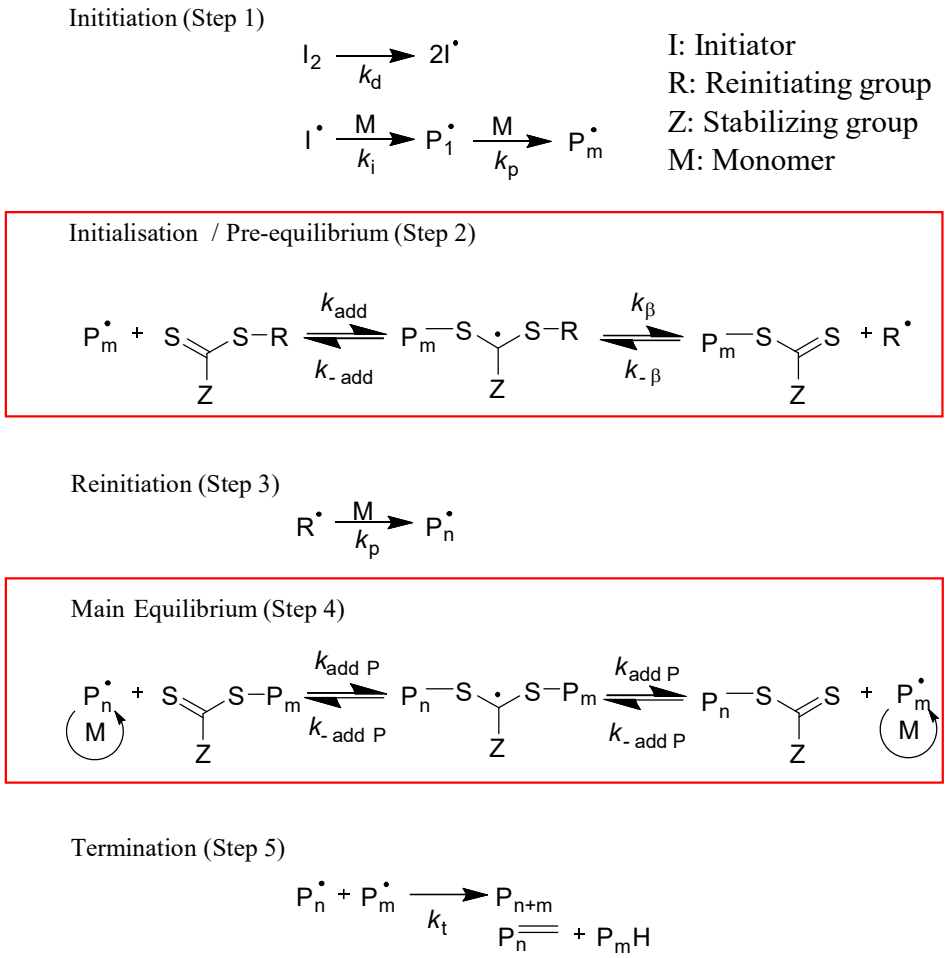

Scheme 1-5: Mechanism of RAFT polymerisation.

Step 1 is the initiation step generating primary radicals, typically via thermal decomposition of an azoinitiator, like in conventional radical polymerisation. This newly formed radical can then react either with monomers, or directly with the CTA prior to reacting with any monomers. The step 2 is the pre-equilibrium step, or initialisation step, in which the initial CTA is consumed by a degenerative chain

transfer mechanism. An intermediate radical is formed and releases the R group which then can reinitiate a new chain (step 3, reinitiation) forming a macroCTA. When all the CTA is consumed, a main equilibrium (step 4) is established which consists of a reversible equilibrium between a dormant (thiocarbonyl-thio capped compound) and an active (growing radical P·) chain. This equilibrium allows all chains to grow simultaneously during the course of the polymerisation. The reversible nature of this fragmentation chain transfer mechanism allows the production of polymer chains with predictable degrees of polymerisation (DP, related to the initial amount of CTA) and with relatively narrow dispersity (Đ < 1.5). As in conventional radical polymerisation, bimolecular terminations (step 5) are unavoidable (i.e. due to the external source of initiator) and lead to dead chains. This can be minimised however by carefully choosing the initiator and minimising its concentration, thus in order to decrease the free radical concentration across the course of the polymerisation.[46] The number of dead chains is related to the number of initiators having initiated a polymer chain (**Equation 4**). For instance, if 10 molecules of initiator (initiator efficiency = 0.5) are initially present in the mixture and if they are all consumed, at the end of the polymerisation there would be both 5 initiator-derived chains and also 5 terminated chains (i.e. if 95 CTAs were initially present, the fraction of dead chains would be 5 %). The previous example showed that it is important to fine tune the RAFT conditions (i.e. by increasing the ratio $[CTA]_0/[I]_{consumed}$) for dead chains are to be kept minimal which is important for the synthesis of complex architectures (e.g. star polymers and multiblock copolymers synthesis).[47-49]

1.2.2 Choice of CTAs and Monomers

A wide range of vinyl monomers can be polymerised by RAFT polymerisation and generally the choice of the CTA will depend highly on the monomer reactivity. Two classes of monomers are normally considered; either the More Activated Monomer (MAM) where the vinyl bond is adjacent to an electron withdrawing group like a carbonyl or aromatic group (e.g. styrene, acrylamide, etc.), or the Less Activated Monomer (LAM) where the double bond is directly adjacent to an electron-donor group such as an oxygen or an nitrogen (e.g. vinyl acetate, N-vinylcarbazole).[38,50] MAM monomers require the use of more activated CTAs such as dithioesters and trithiocarbonates, upon comparison to LAM monomers which require CTAs such as dithiocarbamates or xanthates (**Figure 1-2**).[37,41]

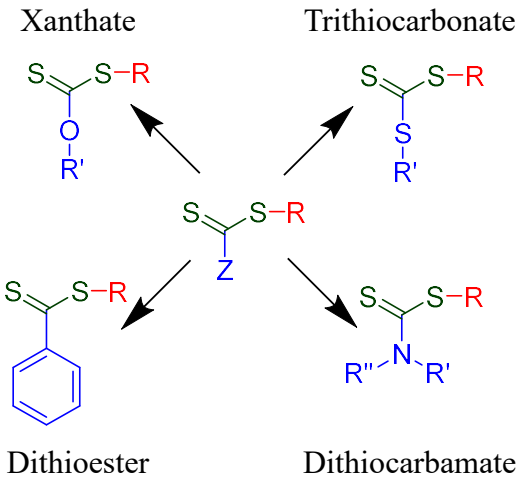

Figure 1-2: General structure of chain transfer agent and its Z-group derivatives.[38]

The choice of the RAFT agent / monomer couple is a critical parameter to control the polymerisation (i.e. control over molecular weight and dispersity), and indeed, the molecular weight distribution is calculated according to the following equation:

$$Đ = 1+(1/C_{tr}) \text{ with } C_{tr} = k_{tr}/k_p \quad \textbf{(Eq. 1-2)}$$

The chain transfer agent should have a high chain transfer constant (C_{tr}) value to achieve low dispersity, and consequently the rate of transfer (k_{tr}) should be higher than the rate of polymerisation (k_p). The transfer rate constant (k_{tr}) is defined by the

following equation and will depend on the reactivity of the intermediate radical formed during the pre-equilibrium step (**Scheme 1-4**):

$$k_{tr} = k_{add}(k_{\beta}/(k_{-add}+k_{\beta})) \quad \textbf{(Eq. 1-3)}$$

A CTA is considered effective towards a monomer if the addition and fragmentation rate is higher than the propagation rate, the CTA is instantaneously consumed, a fast equilibrium between the active and dormant species takes place, and finally, the R-group is able to facilitate the polymerisation reinitiation. Different monomers and CTAs have been studied in the literature and a trend has been found between different R- and Z- groups towards particularly types of monomer (i.e. LAM versus MAM).[38,51] In **Figure 1-3**, Z-groups studied in the literature are presented and it is found from left to right that there is a decrease of the addition rate and an increase of the fragmentation rate.[52]

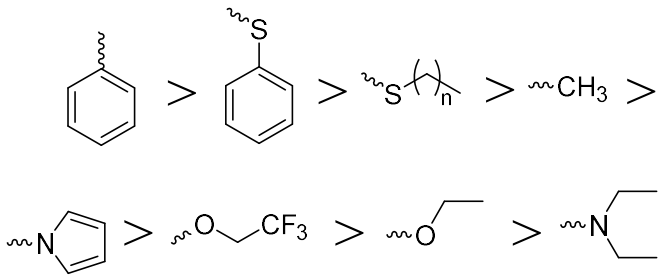

Figure 1-3: Structure of various Z-groups.[37]

The R-group on the other hand is required to be an excellent leaving group and efficient towards reinitiation.[53] The stability of the free radical formed, the steric hindrance and polarity need to be taken into account for the polymerisation of various individual monomers.[54] In **Figure 1-4**, R-groups are presented where the homolytic leaving group ability and fragmentation rates are found to decrease from left to right.

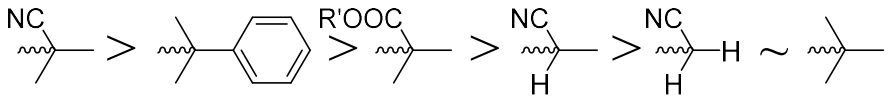

Figure 1-4: Structure of various R-groups.[37]

1.2.3 Aqueous RAFT Polymerisation

RAFT polymerisation can be used in non-stringent conditions such as in water and / or at low temperatures.[55] RAFT is compatible with the use of water soluble monomers (**Figure 1-5**) which could be non-ionic, anionic, cationic or zwitterionic.[56]

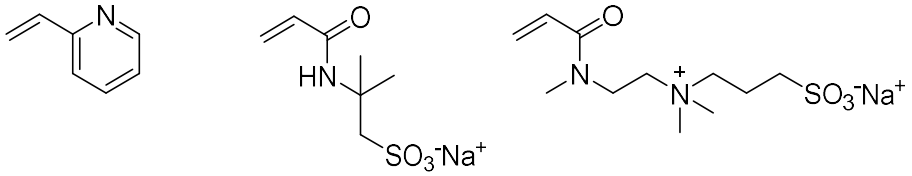

Figure 1-5: Examples of water soluble monomers.

From left to right: 2-vinylpyridine (non-ionic), sodium 2-acrylamido-2-methylpropanesulfonate (ionic) and sodium 3-(dimethyl(2-(*N*-methylacrylamido)ethyl)ammonio) propane-1-sulfonate (zwitterionic).[56]

However, it is important to ensure all the starting reagents (monomer, CTA and initiator) are all water soluble, and that they do not degrade at the pH of the reaction. A wide range of water soluble azoinitiators are commercially available from WAKO with half-life temperatures in water ranging from 44 °C to 87 °C (**Figure 1-6**).

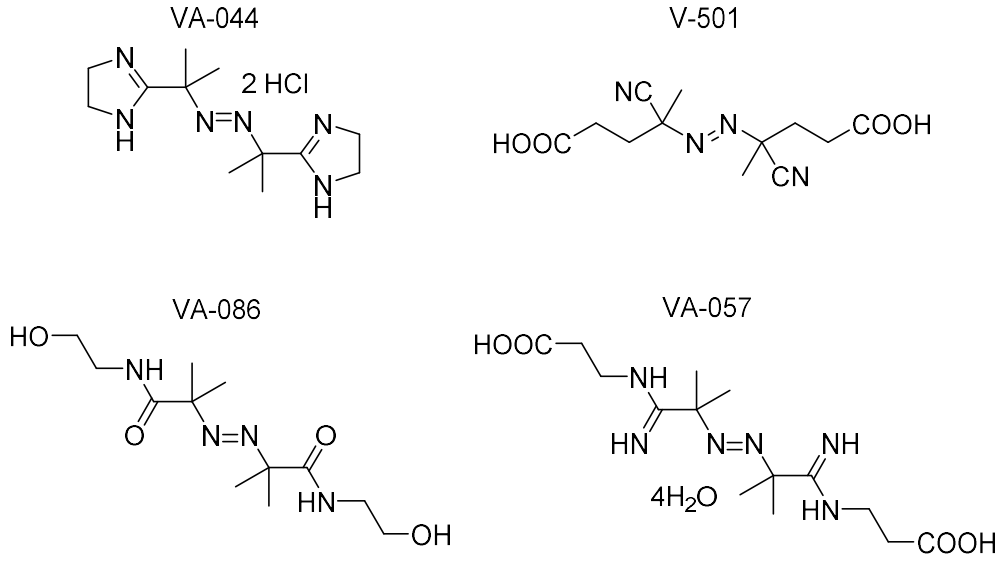

Figure 1-6: Example of water soluble azoinitiators (Wako).

From left to right: 2,2′-azobis[2-(2-imidazolin-2-yl)propane]dihydrochloride (VA-044), 2,2′-azobis[*N*-(2-carboxyethyl)-2-methylpropionamidine]tetrahydrate (VA-057), 2,2′-azobis[2-methyl-*N*-(2-hydroxyethyl)propionamide] (VA-086) and 4,4′-azobis(4-cyanovaleric acid) (V-501, ACVA).

It is important to note that some of them bear either a carboxylic acid or an amine group and that will have an important effect on their solubility depending on the basic, neutral or acidic conditions used. V-501 is likely to be soluble in basic condition while VA-044 more likely in acidic condition. On the other hand, VA-057 and VA086 are likely to be soluble in acidic and basic condition due to the combination of functionalities. Similar observations are made towards the solubility of the chain transfer agent, which, for well-defined materials, it is imperative to ensure an immediate and concurrent initiation of the CTA at the start of the polymerisation (**Figure 1-7**).[57] The pH for aqueous RAFT polymerisation is then a key parameter to ensure the solubility of all compounds, however, the hydrolysis of the chain transfer agent has been widely reported in the literature affecting the polymerisation control. For example, it has been reported in the literature that the hydrolysis of the thiocarbonyl-thio group can occur at high temperatures or in basic conditions. These studies have been mainly performed on dithiobenzoate CTAs which are known to be hydrolytically unstable.[56,58-61] For these reasons, conducting aqueous RAFT polymerisation at low pH (i.e. below 7) is necessary. Recently, work in our group on the synthesis of multiblock copolymers by RAFT polymerisation in aqueous solutions has proven that trithiocarbonates are a hydrolytically stable family of CTAs at neutral pH at 70˚C, or even at higher temperature such as 100 ˚C for several minutes.[62]

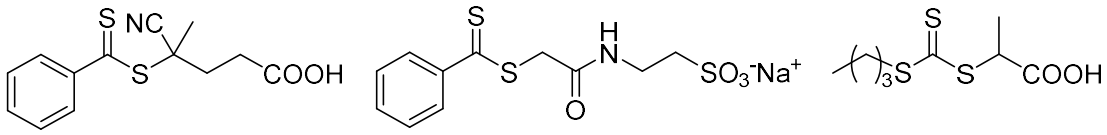

Figure 1-7: Example of water soluble CTAs.

From left to right: 4-cyano-4-(phenylcarbonothioylthio)pentanoic acid, sodium 2-(2-thiobenzoylsulfonylproponylamino) ethanesulfonate and 2-[(butylthio)-carbonothioyl-thio]propanoic acid.[56,63,64]

In the literature, acrylamide monomers have been polymerised in water by RAFT polymerisation and the pH effect has been assessed using buffer solutions (acetic acid / sodium acetate) (**Scheme 1-6**). At pH 7, an inhibition period of ca. 4 hours was observed, followed by non-molecular weight controlled polymerisation (~239,000 g/mol) and high dispersity ($Đ$ = 2.98) after 12 hours. According to this study, the RAFT agent hydrolysed due to the nucleophilic attack of the ammonia released from the monomer hydrolysis. As a consequence, the resulting thiol groups (from the CTA

hydrolysis) acts as a chain transfer stopper and only conventional radical polymerisation is observed. Optimal conditions were suggested to be pH 5 using a buffer solution at 70 °C with a monomer concentration of 2 M. Low dispersity values of around 1.2 were obtained, although after 24 hours monomer conversion was surprisingly low (28 %), due to the low chain transfer constant of the CTA used.[58,59,65] Subsequently, the polymerisation of acrylamides at temperatures up to 50 °C and pH 5.5 in deionised water was attempted. The decrease in temperature from 70 to 50 °C completely suppressed the CTA hydrolysis, resulting in high monomer conversions (~ 93 %) being reached in 2 hours with good molecular weight control and narrow dispersity ($Đ$ = 1.05). It is important to note that in this study they had changed the CTA and used a trithiocarbonate instead of the dithiobenzoate, which dramatically impacted the CTA stability with respect to the pH and temperature.[66]

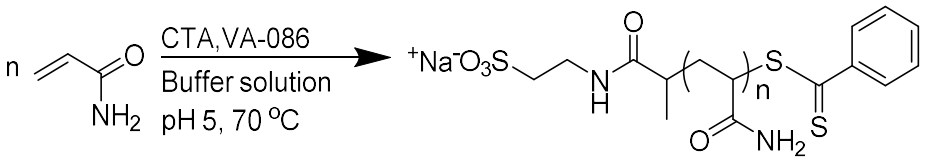

Scheme 1-6: Acrylamide polymerisation conducted by McCormick *et al.*.[65]

Additionally, the pH of the solution can also have a strong influence on the RAFT polymerisation of monomers bearing acidic groups on their side chain (e.g. methacrylic acid (MAA), **Scheme 1-7**).[67,68]

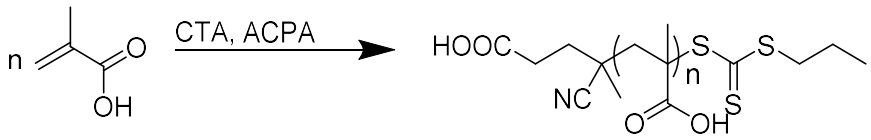

Scheme 1-7: Synthesis of PMAA by RAFT polymerisation with CTPPA and ACPA.[68]

In the case of MAA, homopolymers with dispersity below 1.15 were obtained at pH below the pKa of the monomer (pKa = 4.36), whereas no control of the polymerisation was observed at pH higher than the pKa, (at pH 7, $Đ$ = 2.59). According to the authors, this could be due to electrostatic interactions. Indeed, at pH $\geq$ pKa, MAA is fully ionised and might be responsible for electrostatic repulsion between the growing polymer chain and the monomer.[68] Surprisingly, the effect of the pH on the RAFT agent, which bears a carboxylic acid group, was not studied in this article, although

one would expect that the pH would have a drastic effect on the RAFT agent and consequently on the polymerisation.

Additionally, it has been shown that acrylamide monomers can spontaneously polymerise in acidic conditions by self-initiation.[69-73] This phenomenon has particularly been observed for AMPS® monomer and this could disturb the RAFT process, and consequently the properties of the newly obtained material.[74,75] Indeed, it has been demonstrated that AMPS® in acidic media (pH < 7) can spontaneous self-polymerise without initiators, whilst no spontaneous polymerisation of AMPS® was observed when NaOH, was added in stoichiometry or in excess. On the contrary, when 0.1 to 0.9 equivalent of NaOH with respect to the sulfonic acid group of the monomer was added, monomer conversions between 75 – 88 % after 4 hours at 50 °C were observed. Varying the monomer concentration from 20 to 50 wt. % led to an increase in the initial rate of polymerisation. This observation was explained by a monomer association in concentrated solution that increases the probability of the radical and the monomer reacting with each other. Below 20 wt. %, no spontaneous polymerisation occurred, thus suggesting the solution was too diluted either to create a radical or to create an associated monomer. According to the authors of this work, actives species were formed in associated monomers creating a weak reducing agent: the lone pairs of nitrogen or oxygen act as the reducing agent, while the double carbon bond is the oxidising agent. The size of the counter-ion appeared to be a critical, as the polymerisation rate increased with counter-ion size. Moreover, this reduced the electrostatic repulsion between the growing macroradical and the monomer. Finally, an inhibition time is observed at temperature lower than 60 °C, owing to a low rate of initiation (EA = 21.7 kJ/mol). According to the authors, the system could be initiated by redox activation, as the energy of activation is low. This was demonstrated by the addition of a strong reducing agent to boost the “initiation”, and the induction time was indeed eliminated, and the rate of polymerisation increased.

1.3 AMPS®/AMPS®2405 Monomers

1.3.1 Introduction to AMPS® Based Monomers

AMPS®/AMPS®2405 monomers (**Scheme 1-8**) are a Lubrizol trademark. This monomer was invented more than 30 years ago by the Lubrizol Corporation, and is currently produced in high purity to fulfil its numerous applications in a wide market range due to its remarkable properties. AMPS® is synthesised by a Ritter reaction of acrylonitrile and isobutylene in the presence of sulfuric acid in water.[76,77] AMPS®2405 is prepared from AMPS® at 50 wt. % in water and by adding NaOH to form the salt monomer and have a pH of about 8.

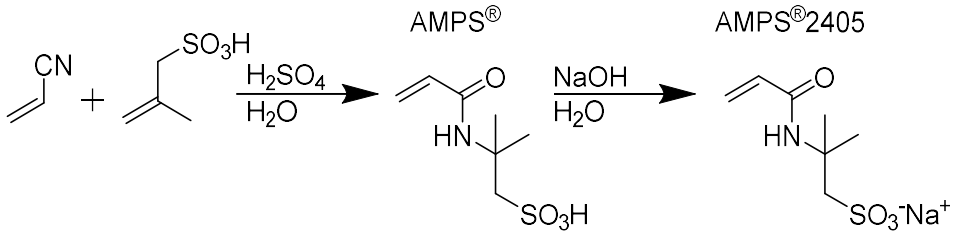

Scheme 1-8: AMPS® and AMPS®2405 monomer synthesis, a Lubrizol trademark.

AMPS®-based monomers are highly charged (negative) monomers, consequently, they are highly soluble in water with a high absorption of water at a wide range of pH.[78] AMPS® based monomers are hydrolytically stable over a broad range of pH, indeed, the steric hindrance with the geminal dimethyl group adjacent to the amide function limits its hydrolysis.[79] Despite, their high stability AMPS®-based monomers can be subject to hydrolysis in extreme conditions. For example, the hydrolysis of AMPS® had been observed at 80 °C with about 40 % of the monomer hydrolysed at pH 1 within 6 days (**Scheme 1-9**). AMPS®2405 can also be hydrolysed, where under basic conditions, at pH 12 and at 80 °C, approximately 60 % of the monomer was hydrolysed after 7 days.[80]

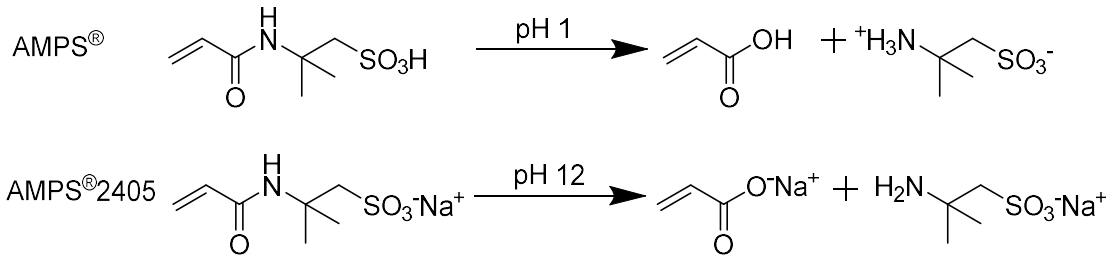

Scheme 1-9: Hydrolysis of AMPS® and AMPS®2405.[80]

Moreover, due to the high thermal stability and mechanical shear stability of the monomer, the polymer (PAMPSA), in its acidic form, does not decompose until 225 °C. Overall, for simplification, polymers made from AMPS® will be named PAMPSA while polymers made from AMPS®2405 monomers will be named PAMPS (**Scheme 1-10**).

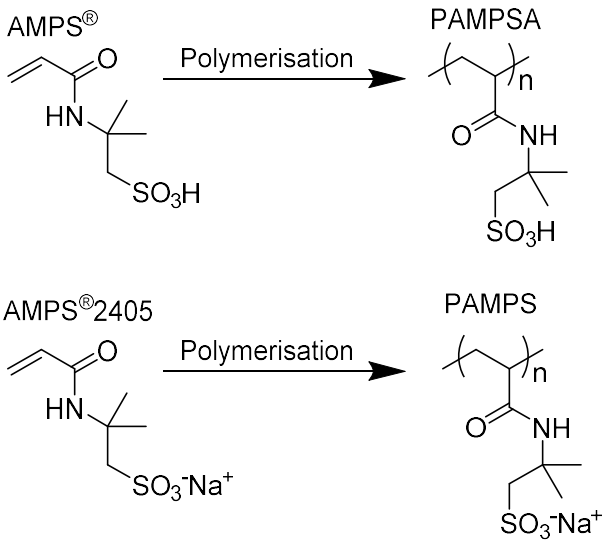

Scheme 1-10: AMPS®-based monomers and polymers nomenclature used in this thesis.

1.3.2 Applications of PAMPS

Polyelectrolytes, and sulfonated polymers in particular, have gradually become key components in important industrial processes such as water purification, oil recovery or fuel cells preparation.[81-83] One of these, PAMPS, are of a particular interest as they combine high thermal stability, resistance to hydrolysis and a high solubility in water over a wide range of pH. PAMPS is used as a rheology modifier, dispersant for oil spills, or as biocompatible hydrogels for various biomedical purposes.[81,84-86]

Specific examples of applications using PAMPS include:

- Water treatment or in the cement industry, as PAMPS is fully ionised in water and reduces cation precipitation. The ability of poly(AMPS-*co*-AA) to limit the nucleation of $CaCO_3$ has been demonstrated by chelation of the Ca^{2+} ion by the carboxylic group present on the AA monomer while AMPS®2405 ensures solubility in aqueous solution.[81]
- In the medical field, PAMPS is used to form cross-linked polymer networks which are able to swell depending on various factors such as the pH, the temperature and the ionic character of the polymer chains.[87] PAMPS is favoured because it has strong ionic properties in a wide range of pH; allowing the polymer to swell uniformly.
- It is also used for cosmetics; the property of PAMPS which is often exploited is the lubricity of the solution.[88]

In conclusion, PAMPS is used in numerous applications from drilling to personal care, however, at present, PAMPS is typically produced on an industrial scale via conventional radical polymerisation.

1.4 Research Aims

The main aim of this project was to optimise the aqueous reversible addition-fragmentation chain transfer (RAFT) polymerisation conditions for the monomer sodium 2-acrylamido-2-methylpropane sulfonate (AMPS®2405), mediated by the chain transfer agent DDMAT, produced and commercialised by Lubrizol (**Scheme 2-6**). In parallel, efficient aqueous RAFT conditions for other water soluble monomers such as *N*,*N*-dimethylacrylamide (DMA), *N*-hydroxyethyl acrylamide (HEAm) or 4-acryloylmorpholine (NAM) will also be investigated. Finally, more advanced complex architectures such as block copolymers and star polymers will be prepared to study the effect of architecture on various applications. A summary of the main objectives are listed below:

CHAPTER 2: Optimization of the RAFT polymerisation conditions for the aqueous homopolymerisation of AMPS®2405, including other water soluble monomers mediated either by the chain transfer agent BDMAT or DDMAT. Comparison between two CTAs with the same R-group but different Z-group, where BDMAT has a shorter alkyl chain compared to DDMAT (C4 versus C12).

CHAPTER 3: Preparation of diblock copolymers using AMPS®2405 macroCTA with a range of other water soluble monomers. Additionally, using AMPS®2405 and HEAm as comonomers, a range of copolymers with different microstructure will be synthesised (i.e. octablock, tetrablock, diblock and statistical copolymers). Thus in order to compare the properties of statistical versus block copolymers for different applications. Preparation of homo- or block- star copolymers using the arm first approach. Arms of different length will be used then arms with different microstructures will be used.

CHAPTER 4: Characterization (SEC, viscometer, rheology, SAXS, DLS, AFM) of the newly synthesised materials in order to support the proposed structures.

CHAPTER 5: Finally, these newly synthesised polymers will be investigated as heparin-mimicking polymers, where the effect of the microstructure will be studied and in addition to the change in charge density and architecture.[89-91]

1.5 References

(1) Nesvadba, P. In *Encyclopedia of Radicals in Chemistry, Biology and Materials*; John Wiley & Sons, Ltd: 2012.

(2) Su, W.-F. In *Principles of Polymer Design and Synthesis*; Springer Berlin Heidelberg: Berlin, Heidelberg, 2013, p 185.

(3) Odian, G. In *Principles of Polymerization*; John Wiley & Sons, Inc.: 2004, p 198.

(4) Ahmad, N. M.; Heatley, F.; Lovell, P. A. *Macromolecules* **1998**, *31*, 2822.

(5) Barner-Kowollik, C.; Vana, P.; Davis, T. P. In *Handbook of Radical Polymerization*; John Wiley & Sons, Inc.: 2003, p 187.

(6) Matyjaszewski, K. In *ACS Symp. Ser.* 2009; Vol. 1023, p 3.

(7) Matyjaszewski, K. In *ACS Symp. Ser.* 2012; Vol. 1100, p 1.

(8) Matyjaszewski, K. In *ACS Symp. Ser.* 2003; Vol. 854, p 2.

(9) Matyjaszewski, K.; Spanswick, J. *Mater. Today* **2005**, *8*, 26.

(10) Matyjaszewski, K. In *Controlled Radical Polymerization*; American Chemical Society: 1998; Vol. 685, p 2.

(11) Quirk, R. P.; Lee, B. *Polym. Int.* **1992**, *27*, 359.

(12) Stenzel, M. H.; Barner-Kowollik, C. *Mater. Horizons* **2016**, *3*, 471.

(13) Nicolas, J.; Guillaneuf, Y.; Lefay, C.; Bertin, D.; Gigmes, D.et al *Prog. Polym. Sci.* **2013**, *38*, 63.

(14) Moad, G.; Rizzardo, E. In *Nitroxide Mediated Polymerization: From Fundamentals to Applications in Materials Science*; The Royal Society of Chemistry: 2016, p 1.

(15) Fischer, H. *Chem. Rev.* **2001**, *101*, 3581.

(16) Hawker, C. J.; Bosman, A. W.; Harth, E. *Chem. Rev.* **2001**, *101*, 3661.

(17) Grubbs, R. B. *Polymer Reviews* **2011**, *51*, 104.

(18) Brusseau, S.; Belleney, J.; Magnet, S.; Couvreur, L.; Charleux, B. *Polym. Chem.* **2010**, *1*, 720.

(19) Groison, E.; Brusseau, S.; D'Agosto, F.; Magnet, S.; Inoubli, R.et al *ACS Macro Lett.* **2012**, *1*, 47.

(20) Braunecker, W. A.; Brown, W. C.; Morelli, B. C.; Tang, W.; Poli, R.et al *Macromolecules* **2007**, *40*, 8576.

(21) Pintauer, T.; Matyjaszewski, K. *Chem. Soc. Rev.* **2008**, *37*, 1087.

(22) Matyjaszewski, K. *Isr. J. Chem.* **2012**, *52*, 206.

(23) Matyjaszewski, K. *Macromolecules* **2012**, *45*, 4015.

(24) Coessens, V.; Pintauer, T.; Matyjaszewski, K. *Prog. Polym. Sci.* **2001**, *26*, 337.

(25) Ding, M.; Jiang, X.; Zhang, L.; Cheng, Z.; Zhu, X. *Macromol. Rapid Commun.* **2015**, *36*, 1702.

(26) Mueller, L.; Matyjaszewski, K. *Macromolecular Reaction Engineering* **2010**, *4*, 180.

(27) Silvestro, G. D.; Yuan, C. M.; Mussini, P. R. *J. Solution Chem.* **2004**, *33*, 923.

(28) Gromada, J.; Spanswick, J.; Matyjaszewski, K. *Macromol. Chem. Phys.* **2004**, *205*, 551.

(29) Strandman, S.; Pulkkinen, P.; Tenhu, H. *J. Polym. Sci., Part A: Polym. Chem.* **2005**, *43*, 3349.

(30) Chan, N.; Cunningham, M. F.; Hutchinson, R. A. *Macromol. Chem. Phys.* **2008**, *209*, 1797.

(31) Tang, W.; Matyjaszewski, K. *Macromolecules* **2006**, *39*, 4953.

(32) Zhang, Q.; Wilson, P.; Li, Z.; McHale, R.; Godfrey, J.et al *J. Am. Chem. Soc.* **2013**, *135*, 7355.

(33) Nikolaou, V.; Simula, A.; Droesbeke, M.; Risangud, N.; Anastasaki, A.et al *Polym. Chem.* **2016**, *7*, 2452.

(34) Jones, G. R.; Li, Z.; Anastasaki, A.; Lloyd, D. J.; Wilson, P.et al *Macromolecules* **2016**, *49*, 483.

(35) Whitfield, R.; Anastasaki, A.; Nikolaou, V.; Jones, G. R.; Engelis, N. G.et al *J. Am. Chem. Soc.* **2017**, *139*, 1003.

(36) Chiefari, J.; Chong, Y. K.; Ercole, F.; Krstina, J.; Jeffery, J.et al *Macromolecules* **1998**, *31*, 5559.

(37) Perrier, S. *Macromolecules* **2017**, *50*, 7433.

(38) Keddie, D. J.; Moad, G.; Rizzardo, E.; Thang, S. H. *Macromolecules* **2012**, *45*, 5321.

(39) Moad, G.; Solomon, D. H. In *The Chemistry of Radical Polymerization*; Second Edi ed.; Moad, G., Solomon, D. H., Eds.; Elsevier Science Ltd: Amsterdam, 2005, p 451.

(40) Moad, G.; Rizzardo, E.; Thang, S. H. *Aust. J. Chem.* **2009**, *62*, 1402.

(41) Perrier, S.; Takolpuckdee, P. *J. Polym. Sci., Part A: Polym. Chem.* **2005**, *43*, 5347.

(42) Semsarilar, M.; Perrier, S. *Nat. Chem.* **2010**, *2*, 811.

(43) Moad, G.; Rizzardo, E.; Thang, S. H. *Polym. Int.* **2011**, *60*, 9.

(44) Willcock, H.; O'Reilly, R. K. *Polym. Chem.* **2010**, *1*, 149.

(45) Moad, G.; Mayadunne, R. T. A.; Rizzardo, E.; Skidmore, M.; Thang, S. H. In *ACS Symp. Ser.* 2003, p 520.

(46) Konkolewicz, D.; Hawkett, B. S.; Gray-Weale, A.; Perrier, S. *Macromolecules* **2008**, *41*, 6400.

(47) Gody, G.; Maschmeyer, T.; Zetterlund, P. B. *Macromolecules* **2014**, *47*, 639.

(48) Gody, G.; Maschmeyer, T.; Zetterlund, P. B.; Perrier, S. *Macromolecules* **2014**, *47*, 3451.

(49) Gody, G.; Maschmeyer, T.; Zetterlund, P. B.; Perrier, S. *Nat. Commun.* **2013**, *4*.

(50) Keddie, D. J. *Chem. Soc. Rev.* **2014**, *43*, 496.

(51) Keddie, D. J.; Guerrero-Sanchez, C.; Moad, G.; Mulder, R. J.; Rizzardo, E.et al *Macromolecules* **2012**, *45*, 4205.

(52) Chiefari, J.; Mayadunne, R. T. A.; Moad, C. L.; Moad, G.; Rizzardo, E.et al *Macromolecules* **2003**, *36*, 2273.

(53) Chong, Y. K.; Krstina, J.; Le, T. P. T.; Moad, G.; Postma, A.et al *Macromolecules* **2003**, *36*, 2256.

(54) Coote, M. L.; Henry, D. J. *Macromolecules* **2005**, *38*, 1415.

(55) Qiu, J.; Charleux, B.; Matyjaszewski, K.; Pierre, Â.; Curie, M. *Prog. Polym. Sci.* **2001**, *26*, 2083.

(56) McCormick, C. L.; Lowe, A. B. *Acc. Chem. Res.* **2004**, *37*, 312.

(57) Lowe, A. B.; McCormick, C. L. *Prog. Polym. Sci.* **2007**, *32*, 283.

(58) Thomas, D. B.; Convertine, A. J.; Hester, R. D.; Lowe, A. B.; McCormick, C. L. *Macromolecules* **2004**, *37*, 1735.

(59) Thomas, D. B.; Convertine, A. J.; Myrick, L. J.; Scales, C. W.; Smith, A. E.et al *Macromolecules* **2004**, *37*, 8941.

(60) Abel, B. A.; McCormick, C. L. *Macromolecules* **2016**, *49*, 465.

(61) Lowe, A. B.; McCormick, C. L. *Chem. Rev.* **2002**, *102*, 4177.

(62) Gody, G.; Barbey, R.; Danial, M.; Perrier, S. *Polym. Chem.* **2015**, *6*, 1502.

(63) Ferguson, C. J.; Hughes, R. J.; Pham, B. T. T.; Hawkett, B. S.; Gilbert, R. G.et al *Macromolecules* **2002**, *35*, 9243.

(64) Donovan, M. S.; Sanford, T. A.; Lowe, A. B.; Sumerlin, B. S.; Mitsukami, Y.et al *Macromolecules* **2002**, *35*, 4570.

(65) Thomas, D. B.; Sumerlin, B. S.; Lowe, A. B.; McCormick, C. L. *Macromolecules* **2003**, *36*, 1436.

(66) Convertine, A. J.; Lokitz, B. S.; Lowe, A. B.; Scales, C. W.; Myrick, L. J.et al *Macromol. Rapid Commun.* **2005**, *26*, 791.

(67) Chaduc, I.; Crepet, A.; Boyron, O.; Charleux, B.; D'Agosto, F.et al *Macromolecules* **2013**, *46*, 6013.

(68) Chaduc, I.; Lansalot, M.; D'Agosto, F.; Charleux, B. *Macromolecules* **2012**, *45*, 1241.

(69) Baker, N. A., University of Connecticut 2001.

(70) Pistoia, G.; Voso, M. A. *Journal of Polymer Science: Polymer Chemistry Edition* **1976**, *14*, 1811.

(71) Salamone, J. C.; Ellis, E. J.; Bardoliwalla, D. F. *Journal of Polymer Science: Polymer Symposia* **1974**, *45*, 51.

(72) Buzanowski, W. C.; Graham, J. D.; Priddy, D. B.; Shero, E. *Polymer* **1992**, *33*, 3055.

(73) Kazantsev, O. A.; Shirshin, K. V.; Sivokhin, A. P.; Kuznetsova, N. A.; Malyshev, A. P. *Russ. J. Appl. Chem.* **2004**, *77*, 303.

(74) Kazantsev, O. A.; Igolkin, A. V.; Shirshin, K. V.; Kuznetsova, N. A.; Spirina, A. N.et al *Russ. J. Appl. Chem.* **2002**, *75*, 465.

(75) Kazantsev, O. A.; Shirshin, K. V. *Polymer* **2004**, *45*, 5021.

(76) Leonard E. Miller, C. F., Donald L. Murfin In *United States Patent Office*; Corporation, T. L., Ed. United States, 1970; Vol. 3 506 707.

(77) Robert E. Quinn, W. M. B. In *The Lubrizol Corporation* United States, 1998; Vol. 6448347B1.

(78) Atta, A. M. *Polym. Adv. Technol.* **2002**, *13*, 567.

(79) Parker, W. O.; Lezzi, A. *Polymer* **1993**, *34*, 4913.

(80) "Lubrizol Internal Report (Proprietary)," 2013.

(81) Dietzsch, M.; Barz, M.; Schüler, T.; Klassen, S.; Schreiber, M.et al *Langmuir* **2013**, *29*, 3080.

(82) Sabhapondit, A.; Borthakur, A.; Haque, I. *Energy Fuels* **2003**, *17*, 683.

(83) Smitha, B.; Sridhar, S.; Khan, A. A. *Macromolecules* **2004**, *37*, 2233.

(84) Koromilas, N. D.; Lainioti, G. C.; Vasilopoulos, G.; Vantarakis, A.; Kallitsis, J. K. *Polym. Chem.* **2016**, *7*, 3562.

(85) Bartlett, R. L.; Panitch, A. *Biomacromolecules* **2012**, *13*, 2578.

(86) Bartlett, R. L.; Medow, M. R.; Panitch, A.; Seal, B. *Biomacromolecules* **2012**, *13*, 1204.

(87) Patrick T. Cahalan, A. H. J., Arthur J. Coury, Michael J. Kallok; Inc, L. B., Ed. United States, 1988; Vol. 4768523.

(88) Larry D. Lundmark, A. M., Ho-Ming Chun; Inc, G. M. C., Ed. United States; Vol. 4128631A.

(89) Moraes, J.; Peltier, R.; Gody, G.; Blum, M.; Recalcati, S.et al *ACS Macro Lett.* **2016**, *5*, 1416.

(90) Kuroki, A.; Sangwan, P.; Qu, Y.; Peltier, R.; Sanchez-Cano, C.et al *ACS Applied Materials & Interfaces* **2017**, *9*, 40117.

(91) Oda, Y.; Kanaoka, S.; Sato, T.; Aoshima, S.; Kuroda, K. *Biomacromolecules* **2011**, *12*, 3581.

CHAPTER 2:
AMPS®2405 POLYMERISATION

2.1 Abstract

RAFT polymerisation in aqueous solution is challenging when compared to being conducted in organic solvent. The hydrolysis of the chain transfer agent at various pH and temperature was shown to affect the chain-end fidelity, and lowered reinitiations were observed when block copolymers were synthesised. Herein, universal conditions were optimised for the polymerisation of acrylamides in aqueous solution by RAFT polymerisation from trithiocarbonates. More specifically, the RAFT polymerisation of a sulfonated monomer, sodium 2-acrylamido-2-methyl-1-propanesulfonate (AMPS®2405), with either 2-(butylthiocarbonothioylthio)-2-methylpropionic acid (BDMAT) or 2-(dodecylthiocarbonothioylthio)-2-methylpropionic acid (DDMAT) as the chain transfer agent in aqueous solution are described. Even though a critical aggregation concentration of DDMAT in aqueous solution (0.005 M) was observed, well-defined polymeric chains could be obtained after optimisation of a few parameters. These newly obtained materials can now be studied for a broader range of applications.

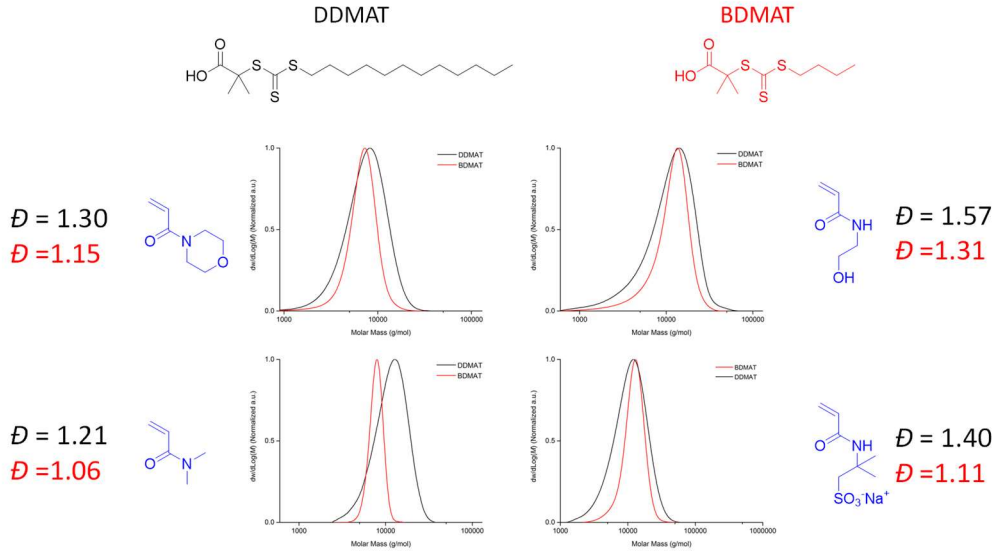

2.2 Introduction

2.2.1 Polymerisation of Sulfonated Polymers

Polyelectrolytes, and sulfonated polymers (**Figure 2-1**) in particular, have gradually become key components in important industrial processes such as water purification, oil recovery or fuel cell preparation.[82,83,92] Amongst them, PAMPS are of a particular interest as they combine high thermal stability, resistance to hydrolysis and a high solubility in water over a wide range of pH.[93] PAMPS is used as rheology modifier, dispersant for oil spills, or as biocompatible hydrogels for various biomedical purposes.[82,84,86,92] In all these applications, the molecular weight, architecture and chain-end functionality of the polyelectrolyte plays an essential role in controlling the physical-chemical properties of the resulting material.

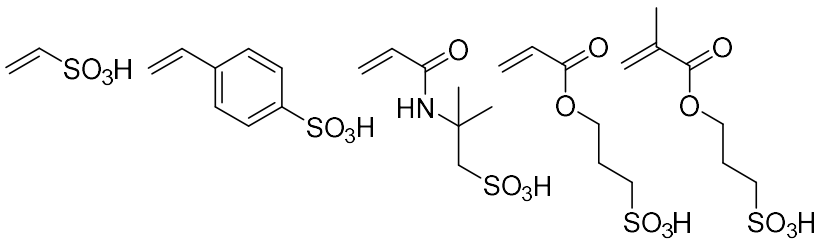

Figure 2-1: Examples of sulfonic acid monomers used in the literature.[56,94]

PAMPS is commonly prepared via conventional radical polymerisation in aqueous solution at low temperature using redox initiation. This process has been widely used for about three decades, albeit with a lack of control over the resulting molecular weight and chain-end functionality of the polymer, typically resulting in dispersities above 1.5.[95-99] Today, the emergence of controlled / living radical polymerisation (NMP,[100] ATRP,[101] or RAFT[42]) allows for the preparation of well-defined polymers, with respect to both molecular weights and architecture.[102] Mincheva *et al.*, optimised the polymerisation of AMPS® by transformation into the sodium salt by addition of NaOH, forming AMPS(Na) (pH 7.5, 8, 9, 10 and 12). They used copper-mediated ATRP in a mixture of methanol and water and reported the influence of pH and ligand type on the resulting materials.[103] The optimal conditions for well-control ATRP of AMPS(Na) in water and methanol (3:1) was found to be with Me_6-TREN ligands at pH 7.5 and room temperature (**Scheme 2-1**). Full monomer conversion was achieved

within 3 hours obtaining narrow and monomodal SEC molecular weight distribution with a dispersity of about 1.29.

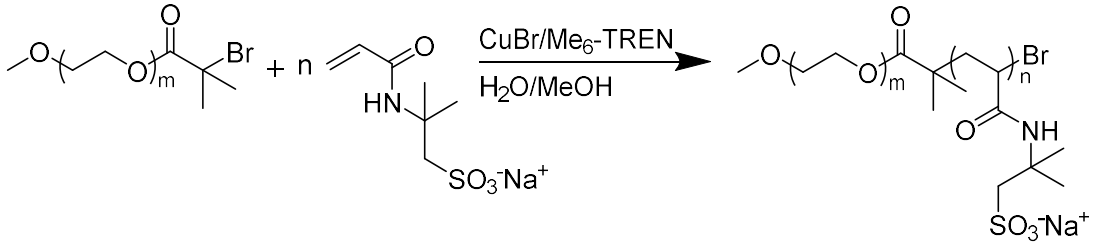

Scheme 2-1: PAMPS synthesised by Mincheva *et al.* using Me_6-TREN ligand.[103]

In another example, Nikolaou *et al.* achieved full monomer conversion in less than 30 minutes by polymerising AMPS®2405 using copper-mediated living radical polymerisation in aqueous solution at 0 °C still with Me_6-TREN.[33] $PAMPS_{DP\leq80}$ with narrow and monomodal molecular weight distributions were prepared by tuning the following ratio [I]:[CuBr]:[Me_6-TREN] and maximising the amount of deactivating species formed during the disproportionation step. This method however yielded poor control over the polymerisation when degree of polymerisation (DP) higher than 80 were targeted. Additionally, the use of a metal-catalyst requires a further step of product purification, which might be an issue for associated applications or scale-up manufacturing.

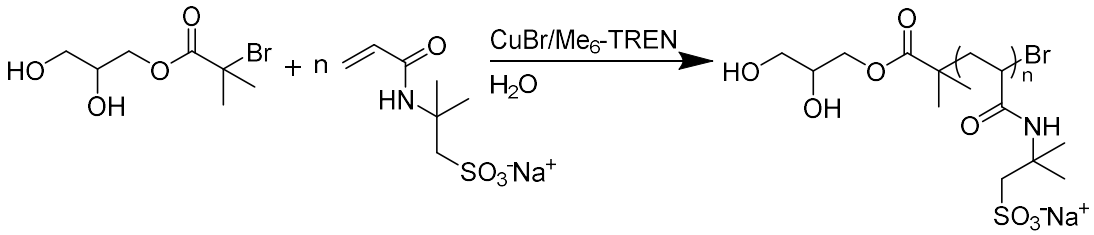

Scheme 2-2: PAMPS synthesised by Nikolaou *et al.* using Me_6-TREN in water.[33]

Another convenient approach to prepare polysulfonated materials is to use RAFT polymerisation. Only a few examples of polysulfonated polymers synthesised by RAFT polymerisation have been reported in the literature using either polar organic solvents (e.g. alcohol) or aqueous solution. Matyjaszewki *et al.* synthesised well-defined AMPS® homopolymer in methanol at 60 °C using cumyl dithiobenzoate as the chain transfer agent and azobisisobutyronitrile (AIBN) as the initiator (**Scheme**

2-3).[104] While a dispersity of 1.36 was obtained the monomer conversion determined by ^{1}H NMR spectroscopy was only about 60 %, with susbsequent purification by dialysis being required to remove the remaining monomer.

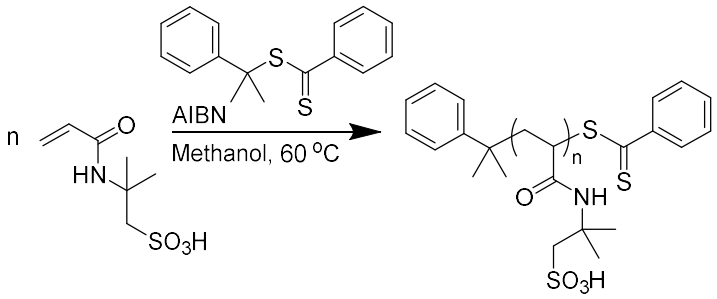

Scheme 2-3: RAFT polymerisation of AMPS® in methanol.[104]

In another example, McCormick and co-workers reported the polymerisation of sodium 4-styrenesulfonate in aqueous solution at 70 °C using 4-cyanopentanoic acid, a dithiobenzoate RAFT agent, and 4,4′-azobis(4-cyanopentanoic acid) (ACVA / V-501) as the initiator.[94] Full monomer conversion was obtained within 8 hours and monomodal SEC chromatograms were obtained depicting dispersities as low as 1.25.

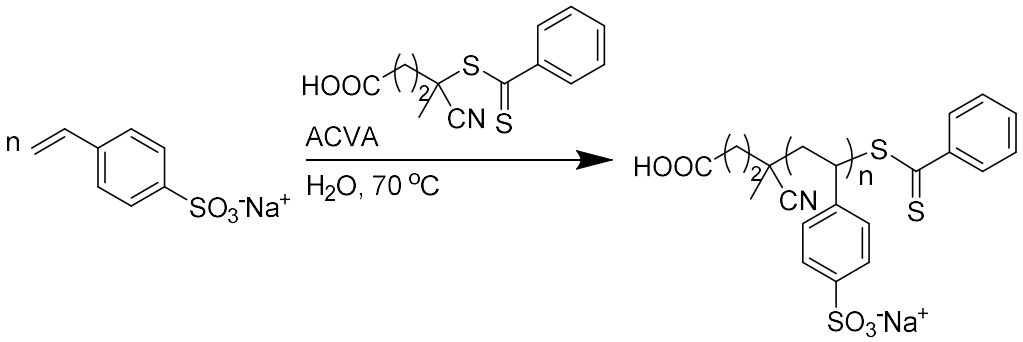

Scheme 2-4: RAFT Polymerisation of sodium styrene sulfonate monomer.[94]

More recently McCormick *et al.* focused their research on the aqueous RAFT polymerisation of AMPS(Na) (AMPS® with NaOH in water) still using 4-cyanopentanoic acid dithiobenzoate as CTA and ACVA as the initiator ($[CTA]_0/[I]_0$ = 5).[58,105-107] They first reported the polymerisation of AMPS(Na) in aqueous solution at 70 °C and pH 9.5 (**Scheme 2-5**).[105,106] Polymers with low dispersity were obtained ($Đ$ < 1.3) and a linear increase of both the molecular weight and first order kinetics with time was observed. However, an induction time of about 1 hour was observed, likely due to the slow rates of reinitiation by the radical created from the R-group of the

CTA. Additionally, the monomer conversion never exceeded 90 %. Finally, an increase in the dispersity was noticeable after 30 % monomer conversion.[105]

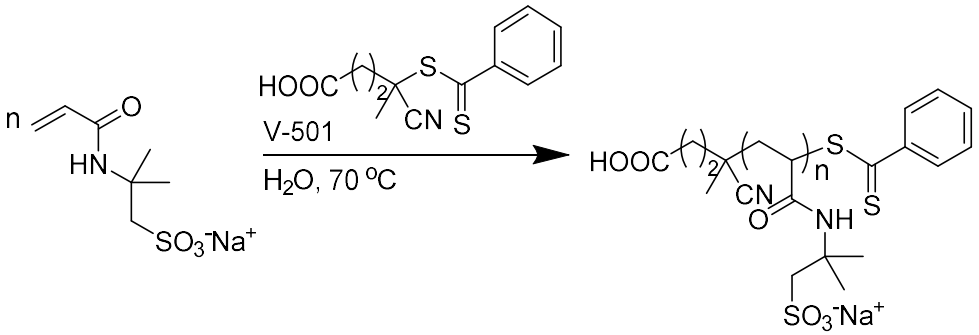

Scheme 2-5: RAFT polymerisation of AMPS(Na) in water using a dithiobenzoate CTA.[58,105-107]

In 2004, McCormick *et al.* reported a study on the potential hydrolysis of a CTA (i.e. dithioesther) at 70 °C and that was shown to be a critical parameter on the polymerisation process, especially at pH higher than 7.[58] They observed an increase of dead chain concentration at higher pH, posing a problem for the synthesis of complex architectures (e.g. diblock synthesis). This explained why in 2010, the RAFT polymerisation of AMPS® in aqueous solution was carried out at lower pH (6.5) and stopped at monomer conversion of approximately 30 % (i.e. to avoid the loss of molecular weight control, $Đ \sim 1.2$).[107] Finally, this AMPS® homopolymer was used as macroCTA to be further chain extended with *N*-acryloyl-L-alanine (AAL). The chain extension was shown to be successful with the observation of a monomodal SEC peak shifted to higher molecular weight than the AMPS® homopolymer used, thus suggesting a good reinitiation of the macroCTA with observed dispersities being lower than 1.3.

The main disadvantage when using aqueous RAFT polymerisation is mainly linked to the loss of chain end fidelity connected to the potential hydrolysis of the chain transfer agents. This hydrolysis has been shown to be not only pH- and temperature- dependent but also CTA-dependent.[58] Indeed, it has been shown in the literature that dithiobenzoates were more prone to hydrolysis than trithiocarbonates and that the rate of hydrolysis increased at pH higher than 7 and temperatures higher than 50 °C.[66,108-110]

2.2.2 RAFT Polymerisation Using DDMAT

2-(Dodecylthiocarbonothioylthio)-2-methylpropionic acid (DDMAT, **Figure 2-2** *left*) is a commercially available trithiocarbonate chain transfer agent synthesised on tonne-scale by the Lubrizol corporation (**Scheme 2-6**).[111]

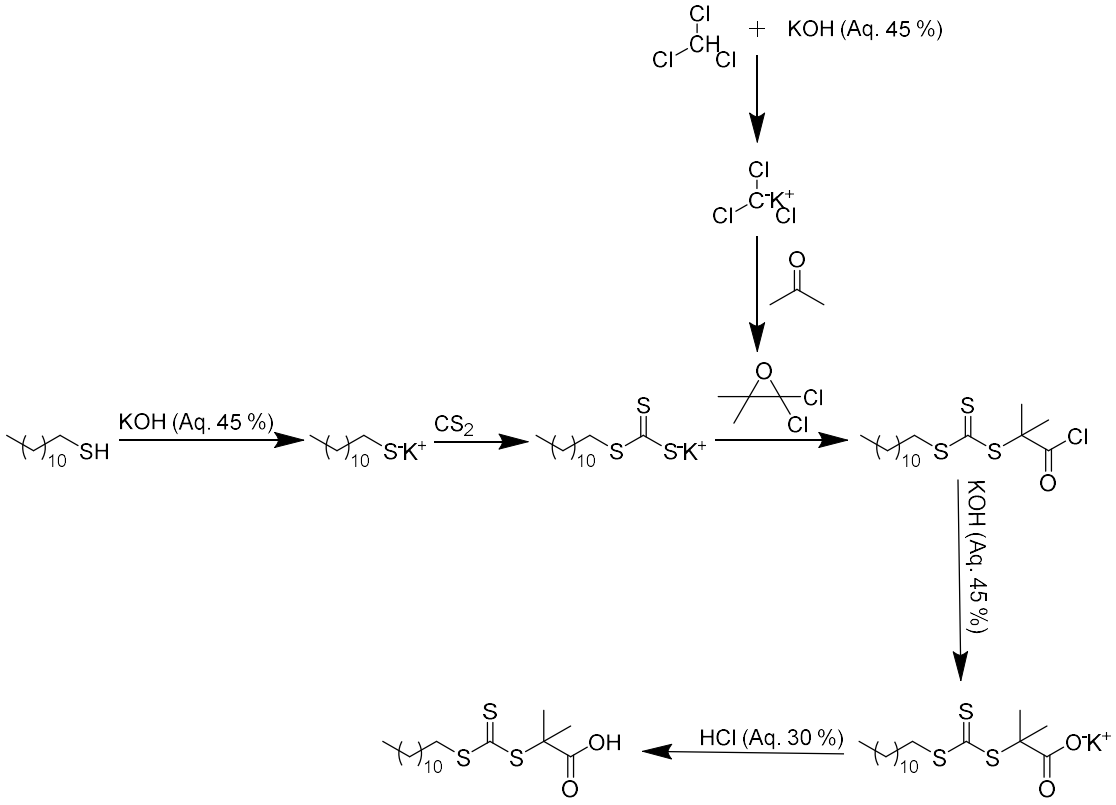

Scheme 2-6: Multistep synthesis of the trithiocarbonate DDMAT patented by the Lubrizol Corporation.[112]

This CTA bears a carboxylic acid group which makes it a viable candidate for use in aqueous solutions, specifically in basic conditions when the carboxylic acid group is potentially deprotonated. However, the use of this CTA for the RAFT polymerisation of different monomers has only been reported either in organic solvents or in bulk polymerisation. For example, Stoffelbach *et al.* reported the RAFT polymerisation of styrene (S) and *n*-butyl methacrylate (BMA) in bulk polymerisation using DDMAT.[113] The polymerisation of styrene using DDMAT was showing control over molecular weight with dispersities below 1.2, however, the monomer conversion was only about 30 % after 20 hours. Conversely, when BMA was used, high dispersities were obtained (> 1.5) even at lower monomer conversions (< 50 %).

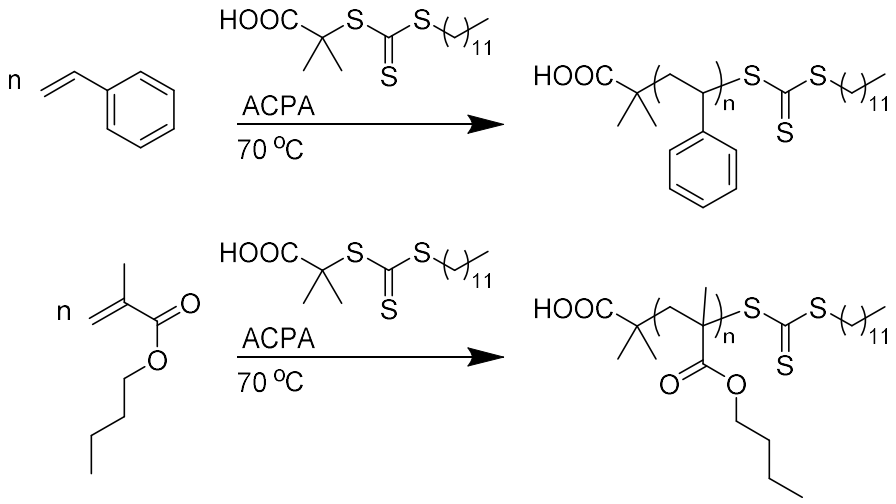

Scheme 2-7: RAFT polymerisation in bulk process using either styrene or *n*-butyl methacrylate.[113]

DDMAT has also been used to mediate the polymerisation of *N*,*N*-dimethylacrylamide (DMA) in 1,4-dioxane with ACPA as the initiator at 80 °C.[114-116] Narrow ($Đ \leq 1.2$) and monomodal SEC chromatograms were observed with full monomer conversion being reached within 1 hour.

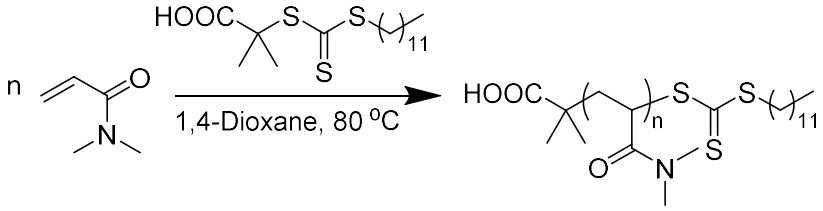

Scheme 2-8: DMA RAFT polymerisation with DDMAT in 1,4-Dioxane.[114]

DDMAT was also shown to successfully mediate the polymerisation of acrylic acid in 1,4-dioxane and polymerisations were stopped at low conversion to retain chain-end fidelity (i.e. 60 %).[117] This PAA-DDMAT was shown to form aggregates in aqueous solution due to the amphiphilic character of this newly synthesised macroCTA. They further chain extended this macroCTA with butyl acrylate yielding stable particles with respect to both colloidal stability and macromolecular structure (**Scheme 2-9**).

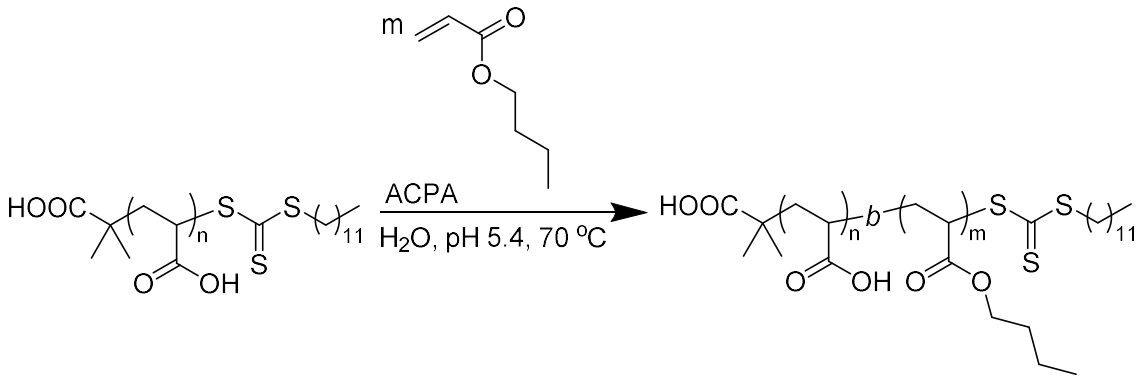

Scheme 2-9: RAFT emulsion polymerisation using PAA-DDMAT macroCTA.[117]

2.2.3 Project Approach

The primary focus of this project is to polymerise AMPS®2405 monomer with the chain-transfer agent DDMAT (**Scheme 2-10**), in aqueous solution using RAFT polymerisation; the overall goal being to synthesise polymers suitable for a wide range of applications from oil recovery to medical usage. DDMAT is first the chain transfer agent of choice due to its potential solubility in water and availability on a large scale.

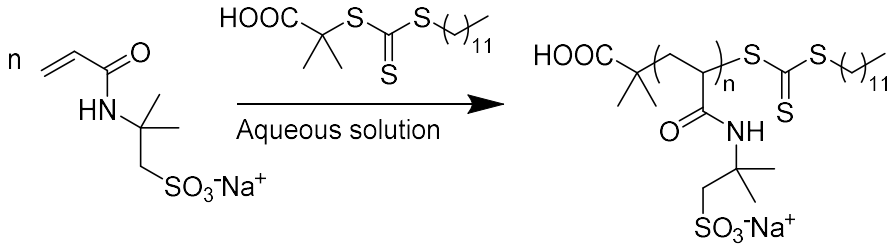

Scheme 2-10: First aim for **CHAPTER 2**.

The initial approach will investigate the RAFT polymerisation of a neutral, water-soluble acrylamide monomer, namely *N*,*N*-dimethylacrylamide. The polymerisation of DMA is known to be controlled by the chain transfer agent DDMAT and similar conditions to that in the literature are used.[56] BDMAT, another chain-transfer agent with a shorter alkyl chain (Z-group) compared to DDMAT, (**Figure 2-2**), will also be used in this study for comparison. Similar control over the polymerisation is expected with two chain transfer agents having the same reinitiating group (R-group) and a similar stabilising group (Z-group, C12 versus C4).

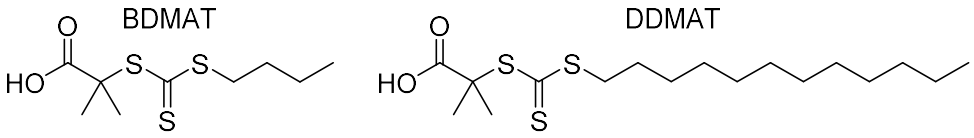

Figure 2-2: Chain-transfer agents used in the focus of this study.

Subsequently, the above conditions will be used to direct the initial RAFT polymerisations of AMPS®2405, with further research being dedicated to the synthesis of well-defined homopolymers of AMPS®2405, with a wide-range of molecular weights. Finally, others acrylamide monomers such as *N*-hydroxyethyl acrylamide (HEAm) and 4-acryloylmorpholine (NAM) will be polymerised with either DDMAT

or BDMAT as the CTA. Thus allowing to evaluate the universality of these conditions for the aqueous RAFT polymerisation of acrylamides (**Scheme 2-11**).

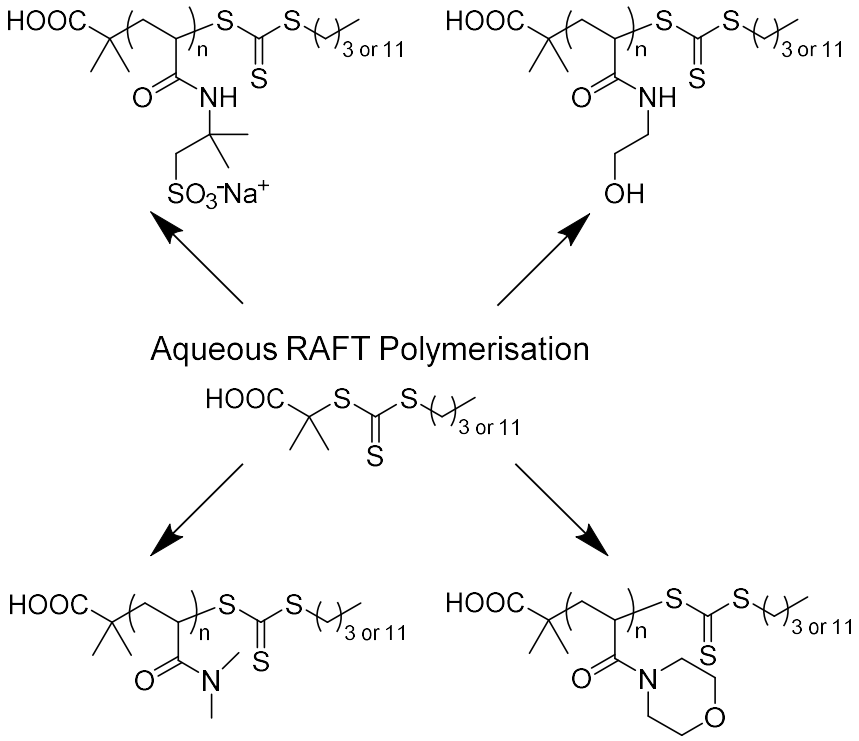

Scheme 2-11: Second aim for **CHAPTER 2**.

2.3 Results and Discussions

It was anticipated that DDMAT would pose a challenge for the RAFT polymerisation in aqueous solution due to the hydrophobic nature of the long alkyl chain, and the known tendency of DDMAT to aggregate in water.[113] Consequently, it was decided to compare the control of polymerisation in aqueous solution with a CTA with a shorter Z-group; using BDMAT. This BDMAT chain transfer agent, was synthesised according to previous literature, as shown in **Scheme 2-12**.[118]

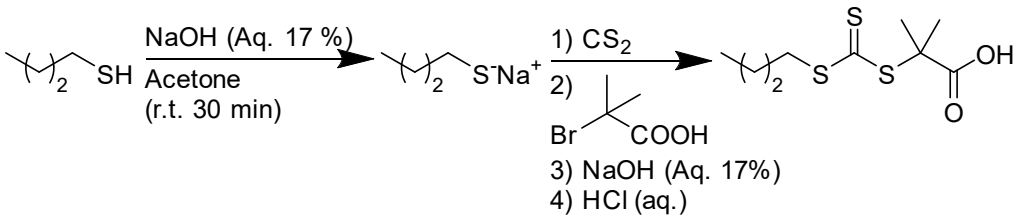

Scheme 2-12: Synthesis of BDMAT chain-transfer agent.

These chain transfer agents were particularly useful in monitoring polymerisation conversion by ^{1}H NMR spectroscopy, using the relative integration of the CTA - $CH_2C\underline{H}_3$ peak at low ppm (δ 0.90ppm) and the vinyl proton of the monomers used (**Figure 2-3**).

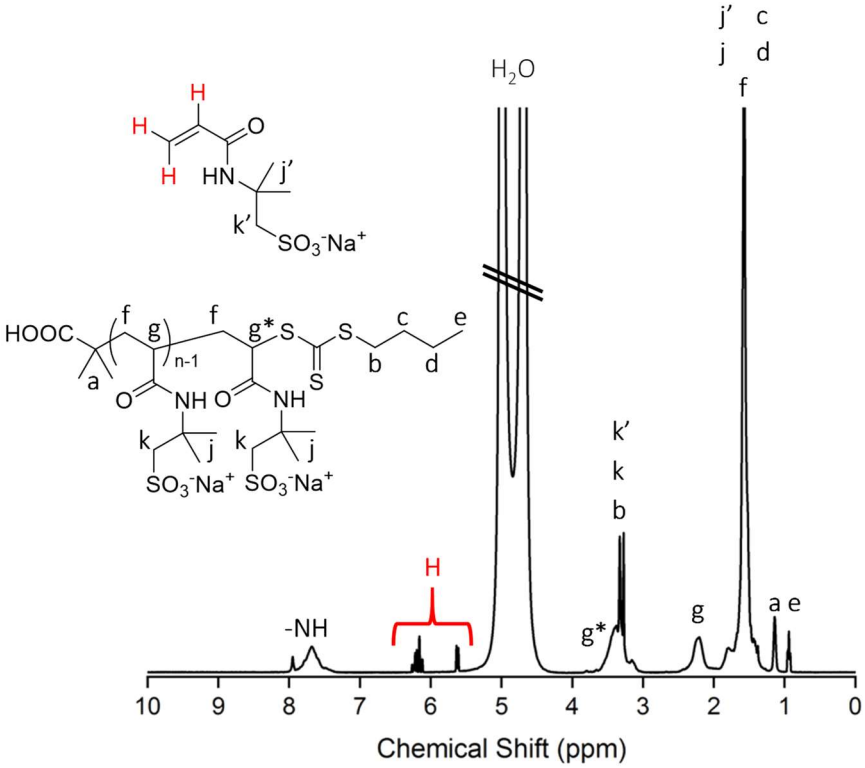

Figure 2-3: ^{1}H NMR spectrum of PAMPS with BDMAT as internal reference in D_2O.

2.3.1 DMA Polymerisation in Water with DDMAT and BDMAT

Initially a range of homopolymers using DMA were prepared by RAFT polymerisation in aqueous solution using either DDMAT or BDMAT for optimisation and comparison of the polymer synthesis changing the Z-group. McCormick *et al.* polymerised DMA in aqueous solution using a similar R-group to our CTAs, however, the Z-group was composed of a C2 alkyl chain. They obtained a well-defined PDMA homopolymer ($Đ$ = 1.07) at 25 °C.[119] Another advantage of using DMA is the solubility of the monomer and polymer in organic solvent. Indeed, Charleux *et al.* polymerised DMA in 1,4-dioxane using DDMAT at 80 °C. While the polymerisation was very well controlled ($Đ$ < 1.1) they did not push the monomer conversion over 50 % and further purifications by precipitation were required.[114]

Table 2-1: Polymerisation data for the RAFT polymerisation of DMA in various solvents.[a]

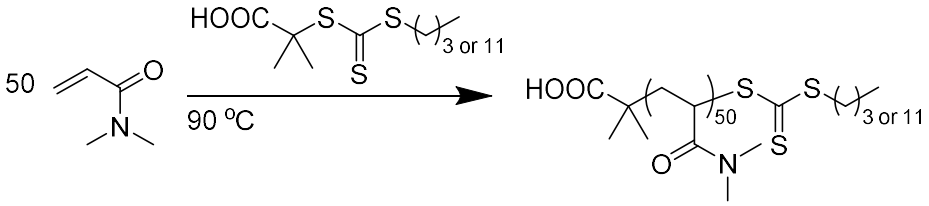

Polymer	Solvent	CTA	pH[b]		Solubility of CTA (°C)		Conv. (%)[c]	$M_{n,th}$ (g/mol)[d]	$M_{n,SEC}$ (g/mol)[e]	$Đ$[e]
			pH_A	pH_B	25	90				
1	Toluene	DDMAT	-	-	✓	✓	96	5,200	6,700	1.08
2	Water	DDMAT	7.9	5.2	×	✓	> 99	5,500	9,400	1.24
3	PB	DDMAT	7.1	6.1	×	✓	> 99	5,400	8,000	1.25
4	Water	BDMAT	4.7	5.1	✓	✓	98	5,000	7,000	1.06
5	PB	BDMAT	6.8	6.4	✓	✓	98	5,000	7,600	1.06

[a] Polymerisations were conducted at 90 °C in toluene, water or phosphate buffer solution ($[DMA]_0$:$[CTA]_0$:$[I]_0$ = 50:1:0.08, $[DMA]_0$ = 1.5 M) with V-40 or VA-086 as the initiator, respectively in toluene and aqueous solution; [b] pH was measured at the start of the reaction before degassing (pH_A) and at the end of the reaction (pH_B) both at room temperature; [c] Conversions were determined by ^{1}H NMR spectroscopy, using **Equation 1**; [d] Theoretical M_n values were calculated using **Equation 2**; [e] Experimental M_n and $Đ$ values were determined by size-exclusion chromatography in DMF with 5 mM NH_4BF_4 using a conventional calibration obtained with PMMA standards.
× not soluble; ×✓ partially soluble; ✓ soluble.

Here, the polymerisation of DMA mediated either by DDMAT or BDMAT was investigated in aqueous solution at 90 °C with VA-086 as the source of initiator. The polymerisation was performed either in deionised water or using a phosphate-buffered saline tablet (**Table 2-1**). The latter was used in order to control the pH and keep it constant at around 6.5, as too basic conditions have been shown to drastically affect

polymerisation control due to the potential CTA hydrolysis.[58,59,65] When DMA was polymerised using BDMAT either in water or PBS, well-defined homopolymers were obtained within 2 hours (**Figure 2-5 – A**) evidenced by narrow molecular weight distributions (**Figure 2-4**). Both conditions yielded 98 % monomer conversion, $Đ$ = 1.06 and molecular weight of about 7,000 g/mol in water and 7,600 in PBS (**Table 2-1**, **Polymers 4** and **5**).

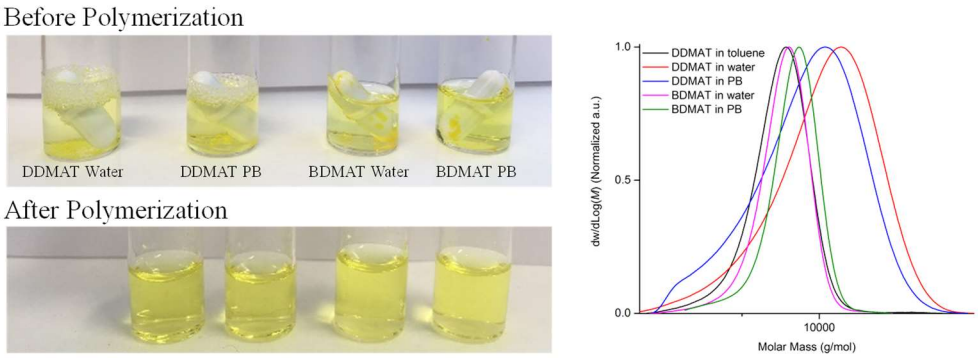

Figure 2-4: On the left; pictures showing the CTA solubility in reaction media; on the right corresponding DMF SEC molecular weight distributions of PDMA prepared by RAFT polymerisation in different solvents using either DDMAT or BDMAT.

However, when DDMAT was used to polymerise DMA either in deionised water or in PBS, broader chromatograms were observed (**Figure 2-4**, **Polymer 2** and **3**) but still obtaining relatively low dispersities ($Đ$ < 1.3). This has been attributed to the lower solubility of the chain transfer agent in water which has been shown to be a critical parameter for the RAFT process (C12 versus C4), (**Pictures Figure 2-4**).[56] The molecular weight obtained with DDMAT (9,400 g/mol) was slightly higher than when BDMAT (7,000 g/mol) was first used in deionised water. To further prove that the challenge was linked to the CTA solubility in water and not linked to the reactivity between monomer and CTA, the polymerisation was carried out in an organic solvent (**Table 2-1**, **Polymer 1**), with toluene being chosen due to its low polarity and high boiling point (110.6 °C). Both DMA and DDMAT were observed to be soluble in toluene, however, V-40 initiator was used instead of VA-086 as VA-086 is only soluble in highly polar solvents (e.g. water or methanol). As V-40 and VA086 both have a similar half-life temperature (86 °C for VA-086 against 88 °C for V-40), then similar initiator quantity would be created / consumed in two hours, and similar kinetics and livingness obtained (**Equation 4**). Well-defined polymers were obtained

with DDMAT when the polymerisation was conducted in toluene instead of water with $M_{n,SEC}$ = 6,700 g/mol and $Đ$ = 1.08, confirming the solubility issue of DDMAT in water compared to when used in toluene. The kinetic study of DMA polymerisation in deionised water using either DDMAT or BDMAT demonstrate a linear first-order kinetics behaviour (**Figure 2-5 – B)**, however, it can be noted a slightly higher apparent rate of polymerisation with DDMAT (k_p^{app} = 14.6x10^{-4} s^{-1}) compared to BDMAT (k_p^{app} = 9.3x10^{-4} s^{-1}). This could explain the lower control over the polymerisation observed with DDMAT.[38] Additionally, the SEC molecular weight distributions were monomodals and shown to be shifted towards higher molecular weight when the monomer conversion was increased (**Figure 2-5 – C** and **D**).

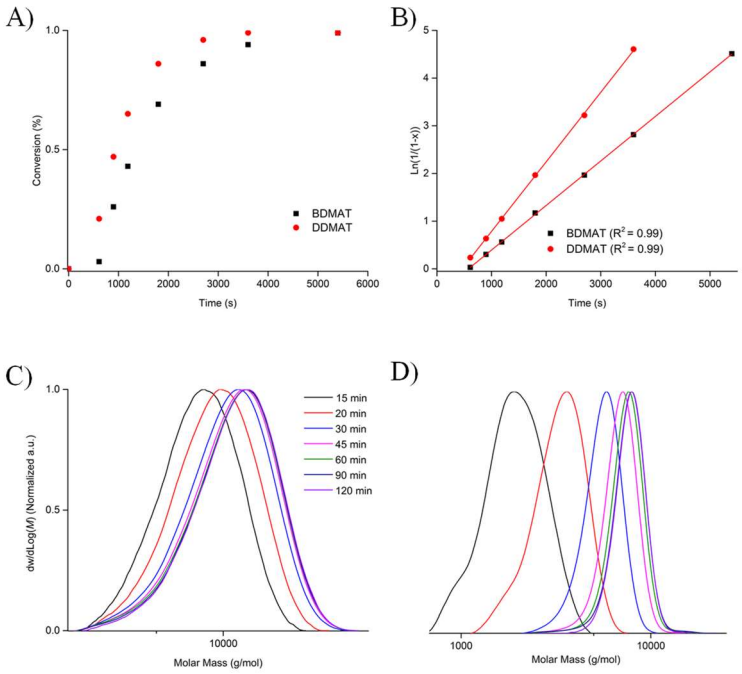

Figure 2-5: Kinetic data for the RAFT polymerisation of DMA using BDMAT or DDMAT targeting a DP 50 in water.

A) Conversion versus time; B) Pseudo first order (Ln([DMA]$_0$/[DMA])) plot versus time; C) Molecular weight distributions showing the evolution (DMF SEC) with time of molecular weight using DDMAT; D) Molecular weight distributions showing the evolution (DMF SEC) with time of molecular weight using BDMAT.

Using DDMAT in deionised water various degrees of polymerisations (DP) ranging from 20 to 200 were targeted. The targeted DP was increased by increasing the ratio of monomer to CTA but keeping the monomer concentration at 1.5 M and the initiator concentration at 2.5x10^{-3} M (**Table 2-2**).

Table 2-2: RAFT polymerisation of DMA using DDMAT in water increasing the DP.[a]

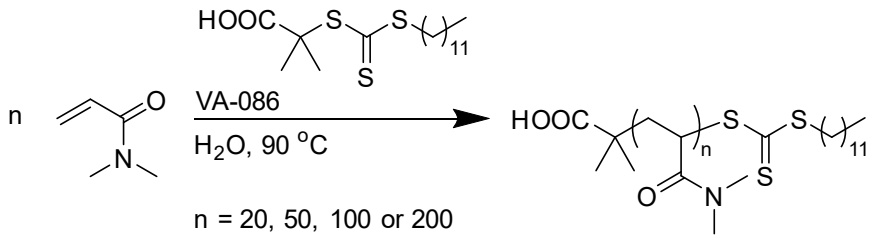

Polymer	DP	$[DMA]_0:[CTA]_0:[I]_0$ (mol/L)	L (%)[b]	Conv. (%)[c]	$M_{n,th}$ (g/mol)[d]	$M_{n,SEC}$ (g/mol)[e]	$Đ$[e]
6	20	20:1:0.033	99.3	> 99	2,300	4,700	1.33
2	50	50:1:0.083	98.4	> 99	5,200	9,900	1.21
7	100	100:1:0.167	96.7	> 99	10,800	15,100	1.17
8	200	200:1:0.333	94.1	> 99	19,100	24,500	1.13

[a] Polymerisations were conducted at 90 °C in water ($[DMA]_0$ = 1.5 M) with VA-086 as the initiator, full conversions were obtained after 2 hours; [b] Theoretical livingness were calculated using **Equation 4**; [c] Conversions were determined by ^{1}H NMR spectroscopy, using **Equation 1**; [d] Theoretical M_n values were calculated using **Equation 2**; [e] Experimental M_n and $Đ$ values were determined by size-exclusion chromatography in DMF with 5 mM NH_4BF_4 using a conventional calibration obtained with PMMA standards.

When the targeted DP was increased (e.g. 20 *versus* 200) a clear shift towards higher molecular weight could be observed (**Figure 2-6 – A**) from the molecular weight distributions. From **Figure 2-6 – B** it can be observed that there is a linear increase of molecular weights determined by SEC when DPs were increased and concurrently a decrease of dispersity from 1.33 (for a DP = 20) to (1.13 for a DP = 200). The better control over the polymerisation obtained when higher DPs were targeted could be explained by a decrease of CTA concentration and consequently an increase of its solubility.

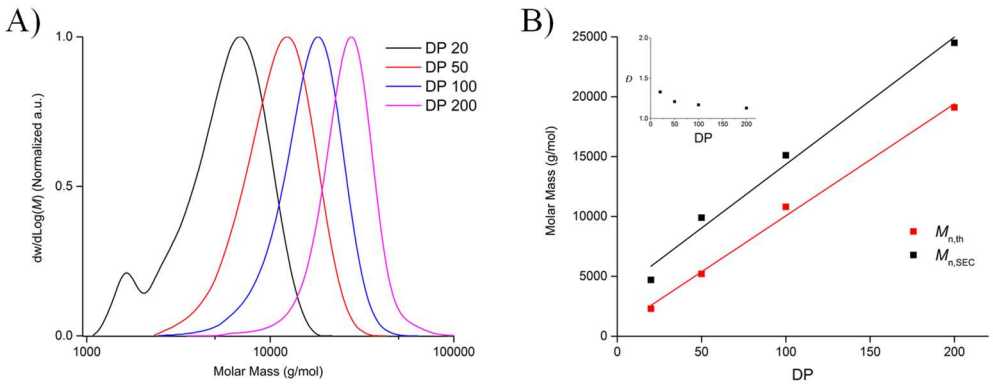

Figure 2-6: PDMA RAFT polymerisation targeting DPs from 20 to 200 (Conv. > 99 %, $[DMA]_0$ = 1.5 M).

A) DMF SEC molecular weight distributions; B) Evolution of molecular weight and dispersity.

The **Polymer 2** (L = 98.4 %) was further chain extended with DMA in order to evaluate the potential use of the system for block copolymer synthesis (**Scheme 2-13**). The **Polymer 9** was synthesised by further adding monomer (DMA) and initiator into the vial already containing **Polymer 2**.

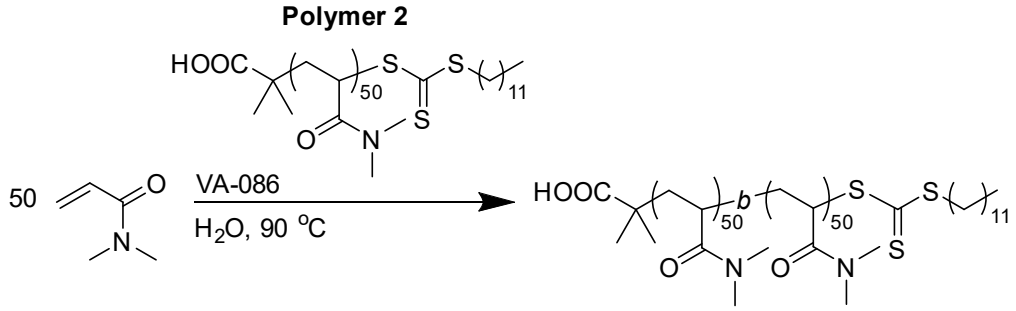

9

Conv.[a] > 99 %
$M_{n,th}$[b] = 10,000 g/mol
$M_{n,SEC}$[c] = 14,100 g/mol
$Đ$[c] = 1.22

Scheme 2-13: Chain extension of PDMA with DMA in water using DDMAT.

[a] Conversion were determined by ^{1}H NMR spectroscopy, using **Equation 1**; [b] Theoretical M_n values were calculated using **Equation 2**; [c] Experimental M_n and $Đ$ values were determined by size-exclusion chromatography in DMF with 5 mM NH_4BF_4 using a conventional calibration obtained with PMMA standards.

The second block was obtained within 2 hours with full monomer conversion and a clear shift towards higher molecular weight was oberved by SEC. A monomodal chromatogram was obtained which is an indication of an efficient reinitiation of the macroCTA (**Polymer 2**, **Figure 2-7**) by DMA itself.

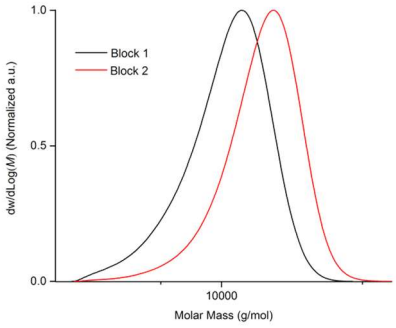

Figure 2-7: DMF SEC molecular weight distribution showing the DMA macroCTA and the corresponding diblock.

2.3.2 AMPS®2405 Polymerisation in Water with DDMAT and BDMAT

The same conditions used to polymerise DMA were then applied to AMPS®2405 (**Table 2-3**). When AMPS®2405 was polymerised from BDMAT either in water or PBS, well-defined homopolymers were obtained within 2 hours ($M_{n,SEC}$ = 11,100 g/mol and $Đ$ = 1.19) with no differences observed using either water or PBS (**Figure 2-8**, **Table 2-3**, **Polymer 12** and **13**).

Table 2-3: Polymerisation data for the RAFT Polymerisation of AMPS®2405 in water or phosphate buffer solution.[a]

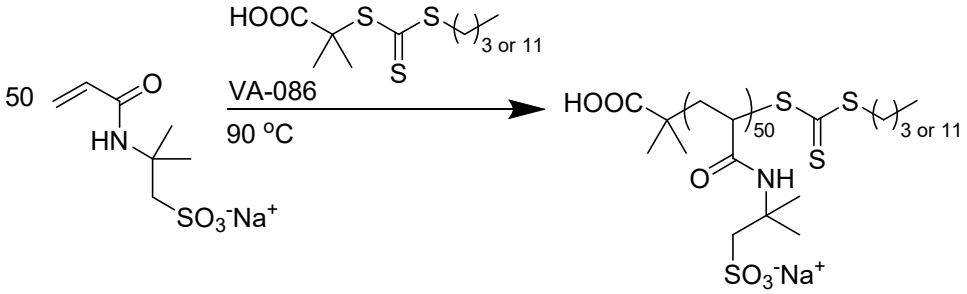

Polymer	Solvent	CTA	pH[b]		Solubility of CTA (°C)		Conv. (%)[c]	$M_{n,th}$ (g/mol)[d]	$M_{n,SEC}$ (g/mol)[e]	$Đ$[e]
			pH_A	pH_B	25	90				
10	Water	DDMAT	6.5	4.8	×	×	> 99	12,100	64,700	2.45
11	PB	DDMAT	6.5	5.7	×	✓	> 99	12,100	25,500	2.20
12	Water	BDMAT	4.2	4.5	×	✓	> 99	11,500	11,100	1.19
13	PB	BDMAT	5.2	5.3	×✓	✓	> 99	11,500	11,100	1.19

[a] Polymerisations were conducted at 90 °C in water or phosphate buffer solution ($[AMPS®2405]_0$:$[CTA]_0$:$[VA\text{-}086]_0$ = 50:1:0.08, $[AMPS®2405]_0$ = 1.5 M); [b] pH was measured at the start of the reaction before degassing (pH_A) and at the end of the reaction (pH_B) both at room temperature; [c] Conversions were determined by ^{1}H NMR spectroscopy, using **Equation 1**; [d] Theoretical M_n values were calculated using **Equation 2**; [e] Experimental M_n and $Đ$ values were determined by size-exclusion chromatography in 20 % MeOH / 80 % 0.1 $NaNO_3$ in milli-Q water eluent using a conventional calibration obtained with PEG/PEO standards. × not soluble; ×✓ partially soluble; ✓ soluble.

However, when AMPS®2405 was polymerised from DDMAT there was little control of the polymerisation, with broader distributions obtained than when BDMAT was used (**Figure 2-8**, **Polymer 10** and **11**). Overall, the control was slightly better in PBS than in water with lower molecular weight obtained (Water: $M_{n,SEC}$ = 64,700 g/mol and $Đ$ = 2.45; PBS: $M_{n,SEC}$ = 25,500 g/mol and $Đ$ = 2.20) but dispersities were well above 1.5. The poorer control obtained can be explained by the low solubility of DDMAT (**Pictures Figure 2-8**) in the presence of AMPS®2405 monomer at the start of the polymerisation. It was important to note that even though BDMAT was not entirely soluble at the start of the reaction it quickly solubilised (i.e. < 5 minutes) after

heating the solution over its melting point (63 °C). The solubilisation of DDMAT by heating was observed to be longer (> 10 minutes).[68]

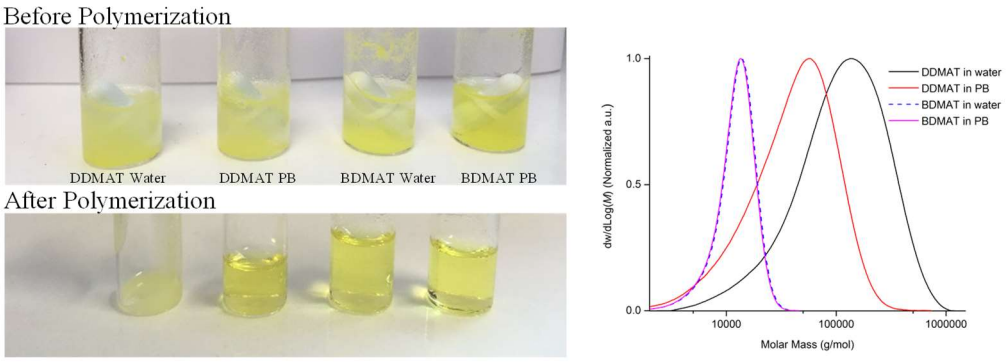

Figure 2-8: On the left, pictures showing CTA solubility in reaction media; on the right, the corresponding aqueous SEC molecular weight distributions of PAMPS prepared by RAFT polymerisation using either DDMAT or BDMAT.

The first attempt to optimise the reaction polymerisation conditions was by increasing the CTA solubility via the addition of sodium hydroxide (**Table 2-4**) in order to deprotonate the carboxylic group of the CTA (R-group) rendering the CTA negatively charged.[106]

Table 2-4: Polymerisation data for the RAFT Polymerisation of AMPS®2405 in aqueous solution adding either 0.5 or 1 equivalent of base per DDMAT.[a]

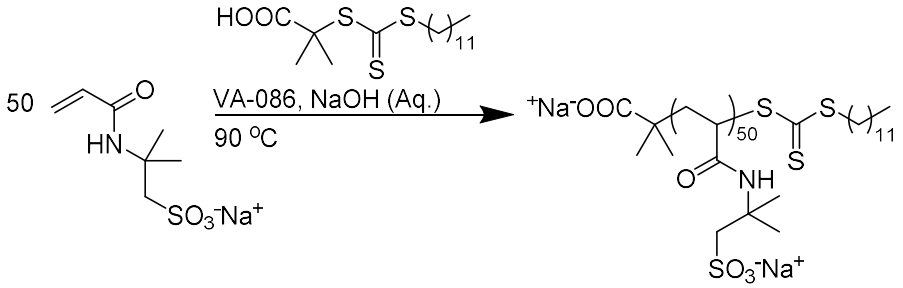

Polymer	Solvent	NaOH[a]	pH[b]		Solubility of CTA (°C)		Conv. (%)[c]	$M_{n,th}$ (g/mol)[d]	$M_{n,SEC}$ (g/mol)[e]	$Đ$[e]
			pH_A	pH_B	25	90				
14	Water	0.5	6.9	6.3	×	✓	> 99	12,000	23,700	2.17
15	PB	0.5	6.6	6.4	×	✓	> 99	11,900	19,500	1.92
16	Water	1	10.6	7.9	×	✓	> 99	12,100	16,700	1.80
17	PB	1	8.8	7.2	×	✓	> 99	12,000	17,800	1.81

[a] Polymerisations were conducted at 90 °C in water or phosphate buffer solution ($[AMPS®2405]_0$:$[DDMAT]_0$:$[VA\text{-}086]_0$ = 50:1:0.08, $[AMPS®2405]_0$ = 1.5 M) adding either 0.5 or 1 equivalent of NaOH per CTA; [b] pH was measured at the start of the reaction before degassing (pH_A) and at the end of the reaction (pH_B) both at room temperature; [c] Conversions were determined by ^{1}H NMR spectroscopy, using **Equation 1**; [d] Theoretical M_n values were calculated using **Equation 2**; [e] Experimental M_n and $Đ$ values were determined by size-exclusion chromatography in 20 % MeOH / 80 % 0.1 $NaNO_3$ in milli-Q water eluent using a conventional calibration obtained with PEG/PEO standards.
× not soluble; ×✓ partially soluble; ✓ soluble.

Two different ratios of NaOH per CTA were tried, using 1 or 0.5 equivalents, both in water and PBS (**Table 2-4**). When the quantity of NaOH was increased from 0 to 0.5 and finally 1, better control was obtained (**Figure 2-9**). This was depicted by an overall decrease of molecular weights and dispersity values being likely due to a slight increase of the CTA solubility. When 1 equivalent of NaOH per CTA was used an increase of the pH could be observed (10.6 in water and 8.8 in PB) that could result in side reactions induced by CTA hydrolysis.[58] Full monomer conversion was obtained in all cases. Slightly faster kinetics was observed with DDMAT (~ 25 minutes) compared to BDMAT (35 minutes), (**Figure 2-10 – A**).

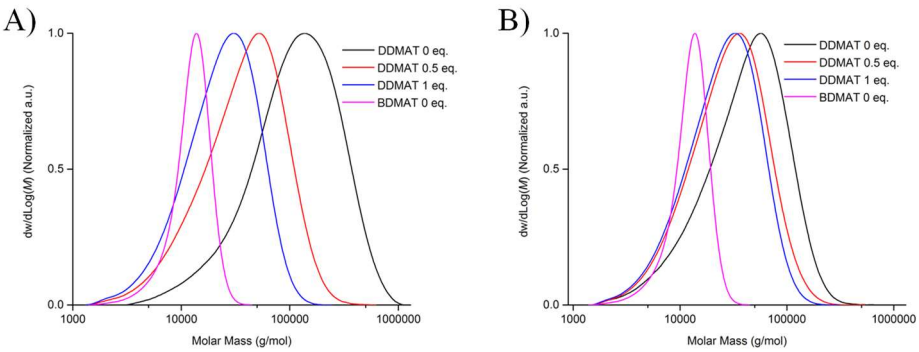

Figure 2-9: Aqueous SEC molecular weight distributions of PAMPS prepared by RAFT polymerisation using DDMAT adding 0, 0.5 and 1 equivalent of NaOH per CTA.

A) Water; B) PB solution. **Polymer 13** was used as a reference.

The kinetic plots of AMPS®2405 polymerisation using either DDMAT (**Polymer 15**) or BDMAT (**Polymer 19**) with 0.5 NaOH per CTA in PB follows a linear first order plot kinetics. However, a slight deviation of the first order plot was observed with DDMAT at higher conversion (**Figure 2-10 – B**). The deviation of the first order plot can be attributed by reaction of termination between propagating radicals.[120,121] Finally, the addition of NaOH did not show any effect on the polymerisation of AMPS®2405 using BDMAT in phosphate buffer solution (**Table S 3-1** and **Figure S 2-3**). The molecular weights obtained were similar and around 10,500 g/mol with dispersities of about 1.20 whether NaOH was added into the starting reaction media or not.

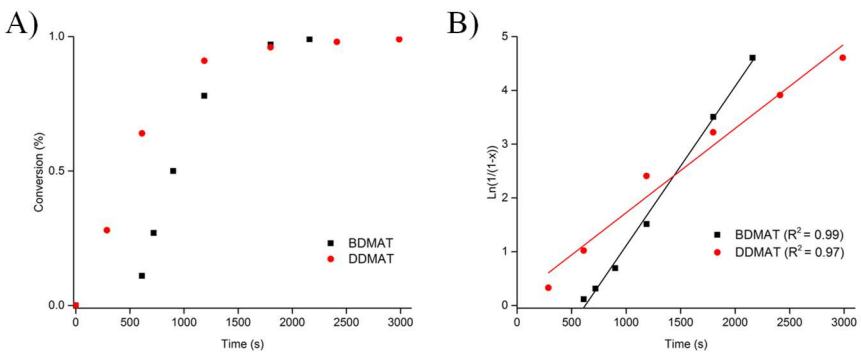

Figure 2-10: Kinetic data for the RAFT polymerisation of AMPS®2405 using BDMAT (black dot - **19**) or DDMAT (red dot- **15**) targeting a DP 50 with 0.5 equivalent of base per CTA in phosphate buffer solution.

A) Conversion versus time; B) Pseudo first order (Ln([AMPS®2405]$_0$/[AMPS®2405])) plot versus time.

The SEC molecular weight distributions (kinetics) using either DDMAT or BDMAT are shown in **Figure 2-11**. The intensity of the monomer peak ($M_{n,SEC}$ ~ 900 g/mol) gradually decreased when consumed while the peak representing the polymer appeared at higher molecular weights. Interestingly, the polymer peaks were not observed to shift towards higher molecular weights as typically observed from consumption of the monomer. This could be an artefact arising from the hydrodynamic volume of the polyelectrolyte in aqueous SEC, as its conformation is usually more extended and is dependent on electrolyte concentration and interaction with the columns.[122,123]

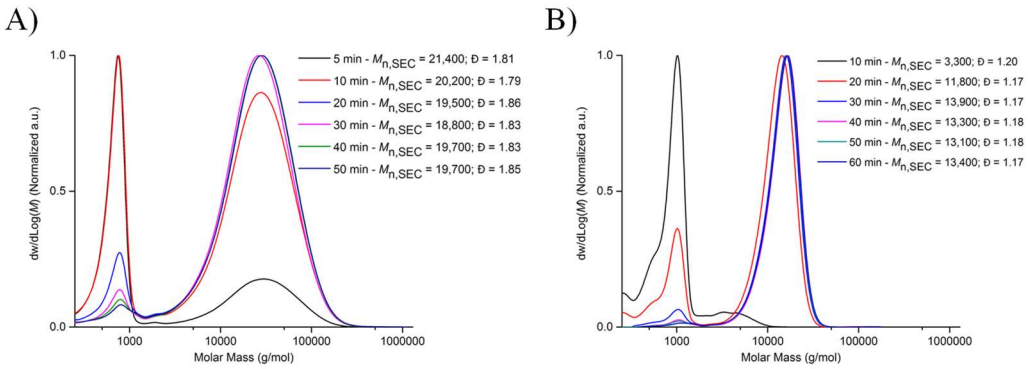

Figure 2-11: Molecular weight distributions showing the evolution (aqueous SEC) with time of molecular weight for the RAFT polymerisation of AMPS®2405 targeting a DP 50 with 0.5 NaOH / CTA in PB.

A) DDMAT (**Polymer 15**); B) BDMAT (**Polymer 19**).

In light of these results, the following experiments were undertaken in phosphate buffer solution at pH 7 (unless specified) to ensure that the pH changes do not affect the kinetics of the reactions or the solubility of the reactants (monomer, CTA and initiator).[66,67] Additionally, sodium hydroxide (0.5 equivalents per CTA) was added to the polymerisation mixture to further ensure the CTA solubility in aqueous solution. A range of homopolymers of AMPS®2405 with degrees of polymerisation varying from 10 to 400 were then prepared using BDMAT. The CTA concentration was decreased from 0.15 M to 3.7×10^{-3} M with increasing DPs (**Table 2-5**) while monomer (1.5 M) and initiator ($2.5\text{x}10^{-3}$ M) concentrations were kept constant across all reactions. Using these conditions, theoretical livingness higher than 90 % were obtained for polymerisations conditions targeting DP lower than 200 (**Table 2-5**). While the theoritical livingness for DP = 400 was found to be slightly below this threshold (L = 87.6 %)

Table 2-5: RAFT polymerisation of AMPS®2405 using BDMAT increasing the DP.[a]

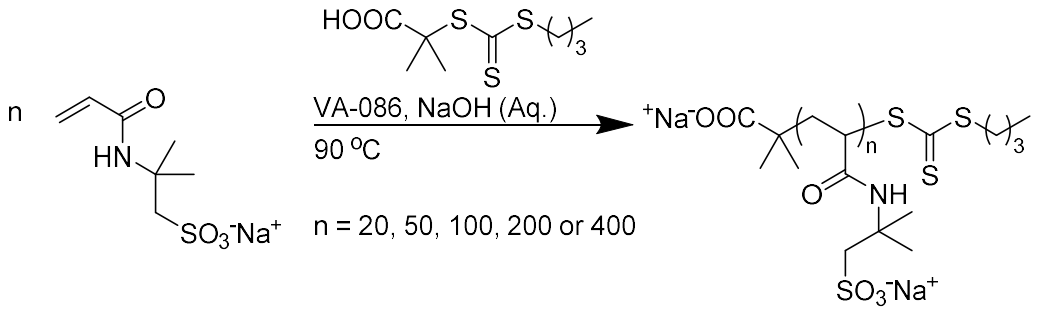

Polymer	DP	[AMPS®2405]$_0$:[BDMAT]$_0$:[I]$_0$ (mol/L)	Conv. (%)[b]	$M_{n,th}$ (g/mol)[c]	$M_{n,NMR}$ (g/mol)[d]	$M_{n,SEC}$ (g/mol)[e]	$Đ$[e]	L (%)[f]
18	20	20:1:0.033	> 99	4,800	5,200	8,100	1.10	99.3
19	50	50:1:0.083	> 99	11,600	11,400	13,000	1.11	98.4
20	100	100:1:0.167	> 99	23,000	21,900	17,600	1.16	96.8
21	200	200:1:0.333	> 99	45,600	46,900	29,900	1.25	93.4
22	400	400:1:0.667	> 99	91,000	115,000	41,300	1.51	87.6

[a] Polymerisations were conducted at 90 °C phosphate buffer solution ([AMPS®2405]$_0$ = 1.5 M) adding 0.5 equivalent of NaOH per CTA; [b] Conversions were determined by ^{1}H NMR spectroscopy, using **Equation 1**; [c] Theoretical M_n values were calculated using **Equation 2**; [d] $M_{n,NMR}$ values were calculated using **Equation 3**; [e] Experimental M_n and $Đ$ values were determined by size-exclusion chromatography in 20 % MeOH / 80 % 0.1 $NaNO_3$ in milli-Q water eluent using a conventional calibration obtained with PEG/PEO standards; [f] Livingness (L) was calculate using **Equation 4**.

Aqueous SEC (**Figure 2-12 - A**) revealed monomodal molecular weight distributions further confirmed by narrow dispersities (≤ 1.25) for polymers with DPs below 200. For the higher DP (**Table 2-5**, **Polymer 22**) a broader molecular weight distribution

(i.e. $Đ$ = 1.51) was obtained with a tail at lower molecular weights. This phenomenon is commonly observed for high molecular weight polymers and is usually referred to as the "gel effect". For higher DPs an increase of the viscosity leads to a decrease in the diffusion of polymer chains and an accumulation of radical species that can affect the kinetics of termination and propagation of the reaction, thus leading to an increased percentage of smaller polymer chains.[124] This can be further confirmed and compared to the theoritical molecular weights plotted against targeted DP on **Figure 2-12 – B**. Indeed, a deviation of the linearity can be observed after a DP of 200 likely due to a loss of polymerisation control.

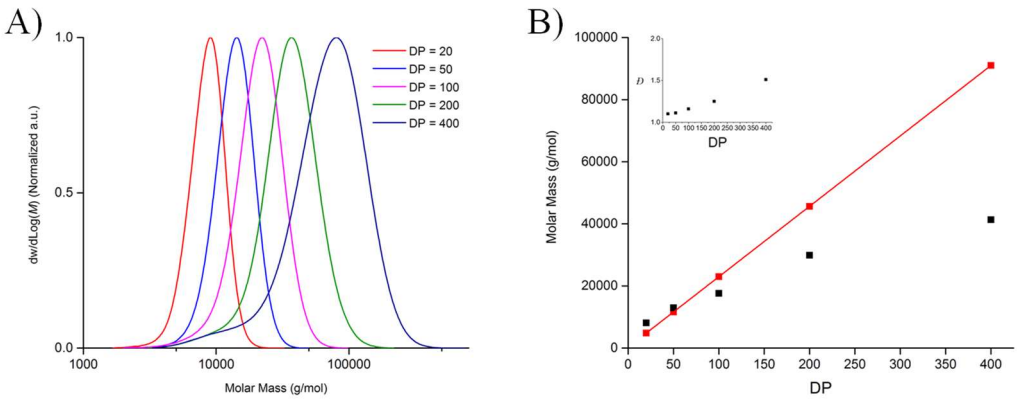

Figure 2-12: AMPS®2405 RAFT polymerisation targeting DPs from 20 to 400 using BDMAT. A) Aqueous SEC molecular weight distributions; B) Evolution of molecular weight and dispersity.

The initiator concentration was kept constant with varying DPs in order to retain similar kinetic profiles for each reaction, however, it can be observed from **Figure 2-13 - A** and **Figure S 2-5** that the monomer was consumed faster when the DP was incresed from 20 (~ 45 minutes, **Polymer 18**) to 200 (~ 15 minutes, **Polymer 21**). Additionally, when the first plot order kinetics were overlayed at increasing DP (20, 50, 100 and 200) the apparent constant of polymerisation was increased from 23.7×10^{-4} s^{-1} (DP 20) to 77.6×10^{-4} s^{-1} (DP 200) (**Figure 2-13**). The three-fold increase of the apparent constant of propagation could be explained by a decrease of the induction period observed at the early stage of the reaction. The decrease of the induction period can be correlated to a faster consumption of the CTA during the pre-equilibrium step. Indeed, when higher DPs are targeted a lower CTA concentration was required and consequently the main equilibrium could take place faster.[125]

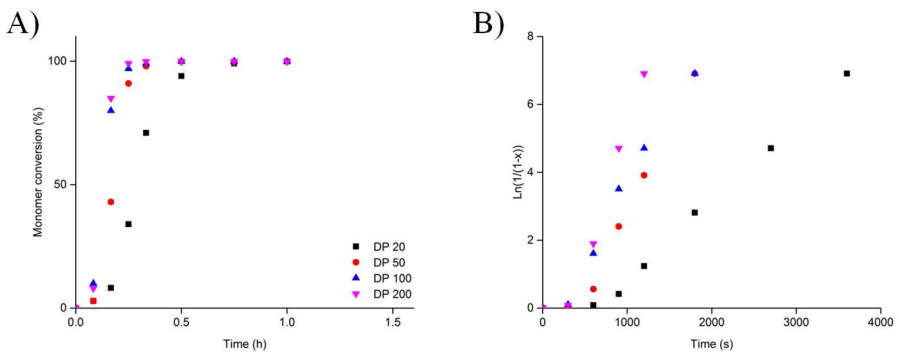

Figure 2-13: Kinetic data of AMPS®2405 RAFT polymerisation in PB solution using BDMAT targeting DPs from 20 to 200.

A) Monomer conversion versus time; B) Ln([AMPS®2405]$_0$/[AMPS®2405]) versus time.

Additionally, using UV-Vis analysis the trithiocarbonate was confirmed to be attached onto the polymer chain.[126] UV-Vis analysis in water of BDMAT, PAMPS-BDMAT and PAMPS synthesised by free radical polymerisation were compared to each other (**Figure S 2-4**). A peak characteristic of BDMAT around 309 nm could be observed for PAMPS synthesised by RAFT polymerisation while no peak at 309 nm was observed when the polymer was synthesised by free radical polymerisation. The PAMPS synthesised by free radical polymerisation was obtained using the same experimental details as for the RAFT polymerisation except that no CTA was added in the media. A transparent gel was formed within minutes, with 60 % conversion that could not be analysed by SEC.[105]

Finally, using DDMAT, different DPs were targeted (20, 50, 100 and 200), as mentioned above, the monomer and the initiator concentrations were kept constant while the CTA concentration was reduced to increase the DP targeted (**Table 2-6**). The molecular weights obtained did not increase when higher DPs were targeted supporting that the polymerisation of AMPS®2405 mediated by DDMAT CTA is not showing the characteristics of a living process (**Figure 2-14 – A** and **B**).

Table 2-6: RAFT polymerisation of AMPS®2405 using DDMAT increasing DP.[a]

Polymer	DP	[AMPS®2405]$_0$:[DDMAT]$_0$:[I]$_0$ (mol/L)	Conv. (%)[b]	CTA_c (%)[c]	$M_{n,th}$ (g/mol)[d]	$M_{n,SEC}$ (g/mol)[e]	$Đ$[e]
23	20	20:1:0.03	99	70	4,900	20,100	1.88
15	50	50:1:0.08	99	70	11,700	19,500	1.87
24	100	100:1:0.17	99	70	23,100	22,700	1.80
25	200	200:1:0.33	99	85	45,500	26,500	1.77

[a] Polymerisations were conducted at 90 °C phosphate buffer solution ([AMPS®2405]$_0$ = 1.5 M) adding 0.5 equivalent of NaOH per CTA; [b] Conversions were determined by ^{1}H NMR spectroscopy, using **Equation 1**; [c] CTA consumption was determined using **Equation 5**; [d] Theoretical M_n values were calculated using **Equation 2**; [e] Experimental M_n and $Đ$ values were determined by size-exclusion chromatography in 20 % MeOH / 80 % 0.1 $NaNO_3$ in milli-Q water eluent using a conventional calibration obtained with PEG/PEO standards.

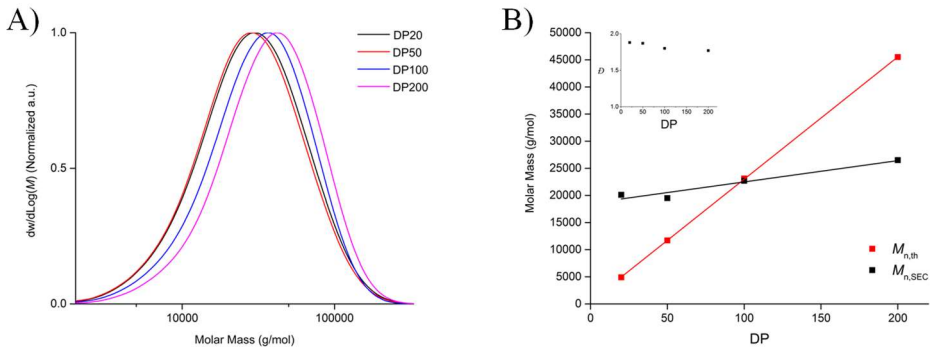

Figure 2-14: AMPS®2405 RAFT polymerisation targeting DPs from 20 to 200 using DDMAT. A) Aqueous SEC molecular weight distributions; B) Evolution of molecular weight and dispersity.

When the DP was increased from 20 to 200 a three-fold increase of the apparent rate of propagation was observed, K_p^{app} = 12.30x10^{-4} s^{-1} and 31.90x10^{-4} s^{-1} respectively. This again is explained by an apparent decrease of the induction period when the DP was increased, which was correlated to the CTA consumption (**Figure 2-15 – A, B** and **C**). Additionally, the CTA consumption never reached 100 % when DDMAT was used, thus explaining the poor control over the RAFT polymerisation (**Table 2-6**). Indeed, one of the imperative requirements of RAFT polymerisation to ensure good control over molecular weight is a rapid and full consumption of the CTA.[127]

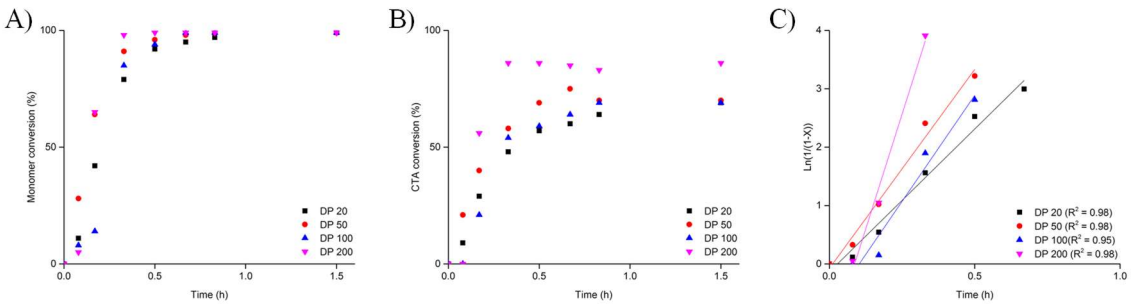

Figure 2-15: Kinetic data for the RAFT polymerisation of AMPS®2405 using DDMAT targeting DPs ranging from 20 to 200.

A) Monomer conversion versus time; B) CTA conversion versus time; C) First plot order ln([AMPS®2405]$_0$/[AMPS®2405]) versus time.

So far it has been shown that the main difference between DDMAT and BDMAT is a difference in the CTA consumption likely due to a difference of solubility in water attributed to a difference of the Z-group (C12 versus C4). To determinate the CTA efficiency, the chain transfer constant (C_{tr} = k_{tr}/k_p) was measured, a value that characterises the efficiency of a RAFT agent for a given monomer, solvent and temperature system. C_{tr} was determined using the Walling method plot, using ^{1}H NMR spectroscopy to follow consumption of CTA and monomer (**Figure 2-17**, **Equation 5**).[38,128] Using this method, the C_{tr}^{app} was estimated to be around 25 for BDMAT and 0.13 for DDMAT (**Equation 6**, **Figure 2-16**). A C_{tr}^{app} higher than 1 means that the rate of transfer is higher than the rate of monomer propagation ($k_{tr} > k_p$) and then control over the polymerisation is expected.[38]

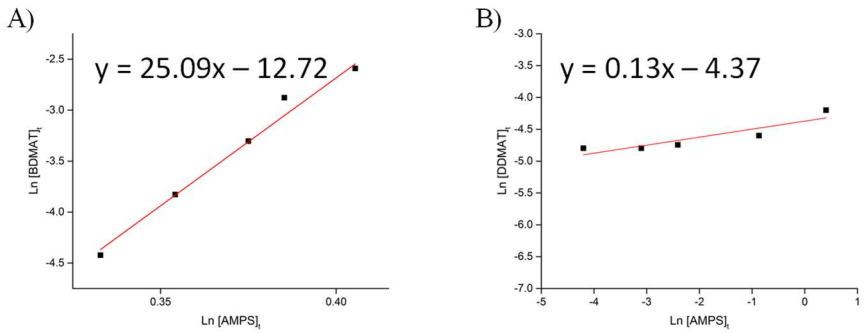

Figure 2-16: Chain transfer constant determined using the Walling plot method for the polymerisation of AMPS®2405 (DP = 20 in PB at 90 °C).

A) BDMAT **Polymer 19** (R^2 = 0.99); B) DDMAT, **Polymer 15** (R^2 = 0.87).

The high value of the chain transfer constant obtained with BDMAT here indicates that the number of monomer units incorporated into the CTA is controlled, and that the CTA was efficient under the conditions studied (i.e. control of molecular weight and low dispersity). On the contrary when DDMAT was used there was little control of the monomer incorporation into the polymeric chains as $k_p >> k_{tr}$.

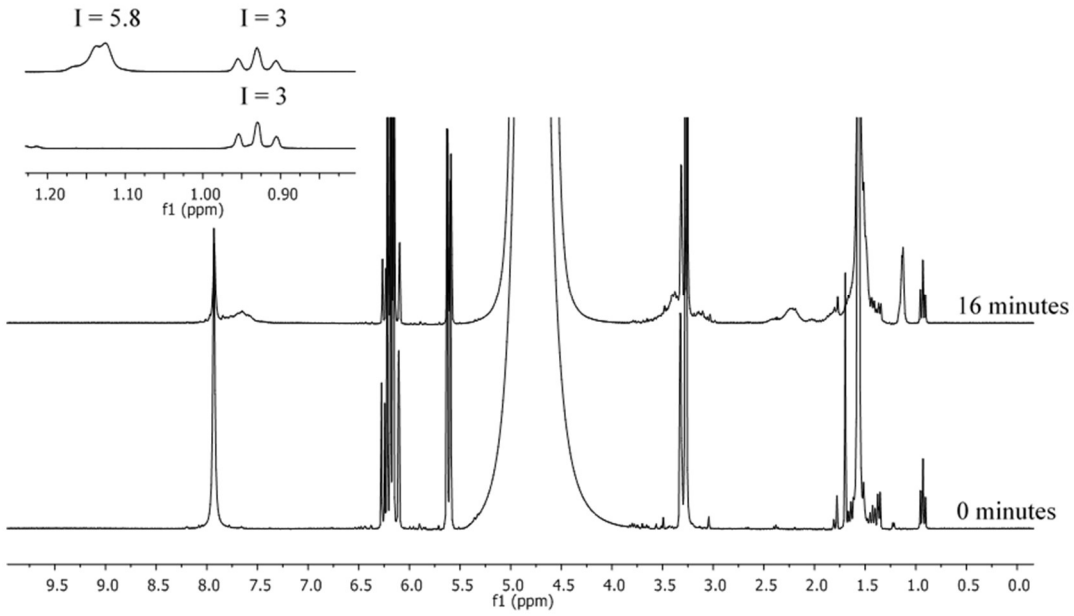

Figure 2-17: ^{1}H NMR spectra (D_2O, 300 MHz) showing the chain transfer agent and monomer consumption after 16 minutes of the polymerisation of AMPS®2405 with BDMAT in water.

2.3.3 Optimisation of AMPS®2405 Polymerisation

The poorer control obtained over the polymerisation of AMPS®2405 with DDMAT is likely due to the poor solubility of the CTA in water in the presence of AMPS®2405 ($Đ > 1.5$) when compared to the previously used DMA ($Đ < 1.5$). DDMAT was shown to be soluble in DMA monomer which is more hydrophobic than AMPS®2405 being a highly charged monomer.

Semi-batch Polymerisation

In order to increase the CTA solubility at the start of the reaction, the monomer was fed into the media containing DDMAT, NaOH, VA-086 and PBS. The monomer was therefore introduced into the system using a syringe pump.[129-131] Klumperman *et al.* have shown that by keeping the ratio $[Monomer]_0/[CTA]_0$ as low as possible it increased the probability of the CTA reacting with one monomer unit at the earliest stage possible of the RAFT polymerisation.[132] Feeding the monomer (DP = 50) over a period of time of 1 hour when BDMAT was used did not reveal any changes on polymerisation control of the newly formed polymer (**Table 2-7**, **Polymer 26**). Similarly, no improvement was observed when DDMAT was used in a starve feed process (e.g. feeding), however, higher molecular weights and dispersity were obtained compared to the batch system ($M_{n,Batch}$ = 19,600 g/mol and $M_{n,Feeding}$ = 30,300 g/mol, **Figure 2-18 – A, Polymer 27**).

Table 2-7: RAFT polymerisation of AMPS®2405 using a semi batch reactor.[a]

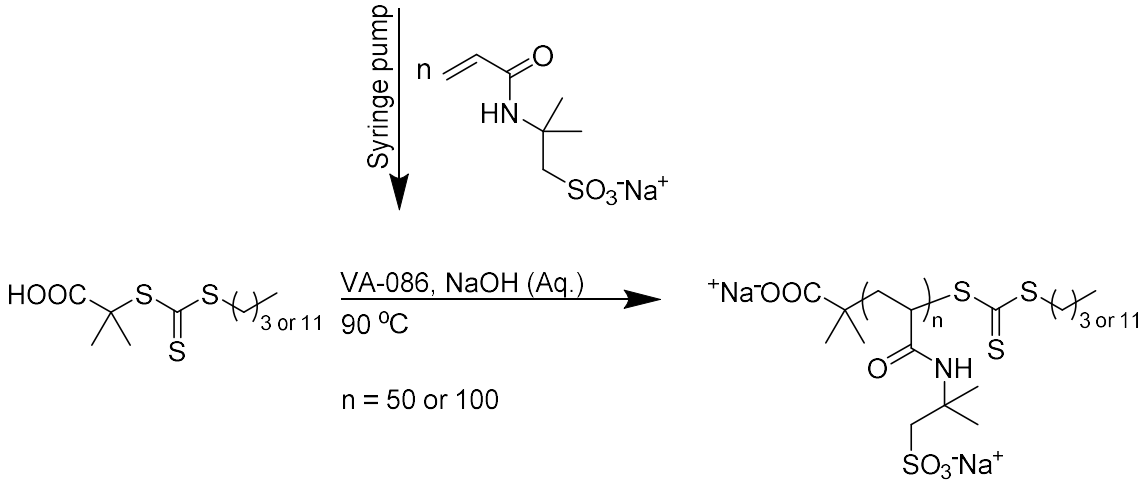

Polymer	DP	CTA	[AMPS®2405]$_0$ (mol/L)	Time of Feeding (hours)	Conv. (%)[b]	$M_{n,th}$ (g/mol)[c]	$M_{n,SEC}$ (g/mol)[d]	$Đ$[d]
19	50	BDMAT	1.5	0	> 99	11,100	14,700	1.19
26	50	BDMAT	1.5	1	> 99	11,700	13,800	1.17
15	50	DDMAT	1.5	0	> 99	11,700	19,600	1.66
27	50	DDMAT	1.5	1	> 99	11,800	30,300	1.77
20	100	BDMAT	1.5	0	> 99	23,100	25,100	1.24
24	100	DDMAT	1.5	0	> 99	23,100	31,900	1.78
28	100	DDMAT	1.5	0.5	> 99	22,900	26,500	1.62
29	100	DDMAT	1.5	1	> 99	23,000	22,900	1.56
30	100	DDMAT	2.5	1	> 99	23,400	32,500	1.81
31	100	DDMAT	0.5	1	> 99	23,600	13,500	1.40

[a] Polymerisations were conducted at 90 °C phosphate buffer solution adding 0.5 equivalent of NaOH per CTA; [b] Conversions were determined by ^{1}H NMR spectroscopy, using **Equation 1**; [c] Theoretical M_n values were calculated using **Equation 2**; [d] Experimental M_n and $Đ$ values were determined by size-exclusion chromatography in 20 % MeOH / 80% 0.1M $NaNO_3$ in milli-Q water eluent using a conventional calibration obtained with PEG/PEO standards.

The effect of the feeding was then evaluated by targeting a DP of 100, as when the CTA concentration was lowered from 0.3 to 0.015 M (**Table 2-6**) an increase of its solubility is then expected. When the time of feeding was increased from 0 to 0.5 h and finally to 1 hour, a small improvement on the control of the polymerisation could be observed. The molecular weight decreased from 31,900 g/mol (no feeding, **Polymer 24**) to 25,600 g/mol (0.5 h, **Polymer 28**) and finally 22,900 g/mol (1 h, **Polymer 29**), unfortunately dispersities were still higher than 1.5 (**Figure 2-18 – B**). The slight improvement is explained by a decrease of monomer concentration at the beginning of the reaction which increased the CTA solubility.[132] The initial CTA concentration was further decreased by changing the starting theoretical monomer concentration, indeed targeting a theoretical monomer concentration of 0.5 M the CTA

concentration was then 0.005 M instead of 0.015 M ($[CTA]_0$ = 0.015 M if $[AMPS^{®}2405]_{0,theoritical}$ = 2.5 M). From **Figure 2-18 - C** it can be observed that the molecular weight distributions are narrower, shifting towards lower molecular weights when the monomer concentration was decreased from 2.5 to 1.5 and finally 0.5 M. It can be noticed that when the theoretical monomer concentration was 2.5 M, similar results were obtained compared to the semi-batch method at 1.5 M (**Table 2-7**, **Polymers 24** and **30**). However, when the theoretical monomer concentration targeted was 0.5 M, while the dispersity was 1.4 the molecular weight was significantly underestimated ($M_{n,SEC}$ = 13,500 g/mol versus $M_{n,theoritical}$ = 23,600 g/mol) even though the monomer conversion was superior at 99 %. This could be attributed by a non-degradative transfer process.[133] All of the above results demonstrated the dependence of monomer and CTA concentrations on the control over the polymerisation process. This is likely worsened by the low solubility of DDMAT in the presence of AMPS®2405 which is highly charged.

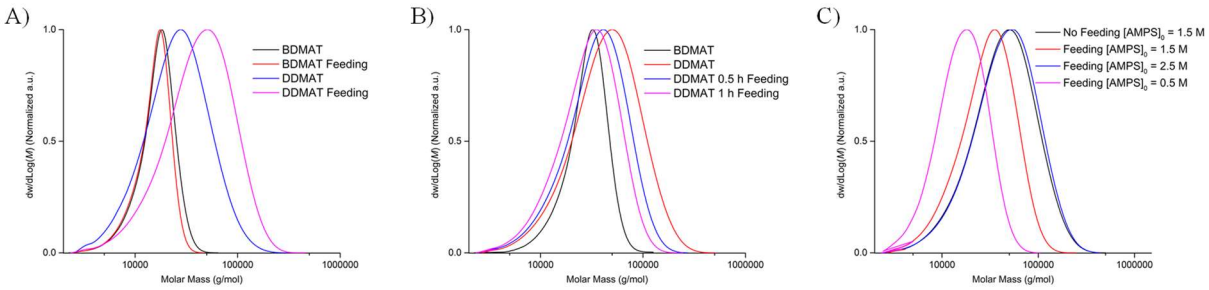

Figure 2-18: Aqueous SEC molecular weight distributions of PAMPS synthesised either in batch or feeding.

A) $PAMPS_{50}$ in batch or by feeding the monomer using either BDMAT or DDMAT at a rate of 1.5 mL per hour; B) $PAMPS_{100}$ in batch or by feeding the monomer using either BDMAT or DDMAT at a rate of 3 or 1.5 mL per hour; C) $PAMPS_{100}$ in batch or by feeding the monomer using DDMAT at a rate of 1.5 mL per hour varying the monomer concentration $[AMPS^{®}2405]_0$ = 1.5 or 2.5 or 0.5 M.

PAMPS Synthesis Using a MacroCTA PDMA

Another way to increase the CTA solubility is to modify this CTA by synthesising a macroCTA. In this section PDMA-macroCTAs synthesised in **Section 2.3.1** were used to polymerise AMPS®2405. This PDMA-macroCTA has been shown to be successfully chain extended by DMA itself and is expected to be efficient for the polymerisation of AMPS®2405 (**Scheme 2-14**).

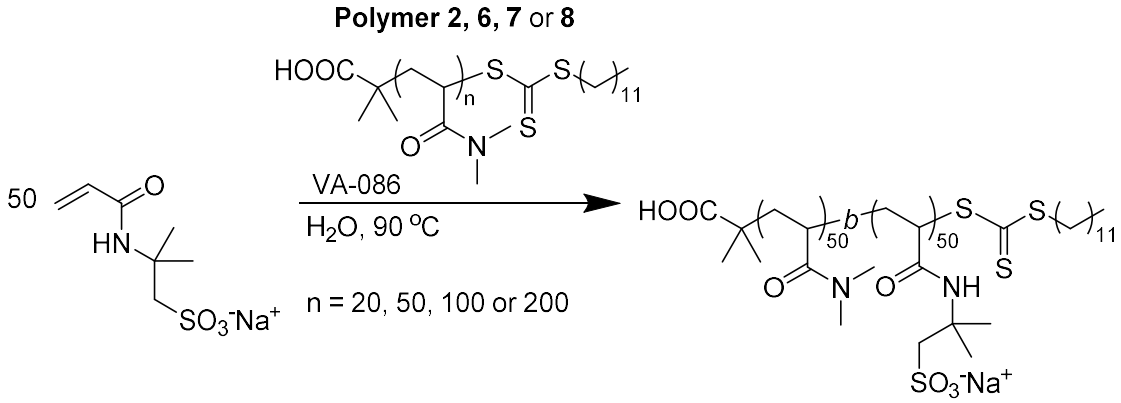

Scheme 2-14: Chain extension of PDMA with AMPS®2405 in PB using DDMAT.

The SEC analysis of these macroCTAs (**Polymer 2**, **6**, **7** and **8**) using both water and DMF solvent was first performed. It could be observed that the dispersities measured were slightly higher when aqueous SEC (**Figure 2-19**) was used compared to DMF SEC (**Table 2-8**). Dispersities were observed to decrease from 1.47 to 1.35 when the DP of the macroCTA was increased from 50 to 200.

Table 2-8: MacroCTA PDMA analysis: DMF versus aqueous SEC.

Polymer	DP	Conv. (%)[a]	$M_{n,th}$ (g/mol)[b]	$M_{n,SEC}$ (g/mol)	$Đ$	$M_{n,SEC}$ (g/mol)	$Đ$
				DMF SEC[c]		Aqueous SEC[d]	
6	20	> 99	2,300	4,700	1.33	-	-
2	50	> 99	5,200	9,900	1.21	7,300	1.47
7	100	> 99	10,800	15,100	1.17	10,500	1.38
8	200	> 99	19,100	24,500	1.13	14,700	1.35

[a] Conversions were determined by ^{1}H NMR spectroscopy, using **Equation 1**; [b] Theoretical M_n values were calculated using **Equation 2**; [c] Experimental M_n and $Đ$ values were determined by size-exclusion chromatography in DMF with 5 mM NH_4BF_4 using a conventional calibration obtained with PMMA standards; [d] Experimental M_n and $Đ$ values were determined by size-exclusion chromatography in 20 % MeOH / 80 % 0.1M $NaNO_3$ in milli-Q water eluent using a conventional calibration obtained with PEG/PEO standards.

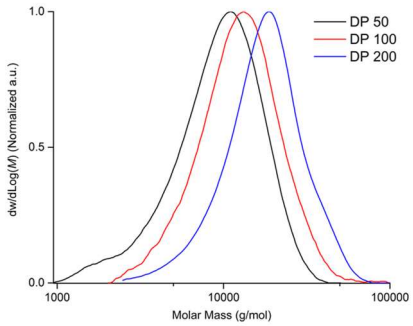

Figure 2-19: Aqueous SEC molecular weight distributions of PDMA with DPs varying from 50 to 200.

MacroCTA of DMA with DPs ranging from 20 to 200 were used to polymerise AMPS®2405 in a one pot process (**Table 2-9**). The second block was synthesised by adding the AMPS®2405 monomer and the initiator into the vial through a syringe. AMPS®2405 concentration was decreased from 1 to 0.33 M when the macroCTA DP was increased from 20 to 200 while the initiator concentration was kept constant to $2.5x10^{-3}$ M.

Table 2-9: Aqueous RAFT polymerisation of AMPS®2405 using PDMA with different DPs (20, 50, 100 and 200) as macroCTA.[a]

Polymer	MacroCTA	Conv. (%)[b]	$M_{n,th}$ (g/mol)[c]	$M_{n,SEC}$ (g/mol)[d]	$Đ$[d]
32	**6** - $PDMA_{20}$	> 99	13,800	31,200	2.02
33	**2** - $PDMA_{50}$	> 99	16,800	25,200	1.81
34	**7** - $PDMA_{100}$	> 99	21,300	15,900	1.69
35	**8** - $PDMA_{200}$	> 99	33,400	19,000	1.43

[a] Polymerisations were conducted at 90 °C during 2 hours in phosphate buffer solution adding AMPS®2405 via a degassed syringe; [b] Conversions were determined by ^{1}H NMR spectroscopy, using **Equation 1**; [c] Theoretical M_n values were calculated using **Equation 2**; [d] Experimental M_n and $Đ$ values were determined by size-exclusion chromatography in 20 % MeOH / 80 % 0.1M $NaNO_3$ in milli-Q water eluent using a conventional calibration obtained with PEG/PEO standards.

Shifts towards higher molecular weights could be observed when macroCTAs were chain extend with AMPS®2405 (**Figure 2-20 – A, B** and **C**) and monomodal peaks were observed due to full reinitiation of the macroCTA by AMPS®2405. However, dispersities higher than 1.5 were obtained when macroCTA with DP of 20, 50 and 100 were used (**Table 2-9, Polymers 32, 33** and **34**). This is likely due to the aggregation of the PDMA-macroCTA due to the long alkyl chain (Z-group).[117,134] The hydrophobicity / hydrophilicity was then shown to be an important parameter as the

hydrophobicity of the C12 alkyl chain was counterbalanced only when the DP of PDMA was over 100 (**Figure 2-20** – **D**).

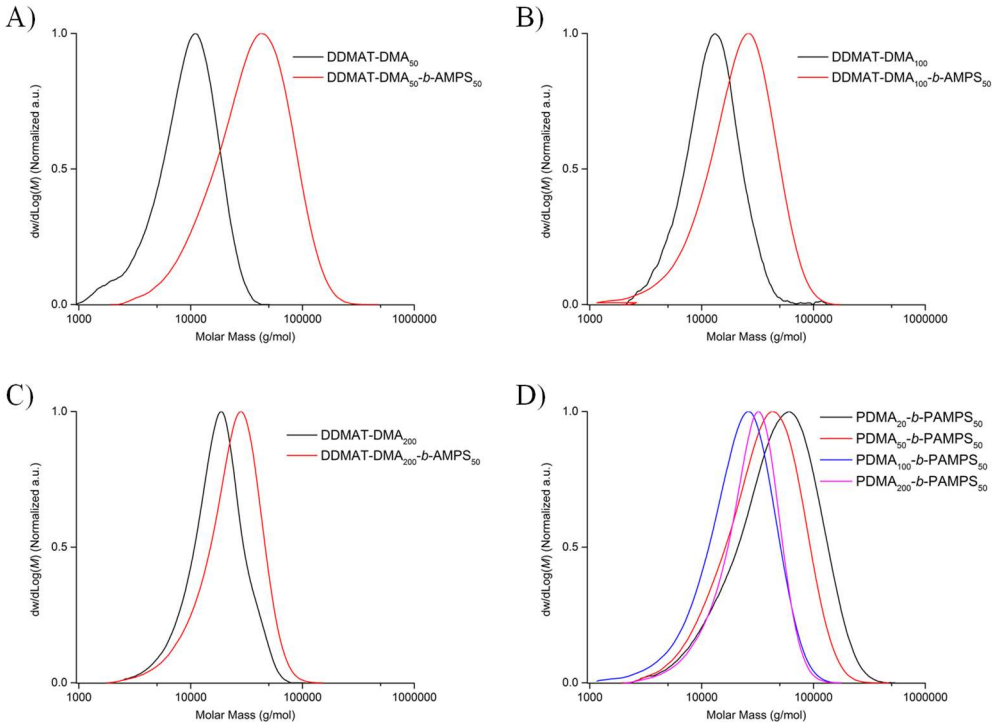

Figure 2-20: Aqueous SEC molecular weight distributions of $PDMA_x$ chain extension with AMPS®2405 (DP50, 2nd block).

A) $PDMA_{50}$; B) $PDMA_{100}$; C) $PDMA_{200}$; D) Overlay of DDMAT-$PDMA_x$-*b*-$PAMPS_{50}$ with x 20, 50,100 and 200.

Use of Organic Solvent

DDMAT was shown to have a poor solubility in water due to the formation of aggregates in aqueous solution. Indeed, this CTA has been widely used in the literature for emulsion polymerisation by RAFT polymerisation without the need of additional surfactants.[113,135] The critical aggregation concentration (CAC) of DDMAT and BDMAT was subsequently determined in PBS by electrical conductivity.[136,137] Conductivities of CTA solutions were measured at increasing concentrations from $5x10^{-5}$ to 0.1 M. Conductivities of BDMAT at increasing concentration was linear, while a variation can be observed when DDMAT conductivities were plotted against CTA concentration (**Figure 2-21**). This change at 0.005 M denoted the CAC of DDMAT in PBS at 25 °C (Stoffelbach *et al*. CAC_{DDMAT} = 0.001 M).[113] Indeed, before the CAC, the conductivity increased due to the increase of electrolyte concentration in solution (i.e. monomer of CTA), while after the CAC the conductivity increased at a lower rate due to the formation of aggregates shielding the charges.

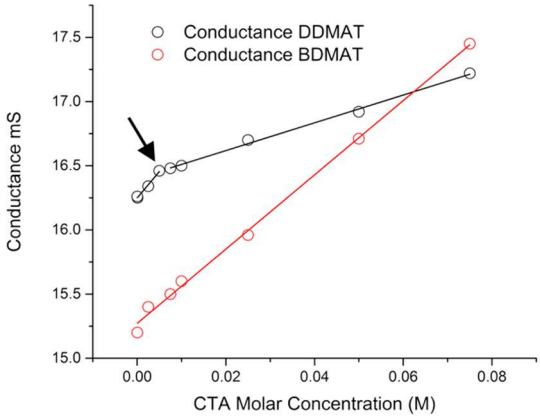

Figure 2-21: Plot of the conductance as a function of the CTA concentration (DDMAT in black and BDMATC in red) in PB. The black arrow denotes the CAC of DDMAT.

The formation of aggregates was further confirmed using ^{1}H NMR spectroscopy, where broad peaks were obtained when DDMAT was analysed in D_2O (**Figure 2-22**), this being in agreement with previous report in the literature.[138,139] [140,141] From the NMR tube of DDMAT in D_2O a few drops of $(CD_3)_2CO$ were added and well-defined peaks were then obtained on the NMR spectra (**Figure 2-22**) due to the breakdown of aggregates. Subsequently, aggregates can be broken either by decreasing DDMAT concentration below its CAC (i.e. 0.005 M but this is likely to be affected by

AMPS®2405) or by conducting the polymerisation in a mixture of water and organic solvent.

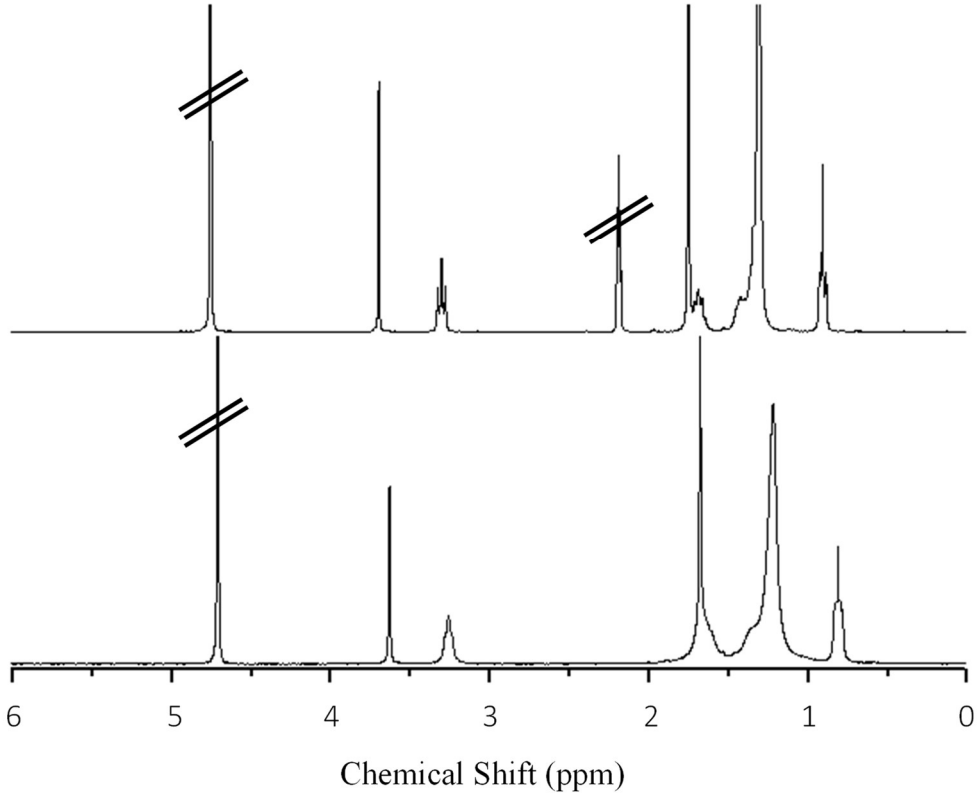

Figure 2-22: ^{1}H NMR (300 MHz) spectra of DDMAT (0.15 M) in D_2O phosphate buffer solution (bottom), addition of a few drops of $(CD_3)_2CO$ (top).

Then, a series of AMPS®2405 polymerisations were conducted in a mixture of water and organic solvent in a ratio of water:organic solvent 80:20 (v:v %) with a monomer concentration of 1.5 M (**Table 2-10**).

Table 2-10: optimisation of the RAFT polymerisation of AMPS®2405 using DDMAT in a mixture of water and organic solvent (80:20 % v:v).[a]

Polymer	Solvent	Reaction Mixture Solubility		Conv. (%)[b]	$M_{n,SEC}$ (g/mol)[c]	$Đ$[c]
		20 °C	90 °C			
36	DMF	No	Yes	> 99	9,100	1.36
37	DMSO	No	Yes	> 99	9,500	1.43
38	Dioxane	No	Yes	> 99	8,900	1.40
39	Acetonitrile	No	Yes	> 99	8,700	1.36
40	*t*-Butanol	Yes	Yes	> 99	9,500	1.46
41	*n*-butanol	Yes	Yes	> 99	9,600	1.51
42	Methanol	No	Yes	> 99	9,300	1.40
43	Formic Acid	No	Yes	96	41,300	3.30
44	Acetic acid	No	Yes	98	31,200	4.50

[a] Polymerisations were conducted at 90 °C during 2 hours in a mixture of phosphate buffer solution 80 % and organic solvent 20 % (v/v %) targeting a DP 50; [b] Conversions were determined by ^{1}H NMR spectroscopy, using **Equation 1**; [c] Experimental M_n and $Đ$ values were determined by size-exclusion chromatography in 20 % MeOH / 80 % 0.1M $NaNO_3$ in milli-Q water eluent using a conventional calibration obtained with PEG/PEO standards.

All polymers formed were shown to be soluble in the series of solvent studied, however, DDMAT itself was only soluble at the beginning of the reaction in *t*-butanol and *n*-butanol. Monomer conversion in a mixture of water and formic acid or acetic acid was lower than 99 %, additionally, the distributions obtained were bimodal and the molecular weight peaks were higher than when DDMAT was used in PBS (**Figure 2-23 – C**). So far the best results were obtained in either of the following solvents ($Đ$ ≤ 1.4): DMF, dioxane, acetonitrile or methanol (**Figure 2-23 – A** and **B**).

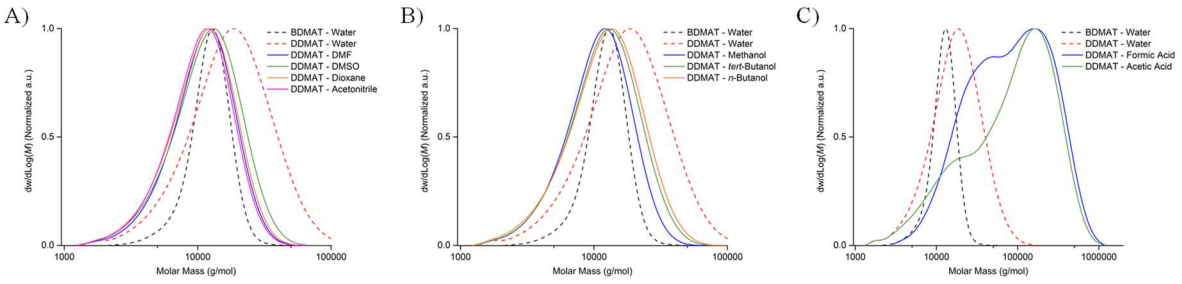

Figure 2-23: Aqueous SEC molecular weight distributions of the RAFT polymerisation of AMPS®2405 in a mixture of water (80 wt. %) and organic solvent (20 wt. %).

$PAMPS_{50}$-DDMAT synthesised in a mixture of water and methanol (80:20 v:v %, **Polymer 42**) was chain extended by AMPS®2405 in a one pot process (**Scheme 2-10**) in order to evaluate the livingness character of the system.

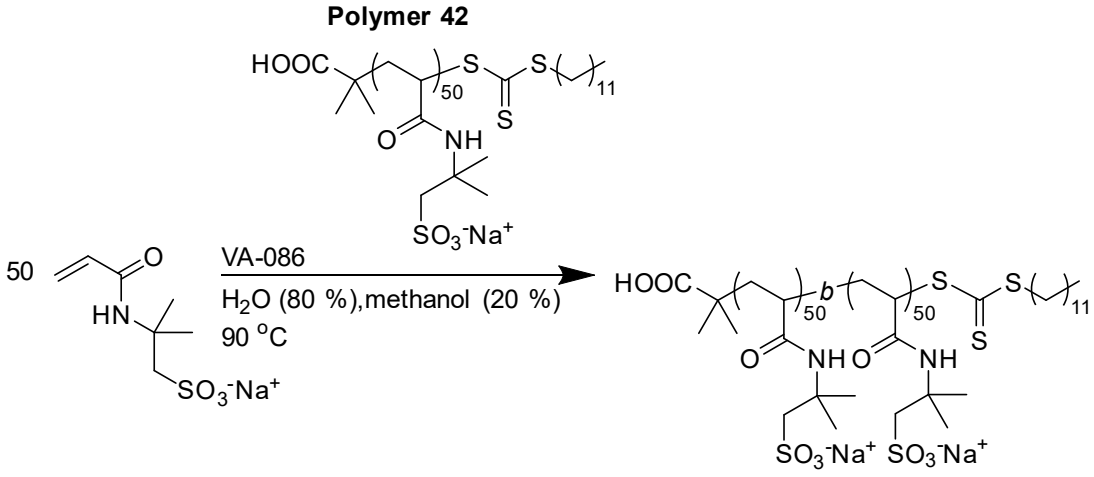

45

Conv.[a] > 99 %

$M_{n,th}$[b] = 23,600 g/mol

$M_{n,SEC}$[c] = 17,400 g/mol

$Đ$[c] = 1.45

Scheme 2-15: Chain extension of PAMPS with AMPS®2405 in water and methanol (80:20 % v:v) using DDMAT.

[a] Conversions were determined by ^{1}H NMR spectroscopy, using **Equation 1**; [b] Theoretical M_n values were calculated using **Equation 2**; [c] Experimental M_n and $Đ$ values were determined by size-exclusion chromatography in 20 % MeOH / 80 % 0.1M $NaNO_3$ in milli-Q water eluent using a conventional calibration obtained with PEG/PEO standards.

Full monomer conversion was obtained and a shift towards higher molecular weight (**Figure 2-24**) was observed, proving a successful chain extension of the macroCTA $PAMPS_{50}$-DDMAT by AMPS®2405 forming the **Polymer 45**.

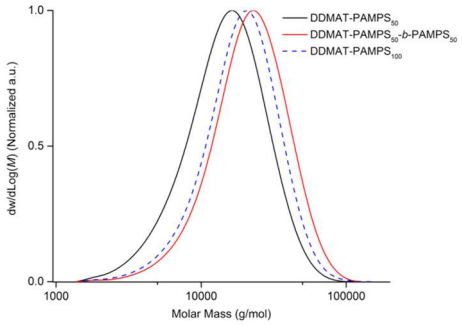

Figure 2-24: Aqueous SEC molecular weight distributions of PAMPS diblock synthesised by RAFT polymerisation in water and methanol (80:20 wt. %) using DDMAT.

2.3.4 Use of Other Acrylamide Monomer

In this section two other acrylamides (4-acryloylmorpholine i.e. NAM and *N*-hydroxyethyl acrylamide (HEAm), **Scheme 2-11**) were polymerised in aqueous solution using either DDMAT or BDMAT (**Table 2-11**).

Table 2-11: Aqueous RAFT polymerisation of NAM and HEAm using either DDMAT or BDMAT as RAFT agent in water (DP = 50).[a]

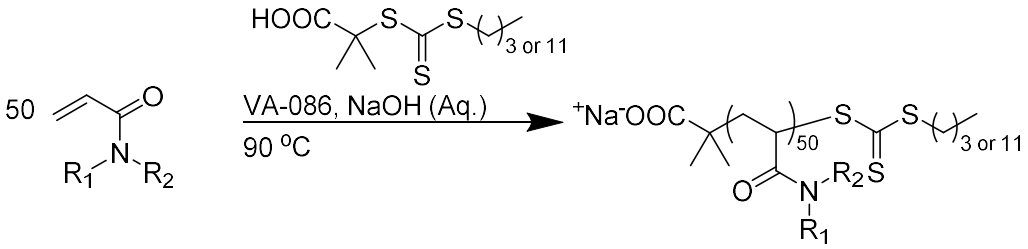

Polymer	CTA	Monomer	Conv. (%)[b]	$M_{n,th}$ (g/mol)[c]	$M_{n,SEC}$ (g/mol)[d]	$Đ$[d]
46	DDMAT	NAM	> 99	7,300	6,300	1.30
47	BDMAT	NAM	> 99	7,300	6,300	1.15
48	DDMAT	HEAm	> 99	6,300	8,200	1.57
49	BDMAT	HEAm	98	6,300	9,500	1.31

[a] Polymerisations were conducted at 90 °C in phosphate buffer solution ($[Monomer]_0$:$[CTA]_0$:$[VA\text{-}086]_0$ = 50:1:0.08, $[Monomer]_0$ = 1.5 M); [b] Conversions were determined by ^{1}H NMR spectroscopy, using Equation 1; [c] Theoretical M_n values were calculated using Equation 2; [d] Experimental M_n and $Đ$ values were determined by size-exclusion chromatography in DMF with 0.1 % LiBr using a conventional calibration obtained with PMMA standards.

The conditions which were found to be optimal for the polymerisation of DMA in **Section 2.3.1 (Polymer 5)** were first applied to NAM. Well-defined $PNAM_{50}$ homopolymers ($Đ$ < 1.5) were obtained using either DDMAT (**Polymer 46**) or BDMAT (**Polymer 47**). When DDMAT was used a slightly higher dispersity (1.3) was obtained compared to when BDMAT was used (1.15), which was likely due to DDMAT aggregation (**Figure 2-25 – A**). Finally, the control over the polymerisation was slightly lowered when HEAm was used. The dispersity with DDMAT was 1.57 (**Polymer 48**) and 1.31 with BDMAT (**Polymer 49**) (**Figure 2-25 – B**). The higher dispersities obtained compared to NAM or DMA can either be explained by column interactions, leading to low molecular weight tailing, or by a poor control of polymerisation due to the higher hydrophilicity of HEAm (hydroxyl group) compared to NAM or DMA. Furthermore, DDMAT was not as readily soluble in HEAm monomer as in NAM or DMA monomers.

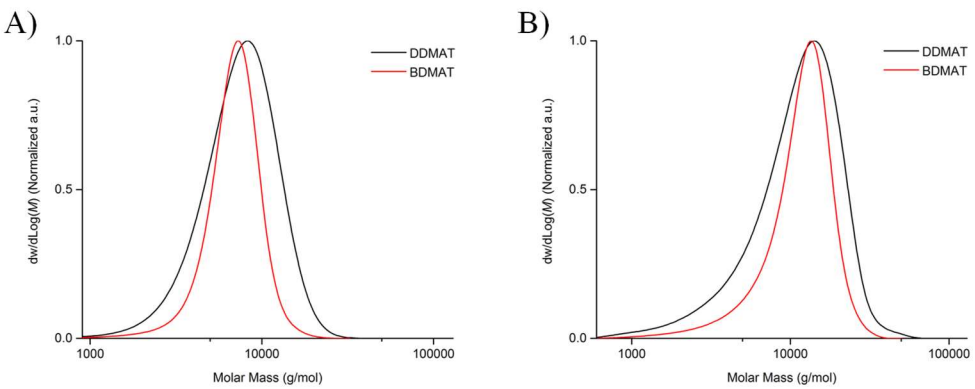

Figure 2-25: DMF SEC molecular weight distributions of acrylamide monomers polymerised by RAFT using either DDMAT (red line) or BDMAT (black line) ($DP_{targeted}$ = 50, $[Monomer]_0$ = 1.5 M, conv. > 98 %).

A) PNAM; B) PHEAm.

2.4 Conclusions

In this chapter the RAFT polymerisation of four different acrylamides were optimised using either DDMAT or BDMAT as the CTA. Overall the polymerisation control was observed to be better when BDMAT was used compared to DDMAT. The polymerisation control was shown to be poorer when DDMAT was used to polymerise HEAm or AMPS®2405 in aqueous solution. The poorest control with DDMAT was attributed to its aggregation in aqueous solution due to the C12 alkyl chain (CTA Z-group) which may then affect the mechanism of RAFT polymerisation (**Figure 2-26**). AMPS®2405 homopolymer using DDMAT was polymerised in a mixture of water and methanol in order to break down the aggregates of DDMAT to obtain well-defined materials ($Đ$ < 1.5). This $PAMPS_{50}$-DDMAT was further chain extended with AMPS®2405 and a diblock homopolymer of AMPS®2405 was obtained. This demonstrated the robustness of the system to synthesise complex architectures, which will be further investigated in **CHAPTER 3**. Finally, using BDMAT, universal conditions were found to polymerise water soluble acrylamides in aqueous solution by RAFT polymerisation. Homopolymers of NAM, DMA, HEAm and AMPS®2405 were obtained within 2 hours. Narrow and monomodal SEC chromatograms of PAMPS were obtained with a dispersity obtained as low as 1.1.

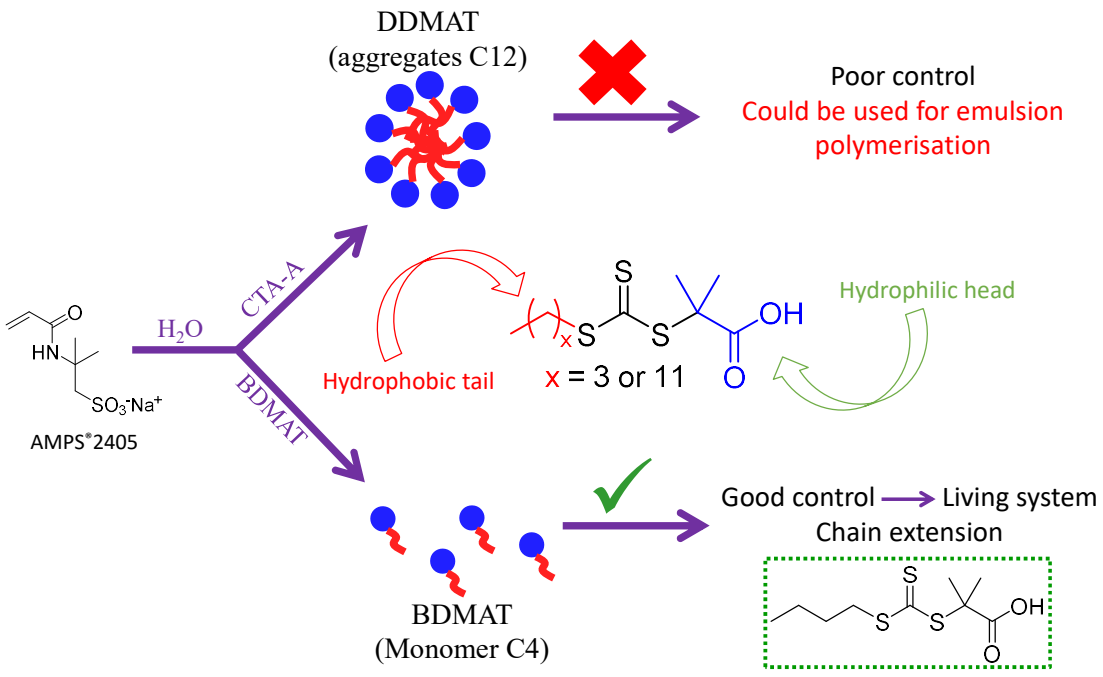

Figure 2-26: Results summary from **CHAPTER 2**.

2.5 Experimental

2-(Butylthiocarbonothioylthio)-2-methylpropionic acid

BDMAT

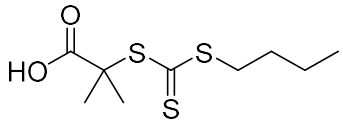

BDMAT was synthesised by adapting a procedure from Lai *et al.*[118] Briefly, a solution of a 17 % (wt. %) NaOH aqueous solution (44 mL, 222.0 mmol) was added to a mixture of butanethiol (24 mL, 222.0 mmol) and acetone (12 mL), and the colourless miscible solution was stirred for 30 minutes at room temperature. Carbon disulfide (15 mL, 244.0 mmol) was then added and stirred for another 30 minutes at room temperature to give an orange solution. The solution was cooled in an ice bath (~ 5 °C) and 2-bromo-2-methylpropanoic acid (38.00 g, 227.0 mmol) was added slowly, keeping the internal temperature below 30 °C, forming a yellow precipitate. Another 17 % NaOH aqueous solution (44 mL) was added (internal temperature again kept below 30 °C) to dissolve the orange precipitate. The solution was left to stir overnight at room temperature. After 17 hours, the reaction mixture was diluted with 200 mL of water before being washed twice with hexane. The aqueous phase was then cooled to 0 °C and hydrochloric acid (200 mL, 1 M) was added dropwise (final pH ~ 2-3) until a yellow precipitate was observed. The solid was collected by suction filtration and washed twice with cold water. Subsequently, the solid was dissolved in chloroform (200 mL) and dried over $MgSO_4$. After filtration and removal of the dichloromethane in *vacuo*, the solid was recrystallised from hexane and finally dried under vacuum, to give the final compound as a bright yellow powder (42.00 g, 76 %); m.p. 57-58 °C, (lit. [142] 52 °C); ν_{max}/cm^{-1} 2948 (br. m, COO-H, stretch), 1690 (s, C=O, stretch), 1050 (s, C=S, stretch), 808 (m, C-S, stretch); δH (500 MHz, CD_3COCD_3) 3.33 (2H, t, J = 7.4 Hz, SCH_2), 1.69 (6H, s, $C(CH_3)_2$), 1.68-1.62 (2H, m, SCH_2CH_2), 1.48-1.35 (2H, m, CH_2CH_3), 0.92 (3H, t, J = 7.4 Hz, CH_2CH_3); δC (125 MHz, CD_3COCD_3), 222.9 (SC(=S)S), 173.6 (COOH), 56.6 ($C(CH_3)_2$), 36.9 (SCH_2), 30.8 (SCH_2CH_2), 25.7 ($C(CH_3)_2$), 22.6 (CH_2CH_3), 13.8 (CH_2CH_3); m/z (ESI Negative Mode, $(M-H^+)$ $C_9H_{15}O_2S_3^-$ requires 251.02), found 251.00.

2-(Dodecylthiocarbonothioylthio)-2-methylpropionic acid

DDMAT

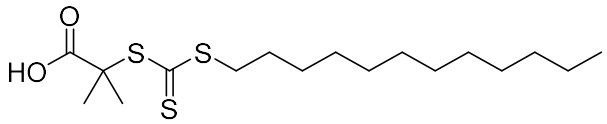

This compound was kindly provided by The Lubrizol Corporation. The crude sample, a brown solid, provided (5.00 g, 14.0 mmol) was purified by recrystallisation in hexane, filtered and dried under vacuum, to give the final compound as a bright yellow powder (4.15 g, 88 %); m.p. 63-64 °C, (lit.[143] 61 °C); ν_{max}/cm^{-1} 2945 (br. m, COO-H, stretch), 1702 (s, C=O, stretch), 1020 (s, C=S, stretch), 800 (m, C-S, stretch); δH (500 MHz, CD_3COCD_3) 3.34 (2H, t, *J* = 7.4 Hz, SCH_2), 1.79-1.59 (8H, br. m, $C(CH_3)_2$ and $SCH_2C\mathit{H}_2$), 1.46-1.38 (2H, m, $SCH_2CH_2C\mathit{H}_2$,), 1.37-1.22 (16H, br. m, $S(CH_2)_3(C\mathit{H}_2)_8CH_3$), 0.88 (3H, t, *J* = 6.8 Hz, $S(CH_2)_{11}C\mathit{H}_3$); δC (125 MHz, CD_3COCD_3), 222.9 (SC(=S)S), 173.6 (COOH), 56.6 ($\mathit{C}(CH_3)_2$), 37.2 (SCH_2), 32.7 ($SCH_2\mathit{C}H_2$), 30.4-29.4 (m, $S(CH_2)_2(\mathit{C}H_2)_7(CH_2)_2CH_3$), 28.8 ($S(CH_2)_9\mathit{C}H_2CH_2CH_3$), 25.8 ($C(\mathit{C}H_3)_2$), 23.4 ($S(CH_2)_{10}\mathit{C}H_2CH_3$),14.4 ($S(CH_2)_{11}\mathit{C}H_3$); m/z (ESI, Negative Mode, ($M\text{-}H^+$) $C_{17}H_{31}O_2S_3^-$ requires = 363.15), found 363.10.

Poly(*N*,*N*-dimethylacrylamide)

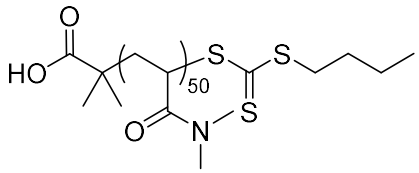

PDMA

Polymer 4, DP50

Synthesis in water: BDMAT (26 mg, 0.1 mmol), DMA (510.0 mg, 5.1 mmol), water (3 mL) and VA-086 (8.6×10^{-3} mmol, 2.5 mg) (from stock solution at 20.0 mg/mL) were introduced into a flask equipped with a magnetic stirrer bar and sealed with a rubber septum. The solution was deoxygenated by bubbling with nitrogen for 10 minutes, and the vial was then placed in a temperature controlled oil bath at the desired temperature (90 °C) for the duration of time required to reach nearly full conversion (~ 2 hours). At the end of the reaction, the mixture was allowed to cool down to room temperature and then opened to the atmosphere. Final materials were characterised using ^{1}H NMR spectroscopy and SEC ($M_{n,SEC}$ and $Đ$ were determined). The compound was then dialysed against water for 48 hours and freeze dried, to give the final compound as a pale yellow powder; m.p. > 300 °C); ν_{max}/cm^{-1} 3431 (br. m, COO-H, stretch), 1616 (s, C=O, stretch), 1142 (s, C-N, stretch), 1047 (s, C=S, stretch); δH (400 MHz, D_2O) 3.00 (3H, br. m, CH_2S and $CH_2CHSC(S)S$), 3.26 – 2.82 (338H, br. m, $N(CH_3)_2$), 2.81 – 2.03 (46H, br. m, CH(CONH)), 2.03 – 1.22 (105H, br. m, $CH_2CH(CON)$ and $CH_3CH_2CH_2$), 1.09 (6H, br. s, $COOHC(CH_3)_2$), 0.88 (3H, br. s, CH_3CH_2); δC (100 MHz, D_2O), 175 ($C(=O)N(CH_3)_2$), 38.5 – 35.5 (br. m, $N(CH_3)_2$ and $CH_2CH(CON)$), 34.8 (br. s, $CH_2CH(CON)$).

Similar polymers with varying degrees of polymerisation and conditions of polymerisation were found to exhibit similar spectroscopic data that of the title compound. The SEC molecular weight distribution for the above product can be seen in **Section 2.3.1**.

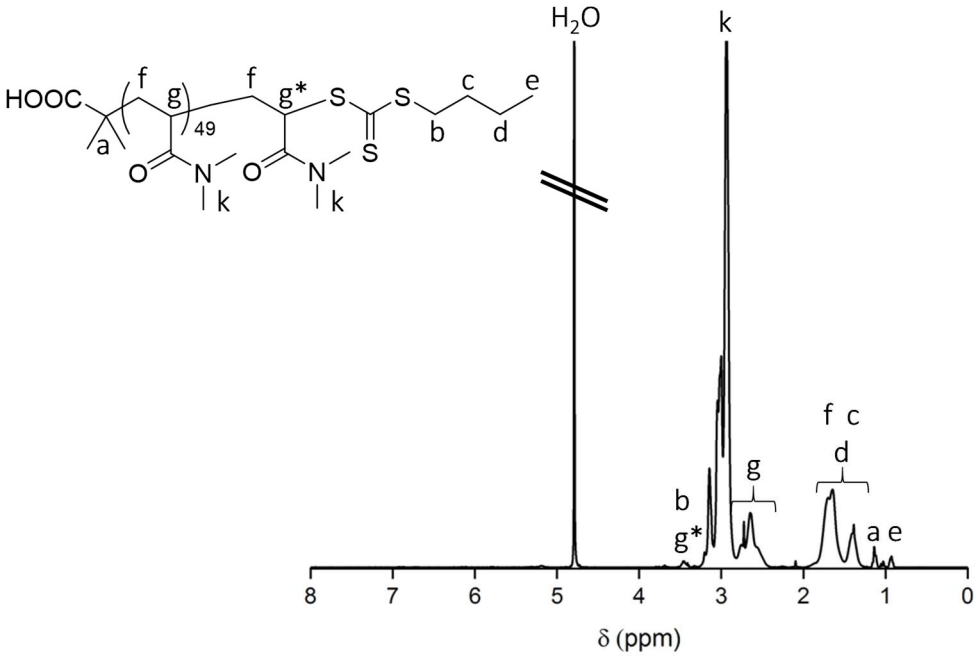

Figure S 2-1: ^{1}H NMR spectrum of PDMA (**Polymer 4**) in D_2O.

Poly(*N*,*N*-dimethylacrylamide)

PDMA

Polymer 1, DP50

Synthesis in toluene: DDMAT (26.0 mg, 0.1 mmol), DMA (510.0 mg, 5.1 mmol), water (3 mL) and V-40 ($8.6\text{x}10^{-3}$ mmol, 2.5 mg) (from stock solution at 20.0 mg/mL) were introduced into a flask equipped with a magnetic stirrer bar and sealed with a rubber septum. The solution was deoxygenated by bubbling with nitrogen for 10 minutes, and the vial was then placed in a temperature controlled oil bath at the desired temperature (90 °C), for the duration of time required to reach nearly full conversion (~ 2 hours). At the end of the reaction, the mixture was allowed to cool down to room temperature and then opened to the atmosphere. Final materials were characterised using ^{1}H NMR spectroscopy and SEC ($M_{n,SEC}$ and $Đ$ were determined). The compound was then precipitated from diethyl ether and dried in vacuum, to yield the final compound as a pale yellow powder.

Similar polymers with varying degrees of polymerisation and conditions of polymerisation were found to exhibit similar spectroscopic data to that of the title compound **Polymer 4**. The SEC molecular weight distribution can be seen in **Section 2.3.1**.

Poly(sodium 2-acrylamido-2-methylpropane sulfonate)

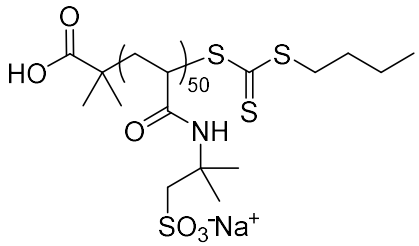

PAMPS

Polymer 19, DP50

BDMAT (26.0 mg, 0.1 mmol), AMPS®2405 (2.00 g, 5.1 mmol), phosphate buffer tablet at pH 6.5 (1.5 mL), sodium hydroxide ($5.1x10^{-2}$ mmol, 2.0 mg) and VA-086 ($8.4x10^{-3}$ mmol, 2.4 mg) (from stock solution at 20.0 mg/mL) were introduced into a flask equipped with a magnetic stirrer bar and sealed with a rubber septum. The solution was deoxygenated by bubbling with nitrogen for 10 minutes, and the vial was then placed in a temperature controlled oil bath at the desired temperature (90 °C), for the duration of time required to reach nearly full conversion (~ 2 hours). At the end of the reaction, the mixture was allowed to cool down to room temperature and then opened to the atmosphere. Final materials were characterised using ^{1}H NMR spectroscopy and SEC ($M_{n,SEC}$ and $Đ$ were determined). The compound was then dialysed against water for 48 hours and freeze dried, to yield the final compound as a pale yellow powder; m.p. > 300 °C; ν_{max}/cm^{-1} 3310 (br. m, COO-H, stretch), 1650 (s, C=O, stretch), 1536 (s, N-H, bend), 1180 (s, C-N, stretch), 1160 (s, C-SO_3^-, stretch), 1042 (s, C=S, stretch); δH (500 MHz, D_2O) 3.95 - 3.04 (99H, br. m, $CH_2SO_3^-Na^+$, CH_2S and $CH_2CHSC(S)S$), 2.70 - 1.88 (47H, br. m, $CH_2CH(CONH)$), 1.86 – 1.29 (374H, br. m, CH_2CH(CONH), $C(CH_3)_2CH_2SO_3^-Na^+$ and $CH_3CH_2CH_2$), 1.16 (6H, br. s, $COOHC(CH_3)_2$), 0.92 (3H, t, J = 7.2 Hz, $CH_3CH_2CH_2$); δC (100 MHz, D_2O), 176 (NHCO), 58.14 ($CH_2SO_3^-Na^+$), 52.47 ($CH_2C(CH_3)_2$), 42.48 ($CH_2CH(CONH)$), 26.44 ($CH_2C(CH_3)_2$), 21.37 ($CH_2CH(CONH)$).

Similar polymers with varying degrees of polymerisation and conditions of polymerisation were found to exhibit similar spectroscopic data to that of the title compound. The SEC molecular weight distribution for the above product can be seen in **Section 2.3.2**.

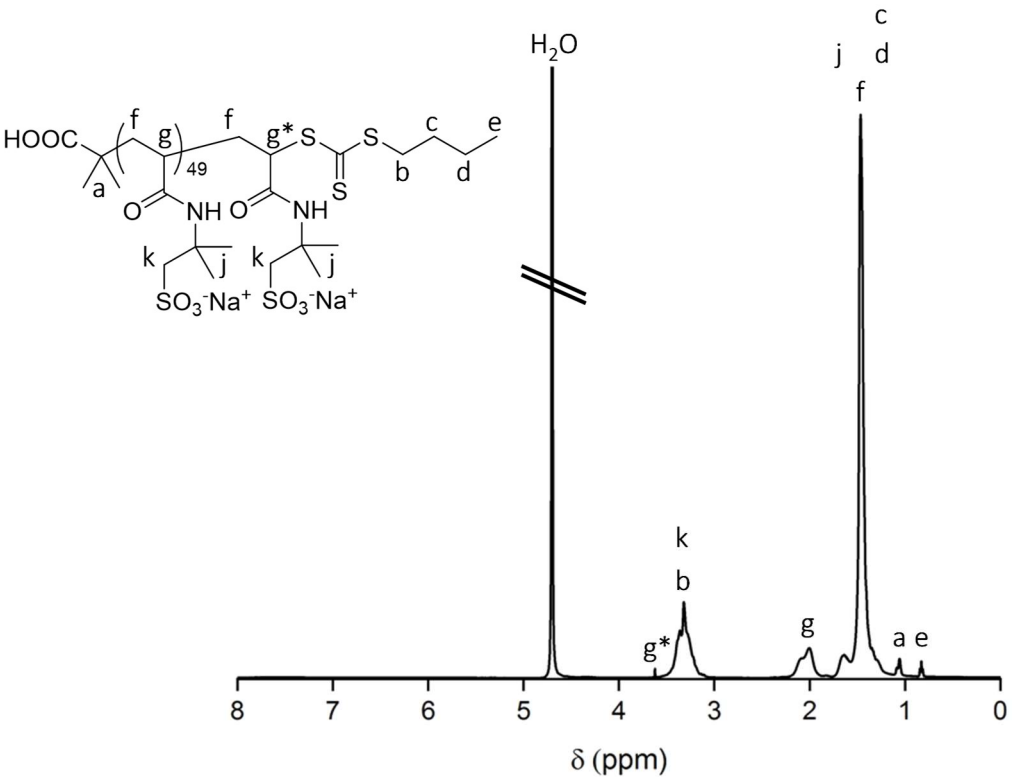

Figure S 2-2: ^{1}H NMR spectrum of PAMPS (**Polymer 19**) in D_2O.

Table S 2-1: Polymerisation data for the RAFT Polymerisation of AMPS®2405 in aqueous solution adding either 0.5 or 1 equivalent of NaOH / BDMAT.[a]

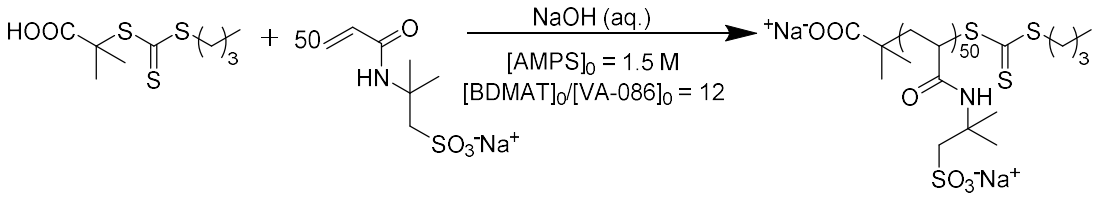

Polymer	Solvent	NaOH	pH[b]		Solubility of CTA (°C)		Conv. (%)[c]	$M_{n,th}$ (g/mol)[d]	$M_{n,SEC}$ (g/mol)[e]	$Đ$[e]
			pH_A	pH_B	25	90				
50	Water	0.5	5.4	5.5	✓	✓	> 99	11,500	10,600	1.19
19	PB	0.5	5.9	6.1	✓	✓	> 99	11,700	10,900	1.19
51	Water	1	6.9	7.2	✓	✓	> 99	11,400	10,500	1.19
52	PB	1	6.6	6.7	✓	✓	> 99	11,500	10,300	1.18

[a] Polymerisations were conducted at 90 °C in water or phosphate buffer solution ([AMPS®2405]$_0$:[BDMAT]$_0$:[VA-086]$_0$ = 50:1:0.08, [AMPS®2405]$_0$ = 1.5 M) adding either 0.5 or 1 equivalent of NaOH per CTA; [b] pH was measured at the start of the reaction before degassing (pH_A) and at the end of the reaction (pH_B) both at room temperature; [c] Conversions were determined by ^{1}H NMR spectroscopy, using **Equation 1**; [d] Theoretical M_n values were calculated using **Equation 2**; [e] Experimental M_n and $Đ$ values were determined by size-exclusion chromatography in 20 % MeOH / 80 % 0.1 $NaNO_3$ in milli-Q water eluent using a conventional calibration obtained with PEG/PEO standards. ✓ Soluble.

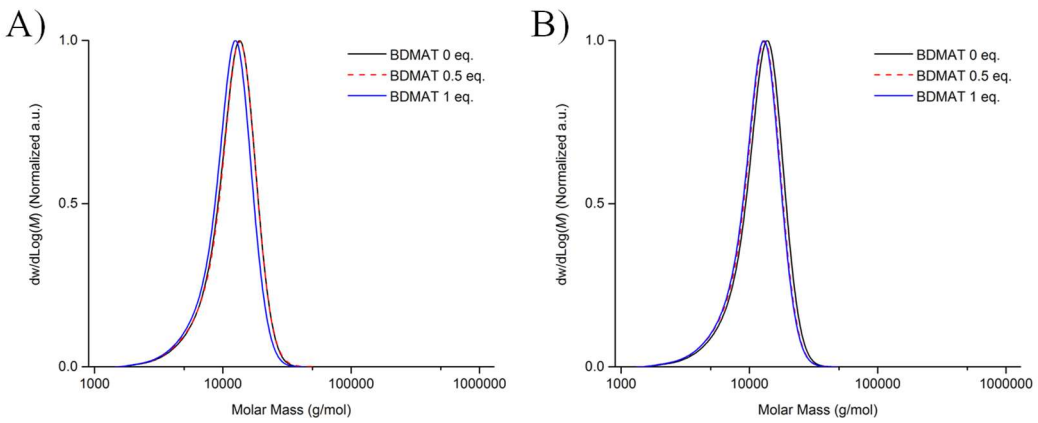

Figure S 2-3: Aqueous SEC molecular weight distributions of PAMPS prepared by RAFT polymerisation using BDMAT adding 0, 0.5 and 1 equivalent of NaOH / CTA.

A) Water; B) PB solution.

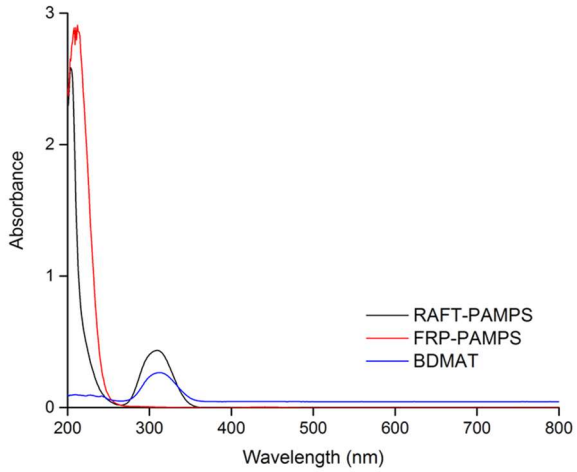

Figure S 2-4: UV-vis spectra of PAMPS synthesised by RAFT polymerisation, free radical polymerisation and BDMAT itself.

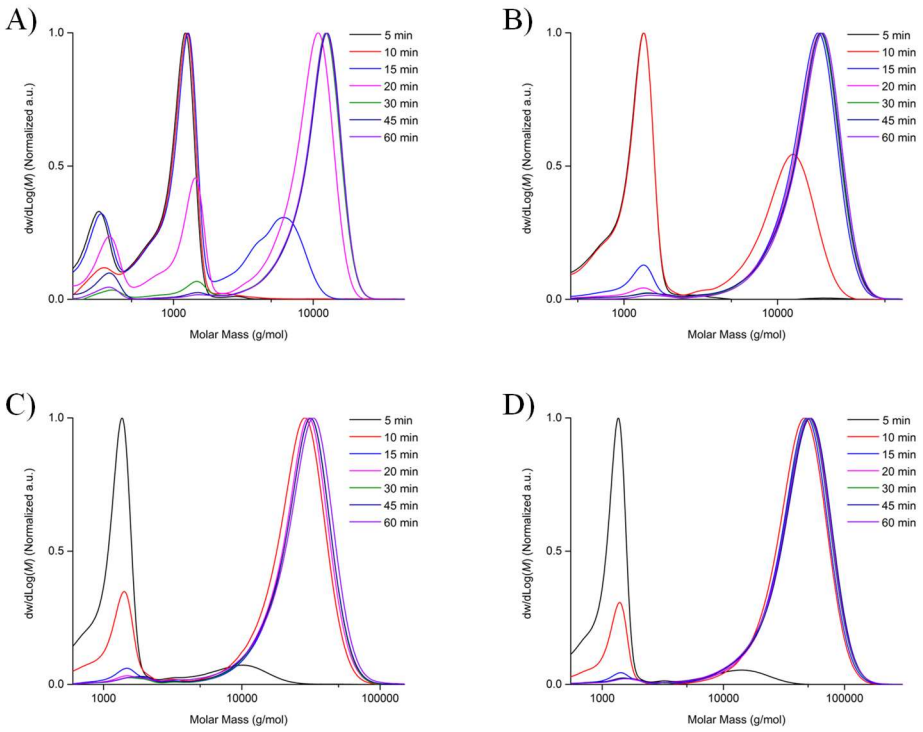

Figure S 2-5: SEC molecular weight distributions showing the evolution (Aqueous SEC) with time of molecular weight using BDMAT.

A) DP 20; B) DP 50; C) DP 100; D) DP 200.

Poly(*N*,*N*-dimethylacrylamide – *block* – sodium 2-acrylamido-2-methylpropane sulfonate)

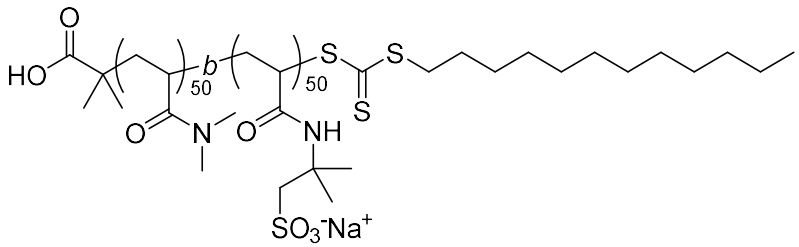

PDMA-*b*-PAMPS

Polymer 33

First block synthesis: DDMAT (37.0 mg, 0.1 mmol), DMA (510.0 mg, 5.1 mmol), water (3 mL) and VA-086 (8.6×10^{-3} mmol, 2.5 mg) (from stock solution at 20.0 mg/mL) were introduced into a flask equipped with a magnetic stirrer bar and sealed with a rubber septum. The solution was deoxygenated by bubbling with nitrogen for 10 minutes, and the vial was then placed in a temperature controlled oil bath at the desired temperature (90 °C), for the duration of time required to reach nearly full conversion (~ 2 hours).

Second block synthesis: a solution containing AMPS®2405 (2.03 g, 5.1 mmol) and further VA-086 (1.7 mg, 5.9×10^{-3} mmol) was degassed and added via a syringe to the polymerisation medium, and allowed to polymerise at the same temperature (90 °C) for the time required to reach full monomer conversion (~ 2 hours). At the end of the reaction, the mixture was allowed to cool down to room temperature and then opened to the atmosphere. Final materials were characterised using ^{1}H NMR spectroscopy and SEC ($M_{n,SEC}$ and $Đ$ were determined). The compound was then dialysed against water for 48 hours and freeze dried, to yield the final compound as a pale yellow powder; m.p. > 300 °C; ν_{max}/cm^{-1} 3325 (br. m, COO-H, stretch), 1632 (s, C=O, stretch), 1547 (m, N-H, bend), 1183 (s, C-N, stretch), 1158 (s, C-SO_3^-, stretch), 1041 (s, C=S, stretch); δH (400 MHz, D_2O) 8.2 – 7.2 (39H, br. s, NH), 3.88 – 3.22 (103H, br. m, $CH_2SO_3^-Na^+$, C*H*$_2$S and $CH_2CHSC(S)S$), 3.20 – 2.88 (347H, br. m, $N(CH_3)_2$), 2.85 – 1.93 (98H, br. m, C*H*(CONH)), 1.91 - 1.20 (515H, br. m, C*H*$_2$CH(CONH), C*H*$_2$CH(CON) and $CH_3(CH_2)_{10}CH_2S$), 1.16 – 1.05 (6H, br. s, $COOHC(CH_3)_2$), 0.88 (3H, br. s, CH_3CH_2); δC (100 MHz, D_2O), 176 (NHCO and *C*(=O)$N(CH_3)_2$), 58.20 ($CH_2SO_3^-Na^+$), 52.27 ($CH_2C(CH_3)_2$), 37.30 ($CH_2CH(CONH)$), 35.89 ($N(CH_3)_2$ and $CH_2CH(CON)$), 26.44 ($CH_2C(CH_3)_2$).

Similar polymers with varying degrees of polymerisation and conditions of polymerisation were found to exhibit similar spectroscopic data that of the title compound. The SEC molecular weight distribution for the above product can be seen in **Section 2.3.3**.

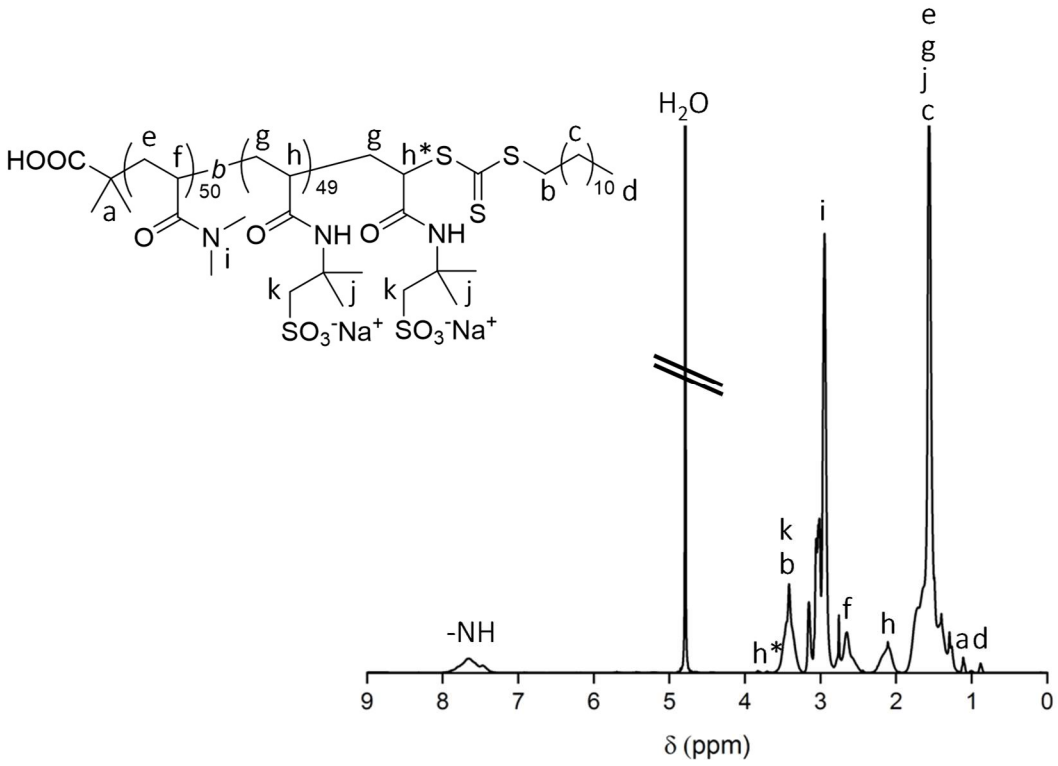

Figure S 2-6: ^{1}H NMR spectrum of PDMA-*b*-PAMPS-DDMAT (**Polymer 33**) in D_2O.

Poly(4-acryloylmorpholine)

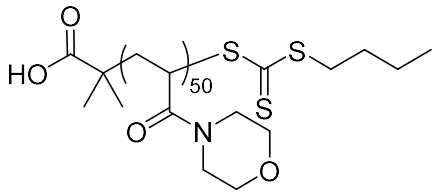

PNAM

Polymer 47, DP50

BDMAT (26.0 mg, 0.1 mmol), NAM (0.72 g, 5.1 mmol), phosphate buffer solution (2.5 mL), sodium hydroxide (5.1×10^{-2} mmol, 2.0 mg) and VA-086 (8.4×10^{-3} mmol, 2.4 mg) (from stock solution at 20.0 mg/mL) were introduced into a flask equipped with a magnetic stirrer bar and sealed with a rubber septum. The solution was deoxygenated by bubbling with nitrogen for 10 minutes, and the vial was then placed in a temperature controlled oil bath at the desired temperature (90 °C), for the duration of time required to reach nearly full conversion (~ 2 hours). At the end of the reaction, the mixture was allowed to cool down to room temperature and then opened to the atmosphere. Final materials were characterised using ^{1}H NMR spectroscopy and SEC ($M_{n,SEC}$ and $Đ$ were determined). The compound was then dialysed against water for 48 hours and freeze dried, to yield the final compound as a pale yellow powder; m.p. > 300 °C; ν_{max}/cm^{-1} 3485 (w, COO-H, stretch), 2961 (w, ar. C-H, stretch), 1631 (s, C=O, stretch), 1438 (br. m, ar. C-C, stretch), 1231 (s, C-N, stretch), 1111 (s, C-O-C, stretch), 1029 (s, C=S, stretch); δH (300 MHz, CD_3OD), 3.98 – 2.96 (395H, br. m, (N-C*H*$_2$C*H*$_2$O) x 2, C*H*$_2$S and CH$_2$C*H*SC(S)S), 2.90 – 2.25 (45H, br. m, CH$_2$C*H*(CON)), 1.95 – 1.09 (94H, br. m, C*H*$_2$CH(CON) and CH$_3$C*H*$_2$C*H*$_2$), 1.07 – 0.92 (6H, br. s, COOHC(C*H*$_3$)$_2$), 0.88 (3H, t, J =7.8 Hz, C*H*$_3$CH$_2$CH$_2$). Carbon NMR signal was too weak for analysis.

Similar polymers with varying degrees of polymerisation and conditions of polymerisation were found to exhibit similar spectroscopic data that of the title compound. The SEC molecular weight distribution for the above product can be seen in **Section 2.3.4**.

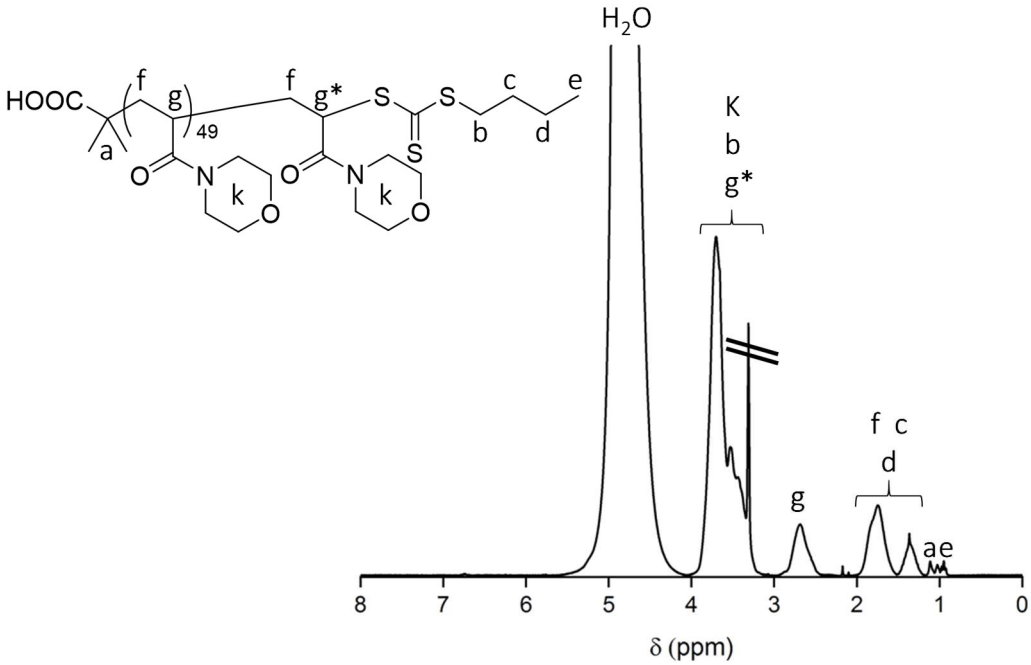

Figure S 2-7: ^{1}H NMR spectrum of PNAM (**Polymer 47**) in CD_3OD.

Poly(*N*-hydroxyethyl acrylamide)

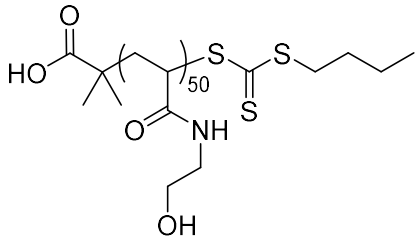

PHEAm

Polymer 49, DP50

BDMAT (26.0 mg, 0.1 mmol), HEAm (0.60 g, 5.1 mmol), phosphate buffer solution (3 mL), sodium hydroxide (5.1×10^{-2} mmol, 2.0 mg) and VA-086 (8.4×10^{-3} mmol, 2.4 mg) (from stock solution at 20.0 mg/mL) were introduced into a flask equipped with a magnetic stirrer bar and sealed with a rubber septum. The solution was deoxygenated by bubbling with nitrogen for 10 minutes, and the vial was then placed in a temperature controlled oil bath at the desired temperature (90 °C), for the duration of time required to reach nearly full conversion (~ 2 hours). At the end of the reaction, the mixture was allowed to cool down to room temperature and then opened to the atmosphere. Final materials were characterised using ^{1}H NMR spectroscopy and SEC ($M_{n,SEC}$ and $Đ$ were determined). The compound was then dialysed against water for 48 hours and freeze dried, to yield the final compound as a pale yellow powder; m.p. > 300 °C; ν_{max}/cm^{-1} 3272 (m, COO-H and O-H, stretch), 2931 (w, C-H, stretch), 1633 (s, C=O, stretch), 1548 (s, N-H, bend), 1057 (s, C=S, stretch); δH (300 MHz, CD_3OD) 3.89 – 2.85 (242H, br. m, NHC*H*$_2$, OHC*H*$_2$, C*H*$_2$S and $CH_2CHSC(S)S$)), 2.32 – 1.90 (57H, br. m, CH_2CH(CONH)), 1.85 – 1.25 (122H, br. m, C*H*$_2$CH(CONH) and $CH_3CH_2CH_2$), 1.11 – 0.99 (6H, br. s, COOH(CH_3)$_2$), 0.94 (3H, t, *J* = 7.2 Hz, $CH_2CH_2CH_3$). Carbon NMR signal was too weak for analysis.

Similar polymers with varying degrees of polymerisation and conditions of polymerisation were found to exhibit similar spectroscopic data that of the title compound. The SEC molecular weight distribution for the above product can be seen in **Section 2.3.4**.

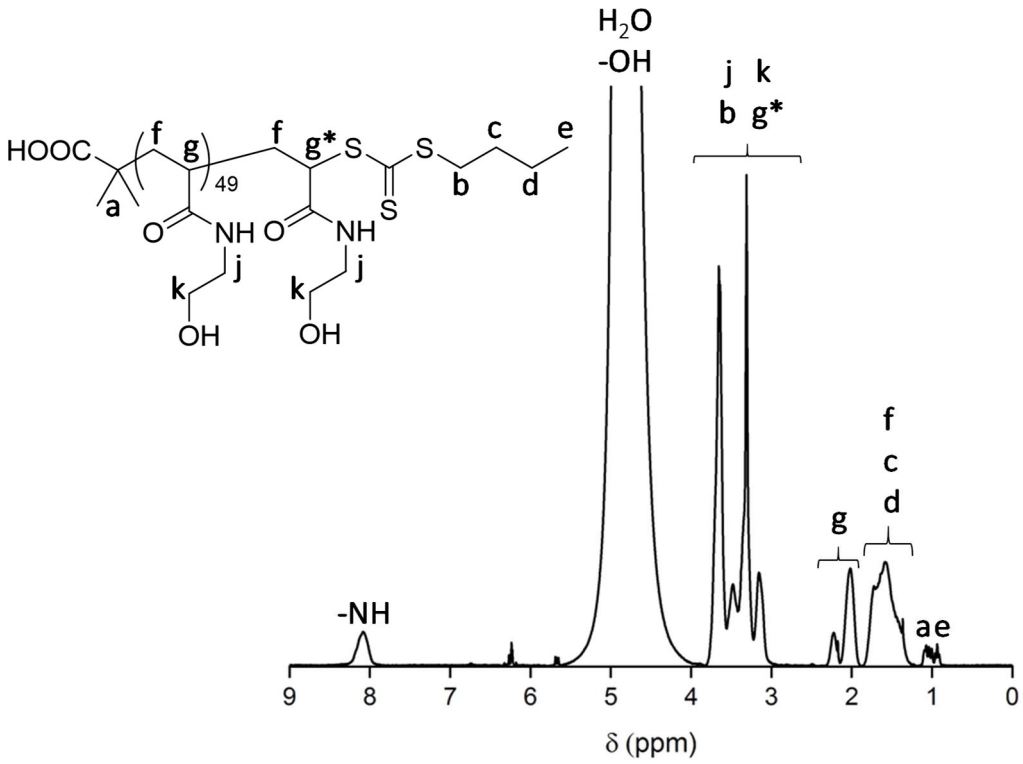

Figure S 2-8: ^{1}H NMR spectrum of PHEAm (**Polymer 49**) in CD_3OD.

2.6 References

(33) Nikolaou, V.; Simula, A.; Droesbeke, M.; Risangud, N.; Anastasaki, A.et al *Polym. Chem.* **2016**, *7*, 2452.

(38) Keddie, D. J.; Moad, G.; Rizzardo, E.; Thang, S. H. *Macromolecules* **2012**, *45*, 5321.

(42) Semsarilar, M.; Perrier, S. *Nat. Chem.* **2010**, *2*, 811.

(56) McCormick, C. L.; Lowe, A. B. *Acc. Chem. Res.* **2004**, *37*, 312.

(58) Thomas, D. B.; Convertine, A. J.; Hester, R. D.; Lowe, A. B.; McCormick, C. L. *Macromolecules* **2004**, *37*, 1735.

(59) Thomas, D. B.; Convertine, A. J.; Myrick, L. J.; Scales, C. W.; Smith, A. E.et al *Macromolecules* **2004**, *37*, 8941.

(65) Thomas, D. B.; Sumerlin, B. S.; Lowe, A. B.; McCormick, C. L. *Macromolecules* **2003**, *36*, 1436.

(66) Convertine, A. J.; Lokitz, B. S.; Lowe, A. B.; Scales, C. W.; Myrick, L. J.et al *Macromol. Rapid Commun.* **2005**, *26*, 791.

(67) Chaduc, I.; Crepet, A.; Boyron, O.; Charleux, B.; D'Agosto, F.et al *Macromolecules* **2013**, *46*, 6013.

(68) Chaduc, I.; Lansalot, M.; D'Agosto, F.; Charleux, B. *Macromolecules* **2012**, *45*, 1241.

(82) Sabhapondit, A.; Borthakur, A.; Haque, I. *Energy Fuels* **2003**, *17*, 683.

(83) Smitha, B.; Sridhar, S.; Khan, A. A. *Macromolecules* **2004**, *37*, 2233.

(84) Koromilas, N. D.; Lainioti, G. C.; Vasilopoulos, G.; Vantarakis, A.; Kallitsis, J. K. *Polym. Chem.* **2016**, *7*, 3562.

(86) Bartlett, R. L.; Medow, M. R.; Panitch, A.; Seal, B. *Biomacromolecules* **2012**, *13*, 1204.

(92) Dietzsch, M.; Barz, M.; Sch??ler, T.; Klassen, S.; Schreiber, M.et al *Langmuir* **2013**, *29*, 3080.

(93) Read, E.; Guinaudeau, A.; James Wilson, D.; Cadix, A.; Violleau, F.et al *Polym. Chem.* **2014**, *5*, 2202.

(94) Mitsukami, Y.; Donovan, M. S.; Lowe, A. B.; McCormick, C. L. *Macromolecules* **2001**, *34*, 2248.

(95) Mccormick, C. L.; Elliott, D. L. *Macromolecules* **1986**, *19*, 542.

(96) McCormick, C. L.; Johnson, B. C. *Macromolecules* **1988**, *21*, 694.

(97) McCormick, C. L.; Johnson, C. B. *Macromolecules* **1988**, *21*, 686.

(98) McCormick, C. L.; Salazar, L. C. *Macromolecules* **1992**, *25*, 1896.

(99) McCormick, C. L.; Middleton, J. C.; Cummins, D. F. *Macromolecules* **1992**, *25*, 1201.

(100) Guillaneuf, Y.; Gigmes, D.; Marque, S. R. A.; Astolfi, P.; Greci, L.et al *Macromolecules* **2007**, *40*, 3108.

(101) Anastasaki, A.; Nikolaou, V.; Nurumbetov, G.; Wilson, P.; Kempe, K.et al *Chem. Rev.* **2016**, *116*, 835.

(102) Moad, G.; Rizzardo, E.; Thang, S. H. *Acc. Chem. Res.* **2008**, *41*, 1133.

(103) Mincheva, R.; Paneva, D.; Mespouille, L.; Manolova, N.; Rashkov, I.et al *J. Polym. Sci., Part A: Polym. Chem.* **2009**, *47*, 1108.

(104) McCullough, L. A.; Dufour, B.; Tang, C.; Zhang, R.; Kowalewski, T.et al *Macromolecules* **2007**, *40*, 7745.

(105) Sumerlin, B. S.; Donovan, M. S.; Mitsukami, Y.; Lowe, A. B.; McCormick, C. L. *Macromolecules* **2001**, *34*, 6561.

(106) Sumerlin, B. S.; Lowe, A. B.; Thomas, D. B.; McCormick, C. L. *Macromolecules* **2003**, *36*, 5982.

(107) Kellum, M. G.; Smith, A. E.; York, S. K.; McCormick, C. L. *Macromolecules* **2010**, *43*, 7033.

(108) Smith, A. E.; Xu, X.; McCormick, C. L. *Prog. Polym. Sci.* **2010**, *35*, 45.

(109) Baussard, J.-F.; Habib-Jiwan, J.-L.; Laschewsky, A.; Mertoglu, M.; Storsberg, J. *Polymer* **2004**, *45*, 3615.

(110) Rizzardo, E.; Chen, M.; Chong, B.; Moad, G.; Skidmore, M.et al *Macromolecular Symposia* **2007**, *248*, 104.

(111) Richard Yodice; John J. Johnson; Ross L. Beebe; Anthony J. Brzytwa, C. D. H.; The Lubrizol Corporation: United States, 2010; Vol. US2010/0261927 A1.

(112) Johnson, A. J. B. J. "Scaled Production of RAFT CTA - a STAR Performer," The Lubrizol Corporation.

(113) Stoffelbach, F.; Tibiletti, L.; Rieger, J.; Charleux, B. *Macromolecules* **2008**, *41*, 7850.

(114) Rieger, J.; Zhang, W.; Stoffelbach, F.; Charleux, B. *Macromolecules* **2010**, *43*, 6302.

(115) Richards, S.-J.; Isufi, K.; Wilkins, L. E.; Lipecki, J.; Fullam, E.et al *Biomacromolecules* **2018**, *19*, 256.

(116) Byard, S. J.; Williams, M.; McKenzie, B. E.; Blanazs, A.; Armes, S. P. *Macromolecules* **2017**, *50*, 1482.

(117) Chenal, M.; Bouteiller, L.; Rieger, J. *Polym. Chem.* **2013**, *4*, 752.

(118) Lai, J. T.; Filla, D.; Shea, R. *Macromolecules* **2002**, *43*, 122.

(119) Convertine, A. J.; Lokitz, B. S.; Vasileva, Y.; Myrick, L. J.; Scales, C. W.et al *Macromolecules* **2006**, *39*, 1724.

(120) Lowe, A. B.; Sumerlin, B. S.; McCormick, C. L. *Polymer* **2003**, *44*, 6761.

(121) Bathfield, M.; D'Agosto, F.; Spitz, R.; Ladavière, C.; Charreyre, M.-T.et al *Macromol. Rapid Commun.* **2007**, *28*, 856.

(122) Rinaudo, M.; Desbrieres, J. *Eur. Polym. J.* **1980**, *16*, 849.

(123) Bruessau, R. J. *Makromolekulare Chemie. Macromolecular Symposia* **1992**, *61*, 190.

(124) Wang, A. R.; Zhu, S. *Macromol. Theory Simul.* **2003**, *12*, 196.

(125) van den Dungen, E. T. A.; Matahwa, H.; McLeary, J. B.; Sanderson, R. D.; Klumperman, B. *J. Polym. Sci., Part A: Polym. Chem.* **2008**, *46*, 2500.

(126) Skrabania, K.; Miasnikova, A.; Bivigou-Koumba, A. M.; Zehm, D.; Laschewsky, A. *Polym. Chem.* **2011**, *2*, 2074.

(127) Mayadunne, R. T. A.; Rizzardo, E.; Chiefari, J.; Chong, Y. K.; Moad, G.et al *Macromolecules* **1999**, *32*, 6977.

(128) Walling, C. *J. Am. Chem. Soc.* **1948**, *70*, 2561.

(129) Cao, G.-P.; Zhu, Z.-N.; Zhang, M.-H.; Le, H.-H.; Yuan, W.-K. *J. Appl. Polym. Sci.* **2001**, *81*, 2068.

(130) Cao, G.-P.; Zhu, Z.-N.; Zhang, M.-H.; Yuan, W.-K. *J. Appl. Polym. Sci.* **2004**, *93*, 1519.

(131) O'Driscoll, K. F.; Burczyk, A. F. *Polym. React. Eng.* **1993**, *1*, 111.

(132) Ilchev, A.; Pfukwa, R.; Hlalele, L.; Smit, M.; Klumperman, B. *Polym. Chem.* **2015**, *6*, 7945.

(133) Loiseau, J.; Doërr, N.; Suau, J. M.; Egraz, J. B.; Llauro, M. F.et al *Macromolecules* **2003**, *36*, 3066.

(134) Wang, X.; Luo, Y.; Li, B.; Zhu, S. *Macromolecules* **2009**, *42*, 6414.

(135) Rieger, J.; Osterwinter, G.; Bui, C.; Stoffelbach, F.; Charleux, B. *Macromolecules* **2009**, *42*, 5518.

(136) Dominguez, A.; Fernandez, A.; Gonzalez, N.; Iglesias, E.; Montenegro, L. *J. Chem. Educ.* **1997**, *74*, 1227.

(137) Pérez-Rodríguez, M.; Prieto, G.; Rega, C.; Varela, L. M.; Sarmiento, F.et al *Langmuir* **1998**, *14*, 4422.

(138) LaPlante, S. R.; Carson, R.; Gillard, J.; Aubry, N.; Coulombe, R.et al *J. Med. Chem.* **2013**, *56*, 5142.

(139) Brown, L. R.; Lauterwein, J.; Wüthrich, K. *Biochimica et Biophysica Acta (BBA) - Protein Structure* **1980**, *622*, 231.

(140) Nash, T. *Journal of Colloid Science* **1959**, *14*, 59.

(141) Rodríguez, A.; del Mar Graciani, M.; Angulo, M.; Moyá, M. L. *Langmuir* **2007**, *23*, 11496.

(142) Skrabania, K.; Laschewsky, A.; Berlepsch, H. v.; Böttcher, C. *Langmuir* **2009**, *25*, 7594.

(143) Deng, L.; Shi, K.; Zhang, Y.; Wang, H.; Zeng, J.et al *J. Colloid Interface Sci.* **2008**, *323*, 169.

CHAPTER 3:
STAR POLYMER SYNTHESIS

3.1 Abstract

Poly(sodium 2-acrylamido-2-methylpropane sulfonate) is a polyelectrolyte currently used in numerous industrial applications. Herein, the use of reversible addition fragmentation chain transfer (RAFT) polymerisation is reported to prepare a range of well-defined diblock copolymers of AMPS®2405 and either one of the following comonomers: *N*-hydroxyethyl acrylamide (HEAm), 4-acryloylmorpholine (NAM), *N*,*N*-dimethylacrylamide (DMA), acrylamide (AM), acrylic acid (AA) with 2-(butylthiocarbonothioylthio)-2-methylpropionic acid (BDMAT). Additionally, the successful synthesis of well-defined octablock copolymers of AMPS®2405 with HEAm in a one-pot process in aqueous solution was reported. Multiblock core cross-linked star copolymers of AMPS®2405 and HEAm with low dispersities (< 1.3) were synthesised. The influence of several parameters on the star formation such as the cross-linker type, cross-linker to chain transfer agent (CTA) ratio, arm length and composition on the polymerisation efficiency were explored using BDMAT RAFT agent. Finally, 2-(dodecylthiocarbonothioylthio)-2-methylpropionic acid (DDMAT) was used as another water soluble RAFT agent to synthesise well-defined star polymers which can now be considered to be scaled up for industrial purposes.

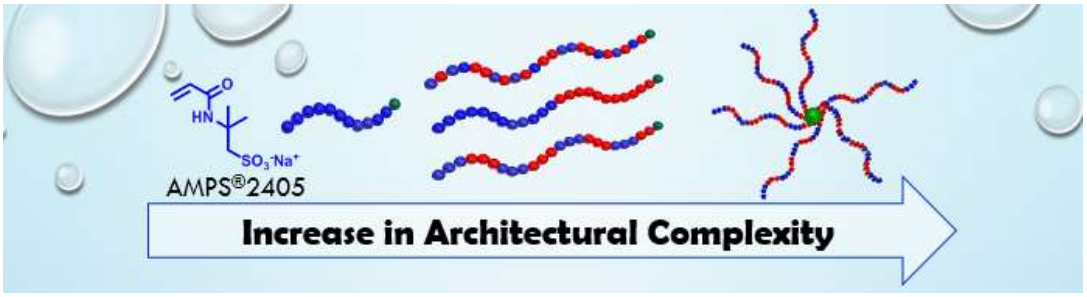

3.2 Introduction

3.2.1 Synthesis of Block Copolymers

The emergence of controlled / living radical polymerisations, such as nitroxide-mediated radical polymerisation (NMP),[100] atom transfer radical polymerisation (ATRP),[101] or reversible addition-fragmentation chain transfer polymerisation (RAFT)[42] allows for the easy preparation of well-defined polymers, both in terms of molecular weight and architecture.[102] In order to diversify its functionality and optimise its physical properties, AMPS®-based monomers are often copolymerised with other monomers such as acrylic acid,[92] acrylamide, *N*,*N*-dimethylacrylamide,[93] sodium 3-acrylamido-3-methylbutanoate,[106] or poly(ethylene glycol).[144] McCormick *et al.* extensively studied the synthesis in aqueous solution of diblock copolymers of AMPS®-based monomers with either sodium 3-acrylamido-3-methylbutanoate (AMBA) or *N*-acryloyl-L-alanine (AALm).[105-107] They investigated the micellization of diblock polymers of AMPS®-based monomers with pH responsive monomers such as AMBA and AALm. In 2001 they first reported the use of PAMPS and PAMBA homopolymers as macroCTA that can be chain extended with either AMBA or AMPS(Na) respectively (**Figure 3-1**), targeting a final diblock composition of about 50/50 mol %.[105] For each diblock copolymer synthesised, they obtained good control over the molecular weight ($Đ$ < 1.2) with the observations of monomodal chromatograms and shifts to higher molecular weights when either macroCTAs were used. However, full conversion was not reached for the homopolymer (< 90 %) even after 6 hours polymerisation. Instead, long reaction times were required to synthesise either of the diblock copolymers (~ 20 hours).

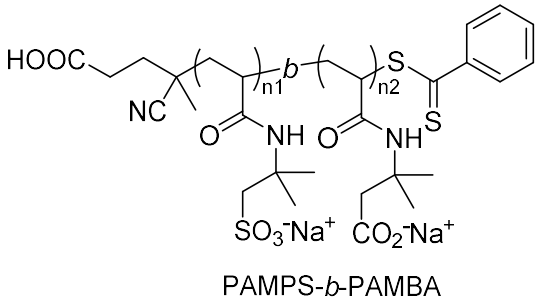

Figure 3-1: First diblock copolymers synthesised by McCormick *et al.* using AMPS(Na).[105]

In 2003, McCormick *et al.* further studied the synthesis of diblock copolymers using $PAMPS_{70}$ as macroCTA to be chain extended with AMBA.[106] These diblock copolymers were synthesised in aqueous solution and well-defined copolymers were obtained within 20 hours (monomodal distribution, $Đ < 1.3$). However, conversions of each block never reached 90 % and further purifications via dialysis was needed. In 2010 they reported the chain extension of PAMPS macroCTA with AALm, (**Scheme 3-1**).[107] In this study, again none of the polymers synthesised reached full monomer conversion (~ 60 % for the macroCTA and 90 % for all diblocks) and extended reaction times were required (~ 7.5 hours). Additionally, further purification via dialysis were necessary between each block to remove leftover monomer.

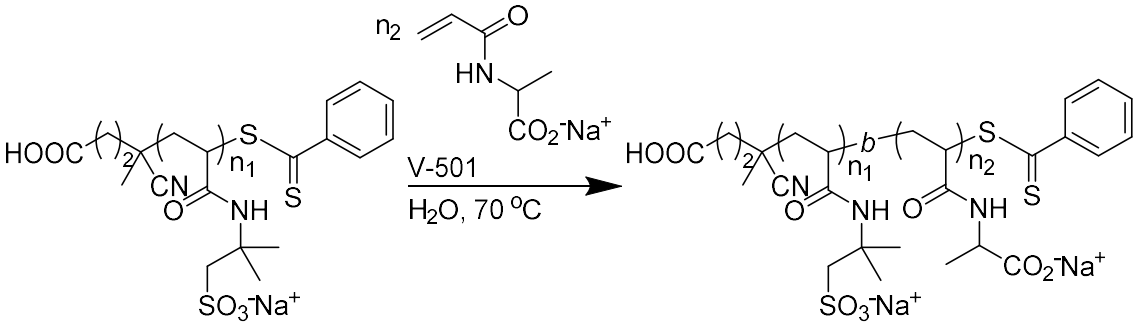

Scheme 3-1: Diblock copolymer synthesised by McCromick *et al.* using PAMPS macro CTA.[107]

Nakashima *et al*. published the synthesis of block copolymers of AMPS(Na) with *N*-isopropylacrylamide (NIPAM).[145] They synthesised diblock copolymers using a $PAMPS_{148}$ macroCTA (conv. ~ 90 %, $Đ = 1.18$) which was chain extended with NIPAM in a mixture of ethanol and water. A poor conversion of the NIPAM block was obtained (~ 26 %) after 4 hours at 70 °C and each block required further purification by dialysis.

In each of the examples mentioned above, long reaction times were required and only low monomer conversions were obtained, introducing the need for additional purification steps. In addition, the range of PAMPS architectures studied to date remain mainly limited to linear homopolymers, linear diblocks or random copolymers. Access to complex PAMPS architectures, such as multiblock or star copolymers, could help to develop a novel class of polyelectrolytes with interesting physical properties (**CHAPTER 4**). Moreover, complex structures such as branched polymers have only been scarcely studied, and to our knowledge, only a single example of a star polymers has been published, which will be further discussed in **Section 3.2.3**.

3.2.2 Synthesis of Multiblock Copolymers

Highly ordered multiblock copolymers can be efficiently obtained by RAFT polymerisation in aqueous solution, especially when using monomers with a high rate of polymerisation (k_p) such as acrylamide.[62] The concentration of initiator was shown to be an essential parameter to optimise the polymerisation. Indeed, the theoretical livingness (**Equation 4**) can be kept high enough to retain the chain end functionality (α- and ω- chain end group) by decreasing the initiator concentration, thus decreasing termination step occurrences.[50,146] Such systems typically allow for the preparation of multiblock copolymers (up to 20 blocks, $Đ < 1.5$) in a one-pot process, where full monomer conversion can be reached for each chain extension step.[48,49,62,146,147] Gody *et al.* first reported the synthesis of decablock homopolymers of 4–acryloylmorpholine and *N*,*N*-dimethylacrylamide by RAFT polymerisation using a trithiocarbonate chain transfer agent in a mixture of water and dioxane.[47] They obtained full monomer conversion between each chain extension (24 hours / block) while retaining high livingness until the last block (~ 97 % after 10 blocks). Their final materials were well-defined with monomodal molecular weight distributions and dispersities as low as 1.15 ($(PNAM_{10})_{10}$). The author further demonstrated that by tuning the initiator concentration, temperature of polymerisation and the solvent, they could decrease the time of reaction for each block from 24 hours to 2 hours per block while still obtaining high monomer conversion (> 99 %) and high livingness (96.6 %).[48] They used this feature to synthesise a more complex dodecablock copolymer (**Figure 3-2**) by alternating the polymerisation of different monomers with a final dispersity of 1.41 and livingness of 92.3 %.

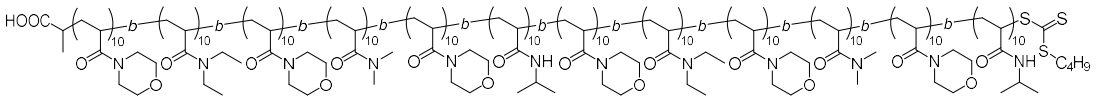

Figure 3-2: Dodecablock copolymer synthesised by RAFT polymerisation.[48]

Recently, Martin *et al.* investigated the synthesis of multiblock copolymers at room temperature using a redox initiation system.[147] This work herein demonstrated the possibility to use acrylate monomers, which are typically prone to side reactions at high temperatures. They synthesised a wide range of copolymers using either

acrylamide, acrylate or alternating acrylates and acrylamides. Synthesis of each copolymer was shown to be controlled ($Đ$ < 1.5) with full monomer conversion between each block extension. However, in this study the polymerisation reaction times were increased (i.e. from 2 hours to 24 hours for each block) when the temperature was decreased from 70 °C to 25 °C. Additionally, a mixture of water and dioxane was still used to ensure full CTA solubilisation at the start of the reaction.

Overall RAFT polymerisation was shown to be particularly advantageous to synthesise multiblock copolymers in that the final materials do not require extensive purification steps due to full monomer conversion and the lowered termination process. In addition, the presence of the CTA in the polymers, which can easily be converted into a thiol, offers a convenient functionalization handle at the end of the polymer chain. Alternately, the CTA can be subsequently removed by post-polymerisation modifications.[43,44,148]

3.2.3 Synthesis of Star Polymers

RAFT polymerisation also provides a suitable method for the preparation of more complex architectures such as star-shaped polymers, hyperbranched polymers and nanoparticles.[149-151] The physical properties of star polymers are known to vary greatly in comparison to their linear counterparts, making them attractive materials for numerous applications ranging from oil recovery to drug delivery.[152] Polymerisation techniques used to prepare star polymers can be divided into two general strategies; core-first or arm-first approach (**Figure 3-3**).[149,153] The core-first approach relies on the use of multifunctional CTAs and typically results in star-shaped polymers with a well-defined number of arms.[154-156] The arm-first approach is a convergent method that consists of chain extending a previously-synthesised arm in the presence of a multifunctional monomer that behaves as a cross-linker.[157-159] The latter typically allows less control over the number of arms incorporated, but provides better control over the length of the arms incorporated.[160,161] The first synthetic star polymer was reported by Flory & Schaefgen using condensation polymerisation, the structure of the star being $R[\text{-}CO[\text{-}NH(CH_2)_6)CO\text{-}]_n\text{-}OH]_v$ with R a v-valent radical and v varying from 1 to 8.[162] The research showed a decrease in intrinsic viscosity and melting point when the branching increased from 1 to 8.

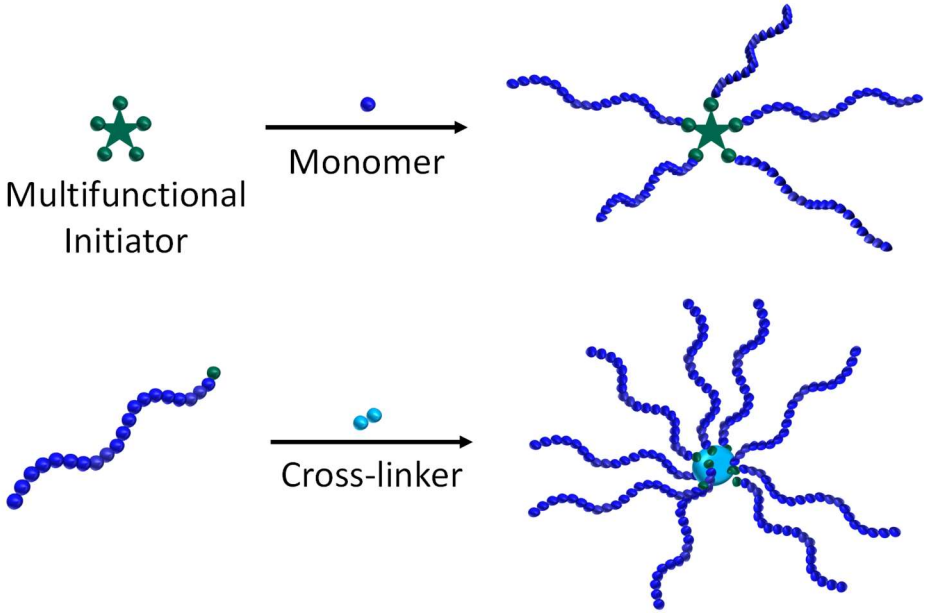

Figure 3-3: Star polymer synthesis using either the core first (top) or arm first approach (bottom).

The use of the core first approach has already been well studied, but remains limited by the need to have multifunctional RAFT agents with high purity in order to get only one well-defined population of star polymers with the desired number of arms.[154,163,164] The principal disadvantage of using these RAFT agents is their poor solubility in water. Thang *et al.* used CTA - **A** (**Figure 3-4**) to polymerise methyl methacrylate (MMA) or styrene (S) in toluene and obtained well-defined star homopolymers ($Đ_{PMMA}$ = 1.16 and $Đ_{PS}$ = 1.18) within 20 hours.[154] Further, they demonstrated the ability to use $(PMMA_{46})_4$ as macroCTA to synthesise a well-defined diblock star copolymer ($P(MMA\text{-}b\text{-}POEGMA)_4$) with dispersity as low as 1.27. Zhang *et al.* used the multifunctional CTA – **B** (**Figure 3-4**) to polymerise *N*-isopropylacrylamide in 1,4-dioxane.[163] Well-defined star homopolymers ($Đ$ < 1.2) were obtained within 2 hours, however, only 64 % of monomer conversion was observed. Another example is the use of CTA – **C** (**Figure 3-4**) by Saeed *et al*. to synthesised a well-defined 4–arms star polymer using 2-(dimethylamino) ethyl acrylate in 2-butanone with dispersities lower than 1.4.[164]

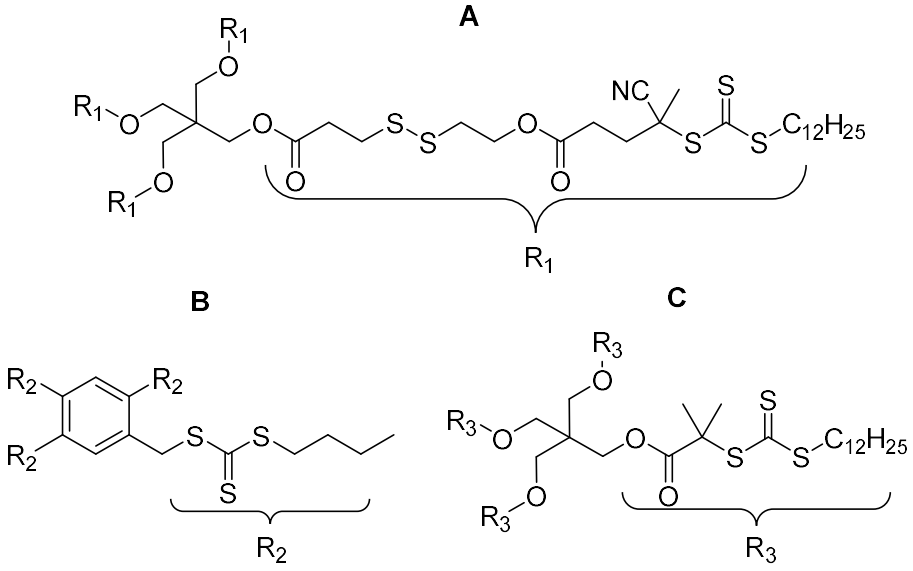

Figure 3-4: Examples of multifunctional RAFT agents used in the literature.[154,163,164]

Synthesising star polymers utilizing the core cross-linked star (CCS) polymer synthesis approach using RAFT polymerisation has previously been shown to be very efficient.[165-167] Boyer *et al.* studied the synthesis of narrow star-shaped polymers using the arm first approach by RAFT polymerisation.[168] They attempted to synthesise star polymers using a wide range of arms (*tert*-butyl acrylate or *N*-isopropylacrylamide or

OEG-A, **Scheme 3-2**) with four different cross-linkers. They studied the effect of compartmentalisation of the cross-linker in toluene on the efficiency of the star polymer formation by emulsion polymerisation. They found that the lower the solubility of the cross-linker, the higher the number of arms incorporated and the lower the dispersity of the final star polymer. For example, when POEG-A was used as arms with the cross-linker **C** (**Scheme 3-2**) the best arm incorporation was obtained (~ 95 %) with a dispersity as low as 1.17. They also studied other parameters than the cross-linker solubility, such as the arm length, the arm composition, the ratio of cross-linker to CTA, the time of polymerisation and finally the solvent. All of the aforementioned parameters were shown to be critical to obtain well-defined star-shaped polymers with high incorporation of arms into the star and low dispersities.

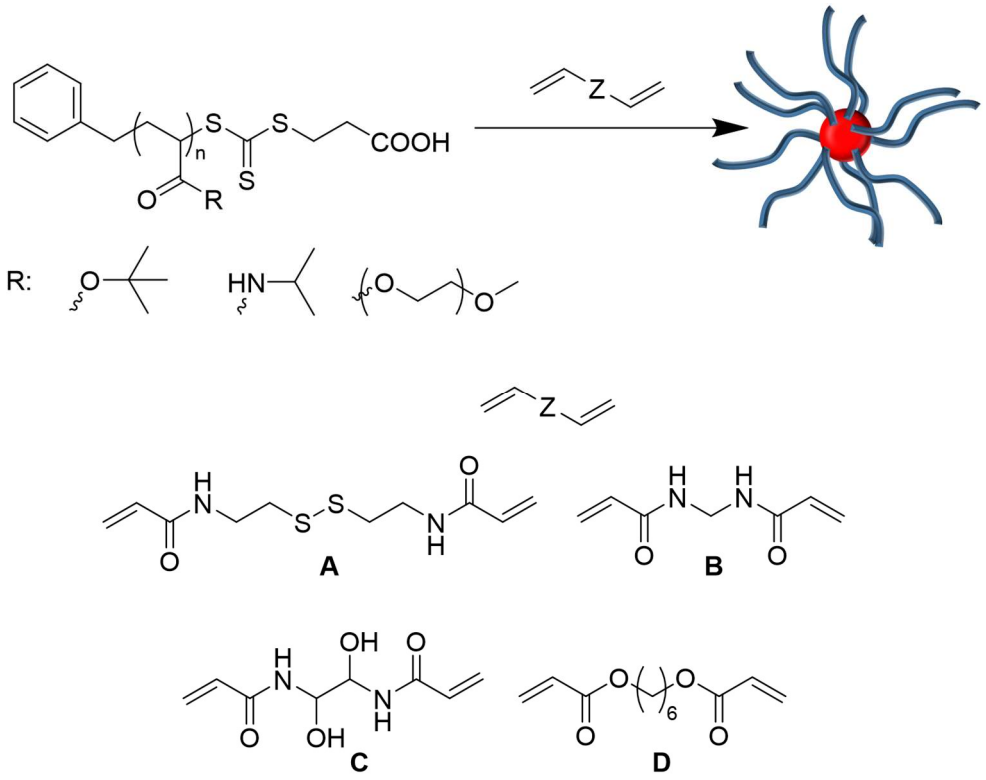

Scheme 3-2: Arms and cross-linkers used by Boyer *et al.* to investigate the synthesis of star polymers by RAFT polymerisation using the arm first approach.[168]

More recently the synthesis of star polymers using the arm first approach by RAFT polymerisation has been studied in aqueous solution.[166] The arm was first synthesised in aqueous solution (P(PEGMA)) and then a hydrophobic cross-linker was added (1,6-hexanediol dimethacrylate). Well-defined core cross-linked star polymers were

obtained with a percentage of arm incorporated higher than 90 % and dispersities lower than 1.1. They confirmed the previous results obtained by Boyer *et al.* and obtained a higher efficiency of the process when the cross-linker was compartmentalised (i.e. emulsion polymerisation). Despite the existence of readily available methods, the preparation of linear and star-shaped multiblock polymers of PAMPS has not been reported so far. As far as we are aware, only one 3-arms diblock star copolymer using AMPS®-based monomer (2nd block) has been reported, by Lund *et al.* in 2015 (**Figure 3-5**).[155] The star polymer was synthesised using the core first approach by ATRP in a mixture of water and DMF at 25 °C. However, a high dispersity of the star polymer was obtained ($Đ$ = 1.58).

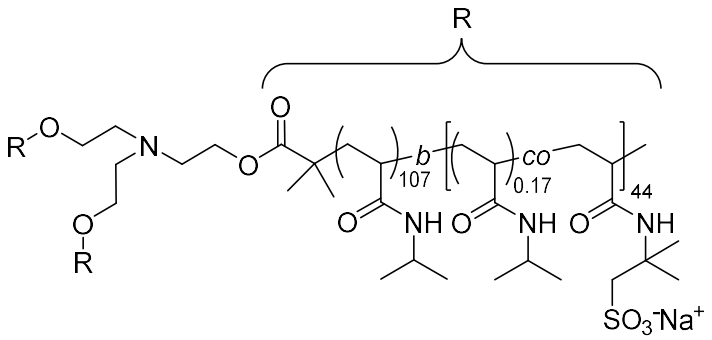

Figure 3-5: Diblock star copolymer (3-arms) synthesised using the arm first approach by ATRP with NIPAM and AMPS® based monomer.[155]

3.2.4 Project Approach

RAFT polymerisation in aqueous solution was described for the preparation of complex architectures using AMPS®2405. This includes the synthesis of diblock copolymers of AMPS®2405 with a wide range of comonomers but also the synthesis of well-defined multiblock and random copolymers of AMPS®2405 with either HEAm or NAM comonomers. Core cross-linked star polymers using the arm-first approach were then synthesised.

- The efficiency of PAMPS macroCTA was first evaluated by reinitiating the polymerisation with AMPS®2405 itself in a one-pot process.

- The effect of the pH on the reinitiation was then evaluated by either increasing the pH to 10 or decreasing it to 2.

- The effect of the reactivity of the newly incorporated monomer on the reinitiation was then studied with four different acrylamides (AM, NAM, HEAm, DMA) and one acrylate monomer (AA).

- High order multiblock copolymers using AMPS®2405 monomer were synthesised, with the effect of block length and comonomer being studied.

- Optimisation of the star polymer synthesis using the arm first approach: effect of cross-linker type, cross-linker to CTA ratio, cross-linker concentration, arm length, time of reaction.

- Synthesis of multiblock star copolymers using the arm first approach by RAFT polymerisation.

- Effect of the CTA used for the star polymer synthesis by using either DDMAT or BDMAT. The use of DDMAT would increase efficiency of the star polymer synthesis by obtaining a better compartmentalisation of the cross-linker into the core of the star polymer.

3.3 Results and Discussions

3.3.1 AMPS®2405 Copolymerisation – Proof of Concept

The preparation of multiblock copolymers was first investigated using blocks solely composed of AMPS®2405. The polymerisation conditions for the first block were optimised in **CHAPTER 2** in order to retain a high "livingness" of the system. RAFT polymerisation typically leads to two types of polymer chains, thiocarbonyl-thio ended chains (living chains) and initiator-ended chains (dead chains). In order to subsequently prepare block copolymers with good precision, it is important to have both a low percentage of dead chains and a good retention of the end group, which is typically referred to as the "livingness" of the system (**Equation 4**).[47] High livingness is typically obtained by either keeping the concentration of initiator low or by using a slowly decomposing initiator. In this study, an optimum concentration of initiator (VA-086) was determined to be of 2.5×10^{-3} M. Using this parameter, 20 % of the initiator is expected to be decomposed after 2 hours (full monomer conversion). When targeting DP = 10, this represented an initial ratio $[BDMAT]_0/[VA\text{-}086]_0 = 60$, a final ratio of $[BDMAT]_0/[VA\text{-}086]_{consumed} = 300$ and a livingness of approximately 99.7 % for the polymerisation (**Table S 3-1**). The macroCTA $PAMPS_{10}$ (**Polymer 53**) prepared using these conditions was characterised using MALDI-ToF (**Figure 3-6**) to confirm the presence of predominantly one population (living chains), using experimental conditions for MALDI-ToF as optimised by Mullen *et al.* for polystyrene sulfonate.[169] The spectrum (**Figure 3-6**) obtained for this macroCTA reveals one narrow main population with m/z corresponding to an experimental DP of 8 (peak 1). A second minor population can be observed (peak 3) which corresponds to the addition of a second Na^+ on the polymeric chains by ionisation of the end group (COOH). A third minor population corresponding to the fragmentation of the C-S bond between the end group and the polymer chains can be observed (peak 4).[170] MALDI-ToF results confirmed a good control over the polymerisation of AMPS®2405 monomer using RAFT polymerisation and renders this macroCTA suitable for the synthesis of multiblock polymers.

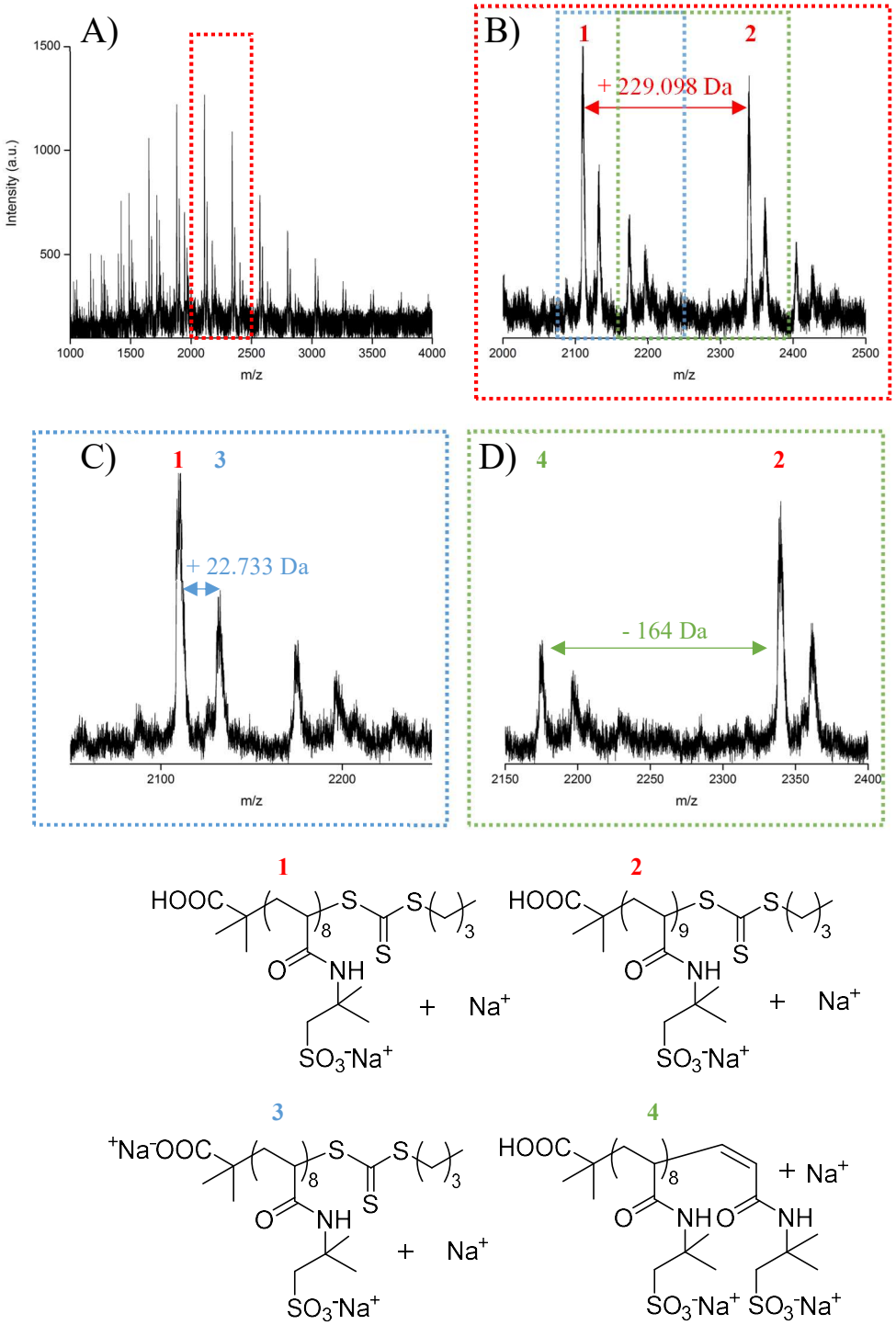

Figure 3-6: MALDI-ToF mass spectra of $PAMPS_{10}$.

A) Full spectra; B) Zoom corresponding to a DP of 8 and 9; C) Zoom corresponding to a DP of 8; D) Zoom corresponding to the CTA degradation.

Using these optimised conditions, an octablock homopolymer (**Table 3-1**, **Polymer 56**) was successfully synthesised by a one-pot sequential monomer addition method targeting a DP of 10 for each chain extension. Full monomer conversion was obtained between each chain extension (**Table S 3-1** and **Figure S 3-1**) despite the monomer

concentrations decreasing from 1.5 to 0.32 M during the polymerisation. It is noteworthy that the first block required a longer reaction time (2 hours) to reach full monomer conversion, with subsequent blocks only taking approximately 1 hour, which can be attributed to the slower consumption of the initial CTA (i.e. induction period) upon comparison to the macroCTA formed later (**Figure 3-7**).

Table 3-1: ^{1}H NMR spectroscopic and SEC data analysis for the multiblock homopolymer $[PAMPS_{10}]_8$ after each chain extension using $PAMPS_{10}$ macroCTA.[a]

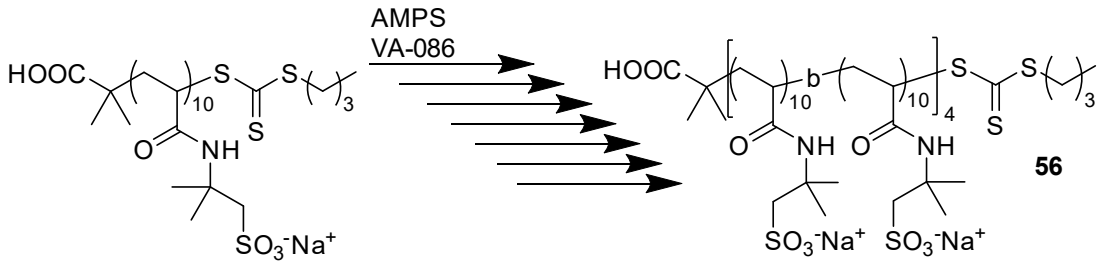

Polymer	Block	Multiblock composition	Conv. (%)[b]	$M_{n,th}$ (g/mol)[c]	$M_{n,SEC}$ (g/mol)[d]	$Đ$[d]
53	1	$PAMPS_{10}$	99	2,500	5,700	1.09
54	2	$[PAMPS_{10}]_2$	99	4,800	8,300	1.09
55	3	$[PAMPS_{10}]_3$	> 99	7,100	9,600	1.09
-	4	$[PAMPS_{10}]_4$	> 99	9,300	12,300	1.10
-	5	$[PAMPS_{10}]_5$	> 99	11,600	14,800	1.12
-	6	$[PAMPS_{10}]_6$	> 99	13,900	17,000	1.13
-	7	$[PAMPS_{10}]_7$	> 99	16,200	17,700	1.16
56	8	$[PAMPS_{10}]_8$	> 99	18,400	18,900	1.18
57	-	$PAMPS_{80}$	> 99	18,800	14,100	1.19

[a] Polymerisations were conducted at 90 °C in phosphate buffer solution; [b] Conversions were determined by ^{1}H NMR spectroscopy, using **Equation 1**; [c] Theoretical M_n values were calculated using **Equation 2**; [d] Experimental M_n and $Đ$ values were determined by size-exclusion chromatography in 20 % MeOH / 80 % 0.1M $NaNO_3$ in milli-Q water eluent using a conventional calibration obtained with PEG/PEO standards.

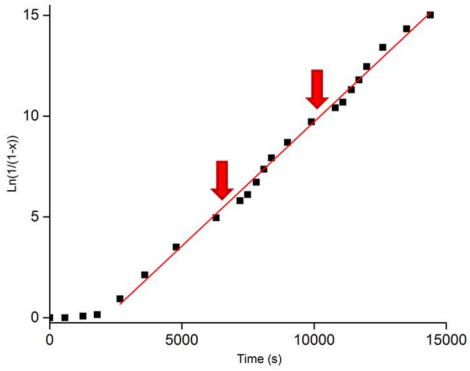

Figure 3-7: Pseudo-first order plot versus the time for the chain extension of PAMPS with AMPS®2405 in water at 90 °C with VA-086. The red arrows denote the monomer addition up to three blocks.

SEC analysis shows monomodal molecular weight distributions and a shift towards higher molecular weight after each monomer addition (**Figure 3-8 – A**). The monodisperse nature of the final octablock homopolymer (i.e. 1.18) confirms the high livingness of the system throughout the whole process (98.5 %) (**Table S 3-1** and **Figure S 3-1**). This is further supported by the relatively linear increase of the number-average molecular weight observed with increasing number of blocks (**Figure 3-8 – B**). The number-average molecular weight measured by SEC was found to be slightly higher than the theoretical values, which can be attributed to dissimilarity in the hydrodynamic volume of PAMPS (polyelectrolyte) and the PEG/PEO standards used for calibrating the aqueous SEC.[147,171]

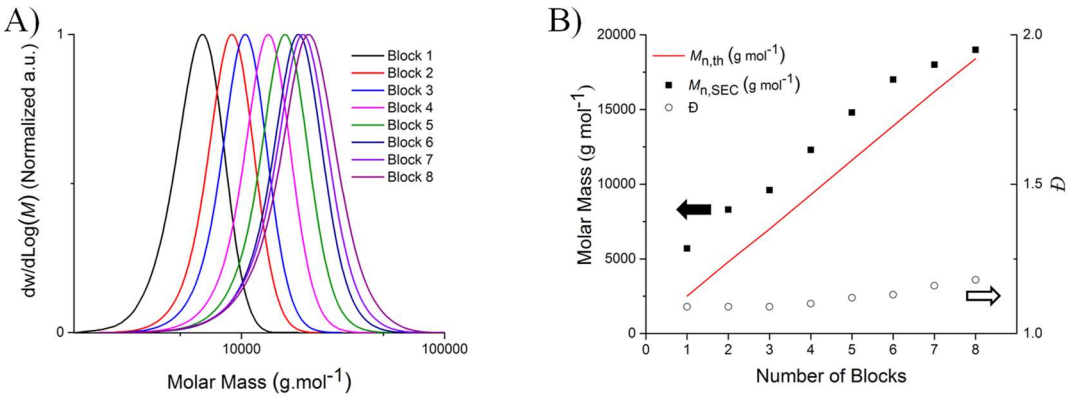

Figure 3-8: Stepwise characterisation of each chain extension of the multiblock AMPS®2405 homopolymer.

A) Aqueous-SEC molecular weight distributions; B) Molecular weight and dispersity versus the number of blocks.

Overlay of the molecular weight distributions of $(PAMPS_{10})_8$ and the corresponding homopolymer $PAMPS_{80}$ (**Figure 3-9**, **Polymer 56** and **57**) shows a slightly higher molecular weight for the octablock ($(PAMPS_{10})_8$: $M_{n,SEC}$ = 18,900 g/mol , $Đ$ = 1.18; $PAMPS_{80}$: $M_{n,SEC}$ = 14,100 g/mol, $Đ$ = 1.18). A similar observation was made by Gody *et al.* for a decablock of poly(*N*,*N*-dimethylacrylamide) (PDMA) versus its homopolymer counterpart.[47]

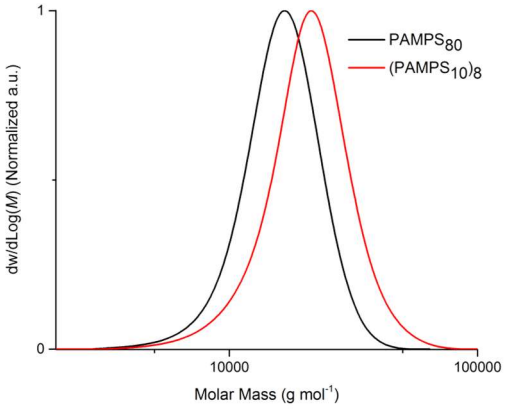

Figure 3-9: Comparison of the final SEC molecular weight distributions (aqueous SEC using PEG/PEO standard) obtained for homopolymer $PAMPS_{80}$ and octablock $(PAMPS_{10})_8$ as synthesised by aqueous RAFT polymerisation.

3.3.2 Block Copolymer Synthesis using PAMPS macro CTA

The copolymerisation of AMPS®2405 using $PAMPS_{50}$-BDMAT macroCTA (**Polymer 19**) (first block) was investigated with other water soluble monomers (second block, DP = 50): acrylamide (AM), acrylic acid (AA), 4-acryloylmorpholine (NAM), *N*-hydroxyethyl acrylamide (HEAm) and *N*,*N*-dimethylacrylamide (DMA). These newly synthesised water soluble diblock copolymers contain different functionalities and may form a new group of polyelectrolytes to be used for a wide range of applications.[172] It is worth noting that the RAFT polymerisation of AA and AM have been shown to be governed by temperature as well as pH.[173] Indeed, Charleux *et al.* have shown that the kinetics of AA polymerisation by RAFT process was governed by the pH and consequently the monomer ionisation, showing that at pH lower than 2 (neutral monomer) the polymerisation was faster than at higher pH (ionic monomer).[67] Similarly, McCormick *et al.* studied the effect of the pH of AM polymerisation in water by RAFT and have shown that the increase of the pH and temperature promoted the hydrolysis of the RAFT agent by the $-NH_2$ group being released as a NH_4^+.[59]

Hence, the effect of pH on the chain extension of PAMPS macroCTA with AMPS itself was then evaluated. The polymerisation of the first block ($PAMPS_{50}$) was conducted at pH 6 while the pH for the second and third block was either reduced to pH 2 by adding drops of HCl or increased to pH 10 by adding drops of $NaOH_{(aq.)}$ after monomer addition into the solution (**Table 3-2**). The pH did not show any effect over the RAFT polymerisation of AMPS®2405 when the second block was polymerised at either pHs (pH 2, 6 and 10), with a similar shift of the SEC peak towards higher molecular weight obtained, alongside low dispersities (~ 1.2) (**Figure 3-10 – A** and **B**). When a third block was synthesised at pH 2 or 6, well-defined polymers were obtained while at pH 10 a bimodal distribution was observed (**Figure 3-10 – C, Polymer 63**) with higher dispersity (1.38). The poor reinitiation at pH 10 can be attributed to the possible hydrolysis of the trithiocarbonate macroCTA in basic conditions. Additionally, the polymerisation medium at the end of the third chain extension was shown to be slightly turbid when the polymerisation was conducted at pH 10 (Z-group precipitation) while the medium was clear at pH 2 and 6.[58]

Table 3-2: Diblock and triblock copolymers synthesised using BDMAT-PAMPS$_{50}$ macroCTA varying the pH (pH, conversions, SEC analysis).[a]

Polymer	MacroCTA	Block	pH	Conv. (%)[b]	$M_{n,th}$ (g/mol)[c]	$M_{n,SEC}$ (g/mol)[d]	$Đ$[d]
58	**19**	2	2.3	> 99	24,700	14,200	1.18
59	**19**	2	5.8	> 99	24,600	14,300	1.18
60	**19**	2	10.1	> 99	24,700	15,400	1.23
61	**58**	3	2.1	> 99	34,200	18,000	1.23
62	**59**	3	5.9	> 99	34,100	18,100	1.25
63	**60**	3	10.1	< 99	-	17,500	1.38

[a] Polymerisations were conducted at 90 °C in phosphate buffer solution; [b] Conversion were determined by ^{1}H NMR spectroscopy, using **Equation 1**; [c] Theoretical M_n values were calculated using **Equation 2**; [d] Experimental M_n and $Đ$ values were determined by size-exclusion chromatography in 20 % MeOH / 80 % 0.1M $NaNO_3$ in milli-Q water eluent using a conventional calibration obtained with PEG/PEO standards.

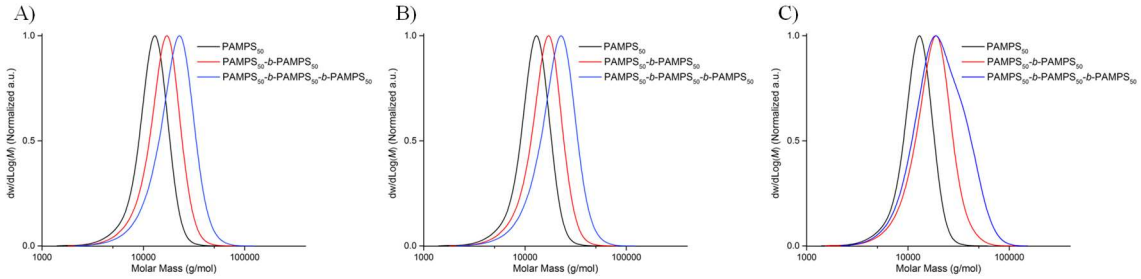

Figure 3-10: Aqueous SEC molecular weight distributions showing the chain extension of PAMPS with AMPS®2405.

A) pH 2; B) pH 6; C) pH 10.

The chain extension of PAMPS$_{50}$-BDMAT macro CTA was then evaluated using different comonomers (**Table 3-3**). Chain extensions were first conducted in the polymerisation medium where pH is mainly governed by the pH of the monomer (i.e. pH 2 for AA, **Table 3-3**, **Polymer 70**). The polymerisations were prepared at pH 6 for NAM, DMA, HEAm and AM but at pH 2 for AA (**Table 3-3**). However, the polymerisation medium of AM at pH 6 became turbid after a few minutes at 90 °C and the pH effect was further investigated for this monomer. The pH for the chain extension of PAMPS$_{50}$ with AM was decreased to pH 2 and the medium was no longer turbid (**Figure S 3-6**).

Table 3-3: Diblock copolymers synthesised in this chapter using BDMAT-PAMPS$_{50}$ macro CTA (pH, conversions, SEC analysis).[a]

PAMPS$_{50}$-*b*-PAMPS$_{50}$, **59**

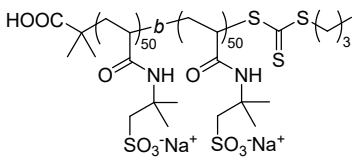

PAMPS$_{50}$-*b*-PNAM$_{50}$, **64**

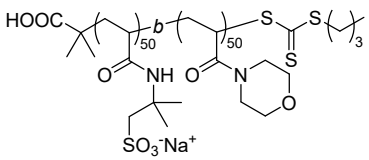

PAMPS$_{50}$-*b*-PDMA$_{50}$, **65**

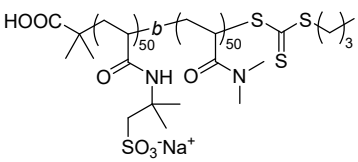

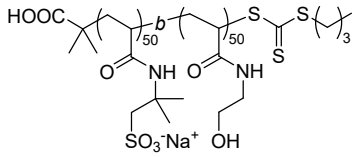

PAMPS$_{50}$-*b*-PHEAm$_{50}$, **66**

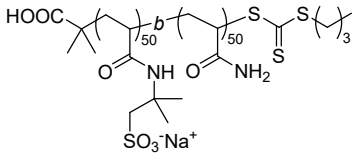

PAMPS$_{50}$-*b*-PAM$_{50}$, **67**

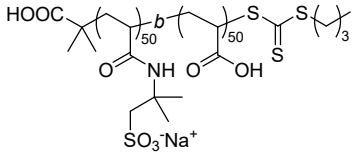

PAMPS$_{50}$-*b*-PAA$_{50}$, **70**

Polymer	Monomer	K_p^{app} (10^{-4}) (s^{-1})	pH	Conv. (%)[b]	$M_{n,th}$ (g/mol)[c]	$M_{n,SEC}$ (g/mol)[d]	$Đ$[d]
64	NAM	10.1	6.3	> 99	18,300	7,400	1.32
65	DMA	6.58	6.5	> 99	16,200	11,200	1.19
66	HEAm	7.22	6.2	> 99	17,500	11,400	1.22
67	AM	12.0, 2.86	2.1	98	14,800	10,500	1.22
68	AM	-	6.2	93	14,700	10,100	1.24
69	AM	-	10.3	39	12,800	11,600	1.19
70	AA	5.18	2.4	92	14,700	15,300	1.12

[a] Polymerisations were conducted at 90 °C in phosphate buffer solution; [b] Conversions were determined by ^{1}H NMR spectroscopy, using **Equation 1**; [c] Theoretical M_n values were calculated using **Equation 2**; [d] Experimental M_n and $Đ$ values were determined by size-exclusion chromatography in 20 % MeOH / 80 % 0.1M $NaNO_3$ in milli-Q water eluent using a conventional calibration obtained with PEG/PEO standards.

For the five different chain extensions, full monomer conversion and low dispersities were obtained, as shown by ^{1}H NMR spectroscopy and aqueous SEC ($Đ$ < 1.5), which indicated that the polymerisation proceeded in a controlled manner. Kinetics of the five different copolymers revealed different reactions rates for each monomer (**Figure 3-11**, **Figure S 3-2** to **Figure S 3-5**). The acrylic acid block (K_p^{app} = 5.18x10^{-4} s^{-1}) showed the slowest reinitiation which is likely due to the difference of reactivity between the acrylamide macroCTA and the newly acrylate monomer added onto the polymeric chains. HEAm (K_p^{app} = 6.58x10^{-4} s^{-1}) and DMA (K_p^{app} = 7.22x10^{-4} s^{-1}) exhibited similar polymerisation rates, which can be attributed to the independence of the pH on the monomer ionisation in aqueous solution. NAM (K_p^{app} = 1.01x10^{-3} s^{-1}) revealed the fastest reinitiation which could be attributed to the reactivity of the double bond being affected by the tertiary amide and conformation restriction of the cyclic ring. When AM was polymerised two different steps were observed; a rapid initiation (K_p^{app} = 1.20x10^{-3} s^{-1}) followed by a decrease of the polymerisation rate (K_p^{app} =

$2.86x10^{-4}$ s^{-1}). This may be explained by possible hydrolysis of the RAFT agent by the ammonium released from the monomer affecting the termination and initiation rates.[59]

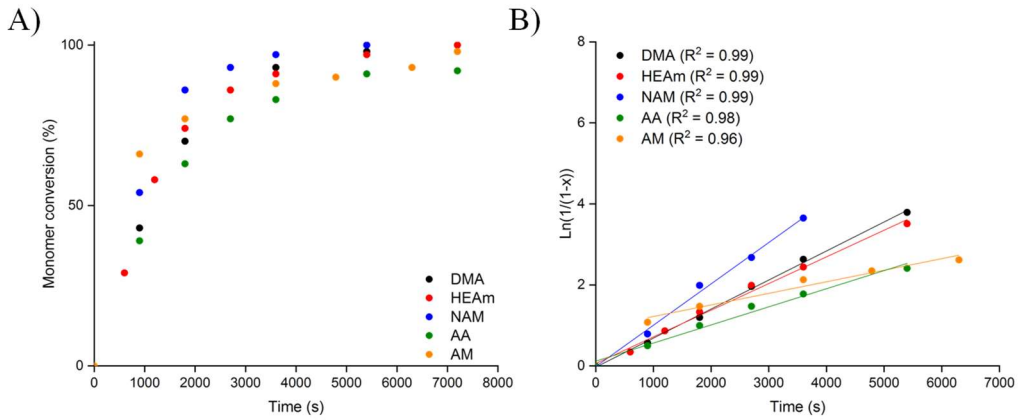

Figure 3-11: $PAMPS_{50}$ chain extension with various acrylamide and acrylic monomers.
A) Monomer conversion versus time; B) First order plot $Ln([Monomer]_0/[Monomer])$ versus time.

Overall, the chain extension of $PAMPS_{50}$ macroCTA with other water soluble monomers has shown narrow and monomodal SEC distributions ($Đ < 1.5$) (**Table S 3-2**), however, only $PAMPS_{50}$-*b*-PAA_{50} showed the expected shift of the SEC distribution towards higher molecular weight (**Figure 3-12 – A, Table S 3-3**). This can be explained by the difference in hydrodynamic volume between the highly charged PAMPS and that the newly blocks synthesised were neutral except in the case of AA. When the diblock copolymers were analysed using DMF SEC (**Figure 3-12 – B**, **Table S 3-3**) with polar gel columns, shifts towards higher molecular weight were observed except for AA. However, the dispersities obtained were close to 1.3 due to the presence of a tail at lower molecular weights.[174] The tailing may be explained by interactions between the macromolecules and the columns.[175] Another way to characterise the diblock copolymers with blocks of different nature (anionic versus neutral) is the use of SEC with triple detection in which the molecular weight is no longer calculated relative to the hydrodynamic volume of standards. As expected, the SEC distributions (**Figure 3-12 – C**, **Table S 3-3**) obtained with triple detection all revealed shifts towards higher molecular weight for the five diblock copolymers.

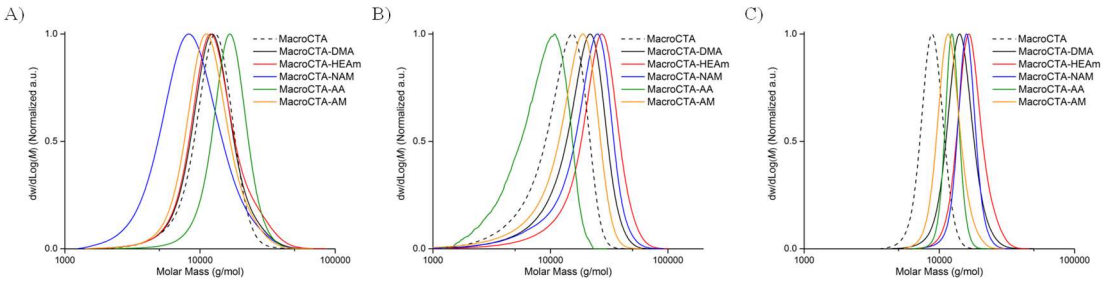

Figure 3-12: SEC molecular weight distributions of the chain extension of $PAMPS_{50}$ with different monomers (DMA, HEAm, NAM, AA, AM) using different SEC eluents and detectors.

A) Aqueous SEC using conventional calibration; B) DMF LiBr SEC using conventional calibration; C) Aqueous SEC using triple detection (LS, RI and VS detectors in series).

In order to further confirm that the artefacts observed with SEC when using conventional calibration (shifts towards lower molecular weights) is mainly linked to the difference of hydrodynamic volume, two different diblock copolymers using either $PAMPS_{50}$ or $PDMA_{50}$ were synthesised as the first block. These two macroCTAs were then chain extended either with DMA or AMPS®2405 respectively (**Scheme 3-3**).

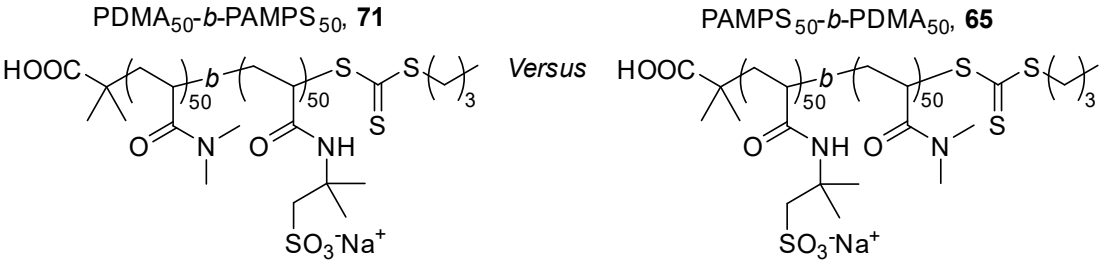

71

Conv.[a] > 99 %

$M_{n,th}$[b] = 16,500 g/mol

$M_{n,SEC}$[c] = 12,700 g/mol

$Đ$[c] = 1.21

65

Conv.[a] > 99 %

$M_{n,th}$[b] = 16,500 g/mol

$M_{n,SEC}$[c] = 10,100 g/mol

$Đ$[c] = 1.21

[a] Conversions were determined by ^{1}H NMR spectroscopy, using **Equation 1**; [b] Theoretical M_n values were calculated using **Equation 2**; [c] Experimental M_n and $Đ$ values were determined by size-exclusion chromatography in 20 % MeOH / 80 % 0.1M $NaNO_3$ in milli-Q water eluent using a conventional calibration obtained with PEG/PEO standards.

Scheme 3-3: Diblock copolymers synthesised using either BDMAT-$PAMPS_{50}$ or $PDMA_{50}$ macro CTA.

When PAMPS was chain extended with DMA, no shift towards higher molecular weight was observed, while a clear shift was observed when PDMA was used for the first block then chain extended with AMPS®2405. This supports the above-mentioned observations and that SEC with conventional calibration has limitations when monomers of different nature were used due to the differences in their respective hydrodynamic volumes.[176]

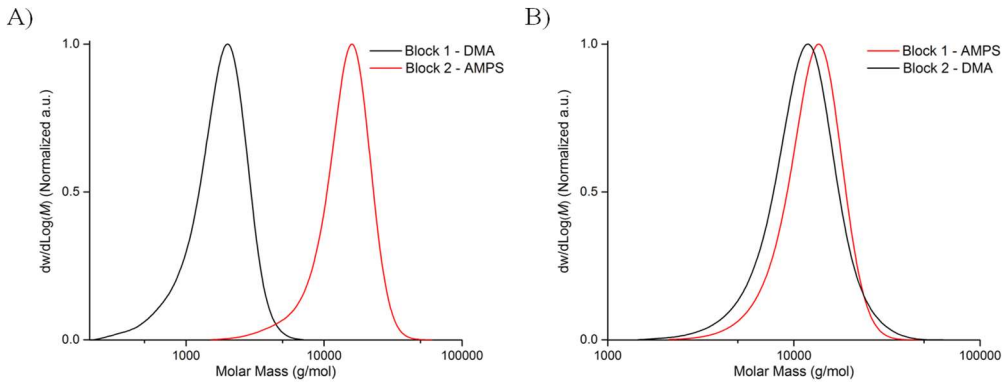

Figure 3-13: Aqueous SEC molecular weight distribution showing the chain extension of $PDMA_{50}$ with AMPS®2405 and the chain extension of $PAMPS_{50}$ with DMA.

A) $PDMA_{50}$-*b*-$PAMPS_{50}$; B) $PAMPS_{50}$-*b*-$PDMA_{50}$

3.3.3 Multiblock Copolymer Synthesis

Copolymerisation of PAMPS with *N*-hydroxyethyl acrylamide (HEAm) and 4-acryloylmorpholine (NAM) were further studied to synthesise multiblock copolymers. These monomers were chosen as representative of acrylamide monomers because of their hydrophilicity and good reactivity. Octablock copolymer PAMPS-*b*-PHEAm and tetrablock copolymer PAMPS-*b*-PNAM were synthesised with an average DP of 10 for each block (**Table 3-4**). Chain extension of PAMPS macroCTA with HEAm or NAM required a longer reaction time to reach full monomer conversion than chain extension with AMPS®2405 itself (1.5 hours versus 1 hour), which can be attributed to differences in the k_p value of each monomer.[48]

Table 3-4: Block copolymers synthesised by aqueous RAFT polymerisation using AMPS®2405 and HEAm targeting an overall DP of 80.

72

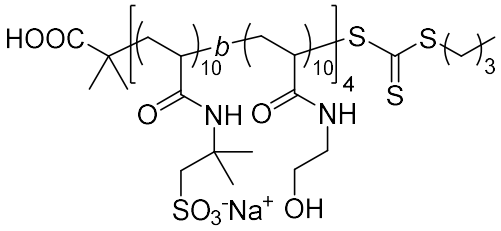

73

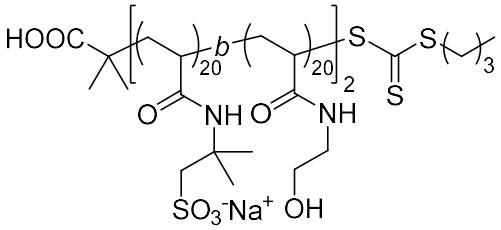

74

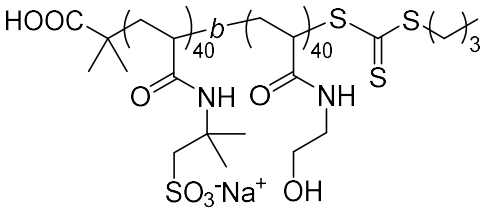

75

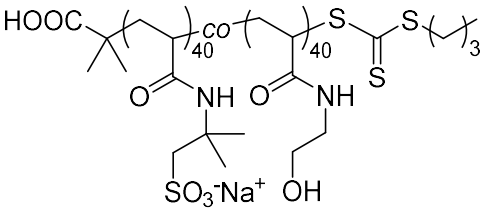

Polymer	Block	Multiblock composition	Conv. (%)[a]	$M_{n,th}$ (g/mol)[b]	$M_{n,SEC}$ (g/mol)[c]	$Đ$ [c]
53	1	$PAMPS_{10}$	99	2,600	5,500	1.09
-	2	$PAMPS_{10}$-*b*-$PHEAm_{10}$	99	3,700	4,000	1.25
-	3	$PAMPS_{10}$-*b*-$PHEAm_{10}$-*b*-$PAMPS_{10}$	> 99	6,000	9,100	1.13
-	4	$[PAMPS_{10}$-*b*-$PHEAm_{10}]_2$	> 99	7,100	8,400	1.18
-	5	$[PAMPS_{10}$-*b*-$PHEAm_{10}]_2$-*b*- $PAMPS_{10}$	> 99	9,400	13,100	1.18
-	6	$[PAMPS_{10}$-*b*-$PHEAm_{10}]_3$	> 99	10,500	11,800	1.25
-	7	$[PAMPS_{10}$-*b*-$PHEAm_{10}]_2$-*b*- $PAMPS_{10}$	> 99	12,800	17,700	1.30
72	8	$[PAMPS_{10}$-*b*-$PHEAm_{10}]_4$	> 99	13,900	16,700	1.48
18	1	$PAMPS_{20}$	99	4,800	6,000	1.09
-	2	$PAMPS_{20}$-*b*-$PHEAm_{20}$	> 99	7,100	6,000	1.13
-	3	$PAMPS_{20}$-*b*-$PHEAm_{20}$-*b*-$PAMPS_{20}$	> 99	11,700	10,000	1.14
73	4	$[PAMPS_{20}$-*b*-$PHEAm_{20}]_2$	> 99	14,100	10,400	1.16
74	-	$PAMPS_{40}$-*b*-$PHEAm_{40}$	> 99	13,600	8,300	1.35
75	-	$PAMPS_{40}$-*co*-$PHEAm_{40}$	> 99	13,900	13,900	1.13
53	1	$PAMPS_{10}$	99	2,500	5,400	1.09
-	2	$PAMPS_{10}$-*b*-$PNAM_{10}$	99	4,000	1,800	1.50
-	3	$PAMPS_{10}$-*b*-$PNAM_{10}$-*b*-$PAMPS_{10}$	> 99	6,200	9,100	1.10
76	4	$[PAMPS_{10}$-*b*-$PNAM_{10}]_2$	> 99	7,600	4,000	1.41

[a] Conversions were determined by ^{1}H NMR spectroscopy, using **Equation 1**; [b] Theoretical M_n values were calculated using **Equation 2**; [c] Experimental M_n and $Đ$ values were determined by size-exclusion chromatography in 20 % MeOH / 80 % 0.1M $NaNO_3$ in milli-Q water eluent using a conventional calibration obtained with PEG/PEO standards.

^{1}H NMR spectroscopy was used to confirm full monomer conversion between each monomer addition (**Table S 3-4** and **Figure S 3-7**). Monomodal distributions were obtained after each block addition, with dispersities ranging from 1.09, for the first block, to 1.48 (**Polymer 72**) for the last block of the octablock copolymer of AMPS®2405 and HEAm.

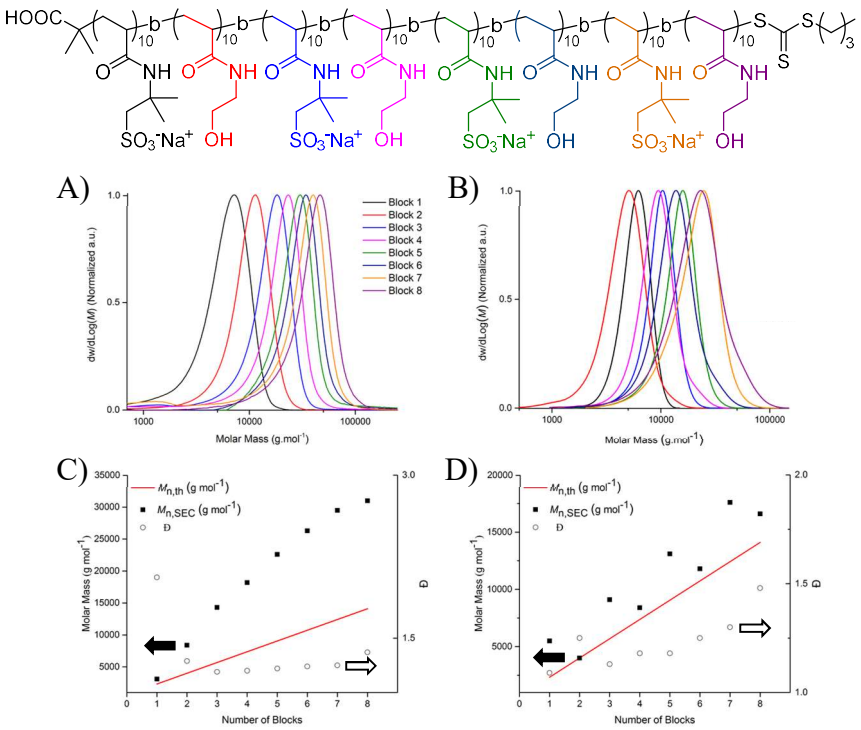

Figure 3-14: Stepwise characterisation of the chain extension of **Polymer 72** [PAMPS$_{10}$-*b*-PHEAm$_{10}$]$_4$.

A) DMF SEC chromatograms with conventional calibration; C) Molar mass and dispersity versus the number of blocks; B) Aqueous SEC molecular weight distribution calculated with conventional calibration; D) Molar mass and dispersity versus the number of blocks.

While the general trend shows a linear evolution of the experimental molecular weight with increasing number of blocks (**Figure 3-14 – B** and **D**), a shift towards lower molecular weight when PAMPS$_{10}$ was chain extended with HEAm, followed by a shift towards higher molecular weight when macroCTA (PAMPS$_{10}$-*b*-PHEAm$_{10}$) was further chain extended with AMPS®2405. This "step effect" can be attributed to differences in the nature of the two monomers (electrolyte versus neutral).[122] As PAMPS is a negatively charged polyelectrolyte, electrostatic interactions are expected to expand the polymer more than in the case of neutral polymer segments (i.e, NAM and HEAm), accounting for the irregular variation of hydrodynamic volumes, and therefore different molecular weights observed. The difference of molecular weights

of the two monomers ($M_{AMPS®2405}$ = 229.2 g/mol and M_{HEAm} = 115.1 g/mol) is expected to further enhance this phenomenon. This is in accordance with an observation made by McKenzie *et al.* for the synthesis of a hexablock copolymer of ethyl acrylate (EA) and methyl acrylate (MA).[177] To verify this hypothesis each block was analysed using DMF SEC with a polar column where a shift for each peak towards higher molecular weight was observed (**Figure 3-14 – A**). The molecular weights determined for each block by DMF-SEC were significantly higher than the theoretical one. Again this is attributed to the difference of hydrodynamic volume between our polymers and the PMMA standards used to calibrate the DMF SEC.

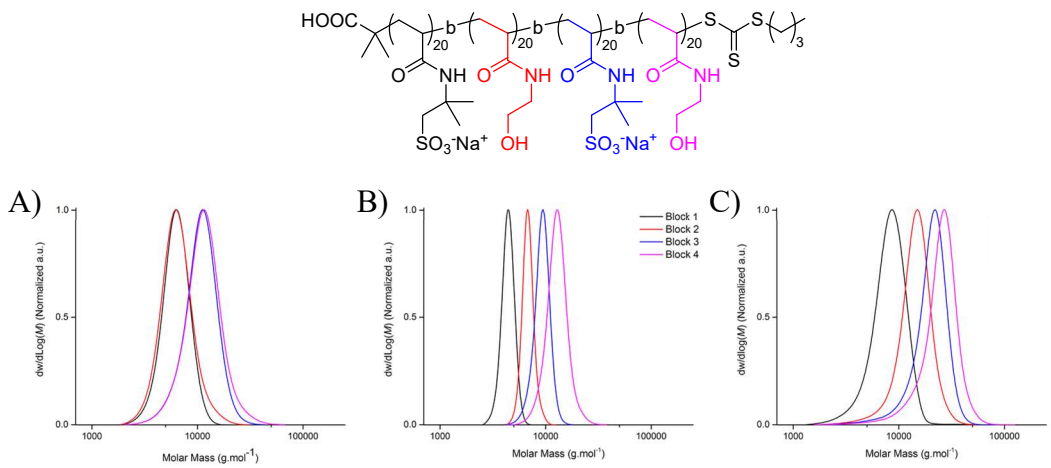

Figure 3-15: Stepwise characterisation for the chain extension of **Polymer 73** [$PAMPS_{20}$-*b*-$PHEAm_{20}$]$_2$.

A) Aqueous SEC molecular weight distributions using conventional calibration); B) Aqueous SEC molecular weight distributions using triple detection (RI, VS, LS detectors); C) DMF SEC chromatograms using conventional calibration.

In order to further investigate the effect of the block length on properties and for biological applications study (**CHAPTER 5**) a tetrablock of PAMPS and HEAm was synthesised, targeting a final DP of 80 ([$PAMPS_{20}$-*b*-$PHEAm_{20}$]$_2$ versus [$PAMPS_{10}$-*b*-$PHEAm_{10}$]$_4$) (**Table S 3-5**). Similar observations for the octablock polymer synthesised previously were found (**Polymer 72**). When conventional aqueous SEC was used an overall increase of molecular weight was observed with steps (**Figure 3-15**), while a linear increase of molecular weight was observed when triple detection when Aqueous SEC was used. Additionally, when DMF SEC was used with conventional calibration a linear increase of molecular weight was observed (**Figure 3-16**). The molecular weights obtained were overestimated due to the nature of the standard for DMF SEC (i.e. PMMA).

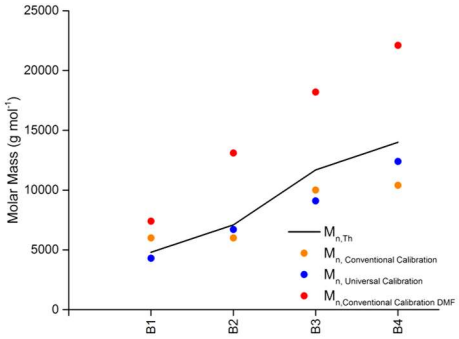

Figure 3-16: Molar mass and dispersity for the chain extension of PAMPS with HEAm using either the aqueous SEC with an RI detector only (orange), triple detection (blue) or DMF SEC with RI detector (red).

NAM, which has been widely used in the literature to synthesise well-defined multiblock homo- and copolymers due to its high reactivity, was used here as an alternative comonomer to demonstrate the robustness of the method.

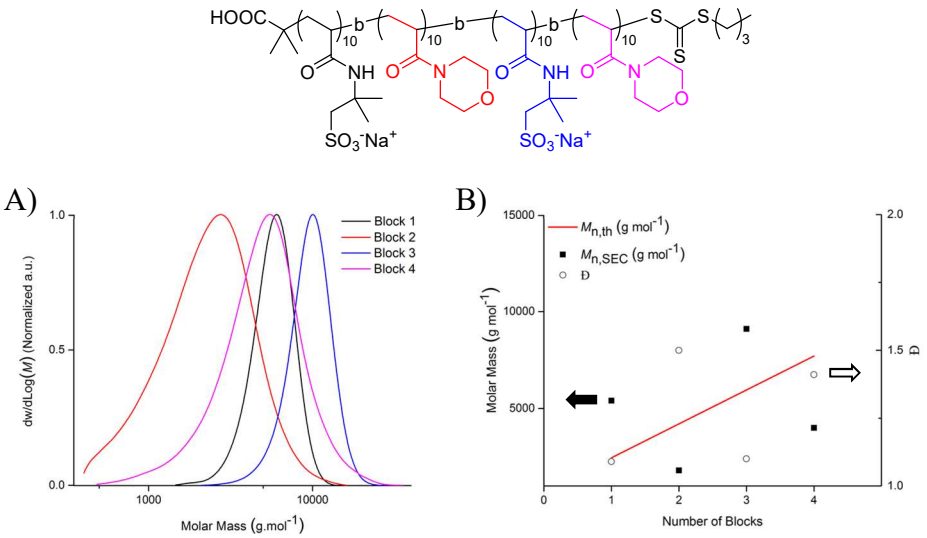

Figure 3-17: Stepwise characterisation of the chain extension of **Polymer 76** [$PAMPS_{10}$-*b*-$PNAM_{10}$]$_2$.

A) Aqueous SEC molecular weight distributions using conventional calibration; B) Molar mass and dispersity versus the number of blocks.

Using similar conditions to those used for HEAm, full monomer conversions (**Table S 3-6** and **Figure S 3-8**) and monomodal chromatograms (**Figure 3-17**, **Table 3-4**) were obtained after each sequential monomer addition. As expected, a similar trend was seen to that of HEAm, with steps observed in the plot of the experimental

molecular weight versus the number of blocks. Similarly, this artefact was attributed to differences in the hydrodynamic volume of AMPS®2405 and NAM segments.

Finally, a diblock and a random copolymer of similar composition and molecular weight to the octablock copolymer of AMPS®2405 and HEAm were prepared for comparison (**Table 3-4**, **Polymer 74** and **75**).

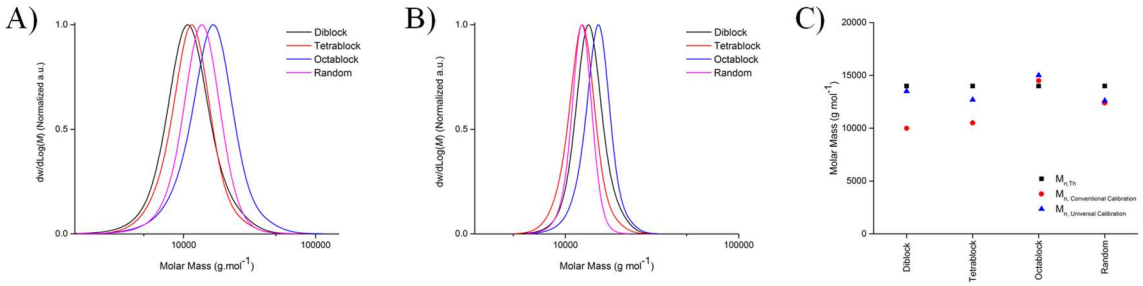

Figure 3-18: Characterisation of the copolymers synthesised with AMPS®2405 and HEAm targeting a DP of 80 (diblock, tetrablock, octablock and random copolymer).

A) Aqueous SEC molecular weight distributions calculated by conventional calibration; B) Aqueous SEC molecular weight distributions calculated by triple detection (LS, RI and VS detectors in series); C) Theoretical and experimental M_n overlaid using either conventional calibration or triple detection.

An induction period of 8 minutes was observed for the random copolymer synthesis (**Figure S 3-9**, **Polymer 75**), when compared to approximately 30 minutes for AMPS®2405 homopolymer synthesis (**Section 2.3.2**). This is likely due to the higher consumption of the CTA with the incorporation of one monomer unit onto each BDMAT molecule, resulting in a faster monomer conversion which was obtained in 45 minutes. **Figure 3-18** shows an overlay of the SEC molecular weight distributions for the copolymers synthesised. All three distributions revealed monomodal distribution with dispersities varying from 1.13 to 1.35. The narrower distribution observed for the random copolymer when compared to the block copolymers is likely due to a better distribution of both monomers along the polymer chains, lowering the repulsion between the negatively charged AMPS®2405. Using SEC with conventional calibration, the experimental molecular weights of octablock, diblock and random copolymers were found to be 16.7, 8.3 and 13.9 kg/mol, respectively. These differences can be attributed to differences in the conformation of the three linear architectures. Indeed, spreading of the negative charge over the backbone is expected to result in a more elongated polymer due to electrostatic repulsion, which explains

why the hydrodynamic volume measured for the diblock is smaller than for its mixed counterparts. However, when the aqueous SEC coupled with triple detection was used the experimental molecular weights obtained were in good agreement with the theoretical molecular weight (**Figure 3-18 – B** and **C**). Again, this is explained in terms of differences between the hydrodynamic volume of the charged AMPS®2405 and the PEG/PEO standards used for conventional calibration. The better distribution of the two monomers in the random copolymer is expected to lessen this effect as such a phenomenon has already been reported in the literature.[89]

3.3.4 Star Shape Polymer Synthesis – Optimisation

The use of RAFT polymerisation to prepare a range of star-shaped polymers using both homopolymers and copolymers of AMPS®2405 was explored. These polymers were synthesised using an "arm-first approach" in which a linear polymer is used as the initial arm, with subsequent addition of a cross-linker, in a one-pot fashion, without any purification step in between (**Scheme 3-4**). At first, the influence of the ratio of cross-linker to CTA was investigated using *N*,*N*′-methylenebisacrylamide (C1) as the cross-linker and homopolymer $PAMPS_{50}$ as the model arm. C1 was chosen as model because its acrylamide functionality ensures similar reactivity between the newly incorporated monomer and the newly reinitiated group (AMPS®2405). Due to the low solubility of C1 in water (20 g/L at 20 °C), the cross-linker was first dissolved in DMSO (150 mg/mL) before being added to the polymerisation mixture alongside additional initiator. The evolution of polymerisation was followed by SEC (**Figure S 3-11**) with the gradual appearance of a peak at shorter retention time due to the transformation of the linear polymer (~ 15 minutes) into a star polymer (~ 12 minutes). Due to the formation of a more complex structure (**Scheme 3-4**) the internal reference (CTA) usually used to determine the monomer conversion disappeared into the core of the star polymer newly formed (**Figure S 3-10**).

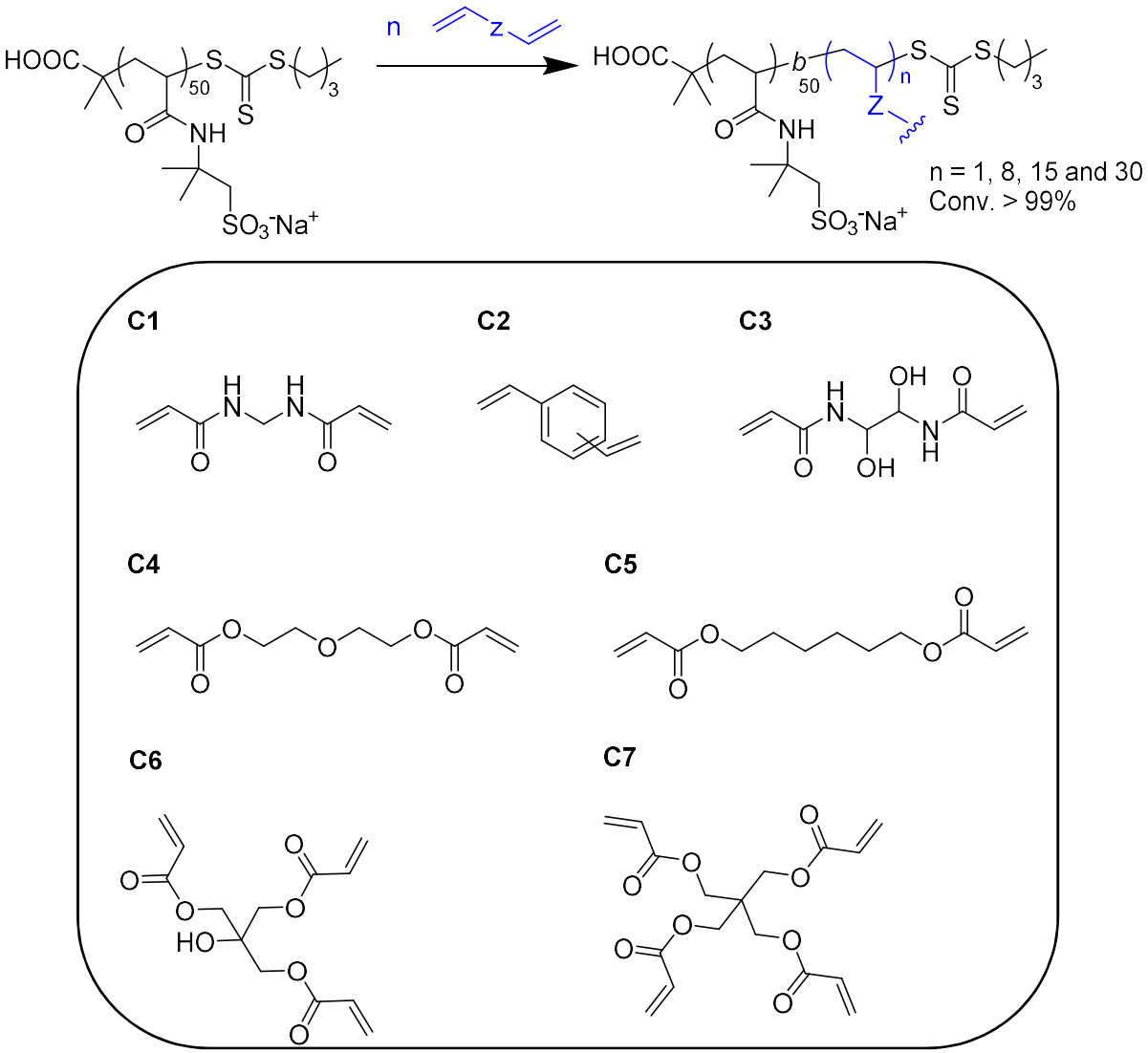

Scheme 3-4: Synthesis of star polymers using the arm-first approach. Bottom insert shows the structure of the different cross-linkers used in this study.

Effect of Cross-linker to CTA Ratio

The ratio of cross-linker to CTA was varied from 1 to 30 (**Scheme 3-4**, **Figure 3-19 – C** and **Table 3-5**, **Polymer 77** to **80**) using C1 as the cross-linker. The molecular weight of the resulting material increased from 33.5 to 125.3 kg/mol with increasing ratio of cross-linker to CTA from 1 to 15. When using a ratio C1:CTA = 30, a gel-like polymer was formed in less than 30 minutes, likely due to the formation of a highly branched polymer that could not be analysed by SEC. For C1:CTA = 1, the percentage of arm incorporated was found to be relatively low (35 %) when compared with the percentage of arm incorporated (91 %) obtained with a C1:CTA = 8. Higher ratios (i.e. 15) led to the observation of a tail by SEC with the peaks at retention times of 16, 13 and 12 minutes corresponding to unreacted arms, star polymer and star-star coupling respectively. In view of these results, a cross-linker to CTA ratio of 8 appeared optimal as it allows low dispersity (1.24), high molecular weight (67 kg/mol), high arm incorporation (91 %) and no visible star-star coupling. It was noteworthy that the percentage of arm incorporated, calculated using **Equation 7**, never reached 100 % in any cases. This could either be due to high electrostatic repulsions between the negatively charged arms, or to the presence of dead chains remaining from the synthesis of the initial arm. This is in agreement with previous reports of star-shaped polymers synthesised by RAFT polymerisation in the literature.[157]

Table 3-5: Star polymers as prepared by RAFT polymerisation using various cross-linker type (C1 to C7), and cross-linker to CTA ratio from 1 to 30.

Polymer	CL	Solvent	[CL]/[CTA]	Arm Incorporation (%)[a]	$M_{n,SEC}$ (kg/mol)[b]	$Đ$[b]
77	C1	DMSO	1	35	33.5	-
78	C1	DMSO	8	91	67.0	1.24
79	C1	DMSO	15	94	125.3	1.89
80	C1	DMSO	30	-	-	-
81	C2	-	8	71	41.7	1.11
82	C3	NaOH (aq)	8	-	12.0	1.27
83	C4	-	4	87	56.5	1.15
84	C4	-	8	89	67.4	1.15
85	C4	-	15	91	73.1	1.17
86	C6	-	8	90	60.2	1.15
87	C7	-	8	93	73.5	1.22

[a] The conversion of the arm into star was determined using **Equation 7**; [b] Experimental M_n and $Đ$ values were determined by size-exclusion chromatography in 20 % MeOH / 80 % 0.1M $NaNO_3$ in milli-Q water eluent using a conventional calibration obtained with PEG/PEO standards.

Next the diacrylate cross-linker C4 was used and the effect on the star polymer formation of three different ratios of C4:CTA was investigated (i.e. 4, 8 and 15) (**Scheme 3-4**, **Table 3-5**, **Polymer 83** to **85**). This cross-linker is liquid at room temperature and was injected alongside the initiator without additional solvent. Similar observations to when C1 was used were made (**Figure 3-19 – D**). When the ratio was increased from 4 to 15, the percentage of arm incorporated into the star increased from 87 to 91 % while the molecular weight increased from 56.5 to 73.1 kg/mol. In contrast with C1, no star-star coupling was observed when a ratio of C4 to CTA of 15 was used. A ratio of 8 was found to be optimum for both cross-linkers and was therefore the ratio of choice for the rest of the study.

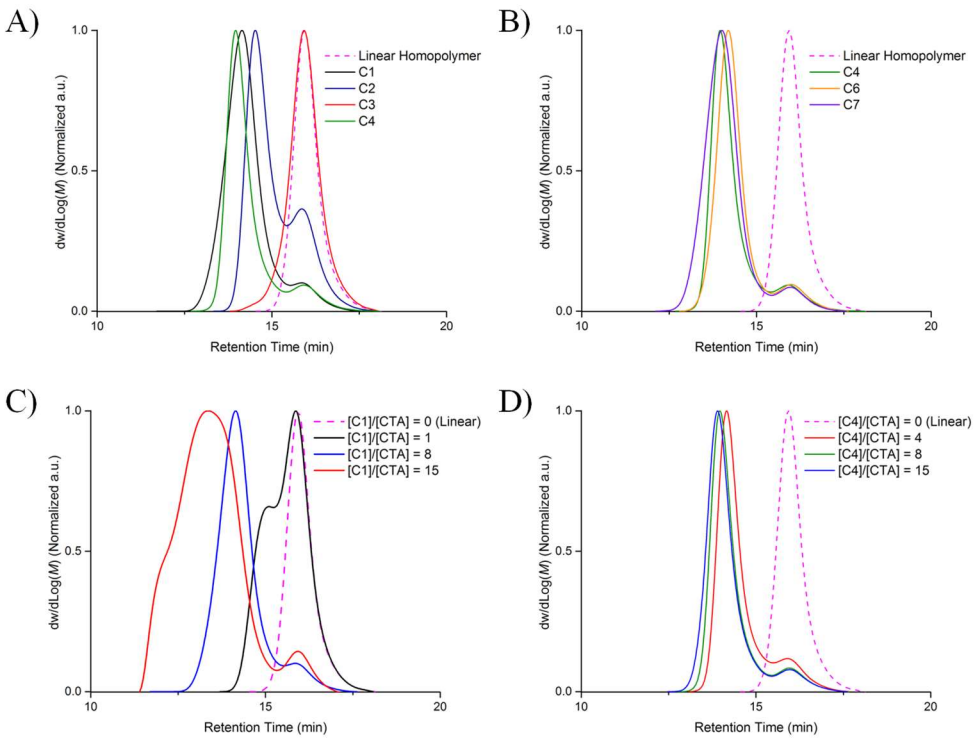

Figure 3-19: Aqueous SEC molecular weight distributions of star polymers prepared by RAFT polymerisation using $PAMPS_{50}$ as arm.

A) Using cross-linker: C1, C2, C3 and C4 ([cross-linker]/$[CTA]_0$ = 8); B) Using cross-linker: C4, C6 and C7 ([cross-linker]/$[CTA]_0$ = 8); C) Using C1 increasing the ratio from 1 to 15; D) Using C4 increasing the ratio from 4 to 15.

Effect of Cross-linker Group

Having determined the optimal cross-linker to CTA ratio for C1 and C4 (CX:CTA = 8), the influence of the cross-linker structures was studied. A range of cross-linkers with different solubility values in aqueous solution were tested, using functionalities such as an aromatic cross-linker (C2), a hydrophilic acrylamide (C3), a hydrophobic acrylate (C4) and acrylate cross-linkers with functionalities higher than two (C6 and C7), (**Scheme 3-4**, **Table 3-5** and **Table 3-6** for C5). C2, C4, C5, C6 and C7 are liquid at room temperature and were injected alongside the initiator without additional solvent. C3 is a solid and was pre-dissolved in sodium hydroxide solution (20 mg/mL), at a concentration of 150 mg/mL, prior to introduction to the polymerisation mixture. The molecular weight distributions obtained using the different bifunctional cross-linkers are shown in **Figure 3-19 – A**, while those with functionalities greater than two are shown in **Figure 3-19 – B**. Acrylate cross-linker (C4) was found to give the narrowest distribution ($Đ$ = 1.15) which can be attributed to the lower reactivity (lower k_p) of acrylates compared to acrylamides, where a better control of arm incorporation into the star was obtained.[147] C2 (**Polymer 81**) resulted in a lower molecular weight attributed to the star polymer when compared to star polymers prepared using either C1 or C4. This can be explained by the known lower reactivity of styrene monomers, which limits the incorporation of the arm into the star (estimated to be 70 % after 24 hours).[170] Interestingly, no star polymers were formed using C3 (**Polymer 82**). In the literature, C3 was used to synthesise a core cross-linked star polymer of poly(oligoethylene glycol-acrylate) (POEG) via emulsion polymerisation, yielding a material with low dispersity (< 1.20) and a high percentage of arm incorporation (> 90 %).[168] In our investigation, absence of star formation can be attributed either to the difference in reactivity of the arms, where acrylamide is typically more reactive than acrylate, or to the influence of solvent (water rather than toluene) and consequently affecting the CL compartmentalisation. C6 (**Polymer 86**) and C7 (**Polymer 87**) which bear functionalities higher than two (three and four respectively), did not show major improvement regarding the arm incorporation when compared to C4 with similar percentage of arm incorporation (~ 90 %) and similar molecular weights obtained ($M_{n,SEC\ C4}$ = 67.4 kg/mol, $M_{n,SEC\ C6}$ = 60.2 kg/mol and $M_{n,SEC\ C7}$ = 73.5 kg/mol).

Table 3-6: Star polymer synthesised from $PAMPS_{50}$ using C5 (**Scheme 3-4**) and changing the ratio of C5 to CTA and the cross-linker concentration.

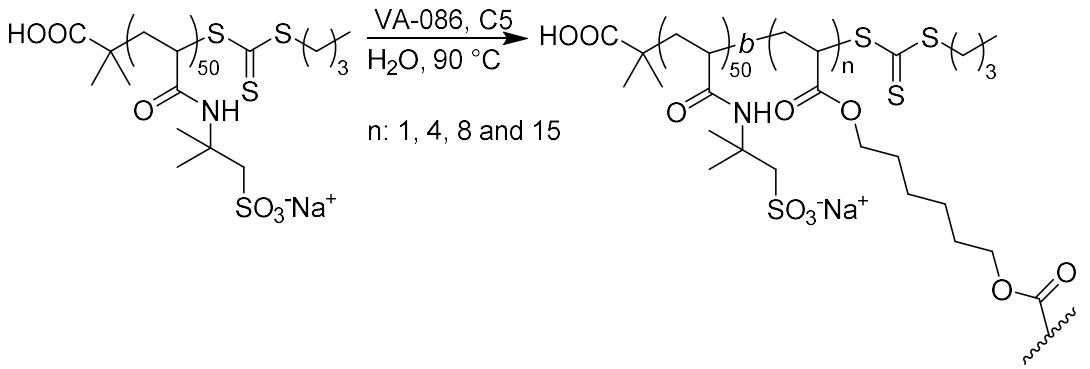

Polymer	[Cross-linker]/[CTA]	[Cross-linker] (mol/L)	Particle Size - Intensity (nm)[a]	*PDI*[a]
88	1	0.03	223.3	0.11
89	4	0.12	221.5	0.06
90	8	0.22	187.0	0.11
91	15	0.40	-	-
92	4	0.06	531.5	0.06
93	4	0.03	1806	0.05
94	4	0.007	-	-

[a] Determined using Dynamic Light Scattering.

Finally, C5 a bifunctional acrylate similar to C4 but with lower solubility in water due to the absence of oxygen in the spacer, was used (**Table 3-6**). While the reaction media became only slightly turbid when C4 was used, the media became turbid within minutes with C5 (**Figure 3-20 – A**), due to an emulsification process relating to the formation of a highly hydrophobic core.[178,179] Well-defined particles were obtained within 4 hours with *PDI* of 0.11 and diameter of about 187 nm measured by DLS (**Figure 3-20 – C** and **D**). Using C5, a few parameters were optimised such as the cross-linker to CTA ratio (1, 4 and 8) and the concentration of cross-linker maintained at a constant ratio of 4. It was shown that when the ratio of cross-linker to CTA was increased from 1 to 8, the concentration of cross-linker was increased from 0.03 to 0.22 M due to the set-up used (monomer injection). The increase of cross-linker to CTA ratio did not show any change of size but the use of a ratio of 4 instead of 8 demonstrated narrower particle distribution, with a *PDI* of 0.06. When the ratio of cross-linker to CTA was maintained at 1:4 and the cross-linker concentration was gradually decreased from 0.12 to 0.06 to 0.03, and finally, 0.007 M, the size of the particles were shown to dramatically increase while retaining good control over the

particles size distribution (*PDI* < 0.1). The particles were further characterised using TEM (**Figure 3-20 – B**) and were shown to be monodisperse.

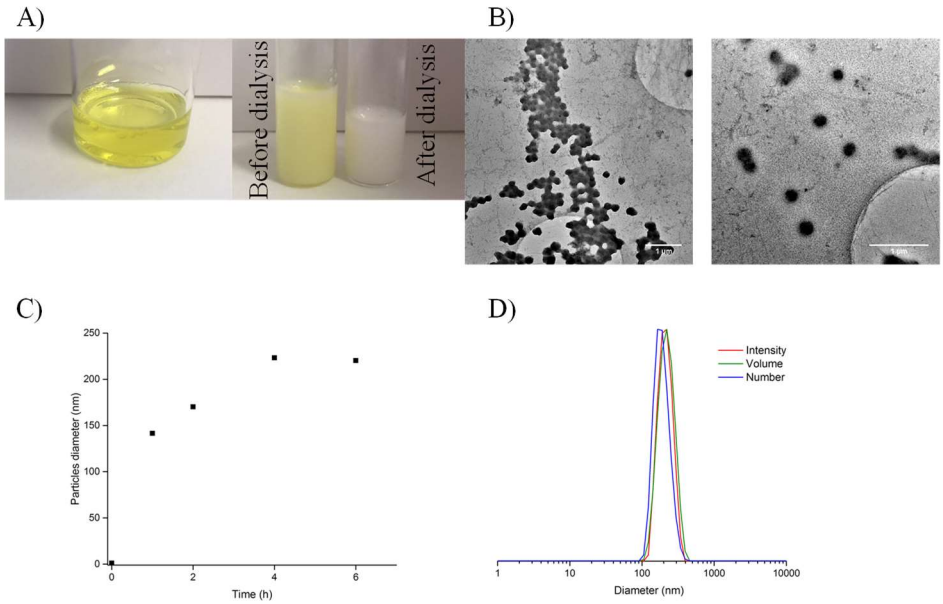

Figure 3-20: Full characterisation of the star particles synthesised using C5 (**Polymer 89**).

A) Pictures of the reaction vial before the reaction (left) and after reaction (right); B) TEM images of the resulting particles; C) Evolution of the star particles size with time measure by DLS in water at 25 °C; D) DLS normalised size distribution of the final particles.

Effect of the Arm Length

Using C1 and C4 as cross-linkers, the influence of arm length on the synthesis of star-architecture PAMPS was investigated. Arm length was initially increased while keeping the ratio of cross-linker to CTA constant and equal to 8, and varying the molecular weight of the initial AMPS®2405 homopolymer arm from 11 to 38 kg/mol (**Table 3-7**). **Figure 3-21 – A** (C1) and **B** (C4) show the molecular weight distributions obtained when increasing the arm length with either C1 or C4 CL. In each case, two peaks were observed which correspond to the star polymer and the unreacted arm. Using C1, increasing the length of the initial arm from DP 50 to 100 and finally 200 resulted in an increase of the molecular weight of the star polymers from 67.8 to 102.0 and 185.1 kg/mol respectively (**Polymer 95** to **97**), while dispersities remained between 1.15 and 1.25. The efficiency of the reaction slightly decreased with increasing arm length and the percentage of calculated arm incorporation reduced from 90 to 79 % (**Figure 3-21 – A**), using the ratio of the RI traces by SEC. This can be attributed to either an increased viscosity of the reaction mixture and a lower arm diffusion, or to the increase of steric hindrance.

Table 3-7: Star polymers prepared by RAFT polymerisation using either C1 or C4 and increasing degrees of arm polymerisation from 50 to 400.

Polymer	CL, DP	Arm	[CL]/[CTA]	[CL] (mol/L)	Arm Incorporation (%)[a]	$M_{n,SEC}$ (kg/mol)[b]	$Đ$[b]
95	C1, 50	**19**	8	0.19	90	67.8	1.23
96	C1, 100	**20**	8	0.11	88	102.0	1.24
97	C1, 200	**21**	8	0.06	79	185.1	1.18
98	C4, 50	**19**	8	0.23	89	67.0	1.15
99	C4, 100	**20**	8	0.12	80	126.0	1.17
100	C4, 100	**20**	15	0.21	85	129.0	1.21
101	C4, 200	**21**	8	0.06	68	199.0	1.16
102	C4, 200	**21**	15	0.11	75	177.0	1.18
103	C4, 200	**21**	30	0.21	74	271.0	1.30
104	C4, 400	**22**	8	0.03	48	385.0	1.19
105	C4, 400	**22**	15	0.06	51	423.0	1.19
106	C4, 400	**22**	30	0.11	47	501.0	1.19

[a] The conversion of the arm into star was determined using **Equation 7**; [b] Experimental M_n and $Đ$ values were determined by size-exclusion chromatography in 20 % MeOH / 80 % 0.1M $NaNO_3$ in milli-Q water eluent using a conventional calibration obtained with PEG/PEO standards.

When C4 was used instead ([C4]/[CTA] = 8), slightly different results were obtained. Indeed, with increasing length of the initial arm, the molecular weight of the resulting stars increased from 67 to 385 kg/mol, while dispersities remained between 1.1 and 1.2. However, the efficiency of the reaction radically decreased with increasing arm length, and the percentage of calculated arm incorporation was reduced from 89 % (DP_{arm} = 50) to 48 % (DP_{arm} = 400) (**Figure 3-21 – B**). In the above experiments, cross-linker concentration was decreased from 0.23 M to 0.03 M from DP 50 to 400 to keep the ratio of cross-linker to CTA equal to 8 (**Table 3-7**). In a separate experiment, the cross-linker to CTA ratio was gradually increased from 8 to 15 and then 30 (**Table 3-7**, **Figure 3-21 – D**) for a DP 200 (**Polymer 101** to **103**). While no improvement in the percentage of arm incorporation was observed, an increase in molecular weight of the resulting star was observed, corresponding to a higher quantity of cross-linker incorporated in the star (higher hydrodynamic volume of the core). Similar observations were made with a DP 100 (**Figure 3-21 – C, Polymer 99** and **100**). No matter the arm length, the star polymers were formed within 40 minutes of reactions (**Figure S 3-12**).

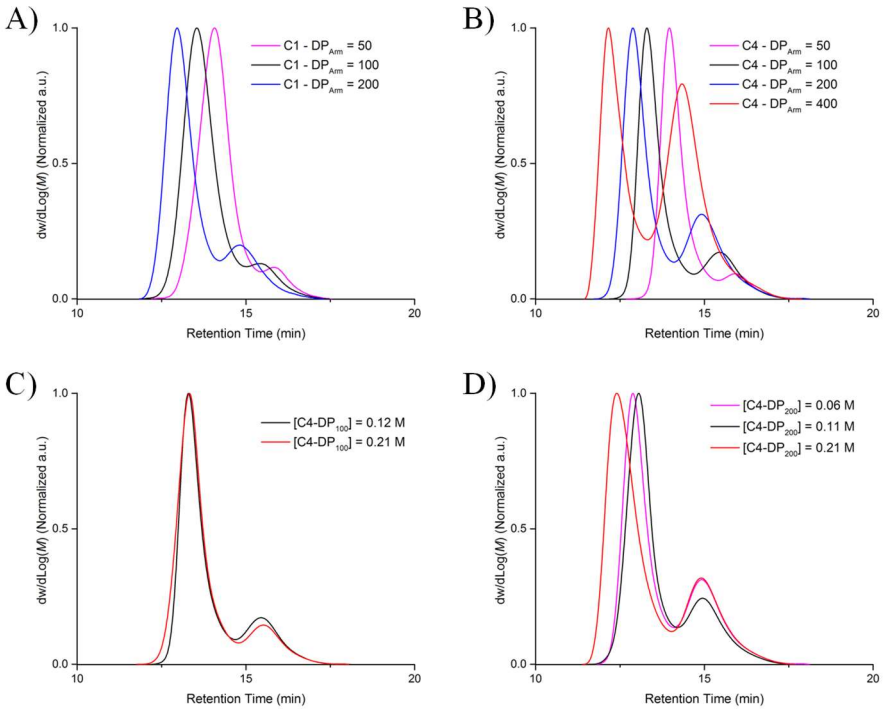

Figure 3-21: Aqueous SEC chromatograms of star polymers obtained by RAFT polymerisation.

A) DP_{arm} = 50, 100 or 200 and [cross-linker]/[CTA] = 8 with C1; B) DP_{arm} = 50, 100 or 200 and [cross-linker]/[CTA] = 8 with C4; C) DP_{arm} = 100 using C4 increasing [cross-linker]/[CTA] from 8 to 15; D) DP_{arm} = 200 using C4 increasing [cross-linker]/[CTA] from 8 to 30.

Using the molecular weight of the SEC peak corresponding to the star and the linear polymers, the number of arms per star was approximated to be around 6 arms for the lower molecular weight arms, but to increase to 10 for the larger molecular weight arms. This result contradicts the decrease in quantity of arms incorporated as calculated previously using the ratio of the two peaks, suggesting that the use of linear PEG to calibrate the aqueous SEC is again responsible for the observed discrepancy between the data. The hydrodynamic volume of a linear system is different from a branched system of equivalent molecular weight, and the discrepancy is expected to increase with increase of the molecular weight. The analysis of star polymers by aqueous SEC with conventional calibration has only given a qualitative comparison between each star polymer. The characterisation of such systems using SEC with triple detection will be investigated in **CHAPTER 4**.

3.3.5 Copolymer Star Shape Synthesis

The effect of arm composition was investigated by preparing star copolymers from copolymers of AMPS®2405 and HEAm (arm), namely octablock, tetrablok, diblock and random copolymers.

Table 3-8: Star polymers as prepared by RAFT polymerisation using C4 as cross-linker and various copolymer as arms (DP_{arm} = 80).

Polymer	Arm	[CL] (mol/L)	Arm Incorporation (%)[a]	$M_{n,SEC}$ (kg/mol)[b]	$Đ$[b]
107	Diblock, **74**	0.22	-	-	-
108	Diblock, **74**	0.16	72	113.5	1.19
109	Diblock, **74**	0.12	71	162.0	1.19
110	Random, **75**	0.14	80	101.8	1.21
111	Octablock, **72**	0.16	67	229.6	1.27
112	Tetrablock, **73**	0.16	79	161.5	1.23

[a] The conversion of the arm into star was determined using **Equation 7**; [b] Experimental M_n and $Đ$ values were determined by size-exclusion chromatography in 20 % MeOH / 80 % 0.1M $NaNO_3$ in milli-Q water eluent using a conventional calibration obtained with PEG/PEO standards.

Synthesis of star polymers using an arm comprised of a diblock and the conditions previously described (0.22 M of C4, C4/CTA = 8) resulted in the formation of a gel-like polymer which could not be analysed by SEC (**Table 3-8**, **Polymer 107**). This behaviour was attributed to the high concentration of cross-linker used. Upon decreasing the concentration of cross-linker to 0.16 and 0.12 M (**Table 3-8**, **Polymer 108** and **109**), star polymers were formed in solution, with a molecular weight of 113.5 kg/mol, a dispersity below 1.2 and 72 % of arm incorporation (**Figure 3-22 – B**). Using a random polymer as the arm and a concentration of C4 equal to 0.14 M, a star copolymer with a molecular weight of 101.8 kg/mol and high arm incorporation (80 %) was obtained (**Figure 3-22 – A, Polymer 110**). A star copolymer derived from the tetrablock arm was synthesised, which resulted in a product with a slightly higher molecular weight (161.5 kg/mol) and arm incorporation (79 %) than for the diblock star copolymer previously synthesised (**Figure 3-22 – C, Polymer 112**). Finally, a star copolymer derived from octablock was synthesised which resulted in a product with a high molecular weight (229.6 kg/mol) but lower arm incorporation (67 %) (**Figure 3-23**, **Polymer 111**). This can either be attributed to differences in the hydrodynamic volume of diblock, tetrablock, octablock and random copolymers which may affect

the mechanism of arm incorporation or the difference of CL concentration used for each star copolymers. Similar kinetics to when the homopolymers were used was observed, where star polymers formed within 40 minutes (**Figure S 3-13**).

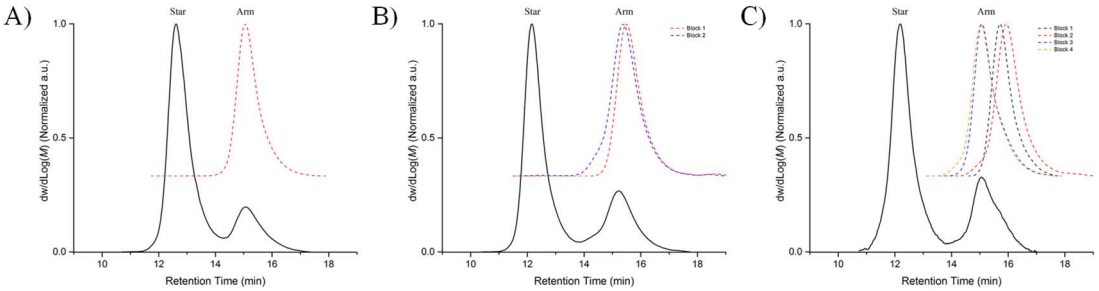

Figure 3-22: Aqueous SEC chromatogram overlay of the linear copolymer used and the corresponding star copolymers newly synthesised using C4 with [C4]/[CTA] = 8.

A) $PAMPS_{40}$-*co*-$PHEAm_{40}$; .B) $PAMPS_{40}$-*b*-$PHEAm_{40}$; C) $[PAMPS_{20}$-*b*-$PHEAm_{20}]_2$.

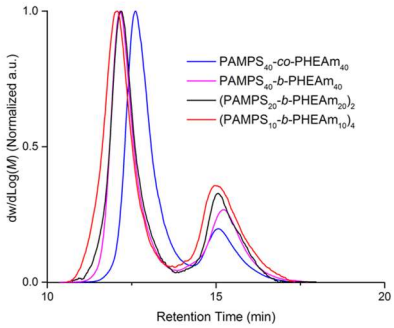

Figure 3-23: Aqueous SEC chromatograms overlaid showing the different star copolymers synthesised using C4 with [C4]/[CTA] = 8.

3.3.6 Star-Shaped Polymer Synthesis using $PDMA_{100}$ as the Arm

Well-defined $PDMA_{100}$ was reported in **CHAPTER 2 – Section 2.3.1** (**Polymer 3** and **5**) using either DDMAT or BDMAT as the chain transfer agent. The synthesis of star polymers using these two homopolymers synthesised from two different RAFT agent was studied.

Table 3-9: Star polymer optimisation as prepared by RAFT polymerisation using C4 as cross-linker and $PDMA_{100}$ as arm with either DDMAT or BDMAT as CTA.

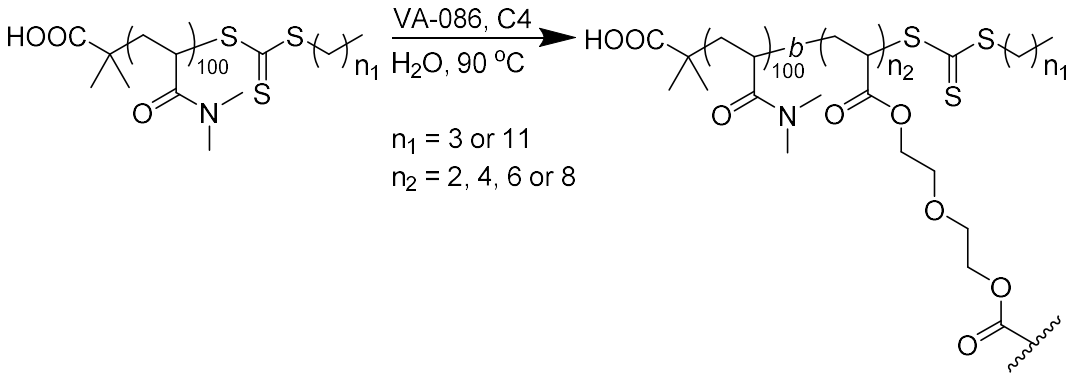

Polymer	CTA, T (°C)	[CL]/[CTA]	[CL] (mol/L)	Arm Incorporation (%)[a]	$M_{n,SEC}$ (kg/mol)[b]	$Đ$[b]
113	BDMAT, 90	8	0.12	86	182	1.07
114	BDMAT, 90	6	0.10	84	174	1.07
115	BDMAT, 90	4	0.06	50	48.7	1.27
116	BDMAT, 90	2	0.03	26	35.7	1.11
117	BDMAT, 90	6	0.05	79	158	1.05
118	BDMAT, 90	6	0.02	64	69.7	1.32
119	BDMAT, 80	6	0.05	72	129	1.12
120	DDMAT, 80	6	0.05	79	210	1.13

[a] The conversion of the arm into star was determined using **Equation 7**; [b] Experimental M_n and $Đ$ values were determined by size-exclusion chromatography in DMF with 5 mM NH_4BF_4 using a conventional calibration obtained with PMMA standards.

The optimum conditions ([C4]:[CTA] = 8, [C4] = 0.12 M, T = 90 °C) established previously for the synthesis of $PAMPS_{100}$ star polymers (**Table 3-7** and **Figure 3-21 – C, Polymer 99**) were first applied to the $PDMA_{100}$-BDMAT (**Polymer 5**) polymerisation system (**Table 3-9**, **Polymer 113**). The SEC depicted a peak at lower retention time linked to the formation of star polymers (**Figure 3-24 – A**). The percentage of arm incorporated (86 %) were comparable to the value obtained when $PAMPS_{100}$ is used. However, a shoulder could be observed at higher molecular weight which may be attributed to the formation of star-star couplings. This could be

accredited to the absence of electrostatic interactions between each arm, in contrast to when PAMPS is used, where the arms are expected to shield the formation of star-star coupling. The newly formed star polymers made of PDMA could react together more readily and form a third population (i.e. star-star coupled).[180,181]

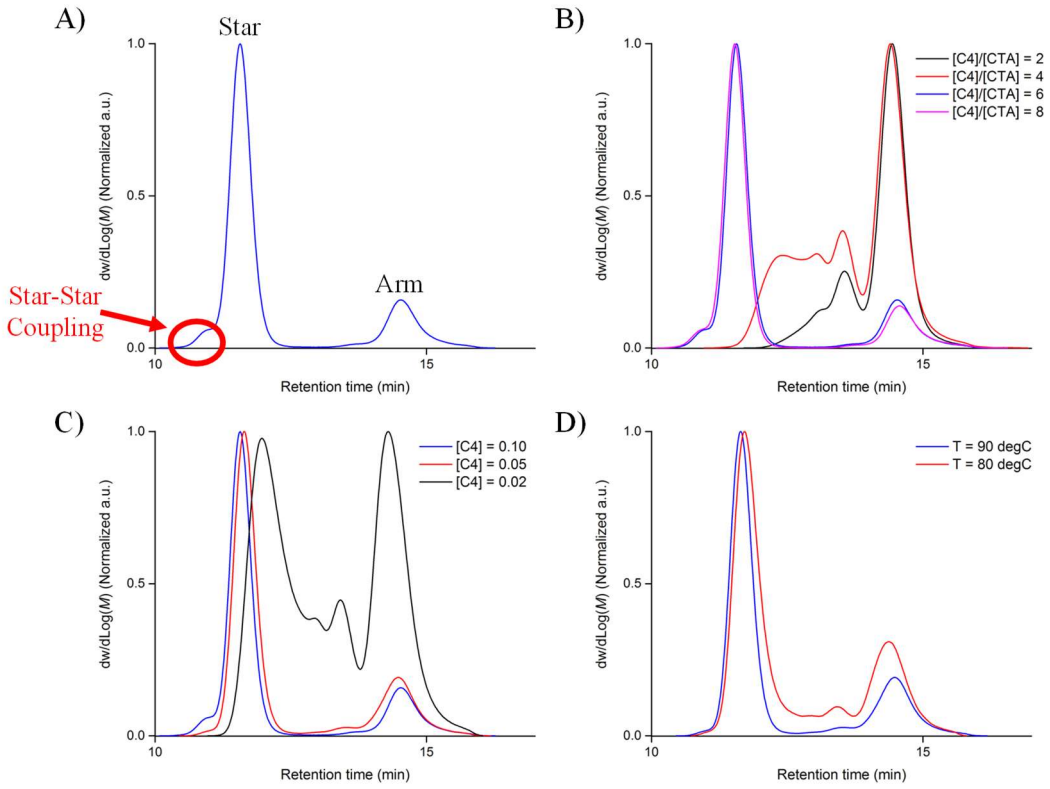

Figure 3-24: Aqueous SEC chromatograms for the optimisation of $PDMA_{100}$-BDMAT star polymers synthesised by RAFT polymerisation.

A) Star polymer synthesised using C4 with [C4]:[BDMAT] = 8 at 90 °C (40 min); B) Star polymer synthesised using C4 with [C4]:[BDMAT] varying from 2 to 8 at 90 °C (40 min), C) Star polymer synthesised using C4 with [C4]:[BDMAT] = 6 decreasing the cross-linker concentration from 0.10 to 0.02 M at 90 °C (40 min), D) Star polymer synthesised using C4 with [C4]:[BDMAT] = 6 and [C4] = 0.05 M either at 90 (40 min) or 80 (3.5 h) °C.

The synthesis of $PPDMA_{100}$ star polymers were optimised in order to reduce, or even eliminate, the formation of this third population of star-star coupling (**Table 3-9**). The ratio of cross-linker to CTA was first gradually reduced from 8 to 6, 4 and finally 2 (**Figure 3-24 – B, Polymer 113** to **116**). Star-star coupling formation was still observed when the ratio of cross-linker to CTA was decreased from 8 to 6 with similar molecular weight and percentage of arm incorporated (182 kg/mol and 86 % for a ratio 8 and 174 kg/mol and 84 % for a ratio 6). When the ratio was further decreased to 4

and 2, the formation of star polymers was a lot less effective with respect to the arm incorporation and the molecular weight ($M_{n,SEC}$ < 50 kg/mol and % arm < 50 %).

Next, keeping a ratio of cross-linker to CTA of 6, the concentration of cross-linker was decreased from 0.10 to 0.05 and finally 0.02 (**Polymer 114**, **117** and **118**). The percentage of arm incorporated was decreased from 84 to 79 and finally 64 % respectively and the molecular weight decreased from 174 to 158 and finally 69.7 kg/mol. When the cross-linker concentration was decreased from 0.1 to 0.05 M, the formation of star-star coupling was no longer observed (**Figure 3-24 – C**). When the cross-linker concentration was further decreased to 0.02 M the formation of other populations could be observed (no star-star coupling) with the appearance of peaks between the arm peak (~ 15 min) and the theoretical main star polymer population (~ 12 min). This likely due to the decrease of the polymerisation rate due to the dilution of the cross-linker. Finally, the temperature of the reaction media was decreased from 90 to 80 °C (**Figure 3-24** – **D, Polymer 119**) to investigate whether this would further decrease the star-star coupling occurrence ([C4] = 0.05 M and [C4]:[CTA] = 6). While there was no significant effect on the star-star coupling, another population of molecular weights between the arm and the main star polymer population was observed. Hence, the cross-linker concentration appeared to be a critical parameter to avoid the formation of star-star coupling, which would dramatically affect the properties of the material obtained (i.e. the viscosity).[182]

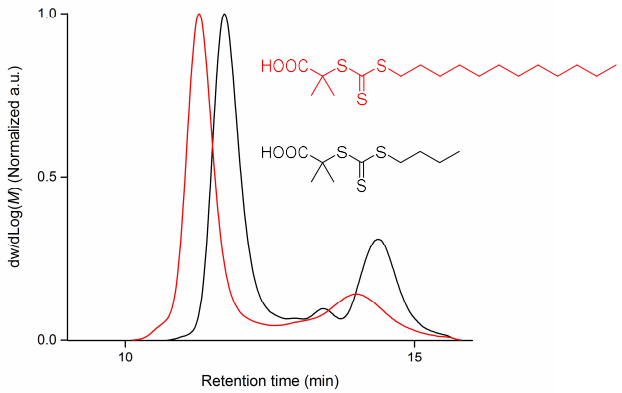

Figure 3-25: Aqueous SEC chromatograms of $PDMA_{100}$ star polymers synthesised by RAFT polymerisation using either DDMAT (red line) or BDMAT (black line) ([C4]:[CTA] = 6, [C4] = 0.05M at 80 °C).

The optimised conditions obtained for the $PDMA_{100}$-BDMAT system were then applied to a $PDMA_{100}$-DDMAT (**Polymer 3**) system (**Table 3-9**). SEC chromatograms of both star polymers using either of the chain transfer agents are overlaid in **Figure 3-25**. Both of the star polymers display high incorporation of the arm into the star (72 % for BDMAT and 79 % for DDMAT), low dispersities (1.12 for BDMAT and 1.13 for DDMAT) and no formation of star-star coupling. However, the molecular weights obtained were dissimilar; 210 kg/mol for DDMAT (**Polymer 120**) and 129 kg/mol for BDMAT. This can be explained by a better compartmentalisation of the cross-linker with DDMAT as the CTA due to the higher hydrophobicity of the Z-group (C12 versus C4, see **CHAPTER 2**) which allowed the incorporation of a higher number of arms into each nanoparticle (14 arms per star for DDMAT against 8 for BDMAT, **Equation 8**).[168,183] Additionally, the longer alkyl chain would induce more steric hindrance, resulting in a lower cross-linker density in the core and an increased swelling ability.[184] Alternatively, the difference of hydrodynamic volume between both star polymers analysed by SEC with the PMMA standards used for conventional calibration, as described in **Section 3.3.4**, is expected to influence those results.

3.3.7 Star Polymer Synthesis using DDMAT-PAMPS$_{100}$ as the Arm

In **CHAPTER 2** it was shown that AMPS®2405 could be polymerised by RAFT polymerisation with DDMAT in a mixture of water and methanol, and that well-defined homopolymers could be obtained. Next, the optimum conditions found to form well-defined star polymers with BDMAT were applied to PAMPS$_{100}$-DDMAT to form star polymers which could be further considered for scale-up by Lubrizol for numerous industrial applications (e.g. for viscosity modifiers).

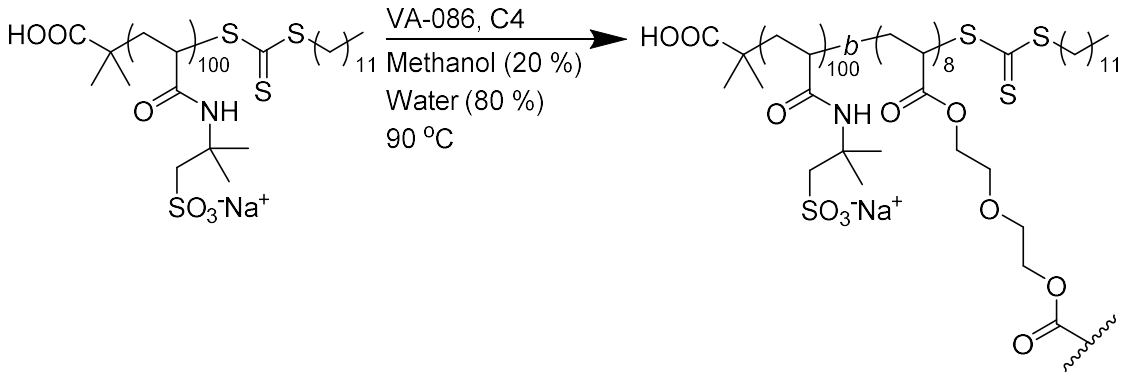

42

121
Arm Incorporated[a] ~ 82 %
$M_{n,SEC}$[b] = 180 kg/mol
$Đ$[b] = 1.11

Scheme 3-5: Star polymer synthesis using DDMAT-PAMPS$_{100}$

[a] The conversion of the arm into star was determined using **Equation 7**; [b] Experimental M_n and $Đ$ values were determined by size-exclusion chromatography in 20 % MeOH / 80 % 0.1M $NaNO_3$ in milli-Q water eluent using a conventional calibration obtained with PEG/PEO standards.

Star polymers were successfully synthesised within 40 minutes using C4 as cross-linker with a ratio of cross-linker to CTA of 8 and maintaining the cross-linker concentration at 0.12 M (**Scheme 3-5**, **Polymer 121**). The percentage of arm incorporation was similar to when BDMAT was used (DDMAT = 82 % and BDMAT = 80 %). However, the molecular weight observed with DDMAT was found to be slightly higher ($M_{n,DDMAT}$ = 180 kg/mol, $Đ_{DDMAT}$ = 1.11 and $M_{n,BDMAT}$ = 126 kg/mol, $Đ_{BDMAT}$ = 1.17), (**Figure 3-26**) compared to the PAMPS$_{100}$-BDMAT star polymer. As previously mentioned for the synthesis of the PDMA$_{100}$-DDMAT star polymer, this can be either explained by a better compartmentalisation of the cross-linker (higher number of arms per star polymer) or to a difference in hydrodynamic volume

associated with a lower cross-linker density into the core (higher swelling ability of the core).[183]

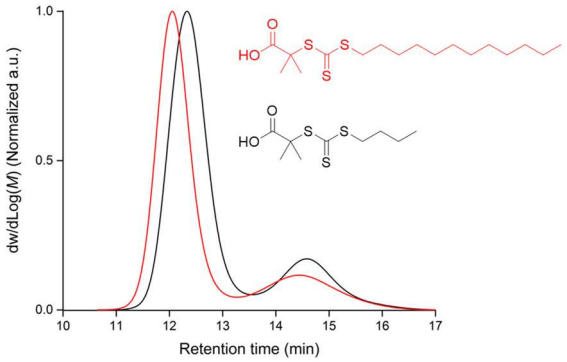

Figure 3-26: RI traces (aqueous SEC) overlay of the star polymers synthesised with either $PAMPS_{100}$-DDMAT (red line) or $PAMPS_{100}$-BDMAT (black line).

3.4 Conclusions

The synthesis of a range of complex architectures of PAMPS using RAFT polymerisation was reported. Highly ordered multiblock homopolymers and copolymers using AMPS®2405 were obtained with full monomer consumption in between each chain extension. A multitude of comonomers with different functionalities (amine, hydroxyl, carboxylic acid) showed good control over molecular weight for the synthesis of diblock copolymers where the pH was shown to be a critical parameter due to the potential hydrolysis of CTA in basic conditions. An octablock copolymer [$PAMPS_{10}$-*b*-$PHEAm_{10}$]$_4$ was successfully synthesised within 9 hours with a final dispersity of 1.48. The influence of monomer distribution on the polymerisation was studied by comparing the octablock polymer with a tetrablock, diblock and random copolymer of analogous composition (i.e. same overall DP and same monomer composition). Finally, AMPS-derived star-shaped polymers with narrow dispersity ($Đ$ < 1.30), high arm incorporation (~ 90 %) and no star-star coupling (**Figure 3-27**) were successfully prepared.

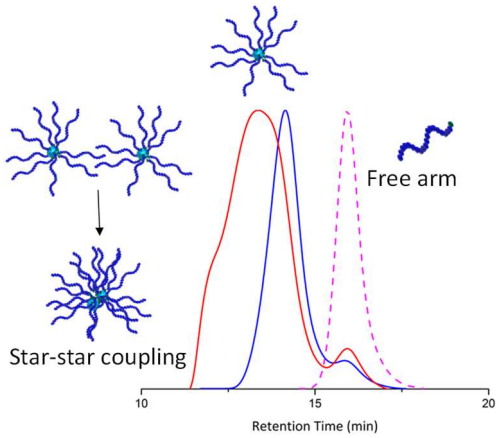

Figure 3-27: Star shaped homopolymer synthesised in this chapter.

This is, to the best of our knowledge, the first example of multiblock core cross-linked star (CCS) copolymerisation via RAFT polymerisation. The ratio of cross-linker to CTA and the nature of the cross-linker were crucial parameters where optimisation resulted in high arm-incorporation and narrow molecular weight distribution in the absence of star-star couplings. Additionally, random and diblock-based CCS copolymers of similar structures were prepared (**Figure 3-28**).

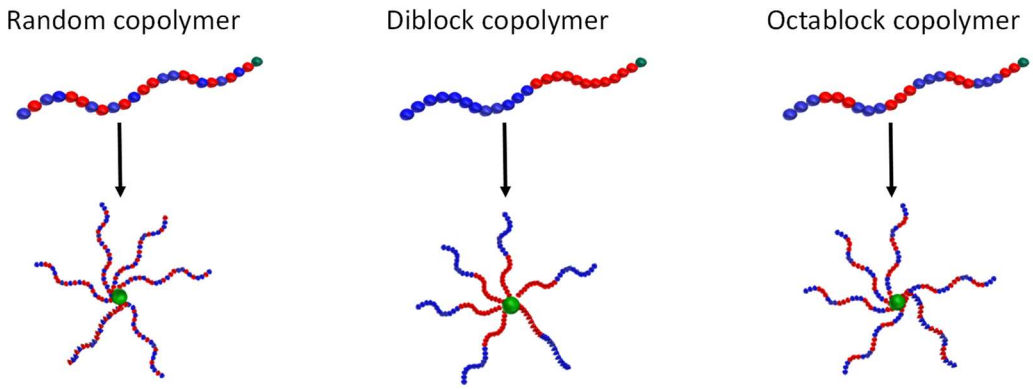

Figure 3-28: Star copolymer synthesised in this chapter.

Additionally, PAMPS synthesised from DDMAT chain transfer agent was used for the synthesis of core cross-linked star polymers, where high percentage of arm incorporated (82 %) and low dispersity (1.11) were obtained. DDMAT, was shown to increase the CL compartmentalisation for the synthesis of well-defined star polymers in aqueous solution. These CCS are good candidates to be scaled-up for industrial purpose as both the monomer and CTA are available in large scale. The investigation of such complex architectures for both physical and rheological properties but also for biological applications are studied in the following two chapters (**CHAPTER 4** and **CHAPTER 5**).

3.5 Experimental

Poly(sodium 2-acrylamido-2-methylpropane sulfonate) Block Homopolymers

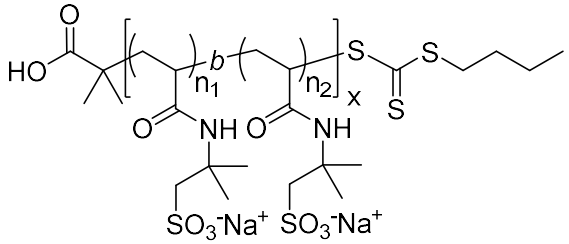

PAMPS

Polymer 59

Example. n1 = n2 = 50, x = 1

First Block Synthesis: BDMAT (26.0 mg, 0.1 mmol), AMPS®2405 (2.00 g, 5.1 mmol), phosphate buffer tablet at pH 6.5 (1.5 mL), sodium hydroxide (5.1×10^{-2} mmol, 2.0 mg) and VA-086 (8.4×10^{-3} mmol, 2.4 mg) (from stock solution at 20.0 mg/mL) were introduced into a flask equipped with a magnetic stirrer bar and sealed with a rubber septum. The solution was deoxygenated by bubbling with nitrogen for 10 minutes, and the vial was then placed in a temperature controlled oil bath at the desired temperature (90 °C), for the duration of time required to reach nearly full conversion (~ 2 hours).

Subsequent Blocks Synthesis: A solution containing AMPS®2405 (2.00 g, 5.1 mmol) and further VA-086 (1.7 mg, 5.9×10^{-3} mmol) was degassed and added via a syringe to the polymerisation medium. The polymerisation mixture was allowed to polymerise at the same temperature (90 °C) for the time required to reach full monomer conversion (~ 1 hour).

At the end of each chain extension a sample was withdrawn and allowed to cool down at room temperature. Each block was characterised using ^{1}H NMR spectroscopy and SEC ($M_{n,SEC}$ and $Đ$ were determined). The final compound was then dialysed against water for 48 hours and freeze dried, to yield the final compound as a pale yellow powder.

Similar polymers with varying degrees of polymerisation were found to exhibit similar spectroscopic data that the homopolymer Poly(sodium 2-acrylamido-2-methylpropane sulfonate) (i.e. **Polymer 19**). The SEC chromatogram for the above products can be seen in **Section 3.3.1**.

Table S 3-1: Conditions used for the preparation of $[PAMPS_{10}]_8$ via RAFT polymerisation in phosphate buffer solution at 90 °C by sequential monomer additions.

Block	1	2	3	4	5	6	7	8
Monomer	AMPS®2405							
$DP_{targeted}$	10	10	10	10	10	10	10	10
$m_{monomer\ added}$ (mg)	580	580	580	580	580	580	580	580
m_{CTA} (mg)	64	-	-	-	-	-	-	-
$m_{VA\text{-}086\ added}$ (mg)	1.22	0.85	0.82	0.89	0.96	1.03	1.11	1.17
m_{NaOH} (mg)	5.06	-	-	-	-	-	-	-
m_{H2O} (mg)	358	-	-	-	-	-	-	-
V_{total} (mL)[a]	1.7	2.5	3.4	4.3	5.2	6.0	6.9	7.8
$VA\text{-}086_{consumed}$ (%)[b]	20	11	11	11	11	11	11	11
$m_{VA\text{-}086\ total}$ (mg)[c]	1.22	1.83	2.46	3.08	3.72	4.35	4.99	5.62
$[AMPS®2405]_0$ (M)[d]	1.50	1.00	0.74	0.59	0.49	0.42	0.37	0.32
$[CTA]_t/[VA\text{-}086]_0$	60	40	30	24	20	17	15	13
$[CTA]_t/[VA\text{-}086]_{consumed}$	301	380	282	225	186	159	139	123
L (%)[e]	99.7	99.8	99.8	99.8	99.8	99.8	99.8	99.8
Cumulative L (%)[f]	99.7	99.5	99.3	99.1	99.0	98.8	98.6	98.5

[a] Represents the sum of the volume of the monomer added + V_{total} from the previous block. [b] Determined using the following equation $VA\text{-}086_{consumed} = [VA\text{-}086]_{consumed}/[VA\text{-}086]_0 *100 = 2f(1\text{-}exp(\text{-}k_d t))(1\text{-}f_c/2)*100$ with $f = 0.5$, $f_c = 0$, $k_d = 3.1x10^{-5}\ s^{-1}$. [c] Represents the total weight of VA-086 at the start of each chain extension characterised by the sum of the weight of VA-086 added plus the weight of VA-086 remaining from the previous block. [d] Represents the concentration of monomer at the beginning of each block extension. [e] Theoretical estimation of the fraction of living chains per block. [f] Theoretical estimation of the cumulated fraction of living chains

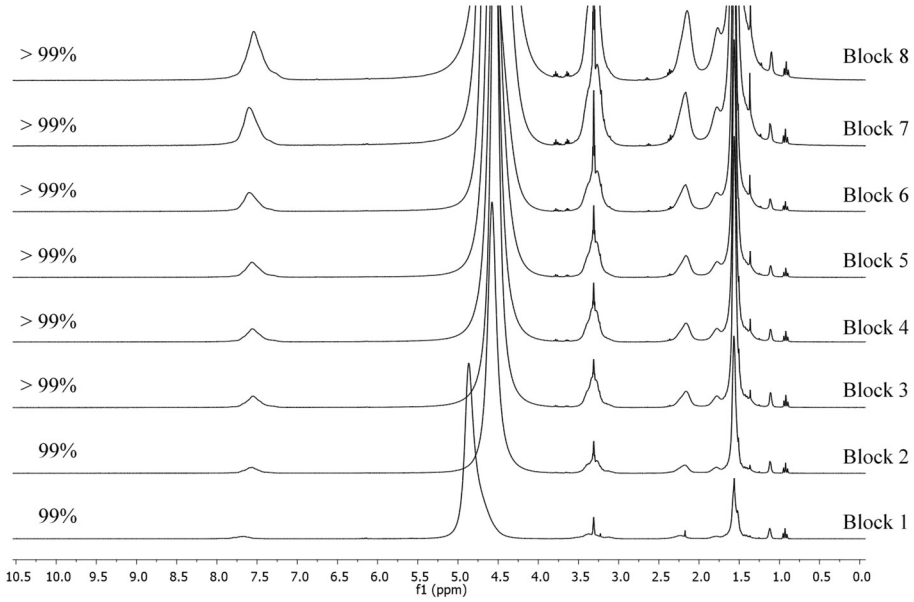

Figure S 3-1: ^1H NMR spectra (CD_3OD, 300 MHz) displaying the monomer conversion for each new chain extension (up to 8 blocks, **Polymer 56**).

Poly(sodium 2-acrylamido-2-methylpropane sulfonate) Block Copolymers

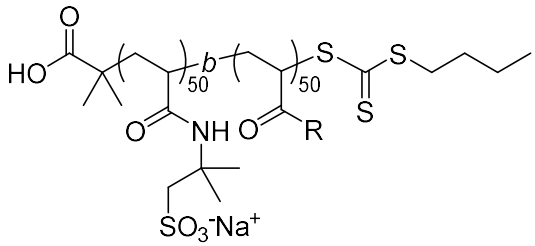

PAMPS Copolymer

Polymers 64 to 70

First Block Synthesis: BDMAT (26 mg, 0.1 mmol), AMPS®2405 (2.00 g, 5.1 mmol), phosphate buffer solution (1.5 mL), sodium hydroxide (5.1×10^{-2} mmol, 2 mg) and VA-086 (8.4×10^{-3} mmol, 2.4 mg) (from stock solution at 20.0 mg/mL) were introduced into a flask equipped with a magnetic stirrer bar and sealed with a rubber septum. The solution was deoxygenated by bubbling with nitrogen for 10 minutes, and the vial was then placed in a temperature controlled oil bath at the desired temperature (90 °C), for the duration of time required to reach nearly full conversion (~ 2 hours).

Subsequent Block Synthesis: A solution containing monomer (5.1 mmol) and further VA-086 was degassed and added via a syringe to the polymerisation medium. The polymerisation mixture was allowed to polymerise at the same temperature (90 °C) for the time required to reach full monomer conversion.

At the end of each chain extension a sample was withdrawn and allowed to cool down at room temperature. Each blocks were characterised using ^{1}H NMR spectroscopy and SEC ($M_{n,SEC}$ and $Đ$ were determined). The final compound was then dialysed against water for 48 hours and freeze dried, to yield the final compound as a pale yellow powder; m.p. > 300 °C;

PAMPS-*b*-PHEAm (**Polymer 66**): ν_{max}/cm^{-1} 3290 (br. m, COO-H and O-H, stretch), 2930 (w, C-H, stretch), 1646 (s, C=O, stretch), 1542 (m, N-H, bend), 1182 (s, C-N, stretch), 1160 (s, C-SO_3^-, stretch), 1040 (s, C=S, stretch); δH (300 MHz, CD_3OD) 3.80 – 3.56 (102H, br. m, $CH_2SO_3^-Na^+$, C*H*$_2$S and $CH_2CHSC(S)S$), 3.55 – 3.05 (207H, br. m, NHC*H*$_2$, OHC*H*$_2$), 2.50 – 1.90 (98H, br. m, $CH_2CH(CONH)$), 1.88 – 1.16 (476H, br. m, C*H*$_2$CH(CONH), $C(CH_3)_2CH_2SO_3^-Na^+$ and $CH_3CH_2CH_2$), 1.09 6H, s, $COOHC(CH_3)_2$), 0.93 3H, t, *J* = 7.3 Hz, $CH_3CH_2CH_2$).

PAMPS-*b*-PNAM (**Polymer 64**): ν_{max}/cm^{-1} 3311 (br. m, COO-H, stretch), 2929 (w, C-H, stretch), 1634 (s, C=O, stretch), 1545 (m, N-H, bend), 1444 (m, ar. C-C, stretch), 1185 (s, C-SO_3^-, stretch), 1112 (m, C-O-C, stretch), 1041 (s, C=S, stretch); δH (300 MHz, CD_3OD) 3.95 – 3.10 (569H, br. m, $CH_2SO_3^-Na^+$, (N-C*H*$_2$C*H*$_2$O) x 2, C*H*$_2$S and CH$_2$C*H*SC(S)S)), 2.95 -2.45 (46H, br. m, CH$_2$C*H*(CON)), 2.42 – 2.05 (42H, br. m, CH$_2$C*H*(CONH)), 2.02 – 1.17 (481H, br. m, C*H*$_2$CH(CON), C*H*$_2$CH(CONH), C(C*H*$_3$)$_2$CH$_2$SO$_3^-$Na$^+$ and CH$_3$C*H*$_2$C*H*$_2$), 1.11 (6H, br. s, COOHC(C*H*$_3$)$_2$), 0.93 (3H, t, *J* = 6.6 Hz, C*H*$_3$CH$_2$CH$_2$).

PAMPS-*b*-PAA (**Polymer 70**): ν_{max}/cm^{-1} 3311 (br. m, COO-H, stretch), 1642 (s, C=O, stretch), 1546 (s, N-H, bend), 1185 (s, C-N, stretch), 1114 (s, C-SO_3^-, stretch), 1042 (s, C=S, stretch); δH (300 MHz, CD_3OD) 3.92 – 2.92 (105H, br. m, $CH_2SO_3^-Na^+$, C*H*$_2$S and CH$_2$C*H*SC(S)S), 2.87 – 2.07 (87H, br. m, CH$_2$C*H*(CONH) and CH$_2$C*H*(COOH)), 2.05 – 1.24 (425H, br. m, C*H*$_2$CH(COOH), C*H*$_2$CH(CONH), C(C*H*$_3$)$_2$CH$_2$SO$_3^-$Na$^+$ and CH$_3$C*H*$_2$C*H*$_2$), 1.17 (6H, br. s, COOHC(C*H*$_3$)$_2$), 0.94 (3H, t, *J* = 7.3 Hz, C*H*$_3$CH$_2$CH$_2$).

PAMPS-*b*-PAM (**Polymer 67**): ν_{max}/cm^{-1} 3311 (br. m, COO-H, stretch), 1643 (s, C=O, stretch), 1544 (s, N-H, bend), 1447 (w, C-N (NH_2C=O), stretch), 1184 (s, C-N, stretch), 1161 (s, C-SO_3^-, stretch), 1041 (s, C=S, stretch); δH (300 MHz, CD_3OD) 3.87 – 2.90 (120H, br. m, $CH_2SO_3^-Na^+$, C*H*$_2$S and CH$_2$C*H*SC(S)S), 2.85 – 2.00 (85H, br. m, CH$_2$C*H*(CONH) and CH$_2$C*H*(CONH$_2$)), 1.99 – 1.17 (437H, br. m, C*H*$_2$CH(CONH$_2$), C*H*$_2$CH(CONH), C(C*H*$_3$)$_2$CH$_2$SO$_3^-$Na$^+$ and CH$_3$C*H*$_2$C*H*$_2$), 1.09 (6H, br. s, COOHC(C*H*$_3$)$_2$), 0.93 (3H, t, *J* = 7.2 Hz, C*H*$_3$CH$_2$CH$_2$).

The SEC chromatogram for the above products can be seen in **Section 3.3.2**.

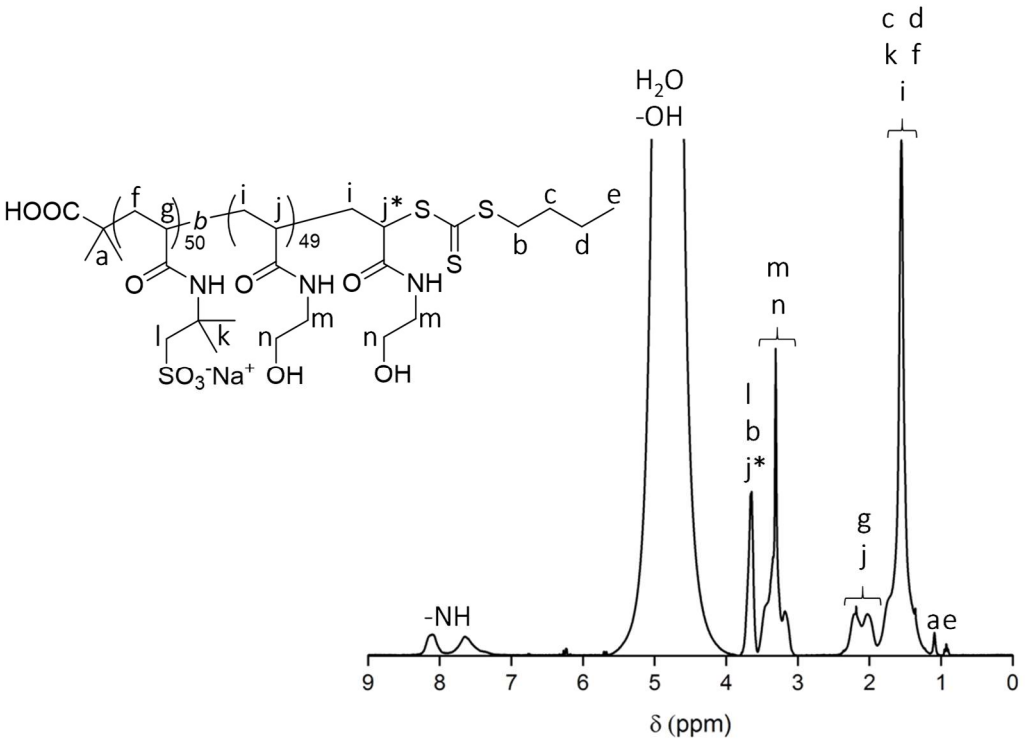

Figure S 3-2: ^{1}H NMR spectrum of PAMPS-*b*-PHEAm (**Polymer 66**) in CD_3OD.

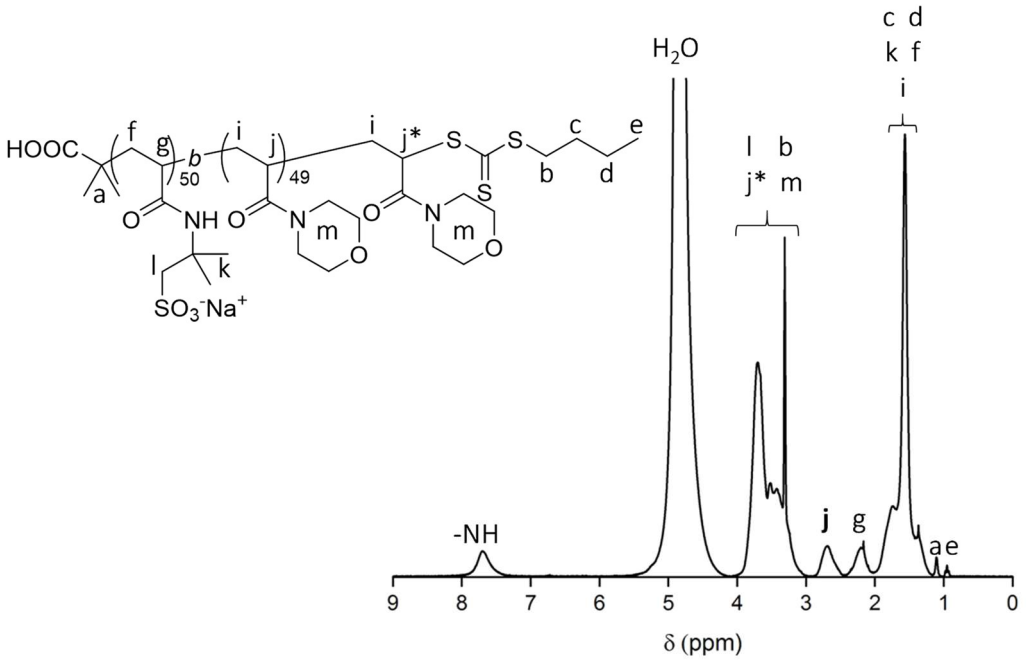

Figure S 3-3: ^{1}H NMR spectrum of PAMPS-*b*-PNAM (**Polymer 64**) in CD_3OD.

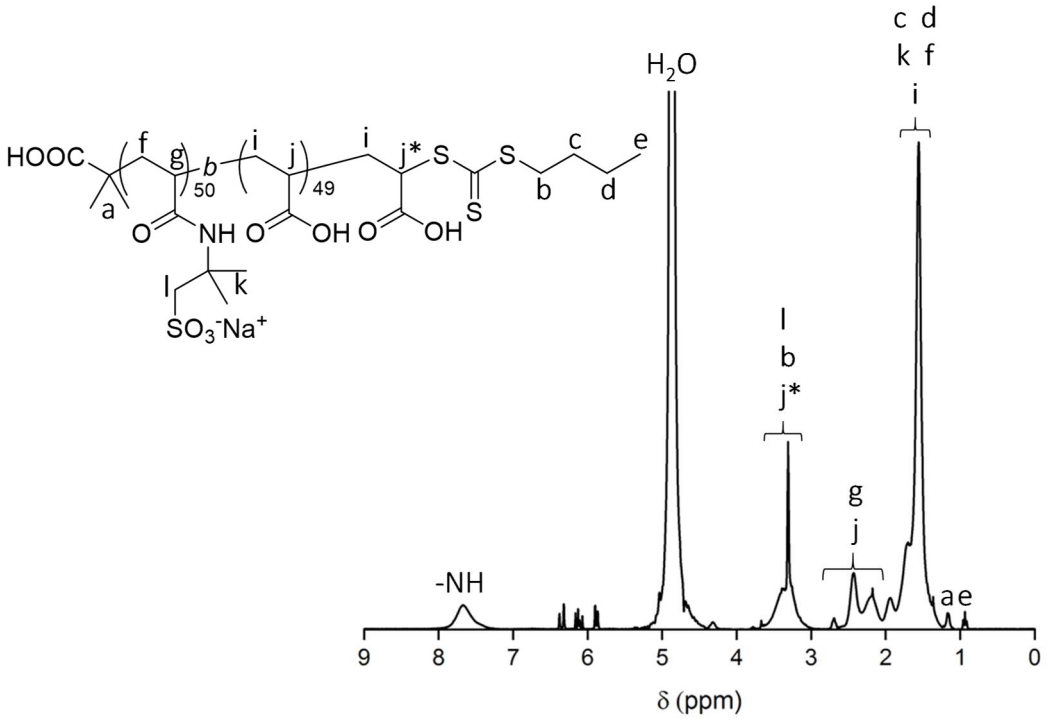

Figure S 3-4: ^{1}H NMR spectrum of PAMPS-*b*-PAA (**Polymer 70**) in CD_3OD.

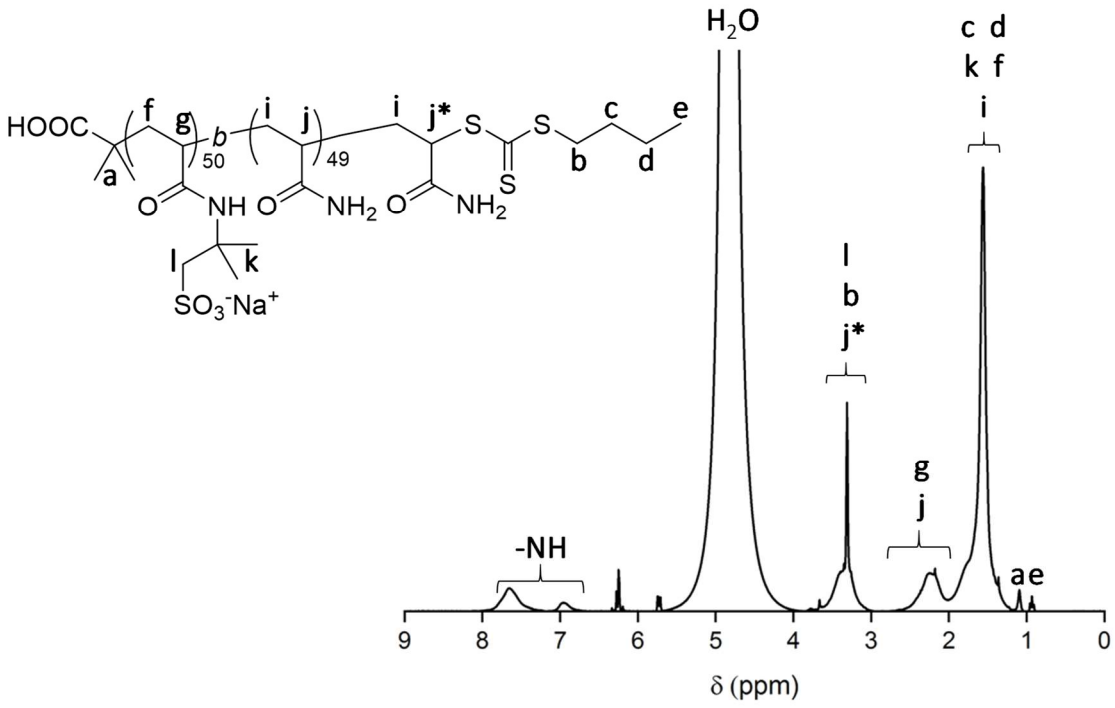

Figure S 3-5: ^{1}H NMR spectrum of PAMPS-*b*-PAM (**Polymer 67**) in CD_3OD.

Table S 3-2: Conditions used for the preparation of block copolymers using $PAMPS_{50}$ as macroCTA for the chain extension via RAFT polymerisation in phosphate buffer solution at 90 °C by sequential monomer additions of the following monomers: AMPS®2405, NAM, DMA, HEAm, AM and AA.

Block	1	2	2	2	2	2	2
Monomer	AMPS®2405	AMPS®2405	NAM	DMA	HEAm	AM	AA
$DP_{targeted}$	50	50	50	50	50	50	50
$m_{monomer\ added}$ (mg)	2000	580	580	580	580	580	580
m_{CTA} (mg)	26	-	-	-	-	-	-
$m_{VA\text{-}086\ added}$ (mg)	2.43	1.69	0.94	0.86	0.86	0.86	074
m_{NaOH} (mg)	2.03	-	-	-	-	-	-
m_{H2O} (mg)	487	-	-	-	-	-	-
V_{total} (mL)[a]	3.38	5.1	4.1	3.90	3.90	3.90	3.70
$VA\text{-}086_{consumed}$ (%)[b]	20	11	20	20	20	20	20
$m_{VA\text{-}086\ total}$ (mg)[c]	2.43	2.81	2.89	2.81	2.81	2.81	2.69
$[Monomer]_0$[d] (M)	1.5	1.0	1.3	1.3	1.3	1.3	1.4
$[CTA]_t/[VA\text{-}086]_0$	12	8	10	10	10	10	11
$[CTA]_t/[VA\text{-}086]_{consumed}$	60	52	51	52	52	52	55
L (%)[e]	98.4	98.9	98.4	99.2	98.4	98.4	98.4
Cumulative L (%)[f]	98.4	97.2	96.8	97.6	96.8	96.8	96.8

[a] Represents the sum of the volume of the monomer added + V_{total} from the previous block. [b] Determined using the following equation $VA\text{-}086_{consumed} = [VA\text{-}086]_{consumed}/[VA\text{-}086]_0 *100 = 2f(1\text{-}exp(\text{-}k_d t))(1\text{-}f_c/2)*100$ with $f = 0.5$, $f_c = 0$, $k_d = 3.1x10^{-5}\ s^{-1}$. [c] Represents the total weight of VA-086 at the start of each chain extension characterised by the sum of the weight of VA-086 added plus the weight of VA-086 remaining from the previous block. [d] Represents the concentration of monomer at the beginning of each block extension. [e] Theoretical estimation of the fraction of living chains per block. [f] Theoretical estimation of the cumulated fraction of living chains

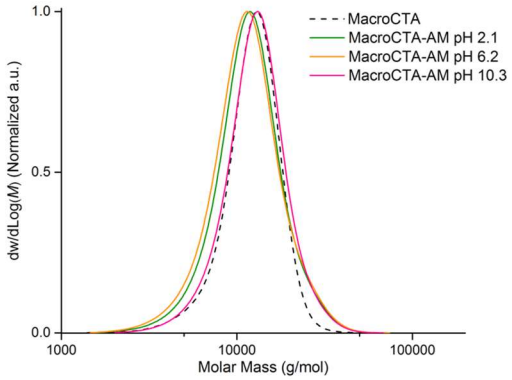

Figure S 3-6: Aqueous SEC molecular weight distributions showing the macroCTA BDMAT-$PAMPS_{50}$ (black dotted line) and the corresponding chain extension using AM varying the pH from 2 to 10.

Table S 3-3: SEC analysis data of the diblock copolymers synthesised in this chapter using BDMAT-PAMPS$_{50}$ macro CTA with different eluents and detectors.

Polymer	Monomer	$M_{n,th}$ (g/mol)[a]	$M_{n,SEC}$ (g/mol) Aqueous (RI)[b]	$Đ$	$M_{n,SEC}$ (g/mol) Aqueous (RI, LS, VS)[c]	$Đ$	$M_{n,SEC}$ (g/mol) DMF (RI)[d]	$Đ$
19	MacroCTA	11,600	11,200	1.15	8,600	1.04	10,100	1.31
64	NAM	18,300	7,400	1.32	15,600	1.03	16,000	1.39
65	DMA	16,200	11,200	1.19	13,800	1.06	14,500	1.36
66	HEAm	17,500	11,400	1.22	16,500	1.05	19,600	1.33
67	AM	14,800	10,500	1.22	11,600	1.04	12,000	1.39
70	AA	14,700	15,300	1.12	12,300	1.02	7,000	1.29

[a] Theoretical M_n values were calculated using **Equation 2**; [b] Experimental M_n and $Đ$ values were determined by size-exclusion chromatography in 20 % MeOH / 80 % 0.1M $NaNO_3$ in milli-Q water eluent using a conventional calibration obtained with PEG/PEO standards; [c] Experimental M_n and $Đ$ values were determined by size-exclusion chromatography in 20 % MeOH / 80 % 0.1M $NaNO_3$ in milli-Q water eluent using an universal calibration; [d] Experimental M_n and $Đ$ values were determined by size-exclusion chromatography in DMF with 0.1 % LiBr using a conventional calibration obtained with PMMA standards.

Poly(sodium 2-acrylamido-2-methylpropane sulfonate – *Block* – *N*-hydroxyethyl acrylamide)

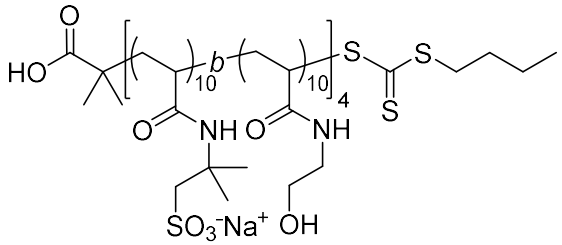

PAMPS-*b*-PHEAm
Polymer 72

First Block Synthesis: BDMAT (26.0 mg, 0.1 mmol), AMPS®2405 (1.00 g, 2.5 mmol), phosphate buffer tablet at pH 6.5 (1.5 mL), sodium hydroxide ($1.3x10^{-1}$ mmol, 5.0 mg) and VA-086 ($4.2x10^{-3}$ mmol, 1.2 mg) (from stock solution at 20.0 mg/mL) were introduced into a flask equipped with a magnetic stirrer bar and sealed with a rubber septum. The solution was deoxygenated by bubbling with nitrogen for 10 minutes, and the vial was then placed in a temperature controlled oil bath at the desired temperature (90 °C), for the duration of time required to reach nearly full conversion (~ 2 hours).

Subsequent Block Synthesis: A solution containing monomer (2.5 mmol) and further VA-086 was degassed and added via a syringe to the polymerisation medium. The polymerisation mixture was allowed to polymerise at the same temperature (90 °C) for the time required to reach full monomer conversion.

At the end of each chain extension a sample was withdrawn and allowed to cool down at room temperature. Each block was characterised using ^{1}H NMR spectroscopy and SEC ($M_{n,SEC}$ and $Đ$ were determined). The final compound was then dialysed against water for 48 hours and freeze dried, to yield the final compound as a pale yellow powder.

Similar polymers with varying degrees of polymerisation were found to exhibit similar spectroscopic data to that of the title compound diblock PAMPS-*b*-PHEAm (**Polymer 66**). ^{1}H NMR spectra of the diblock, random and octablock copolymer of AMPS®2405 with HEAm (DP = 80) are displayed in **Figure S 5-3**. The SEC chromatogram for the above products can be seen in **Section 3.3.3**.

Similar conditions were used for the synthesis of the tetrablock copolymer of AMPS®2405 with NAM ($[PAMS_{10}$-*b*-$PNAM_{10}]_2$) which exhibit similar spectroscopic

data that the diblock PAMPS-*b*-PNAM (i.e. **Polymer 64**). The SEC chromatogram for the above products can be seen in **Section 3.3.3**.

Table S 3-4: Conditions used for the preparation of [$PAMPS_{10}$-*b*-$PHEAm_{10}$]$_8$ via RAFT polymerisation in phosphate buffer solution at 90 °C by sequential monomer additions.

Block	1	2	3	4	5	6	7	8
Monomer	AMPS® 2405	HEAm	AMPS® 2405	HEAm	AMPS® 2405	HEAm	AMPS® 2405	HEAm
$DP_{targeted}$	10	10	10	10	10	10	10	10
$m_{monomer\ added}$ (mg)	1000	292	1000	292	1000	292	1000	292
m_{CTA} (mg)	64	-	-	-	-	-	-	-
$m_{VA\text{-}086\ added}$ (mg)	1.22	0.47	0.91	0.43	1.08	0.53	1.25	0.64
$M_{NaOH\ added}$ (mg)	5.06	-	-	-	-	-	-	-
V_{H2O}	358	-	-	-	-	-	-	-
V_{total} (mL)[a]	1.69	1.99	2.85	3.15	4.01	4.33	5.19	5.51
$VA\text{-}086_{consumed}$ (%)[b]	20	20	11	20	11	20	11	20
$m_{VA\text{-}086\ total}$ (mg)[c]	1.22	1.42	2.06	2.26	2.89	3.11	3.73	3.98
$[Monomer]_0$ (M)[d]	1.50	1.27	0.89	0.80	0.63	0.59	0.49	0.46
$[CTA]_t/[VA\text{-}086]_0$	60	51	36	32	25	23	20	18
$[CTA]_t/[VA\text{-}086]_{consumed}$	301	255	338	161	240	117	186	92
L (%)[e]	99.7	99.7	99.8	99.7	99.8	99.7	99.8	99.7
Cumulative L %)[f]	99.7	99.3	99.2	98.8	98.7	98.3	98.2	97.8

[a] Represents the sum of the volume of the monomer added + V_{total} from the previous block. [b] Determined using the following equation $VA\text{-}086_{consumed} = [VA\text{-}086]_{consumed}/[VA\text{-}086]_0 *100 = 2f(1\text{-}\exp(\text{-}k_d t))(1\text{-}f_c/2)*100$ with $f = 0.5$, $f_c = 0$, $k_d = 3.1 \times 10^{-5}\ s^{-1}$. [c] Represents the total weight of VA-086 at the start of each chain extension characterised by the sum of the weight of VA-086 added plus the weight of VA-086 remaining from the previous block. [d] Represents the concentration of monomer at the beginning of each block extension. [e] Theoretical estimation of the fraction of living chains per block. [f] Theoretical estimation of the cumulated fraction of living chains

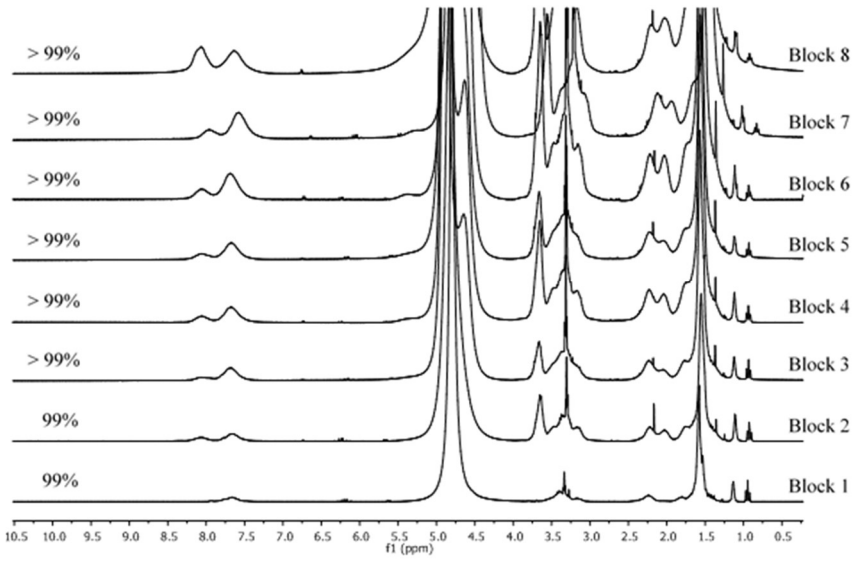

Figure S 3-7: ^{1}H NMR spectra (CD_3OD, 300 MHz) for each new chain extension (up to 8 blocks) alternating AMPS®2405 and HEAm blocks.

Table S 3-5: Conditions used for the preparation of [$PAMPS_{20}$-*b*-$PHEAm_{20}$]$_2$ via RAFT polymerisation in phosphate buffer solution at 90 °C by sequential monomer additions.

Block	1	2	3	4
Monomer	AMPS®2405	HEAm	AMPS®2405	HEAm
$DP_{targeted}$	20	20	20	20
$m_{monomer\ added}$ (mg)	725	211	725	211
m_{CTA} (mg)	23	-	-	-
$m_{VA\text{-}086\ added}$ (mg)	0.88	0.32	0.65	0.29
$m_{NaOH\ added}$ (mg)	1.84	-	-	-
V_{H2O} (mL)	0.620	-	-	-
V_{total} (mL)[a]	1.22	1.43	2.07	2.29
$VA\text{-}086_{consumed}$ (%)[b]	20	20	11	20
$m_{VA\text{-}086\ total}$ (mg)[c]	0.88	1.02	1.50	1.64
$[Monomer]_0$ (M)[d]	1.50	1.30	0.90	0.81
$[CTA]_t/[VA\text{-}086]_0$	60	51	36	32
$[CTA]_t/[VA\text{-}086]_{consumed}$	301	355	338	161
L (%)[e]	99.3	99.3	99.6	99.3
Cumulative L (%)[f]	99.3	98.7	98.3	97.7

[a] Represents the sum of the volume of the monomer added + V_{total} from the previous block. [b] Determined using the following equation $VA\text{-}086_{consumed} = [VA\text{-}086]_{consumed}/[VA\text{-}086]_0 *100 = 2f(1\text{-}\exp(\text{-}k_d t))(1\text{-}f_c/2)*100$ with $f = 0.5$, $f_c = 0$, $k_d = 3.1\text{x}10^{-5}$ s^{-1}. [c] Represents the total weight of VA-086 at the start of each chain extension characterised by the sum of the weight of VA-086 added plus the weight of VA-086 remaining from the previous block. [d] Represents the concentration of monomer at the beginning of each block extension. [e] Theoretical estimation of the fraction of living chains per block. [f] Theoretical estimation of the cumulated fraction of living chains

Table S 3-6: Conditions used for the preparation of [$PAMPS_{10}$-*b*-$PNAM_{10}$]$_2$ via RAFT polymerisation in phosphate buffer solution at 90 °C by sequential monomer additions.

Block	1	2	3	4
Monomer	AMPS®2405	NAM	AMPS®2405	NAM
$DP_{targeted}$	10	10	10	10
$m_{monomer\ added}$ (mg)	1160	715	1160	715
m_{CTA} (mg)	128	-	-	-
$m_{VA\text{-}086\ added}$ (mg)	2.43	0.74	1.61	0.97
$M_{NaOH\ added}$ (mg)	10.13	-	-	-
V_{H2O}	1080	-	-	-
V_{total} (mL)[a]	3.38	4.07	5.79	5.63
$VA\text{-}086_{consumed}$ (%)[b]	20	20	11	20
$m_{VA\text{-}086\ total}$ (mg)[c]	1.22	1.45	1.98	2.25
$[Monomer]_0$ (M)[d]	1.50	1.24	0.88	0.90
$[CTA]_t/[VA\text{-}086]_0$	60	50	35	31
$[CTA]_t/[VA\text{-}086]_{consumed}$	301	325	334	203
L (%)[e]	99.6	99.6	99.8	99.7
Cumulative L (%)[f]	99.6	99.3	99.1	98.8

[a] Represents the sum of the volume of the monomer added + V_{total} from the previous block. [b] Determined using the following equation $VA\text{-}086_{consumed} = [VA\text{-}086]_{consumed}/[VA\text{-}086]_0 *100 = 2f(1\text{-}exp(\text{-}k_d t))(1\text{-}f_c/2)*100$ with $f = 0.5$, $f_c = 0$, $k_d = 3.1x10^{-5}$ s^{-1}. [c] Represents the total weight of VA-086 at the start of each chain extension characterised by the sum of the weight of VA-086 added plus the weight of VA-086 remaining from the previous block. [d] Represents the concentration of monomer at the beginning of each block extension. [e] Theoretical estimation of the fraction of living chains per block. [f] Theoretical estimation of the cumulated fraction of living chains

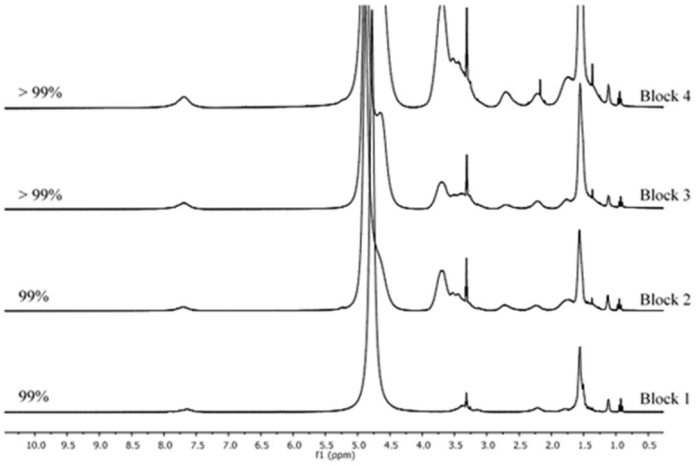

Figure S 3-8: ^1H NMR spectra (CD_3OD, 300 MHz) for each new chain extension (up to 4 blocks) alternating AMPS®2405 and NAM blocks.

Poly(sodium 2-acrylamido-2-methylpropane sulfonate – *Copolymer* – *N*-hydroxyethyl acrylamide)

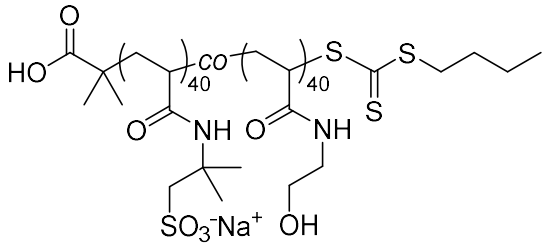

PAMPS-*co*-PHEAm

Polymer 75, DP80

BDMAT (26.0 mg, 0.1 mmol), HEAm (0.47 g, 4.1 mmol), AMPS®2405 (1.60 g, 4.1 mmol), phosphate buffer solution (2.5 mL), sodium hydroxide (5.1×10^{-2} mmol, 2.0 mg) and VA-086 (1.4×10^{-2} mmol, 4.0 mg) (both taken from a stock aqueous solution at 20.0 mg/mL) were introduced into a flask equipped with a magnetic stirrer bar, and sealed with a rubber septum. The solution was deoxygenated by bubbling with nitrogen for 10 minutes, and the vial was placed in a temperature controlled oil bath at the desired temperature (90 °C) for the time required to reach nearly full conversion (~ 1 hour). After the reaction, the mixture was cooled down to room temperature and opened to the atmosphere. The monomer conversion was then determined using ^{1}H NMR spectroscopy and the material was analysed by SEC ($M_{n,SEC}$ and Đ were determined). The compound was then dialysed against water for 48 hours and freeze dried, to yield the final compound as a pale yellow powder; m.p. > 300 °C; ν_{max}/cm^{-1} 3291 (br. m, COO-H and O-H, stretch), 2931 (w, C-H, stretch), 1648 (s, C=O, stretch), 1542 (m, N-H, bend), 1183 (s, C-N, stretch), 1160 (s, C-SO_3^-, stretch), 1040 (s, C=S, stretch).

Polymer 75 exhibits similar spectroscopic data to the title compound diblock PAMPS-*b*-PHEAm (**Polymer 66**). Overlaid ^{1}H NMR spectra of the diblock, random and octablock copolymer of AMPS®2405 with HEAm are displayed **Figure S 5-3**. The SEC chromatogram for the above products can be seen in **Section 3.3.3**.

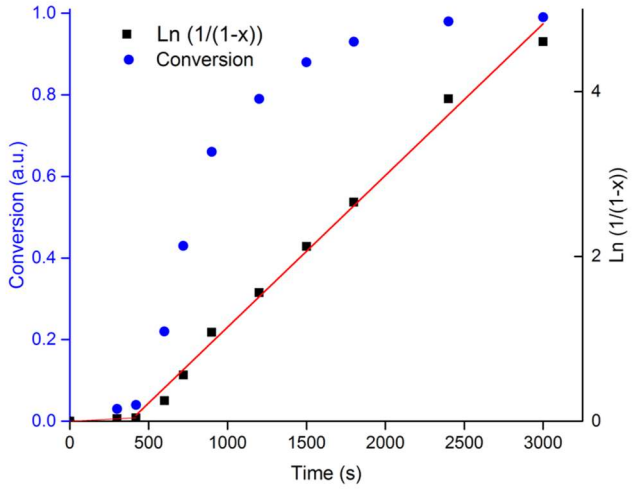

Figure S 3-9: Monomer conversion (blue) and Ln([Monomer]$_0$/[Monomer]) (black) versus time for the synthesis of random copolymer with AMPS®2405 and HEAm monomer.

Star Polymer Synthesis – General Procedure

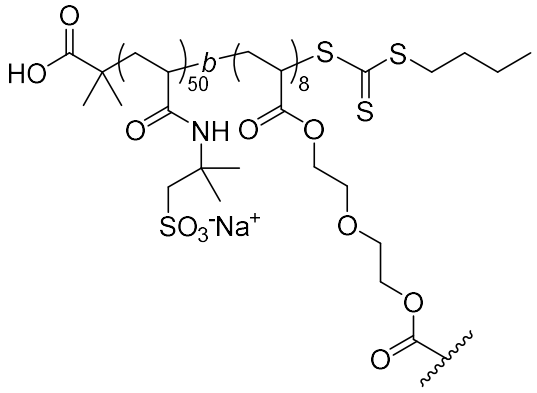

PAMPS-*b*-PC4

Polymer 84

Arm Synthesis: For the synthesis of the initial arms refer to the previous synthesis from **Sections 2.5 and 3.5** – Poly(sodium 2-acrylamido-2-methylpropane sulfonate), Poly(sodium 2-acrylamido-2-methylpropane sulfonate – *Block* – *N*-hydroxyethyl acrylamide) and Poly(sodium 2-acrylamido-2-methylpropane sulfonate – *Copolymer* – *N*-hydroxyethyl acrylamide).

Star Synthesis: Star polymer synthesis was carried out using a similar protocol as for block copolymer synthesis. An example of the synthesis is given here for a star comprised of $PAMPS_{50}$ homopolymer. A solution of additional initiator (0.6 mg, $2.2x10^{-3}$ mmol) and cross-linker (0.17g, $8.1x10^{-1}$ mmol) was degassed and added via a syringe to the polymerisation media. The polymerisation mixture was allowed to polymerise at the same temperature (90 °C) for the time required to reach full cross-linker conversion and maximum conversion of the arm into the star (45 min).

At the end of each chain extension a sample was withdrawn and allowed to cool down at room temperature. Each block was characterised using ^{1}H NMR spectroscopy and SEC ($M_{n,SEC}$ and $Đ$ were determined). The final compound was then dialysed against water for 48 hours and freeze dried, to yield the final compound as a white-ish yellow powder; m.p. > 300 °C; ν_{max}/cm^{-1} 3431 (br. m, COO-H, stretch), 1731 (w, C=O, stretch), 1650 (s, C=O, stretch), 1538 (s, N-H, bend), 1181 (s, C-N, stretch), 1160 (s, $C\text{-}SO_3^-$, stretch), 1040 (s, C=S, stretch).

Similar experimental conditions were used for the synthesis of star polymers with varying cross-linker type, the degrees of polymerisation and the cross-linker concentrations. The SEC chromatograms for the above products can be seen in **Sections 3.3.4**, **3.3.5**, **3.3.6** and **3.3.7**. For NMR analysis the internal reference (i.e. chain end CH_2CH_3) disappeared when the star polymer was formed due to its

internalisation into the core of the star polymer. For the star polymer similar spectra to the linear were obtained with the same characteristic peaks observed for the NMR of Poly(sodium 2-acrylamido-2-methylpropane sulfonate). Additionally, due to the formation of bigger macromolecules, the peaks observed by ^{1}H NMR spectroscopy were broader.

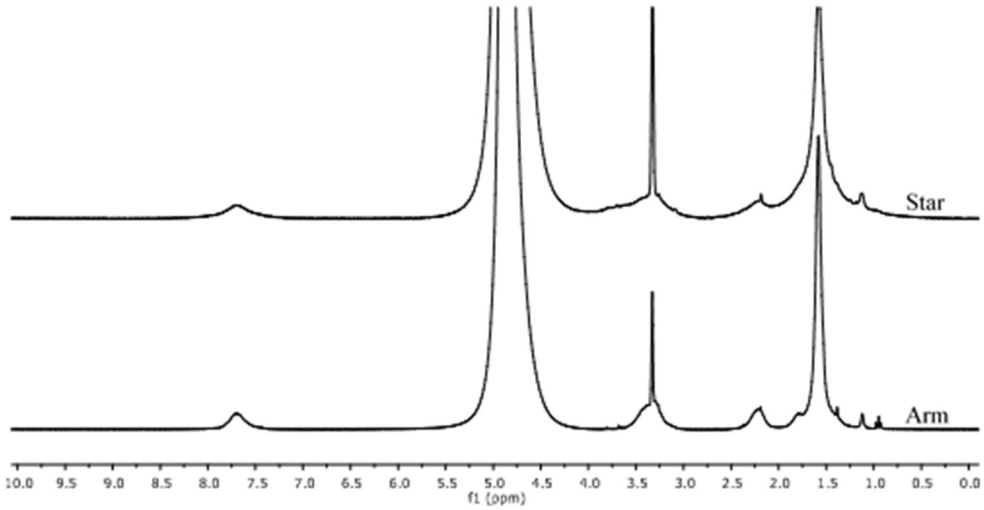

Figure S 3-10: ^{1}H NMR spectra (CD_3OD, 300 MHz) showing the monomer conversion for the arm (bottom) after 2 hours and the cross-linker conversion for the star (top) after 1 hour using $PAMPS_{100}$ as arm.

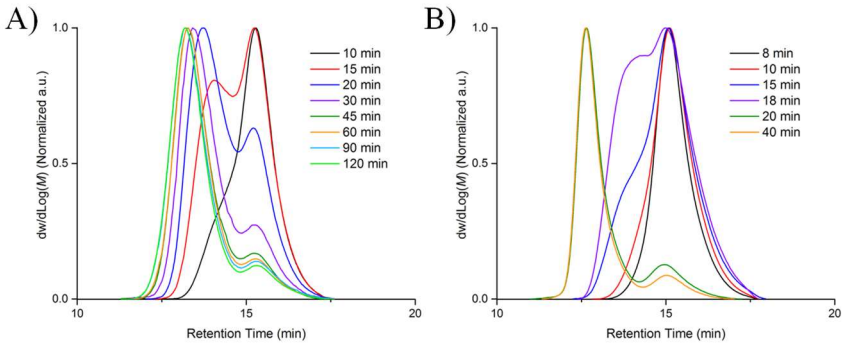

Figure S 3-11: Aqueous SEC chromatograms of the kinetic of the star polymers synthesised with DP_{arm} = 50 and [cross-linker]:[CTA] = 8.

A) C1; B) C4.

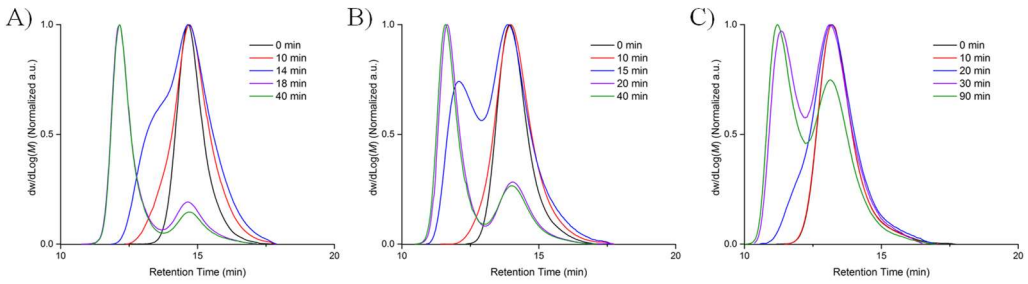

Figure S 3-12: Aqueous SEC chromatograms for the kinetic of the star polymers synthesised using C4 and [cross-linker]:[CTA] = 8.

A) DP_{arm} = 100; B) DP_{arm} = 200; C) DP_{arm} = 400.

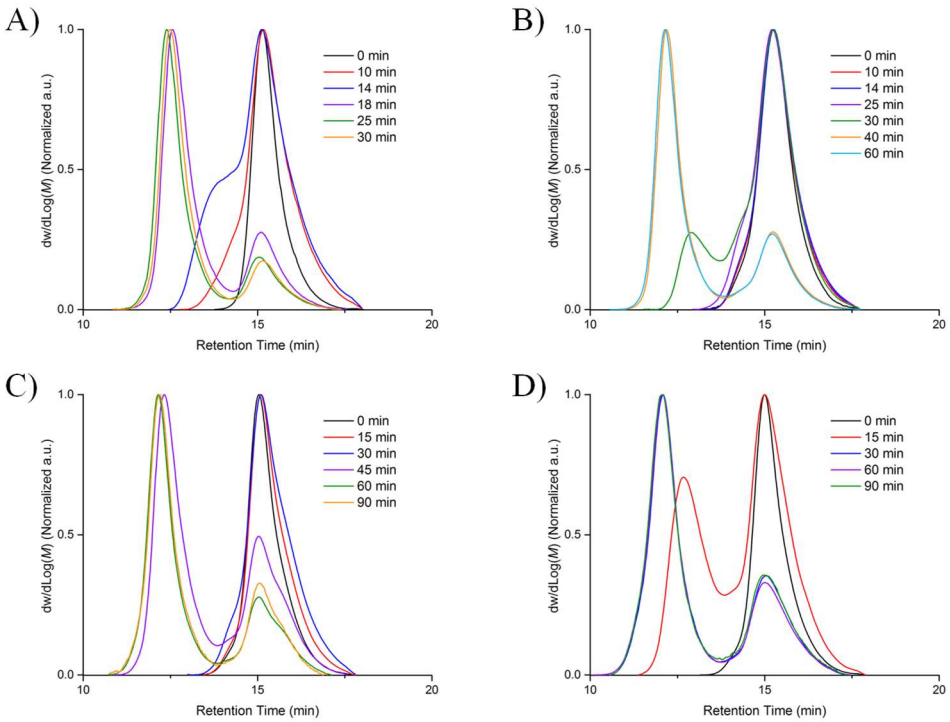

Figure S 3-13: Aqueous SEC chromatograms of the kinetic of the star copolymers synthesised using C4 with [C4]:[CTA] = 8.

A) $PAMPS_{40}$-*co*-$PHEAm_{40}$; B) $PAMPS_{40}$-*b*-$PHEAm_{40}$; C) $[PAMPS_{20}$-*b*-$PHEAm_{20}]_2$; D) $[PAMPS_{10}$-*b*-$PHEAm_{10}]_4$.

3.6 References

(42) Semsarilar, M.; Perrier, S. *Nat. Chem.* **2010**, *2*, 811.

(43) Moad, G.; Rizzardo, E.; Thang, S. H. *Polym. Int.* **2011**, *60*, 9.

(44) Willcock, H.; O'Reilly, R. K. *Polym. Chem.* **2010**, *1*, 149.

(47) Gody, G.; Maschmeyer, T.; Zetterlund, P. B. *Macromolecules* **2014**, *47*, 639.

(48) Gody, G.; Maschmeyer, T.; Zetterlund, P. B.; Perrier, S. *Macromolecules* **2014**, *47*, 3451.

(49) Gody, G.; Maschmeyer, T.; Zetterlund, P. B.; Perrier, S. *Nat. Commun.* **2013**, *4*.

(50) Keddie, D. J. *Chem. Soc. Rev.* **2014**, *43*, 496.

(58) Thomas, D. B.; Convertine, A. J.; Hester, R. D.; Lowe, A. B.; McCormick, C. L. *Macromolecules* **2004**, *37*, 1735.

(59) Thomas, D. B.; Convertine, A. J.; Myrick, L. J.; Scales, C. W.; Smith, A. E.et al *Macromolecules* **2004**, *37*, 8941.

(62) Gody, G.; Barbey, R.; Danial, M.; Perrier, S. *Polym. Chem.* **2015**, *6*, 1502.

(67) Chaduc, I.; Crepet, A.; Boyron, O.; Charleux, B.; D'Agosto, F.et al *Macromolecules* **2013**, *46*, 6013.

(89) Moraes, J.; Peltier, R.; Gody, G.; Blum, M.; Recalcati, S.et al *ACS Macro Lett.* **2016**, *5*, 1416.

(92) Dietzsch, M.; Barz, M.; Sch??ler, T.; Klassen, S.; Schreiber, M.et al *Langmuir* **2013**, *29*, 3080.

(93) Read, E.; Guinaudeau, A.; James Wilson, D.; Cadix, A.; Violleau, F.et al *Polym. Chem.* **2014**, *5*, 2202.

(100) Guillaneuf, Y.; Gigmes, D.; Marque, S. R. A.; Astolfi, P.; Greci, L.et al *Macromolecules* **2007**, *40*, 3108.

(101) Anastasaki, A.; Nikolaou, V.; Nurumbetov, G.; Wilson, P.; Kempe, K.et al *Chem. Rev.* **2016**, *116*, 835.

(102) Moad, G.; Rizzardo, E.; Thang, S. H. *Acc. Chem. Res.* **2008**, *41*, 1133.

(105) Sumerlin, B. S.; Donovan, M. S.; Mitsukami, Y.; Lowe, A. B.; McCormick, C. L. *Macromolecules* **2001**, *34*, 6561.

(106) Sumerlin, B. S.; Lowe, A. B.; Thomas, D. B.; McCormick, C. L. *Macromolecules* **2003**, *36*, 5982.

(107) Kellum, M. G.; Smith, A. E.; York, S. K.; McCormick, C. L. *Macromolecules* **2010**, *43*, 7033.

(122) Rinaudo, M.; Desbrieres, J. *Eur. Polym. J.* **1980**, *16*, 849.

(144) Yusa, S. I.; Yokoyama, Y.; Morishima, Y. *Macromolecules* **2009**, *42*, 376.

(145) Guragain, S.; Bastakoti, B. P.; Ito, M.; Yusa, S.-i.; Nakashima, K. *Soft Matter* **2012**, *8*, 9628.

(146) Zetterlund, P. B.; Gody, G.; Perrier, S. *Macromol. Theory Simul.* **2014**, *23*, 331.

(147) Martin, L.; Gody, G.; Perrier, S. *Polym. Chem.* **2015**, *6*, 4875.

(148) Chen, M.; Moad, G.; Rizzardo, E. *J. Polym. Sci., Part A: Polym. Chem.* **2009**, *47*, 6704.

(149) Gregory, A.; Stenzel, M. H. *Prog. Polym. Sci.* **2012**, *37*, 38.

(150) Gurnani, P.; Lunn, A. M.; Perrier, S. *Polymer* **2016**, *106*, 229.

(151) Wang, D.; Li, X.; Wang, W. J.; Gong, X.; Li, B. G.et al *Macromolecules* **2012**, *45*, 28.

(152) N. H. Aloorkar, A. S. K., R. A. Patil, D. J. Ingale *IJPSN* **2012**, *5*, 1675.

(153) Ren, J. M.; McKenzie, T. G.; Fu, Q.; Wong, E. H. H.; Xu, J.et al *Chem. Rev.* **2016**, *116*, 6743.

(154) Rosselgong, J.; Williams, E. G. L.; Le, T. P.; Grusche, F.; Hinton, T. M.et al *Macromolecules* **2013**, *46*, 9181.

(155) Bekhradnia, S.; Diget, J. S.; Zinn, T.; Zhu, K.; Sande, S. A.et al *Macromolecules* **2015**, *48*, 2637.

(156) Wenn, B.; Martens, A. C.; Chuang, Y.-M.; Gruber, J.; Junkers, T. *Polym. Chem.* **2016**, *7*, 2720.

(157) Blencowe, A.; Tan, J. F.; Goh, T. K.; Qiao, G. G. *Polymer* **2009**, *50*, 5.

(158) Boyer, C.; Derveaux, A.; Zetterlund, P. B.; Whittaker, M. R. *Polym. Chem.* **2012**, *3*, 117.

(159) Ding, H.; Park, S.; Zhong, M.; Pan, X.; Pietrasik, J.et al *Macromolecules* **2016**, *49*, 6752.

(160) Gao, H.; Ohno, S.; Matyjaszewski, K. *J. Am. Chem. Soc.* **2006**, *128*, 15111.

(161) Wiltshire, J. T.; Qiao, G. G. *Macromolecules* **2006**, *39*, 9018.

(162) Schaefgen, J. R.; Flory, P. J. *J. Am. Chem. Soc.* **1948**, *70*, 2709.

(163) Qu, Y.; Chang, X.; Chen, S.; Zhang, W. *Polym. Chem.* **2017**, *8*, 3485.

(164) Liao, X.; Walden, G.; Falcon, N. D.; Donell, S.; Raxworthy, M. J.et al *Eur. Polym. J.* **2017**, *87*, 458.
(165) Wu, Z.; Liang, H.; Lu, J. *Macromolecules* **2010**, *43*, 5699.
(166) Chen, Q.; Xu, Y.; Cao, X.; Qin, L.; An, Z. *Polym. Chem.* **2014**, *5*, 175.
(167) Cao, X.; Zhang, C.; Wu, S.; An, Z. *Polym. Chem.* **2014**, *5*, 4277.
(168) Ferreira, J.; Syrett, J.; Whittaker, M.; Haddleton, D.; Davis, T. P.et al *Polym. Chem.* **2011**, *2*, 1671.
(169) Räder, H. J.; Spickermann, J.; Müllen, K. *Macromol. Chem. Phys.* **1995**, *196*, 3967.
(170) Moriceau, G.; Gody, G.; Hartlieb, M.; Winn, J.; Kim, H.et al *Polym. Chem.* **2017**, *8*, 4152.
(171) Mühlebach, A.; Gaynor, S. G.; Matyjaszewski, K. *Macromolecules* **1998**, *31*, 6046.
(172) Mecerreyes, D. *Prog. Polym. Sci.* **2011**, *36*, 1629.
(173) Kocak, G.; Tuncer, C.; Bütün, V. *Polym. Chem.* **2017**, *8*, 144.
(174) Wang, K.; Song, Z.; Liu, C.; Zhang, W. *Polym. Chem.* **2016**, *7*, 3423.
(175) Bouvier, E. S. P.; Koza, S. M. *TrAC, Trends Anal. Chem.* **2014**, *63*, 85.
(176) Malheiro, D. In *Modern Size-Exclusion Liquid Chromatography*; John Wiley & Sons, Inc.: 2009, p 322.
(177) McKenzie, T. G.; Ren, J. M.; Dunstan, D. E.; Wong, E. H. H.; Qiao, G. G. *J. Polym. Sci., Part A: Polym. Chem.* **2016**, *54*, 135.
(178) Lesage de la Haye, J.; Martin-Fabiani, I.; Schulz, M.; Keddie, J. L.; D'Agosto, F.et al *Macromolecules* **2017**, *50*, 9315.
(179) Zhou, W.; Yu, W.; An, Z. *Polym. Chem.* **2013**, *4*, 1921.
(180) Furukawa, T.; Ishizu, K. *Macromolecules* **2003**, *36*, 434.
(181) Hui; Likos, C. N.; Blaak, R. *Soft Matter* **2011**, *7*, 8419.
(182) Lee, H.-J.; Lee, K.; Lee, S. N. *J. Polym. Sci., Part A: Polym. Chem.* **2006**, *44*, 2579.
(183) Lu, F.; Luo, Y.; Li, B. *Macromol. Rapid Commun.* **2007**, *28*, 868.
(184) Huang, R.; Chen, D.; Jiang, M. *J. Mater. Chem.* **2010**, *20*, 9988.

CHAPTER 4:

STAR POLYMER CHARACTERISATION

4.1 Abstract

The star shaped polymers synthesised in **CHAPTER 3** were fully characterised by numerous techniques: SEC with triple detection (refractive index (RI), light scattering (LS) and viscosity (VS)), AFM, DLS, rheology, and SAXS. Techniques such as SEC with triple detection allowed for determination of the star polymers molecular weight which is underestimated when conventional calibration is used. Given the likelihood of hydrogen bonding between the HEAm blocks in the PAMPS-*co*-PHEAm star polymers, interesting shear thinning properties were observed, which was regulated by the length of the PHEAm block. Finally, these particular star polymers synthesised using the arm first approach were shown to be more similar to nanoparticles regarding their structures than conventional star polymers synthesised by the core first approach. The star shaped polymers revealed a spherical shape by AFM which was further confirmed by SAXS. SAXS data were fitted against a core-shell sphere model.

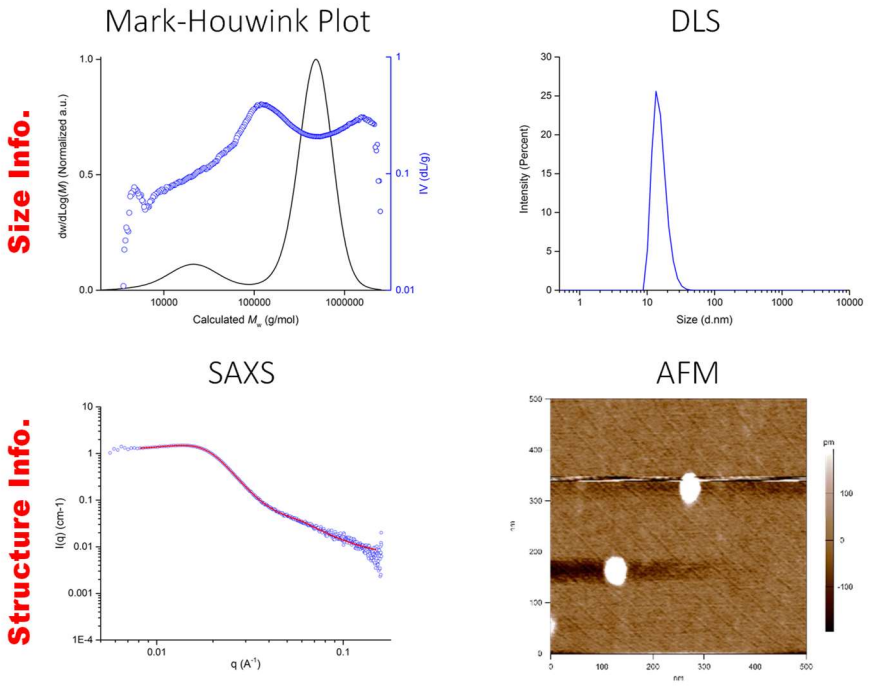

4.2 Introduction

Controlled radical polymerisations (RAFT, ATRP, NMP) allow for not only the control over the molecular weight, but access to different architectures (such as block, comb and star polymers) in a one-pot process. The use of the arm first approach to synthesise star polymers has been widely studied in the literature and has been a breakthrough for the synthesis of higher functionality star polymers with a narrow dispersity.[152] Star polymers can be associated to a wide range of application areas from drug delivery,[185] imaging[186] and surface modification.[187] Due to the large number of applications of star polymers linked to their high functionality and arm density, high molecular weight, globular structure (core, inner and outer shell) and unique solution properties (viscosity and rheological), their full characterisation is an important research area especially for biomedical applications. Due to the branching and the high molecular weight of such structures, traditional tools such as NMR or SEC with conventional calibration (i.e. with a polymer standard), provide only rudimentary information, and often leads to an underestimation of the molecular weight. Owing to this, more advanced techniques are used such as SEC with triple detection, DLS, rheology, or even SAXS. These techniques permit the access of the star polymer functionalities, sizes and structures.

4.2.1 Chromatography with Triple Detection

SEC is a convenient analytical tool which is widely used in polymer analysis. This technique allows the characterisation of a polymer sample, yielding molecular weight averages (relative to standards such as PEG if RI is used as a detector) and molecular weight distribution ($Đ \leq 1.5$). Polymer samples are injected through columns containing packed beads allowing for the separation of macromolecules based on their hydrodynamic volume in a given solvent. The pores in the beads loaded into the column can have varying sizes depending on the column chosen. Choice of columns including taking into account the chemistry, pore size, solvent and molecular weight range are all crucial for developing a suitable SEC method. The separation of analytes is proportional to the number of pores entered by molecules and larger molecules elute before smaller ones due to navigation through fewer pores. By using concentration sensitive detectors (typically differential refractometer but also UV) it is possible to obtain a relationship between the molecular weight of the polymer and the elution volume via the calibration curve. This calibration curve is generated using narrow calibrants of a known molecular weight (**Figure 4-1**).[188-190]

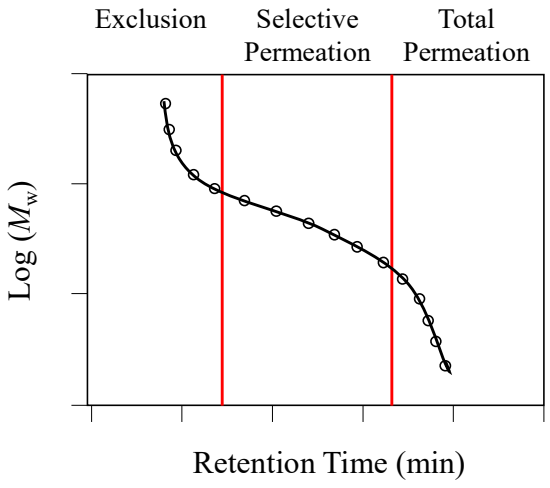

Figure 4-1: Typical calibration curve obtained with a RI detector in SEC.

However, inconsistencies and deviations are observed when polymers with complex architectures and chemistries (e.g. star or charged polymers) are analysed with conventional SEC. This is mainly due to the fact that the separation of the macromolecules depends on the hydrodynamic volume of the sample and not its actual

molecular weight. It is well known that a branched polymer and its linear homologue, having the same molecular weight, have different hydrodynamic volumes.[191] Branched polymers are smaller and more compact than their linear homologues, at a given molecular weight, which are more diffuse. The apparent molecular weight of branched polymers are underestimated when using a linear standard for conventional calibration which is typically the case. To overcome this challenge multiple SEC detectors can be used to obtain the true molecular weight.

Triple detection SEC uses a combination of three detectors, setup in a series, and consists of a refractometer, a viscometer and a light scattering detector. While the viscometer allows for the measurement of the intrinsic viscosity of the sample, the light scattering detector allows the determination of the molecular size. This combination makes it possible to determine not only the true molecular weight but also gives information on the branching functionality. The Mark-Houwink plot (**Figure 4-2** – **A**) can easily be determined by plotting the intrinsic viscosity across the molecular weight of the polymer. The mark-Houwink equation, $[\eta] = KM^{\alpha}$ allows for the determination of two parameters, alpha and k. These parameters are specific for a given polymer-solvent system. Alpha values range from 0 to 2 and give information on the solvent and the structure obtained. Indeed, typical values of alpha below 0.5 are characteristic of a solid sphere (branching) while a value of 2 is typical of a rigid rod. Additionally, alpha values of about 0.5 are typical of a theta solvent while value of 0.8 are obtained for a good solvent.[192] A good solvent is a solvent which favour energetically the interactions between the polymers and solvent, consequently, the polymer chains have more expended conformation. In a theta solvent the polymer-polymer interactions and polymer-solvent interactions are both identical and then the polymer chain is considered as an ideal chain.

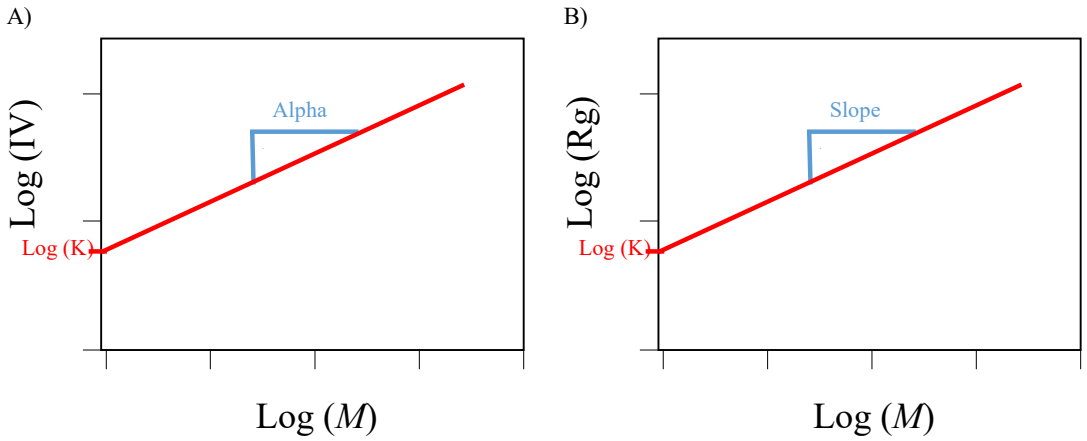

Figure 4-2: A) Mark-Houwink plot using SEC with viscometer; B) Conformation plot using SEC with light scattering.

Multi-angle laser light scattering in SEC is used to determine the true weight averaged molecular weight and uses the light scattered by macromolecules which is proportional to size, where bigger molecules scatter more light than smaller ones. Using light scattering, it is then possible to generate a conformational plot (**Figure 4-2 – B**) allowing size information (radius of gyration Rg) of the polymer to be determined. The combination of the three detectors with SEC allows for determination of the true molecular weight from which the number of arms per star (i.e. functionality) can be calculated using **Equation 8**.[193]

4.2.2 Viscosity Properties of Star Polymers

Viscosity refers to the thickness of a fluid. It is a measure of the resistance of a fluid to flow under applied forces (i.e. shear stress) mainly due to intramolecular interactions. For core cross-linked star polymers, interesting viscosity properties are usually observed. Even though such structures have a high molecular weight, the viscosity observed is usually similar to linear polymers of low molecular weights. Additionally, the viscosity of star polymers was shown to be greatly altered by the arm length more than the overall molecular weight. A decrease of arm length induces a decrease in viscosity due to a change in hydrodynamic radius; indeed, the structure is more compact when the arm length is decreased.[194,195] Pearson *et al.* have shown that the viscosity of star shape polyisoprenes increased exponentially with increasing arm molecular weight, while an increase of functionality (i.e. number of arms per star) did not show any effect on viscosity.[196] Mark and co-workers studied the effect of temperature and solvent on the viscosity of polystyrene and rubber.[197] They found that the viscosities of polymer solutions decreased when the temperature increased from 25 to 60 °C. They furthermore demonstrated that the viscosity is higher in a good solvent than poor solvent, which is likely due to change in conformations.

Viscosity can be measured with a viscometer: rheometer, capillary viscometer, falling sphere viscometer, vibrational viscometer and rotational viscometer.[198]

- Capillary viscometer:[199] The viscosity of a Newtonian liquid is determined by measuring the time taken for a known volume of a liquid with a known density to go through capillary tubes, with a pre-identified diameter and length.
- Falling sphere viscometer:[200] This method is used to determine the viscosity only of Newtonian liquids and gases. It uses the Stokes and Newton laws to measure the viscosity of a liquid. It measures the time required for a ball to fall through the solution under gravity.
- Vibrational viscometer:[201] The viscosity is measured by the frequency response when external force is applied such as an electric current. This technique is being more and more used due to the small instrument size, and also the possibility for on-line use.

- Rotational viscometer:[202] The viscosity is measured by the torque required to turn a disk or a bob at a known speed when immersed in a fluid.
- Rheometer:[203] The viscosity is usually calculated from rheological parameters such as the resistance due to rotational force. Rheology allows the measurement of the viscosity of Newtonian and non-Newtonian fluids.

The choice of the technique will greatly depend on the viscosity range of the sample to analyse, the availability of the compound to analyse, if the fluid is Newtonian or not, and the time and ease of analysis.

The combination of results obtained with SEC triple detection can easily be correlated with the viscosity properties observed. SEC with triple detection gives information on the true molecular weight, the branching system information ($\alpha < 0.5$) and the size of the star polymers, while the viscosity measurement gives evidence of the flow properties of the solutions.

4.2.3 Other Techniques to Characterise Star Polymers

Other techniques available to determine the structure of branched polymers include DLS, AFM and SAXS. Dynamic light scattering is a well-known method which allows for the measurement of hydrodynamic particle size and size distribution. DLS is based on the principle that the Brownian motion of particles causes scattering at different intensities, which can be used to determine a diffusion coefficient. The Stokes-Einstein relationship can then be used to determine the size of the particles, dependent on the solvent viscosity and temperature.[204] The hydrodynamic radius determined by DLS can then be compared by the hydrodynamic radius determined by SEC (viscometer detector), both results being complementary to each other.[177] Atomic force microscopy has also been used to get not only morphological but also the size properties of star polymers in 3-dimension. Aoshima *et al.* used AFM (**Figure 4-3**) on mica discs to characterise the structure of their poly(*p*-methoxystyrene) star-shaped polymer. They obtained a radius of 20 nm while the height was only 2.5 nm which was in accordance to the hydrodynamic radius measured by SEC. [205]

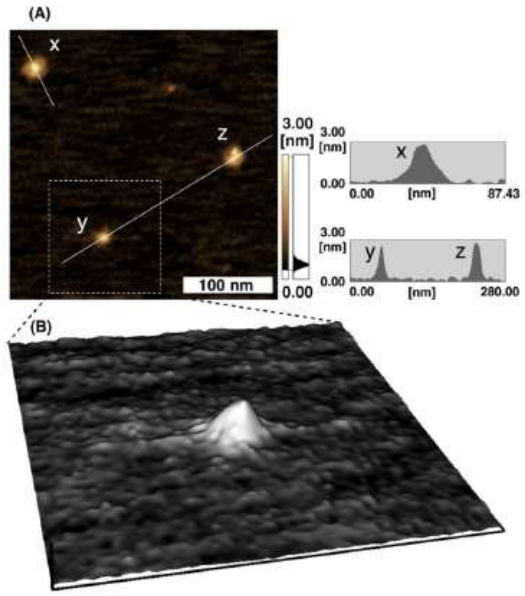

Figure 4-3: AFM of poly(*p*-methoxystyrene) obtained by Aoshima *et al.*.[205]

Another technique to study the conformation and structure of star polymers obtained is small-angle X-ray scattering (SAXS). SAXS measurements involve analysing the elastic scattering of X-rays when travelling through a solution. Differences in electron

density give rise to different scattering intensities, including the solvent, which can then be analysed to provide the structural information.[206] While DLS only gives information on the size of spherical objects, SAXS can give information on both the intra- and inter- molecular structure, including the shape, conformation and internal structure for structures other than spherical. Neutral star polymers have been widely studied using SAXS, while polyelectrolytes and block star copolymers have been rarely studied.[207,208] The scattering intensity of a monodisperse system of particles can be described by the following equation:

$$I(Q) = NP(Q)S(Q) \quad \textbf{(Eq. 4-1)}$$

With I(Q) being the experimental scattering intensity, N the number of particles, P(Q) the single particle scattering function (form factor) and finally S(Q) the inter-particle scattering function (interaction between particles).[209] Kawaguchi *et al.* characterised the core of a cross-linked star polymer, with PHEAm as the arm, using SAXS and confirmed the structure obtained by fitting a star-shaped structure existing as a single molecule in water.[210] Moinard *et al.* analysed polyelectrolyte star polymers synthesised using the core first approach and characterised these structures using SAXS. They have shown that the counter ion (Cs^+ or Na^+) and the 4-arms star copolymer concentration had a critical effect on the intensity q_{max} (**Figure 4-4**).[211]

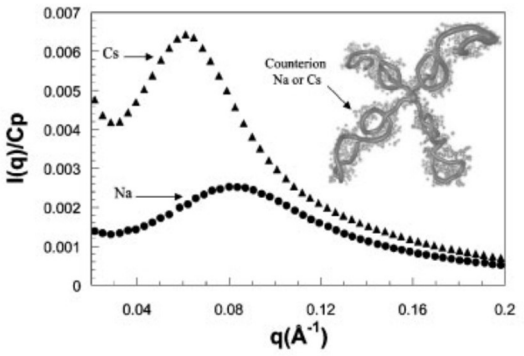

Figure 4-4: SAXS results of the 4-arms star polyelectrolyte, Moinard *et al.*.[211]

Lund *et al.* characterised a 3-arms PNIPAM-*b*-PAMPS star polymer in water at 25 °C using SAXS. They have shown that when a salt was added, the electrostatic repulsion was lowered, and that when the polymer concentration increased these interactions increased.[155]

4.2.4 Project Approach

This chapter discusses the full characterisation of the star polymers synthesised in **CHAPTER 3**.[212] Core cross-linked star (CCS) polymers synthesised using the arm first approach (**Figure 4-5**) allow for the formation of complex soluble core-shell structures, which are of interest for a wide range of biomedical applications such as drug and gene delivery, tissue engineering and diagnosis.[186] Here the aim is to use these star polymers in a wide range of biological applications, such as heparin-mimicking polymers described in **CHAPTER 5**, but also as a stabiliser for contrast agents in MRI, carried out in collaboration with Dr Gemma-Louise Davies.[213,214] These polymers were then analysed using a wide range of techniques. The size of these star polymers and their shape was determined using a battery of techniques available including dynamic light scattering (DLS), size exclusion chromatography (SEC) with triple detection, atomic force microscopy (AFM) and small-angle X-ray scattering (SAXS). Their rheological and viscosity properties in different solutions were also explored using a rheometer. It is important to look at these properties in both water and phosphate-buffered saline due to the type of applications targeted. The final aim is to correlate the properties of each star in response to changes in structure, such as the dependence of the molecular weight on the rheological behaviour and how this affects the microstructure. Indeed, at a constant arm length the different properties of random, diblock and tertrablock star copolymers were compared. In a second study, the effect of the position of the charged block, either outside or inside of the star polymer, was also studied.

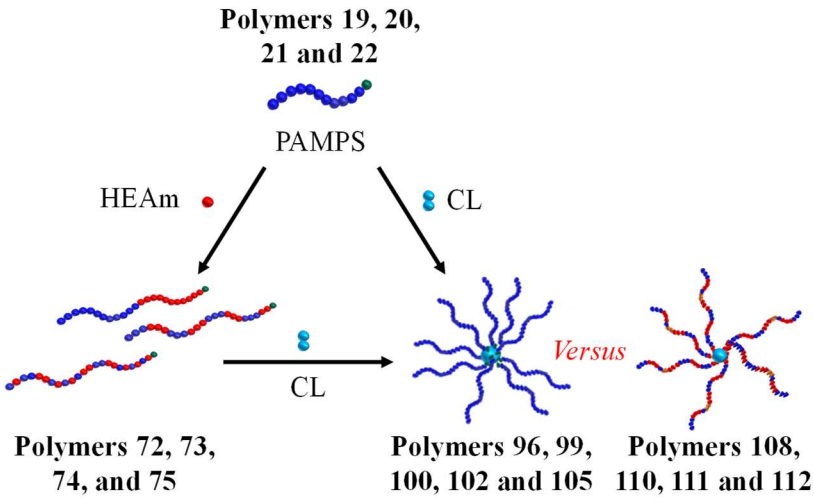

Figure 4-5: Structure of the star polymers studied in this chapter.

4.3 Results and Discussions

4.3.1 Triple Detection – LS, VS and RI Detectors

In this section, the molecular weight of each star polymer obtained using either conventional calibration or triple detection was compared. When polymers are analysed by light scattering it is important to determine the refractive index increment (dn/dc). This value is representative of the change in the refractive index of a solution when the concentration of solute is changed. The dn/dc value is dependent on several parameters such as the temperature, solvent, chemistry of the solute, and finally the molecular weight. For example, lower molecular weight polymers are more likely to be affected by the end-group functionalities.[215-217] The dn/dc values of common polymers at different temperatures, molecular weights, and solvent can be found in various databases.[218,219] However, for more novel polymers or architectures, such as PAMPS or star polymers, it is less likely to find dn/dc values in a database, therefore it is more convenient to measure it. The dn/dc can be determined online using the Agilent GPC/SEC software by entering the concentration of the polymer injected it will then calculate the dn/dc using the differential refractive index (DRi) (**Table 4-1** and **Table 4-2**). It can also be determined offline using a refractometer, where the refractive index of increasing polymer concentrations is measured and the dn/dc calculated using **Equation 9**. For linear PAMPS with a DP of 50, the dn/dc calculated online using SEC was 0.153 mL/g (**Table 4-1**, **Polymer 19**) while the dn/dc calculated offline using a refractometer was 0.155 mL/g (**Figure S 4-1**). As these values were in good agreement the SEC method was the method of choice as it is easier and faster to use. Overall, all polymers analysed in this study had dn/dc values varying between 0.122 to 0.163 mL/g.

Table 4-1: Aqueous SEC results of the linear precursors used for the synthesis of star polymers using triple detection.

Polymer	Structure	$M_{n,th}$ (g/mol)[a]	$M_{n,SEC}$ (g/mol)	dn/dc (mL/g)	$M_{n,SEC}$ (g/mol)	$Đ$	α	K (10^{-5} dL/g)
			RI Detector[b]		RI, MALS, VS Detectors[c]			
19	DP50	11,600	9,900	0.153	8,300	1.05	0.50	81.94
20	DP100	23,000	15,400	0.161	15,700	1.04	0.61	30.40
21	DP200	45,600	26,200	0.160	30,800	1.08	0.70	13.65
22	DP400	91,000	47,600	0.154	64,500	1.12	0.89	1.83
75	DP80, Random	13,900	12,400	0.146	12,000	1.03	0.80	5.03
74	DP80, Diblock	13,600	10,000	0.151	13,200	1.07	0.58	36.31
73	DP80, Tetrablock	13,900	10,500	0.147	11,900	1.04	0.51	70.34
72	DP80, Octablock	14,100	14,500	0.163	14,900	1.04	0.56	54.86

[a] Theoretical M_n values were calculated using **Equation 2**; [b] Experimental M_n values were determined by size-exclusion chromatography in 20 % MeOH / 80 % 0.1M $NaNO_3$ in milli-Q water eluent using a conventional calibration obtained with PEG/PEO standards; [c] Experimental M_n, $Đ$, α, K and dn/dc values were determined by size-exclusion chromatography in 20 % MeOH / 80 % 0.1M $NaNO_3$ in milli-Q water eluent using the triple detection options in Agilent GPC/SEC Software which used a combination of a Refractive Index (RI), a Multi-Angle Light Scattering (MALS) and a Viscometer (VS) detectors.

The linear polymers (i.e. arms) used to synthesise the star polymers were first analysed by SEC with triple detection. AMPS®2405 homopolymers with an increasing theoretical molecular weight from 11.6 to 91.0 kg/mol were then analysed. The molecular weights obtained using triple detection were slightly higher than when a conventional calibration was used (**Figure 4-6** – **A** and **B**), however, there were still discrepancies with the theoretical molecular weight which could be due to the nature of the polymers analysed (i.e. highly charged) or to the chemistry (i.e. termination). For example, analysing PAMPS with a DP of 400 (**Polymer 22**), a shoulder at lower molecular weight is observed which will greatly affect the average molecular weight due to a bimodal distribution. Additionally, the use of triple detection SEC allowed the determination of different constants, which are characteristic of a specific polymer-solvent system at a given temperature (i.e. α and K). Alpha values were all between 0.5 and 0.9 suggesting here that all chains are random coiled polymers in a good solvent.[220]

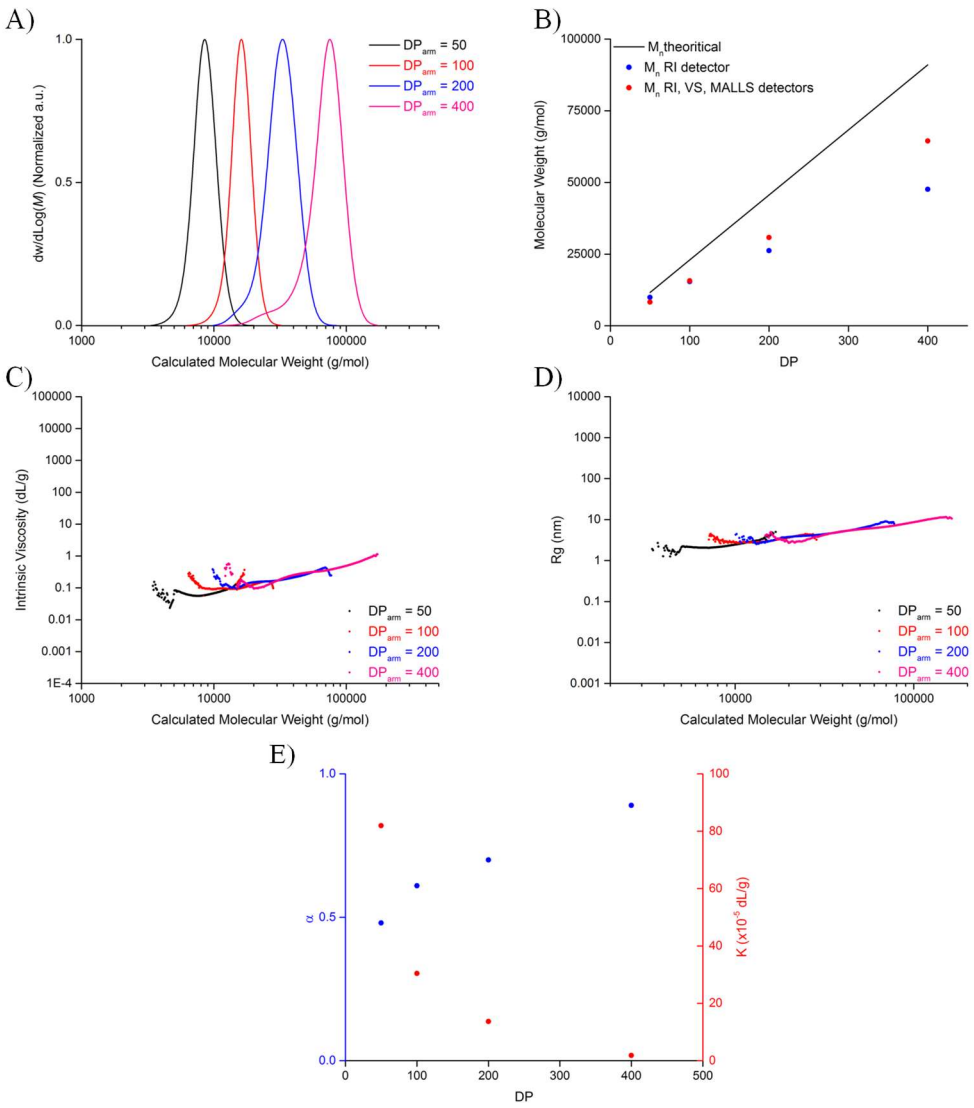

Figure 4-6: SEC triple detection analysis (RI, VS, MALS) of linear AMPS®2405 homopolymers. A) Molecular weight distributions; B) Comparison of the theoretical molecular weight with the molecular weight determined using either conventional (RI) or triple detection (RI, VS, MALS); C) Intrinsic viscosity versus calculated molecular weight (Mark-Houwink plot); D) Radius of gyration versus calculated molecular weight (conformation plot); E) Mark-Houwink parameters (α and K) for different DPs at 35 °C.

The intrinsic viscosity obtained using the viscometer detector and the Rg values obtained by light scattering (**Figure 4-6** – **A** and **B**) gradually increased when the molecular weight increased. A linear fit of the intrinsic viscosity and Rg along a wider molecular weight range (**Figure S 4-2** – **A** and **B**) could then be used for extrapolation at higher molecular weights and comparison with the star polymers. It should be noted that when the molecular weight was increased from 11.6 to 91.0 kg/mol, the alpha value increased from 0.5 to 0.89 perhaps indicating a difference in conformation when the molecular weight was increased. This can be explained by an increase of solvation.

In opposition, when the molecular weight was increased the K values decreased (**Figure 4-6 – E**).

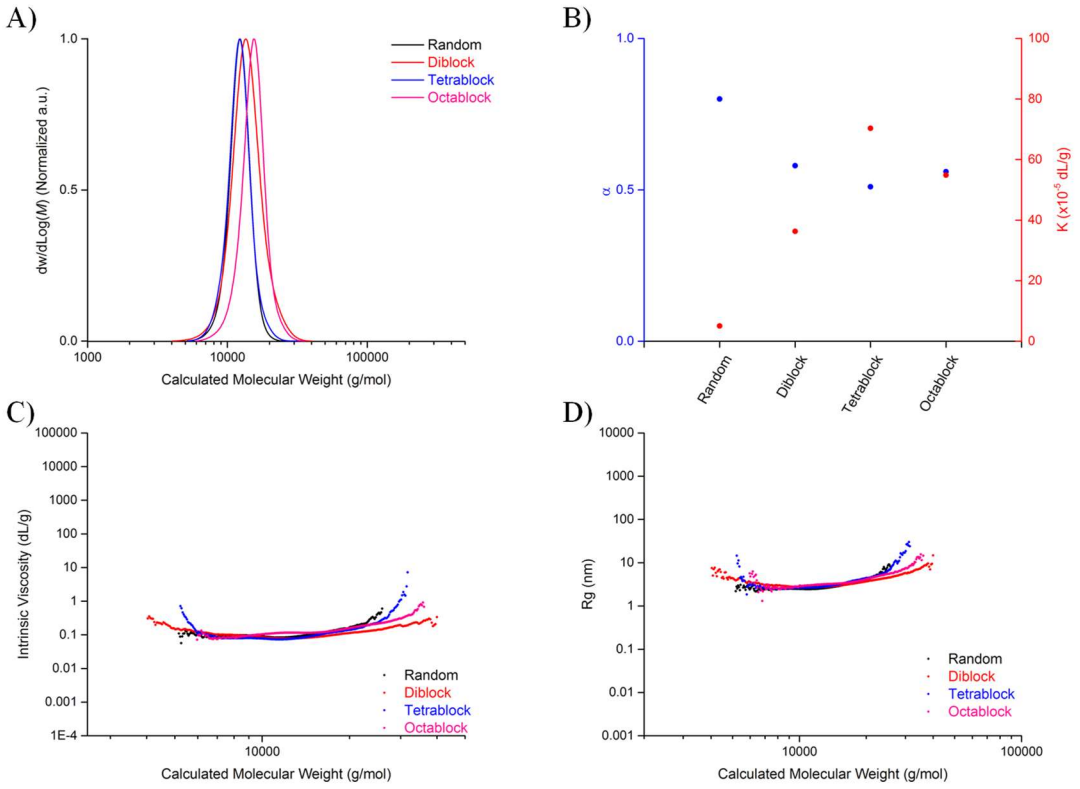

Figure 4-7: SEC triple detection analysis (RI, VS, MALS) of linear copolymers (AMPS®2405 and HEAm) targeting a total DP of 80.

A) Molecular weight distributions; B) Mark-Houwink parameters (α and K) for different monomer distribution at 35 °C, C) Intrinsic viscosity versus calculated molecular weight (Mark-Houwink plot); D) Radius of gyration versus calculated molecular weight (conformation plot).

When selected copolymers were analysed using triple detection, a different behaviour from the linear homopolymers was observed. Firstly, the molecular weights obtained were closer to theoretical ones (**Figure 4-7** – **A**). Additionally, the alpha values for the diblock, tetrablock and octablock copolymers were closer to 0.5 being typical for a theta solvent. These results suggest that the polymer chains are ideal chains due to a balance of interactions between solvent and polymer chains. However, when the random copolymer was analysed an alpha value of about 0.8 was obtained being indicative of a good solvent (**Figure 4-7 – B**). Finally, the intrinsic viscosity and Rg values were similar for all four copolymers as shown in **Figure 4-7** – **C** and **D**.

Branched polymers are usually smaller and more compact than their homologous counterparts at a given molecular weight and the addition of branching renders the molecular weights calculated using conventional calibration underestimated. SEC using triple detection is then the technique of choice to characterise branched polymers (e.g. star polymers).[191] When the molecular weights obtained by conventional calibration or by triple detection were compared (**Table 4-2**), the ratio of the molecular weights obtained by triple detection were 3.5-fold higher for the star homopolymers (**Figure 4-8 – A** and **B**). However, comparison of the copolymers was more complex, with ratios varying from 3.2-fold for the random star copolymer up to 5.9-fold for the octablock star copolymer being obtained (**Figure 4-10 – A** and **B**).

Table 4-2: Aqueous SEC results of the star polymers synthesised using triple detection (C4 was used in all cases except for **Polymer 95** where C1 was used).

Polymer	Structure	$M_{n,SEC}$ (kg/mol)	dn/dc (mL/g)	$M_{n,SEC}$ (kg/mol)	f[c]	$Đ$	α	K (10^{-5} dL/g)
		RI Detector[a]		RI, MALS, VS Detectors[b]				
95	DP50	60	0.142	130	16	1.12	0.24	747
98	DP50	91	0.137	307	37	1.01	0.19	1024
99	DP100	156	0.137	526	34	1.01	0.23	1085
101	DP200	240	0.126	838	27	1.01	0.25	1143
104	DP400	416	0.122	1,459	23	1.01	0.27	1328
110	DP80, Random	131	0.147	427	36	1.01	0.34	241
108	DP80, Diblock	153	0.147	697	53	1.01	0.27	438
112	DP80, Tetrablock	158	0.151	665	56	1.02	0.30	317
111	DP80, Octablock	247	0.148	1,458	98	1.22	0.28	418

[a] Experimental M_n values were determined by size-exclusion chromatography in 20 % MeOH / 80 % 0.1M $NaNO_3$ in milli-Q water eluent using a conventional calibration obtained with PEG/PEO standards; [b] Experimental M_n, $Đ$, α, K and dn/dc values were determined by size-exclusion chromatography in 20 % MeOH / 80 % 0.1M $NaNO_3$ in milli-Q water eluent using the triple detection options in Agilent GPC/SEC Software which used a combination of a Refractive Index (RI), Multi-Angle Light Scattering (MALS) and Viscometer (VS) detectors; [c] The functionality of star polymers was determined using **Equation 8** from the M_n determined by triple detection SEC.

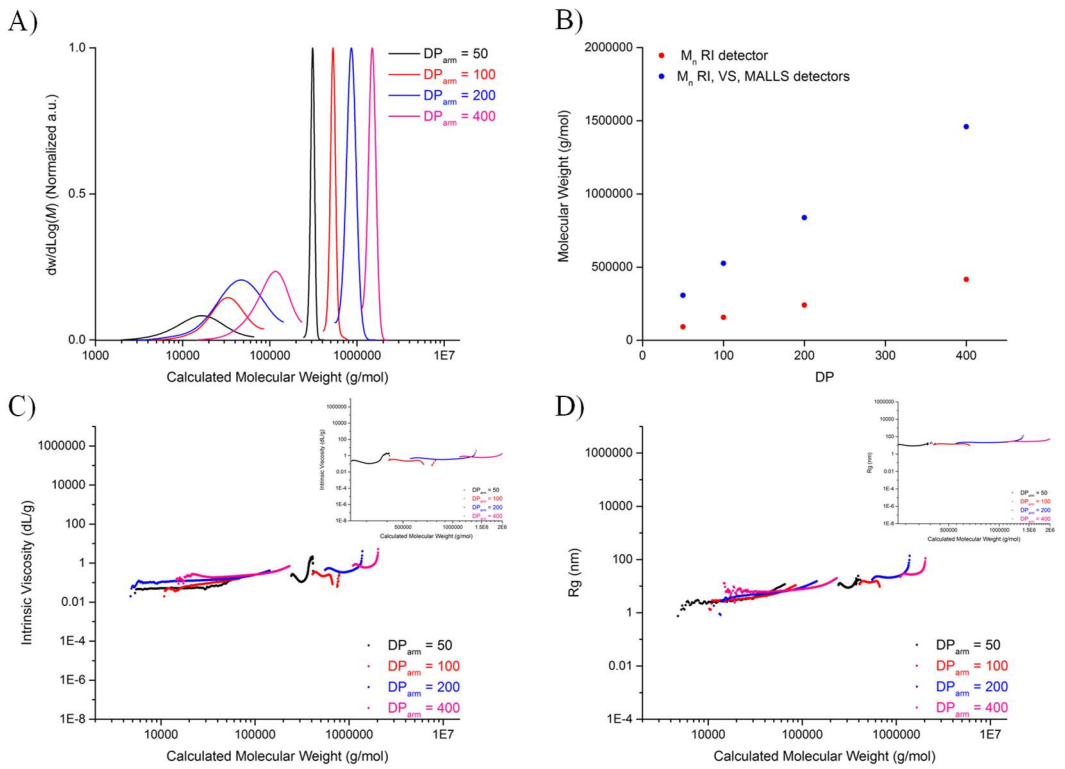

Figure 4-8: SEC triple detection analysis (RI, VS, MALS) of star AMPS®2405 homopolymers.

A) Molecular weight distributions; B) Comparison of the molecular weight determined using either single (RI) or triple detection (RI, VS, MALS); C) Intrinsic viscosity versus calculated molecular weight (Mark-Houwink Plot); D) Radius of gyration versus calculated molecular weight (conformation plot).

The Mark-Houwink plot (**Figure 4-8 – C**) of the star homopolymers gave further details about the structure. At higher molecular weights of each individual star polymer there was an increase in the intrinsic viscosity which is likely due to the formation of star-star coupling. Similarly at lower molecular weights the intrinsic viscosity determined is less reliable since the intrinsic viscosity of the material is too low to affect the actual viscosity of the solution (i.e. similar to the viscosity of the eluent). Additionally, at either edge of the material distribution the material concentration will be lower, and therefore, the IV determined will be less reliable. The alpha values decreased from linear (> 0.5) to star polymer formation (< 0.5), supporting the formation of branching. AMPS®2405 star homopolymers with increasing arm length had different properties. A linear increase in intrinsic viscosity (**Figure 4-9** – **B**) and radius of gyration (**Figure 4-9 – C**) was observed. The increase in Rg is in good correlation with the increase in alpha value when the arm length is increased. The increase in alpha value suggests a more extended conformation of the

star polymers which could be due to steric hindrance but also may be due to the fact that the functionality (**Figure 4-9 – A**) of each star polymer was decreased and a less branched structure expected.

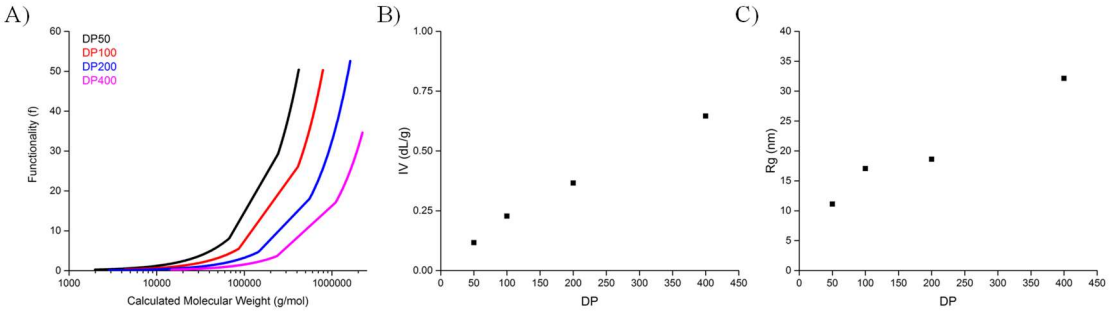

Figure 4-9: A) Calculated functionality of the star polymers by increasing the arm length; B) Intrinsic viscosity against DPs; C) Radius of gyration against DP.

In the second phase, the properties of two star polymers, with the same arm length (DP50) but synthesised with different cross-linkers, were compared. One of the cross-linkers was a diacrylamide (**Polymer 95**, C1) with one carbon separating the two functionalities, while the second cross-linker was a diacrylate having a spacer with 4 carbons (**Polymer 98**, C4). The functionalities (i.e. number of arms per stars) obtained for the star **Polymer 95** (C1) was found to be only 16 while it increased to 37 when the diacrylate CL (C4) was used. This explained the alpha value of 0.24 for the star using C1 to 0.19 for C4, when C4 was used, the star was denser due to the increased number of arms in the star.

Finally, the properties of star copolymers were examined, comparing the effect of microstructure (**Polymers 108**, **110**, **111**, **112**). The properties of random, diblock, tetrablock and octablock star copolymers (DP = 80) synthesised using an arm first approach with cross-linker 4 (C4) were compared (**Figure 4-10**).

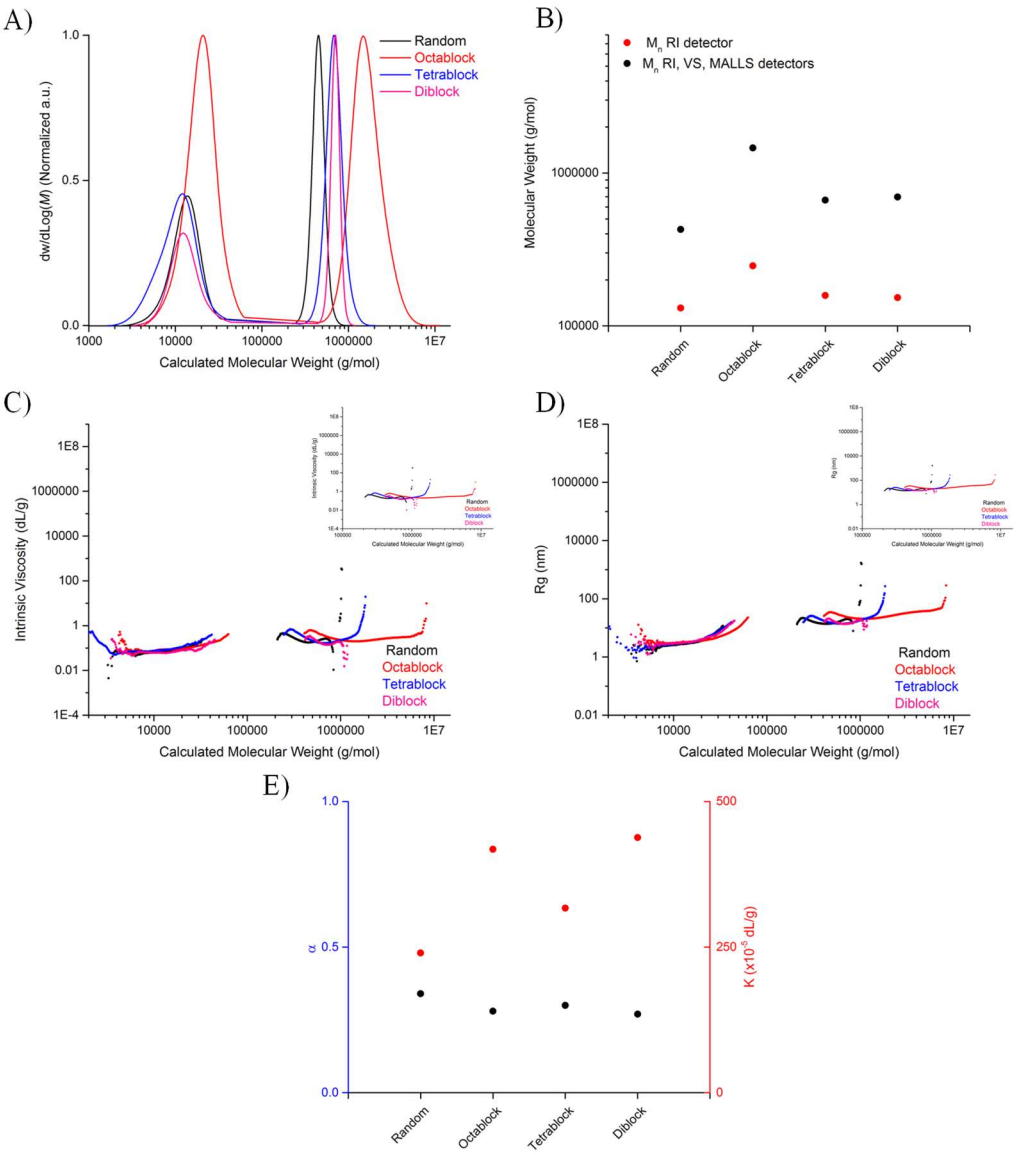

Figure 4-10: SEC triple detection analysis (RI, VS, MALS) of star AMPS®2405 copolymers (AMPS®2405 and HEAm).

A) Molecular weight distributions; B) Comparison of the molecular weight determined using either conventional (RI) or triple detection (RI, VS, MALS); C) Intrinsic viscosity versus calculated molecular weight (Mark-Houwink plot); D) Radius of gyration versus calculated molecular weight (conformation plot); E) Mark-Houwink parameters (α and K) for different monomer distributions at 35 °C.

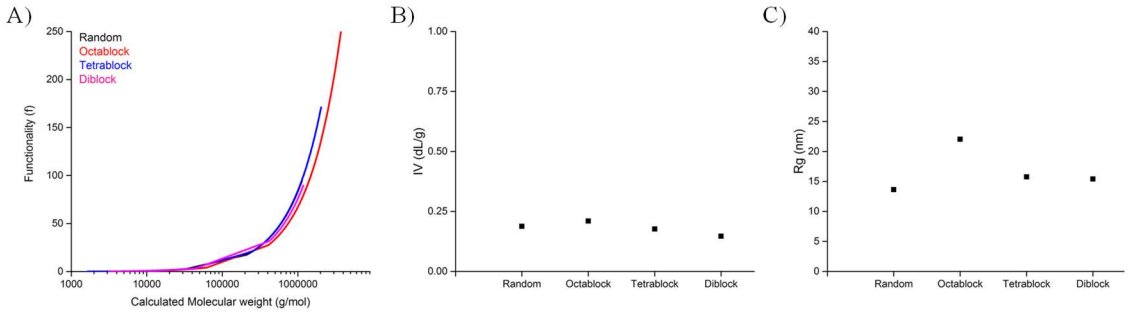

Figure 4-11: A) Calculated functionality of the star copolymers; B) Intrinsic viscosity against monomer distribution; C) Radius of gyration against monomer distribution.

It can be first observed that the K values of the star copolymers were lower (< 500 dL/g) compared to the homopolymers (> 1000 dL/g). But overall K values of the star polymers were higher than for the linear polymer (**Table 4-1** and **Table 4-2**). The importance of the polymer architecture and composition on the K value was successfully demonstrated with this study. Additionally, the functionalities determined were higher for the star copolymers compared to the star homopolymers (**Figure 4-11 – A**). The alpha values were observed to be below 0.5 suggesting the formation of a branched system (**Figure 4-10 – E**) compared to linear arms ($\alpha > 0.5$). It was observed that the molecular weight of the octablock star copolymer was higher than the other star copolymers synthesised (**Figure 4-10**). An increase of the radius of gyration and intrinsic viscosity would be expected due to the differences in molecular weight obtained for different copolymer arms, but, there was no observed increase of intrinsic viscosity (IV) (~ 0.200 dL/g) (**Figure 4-11 – B**). However, a higher Rg for the octablock copolymer (~ 22 nm) compared to other star copolymers (~ 15 nm) was found. Furthermore, higher functionalities were obtained for the octablock star copolymer (f = 98) compared to the random star copolymer (f = 36). This was likely due to a difference of conformation between the octablock and random linear copolymer, affecting the star polymer synthesis (i.e. CL compartmentalisation).

4.3.2 Rheology

Star polymers are formed by the assembly of a large number of linear polymer chains around one central point, the core. The diffusion observed for linear polymers (i.e arms) is consequently reduced when incorporated into a star polymer due to the link onto a central point. Consequently, this difference in conformation between a star and a linear polymer induces different rheological properties. For example it is well known that linear polymers of comparable molecular weights and chemistry exhibit higher solution viscosity than their counterparts star polymers.[186] It is also important to note that the viscosity of star shaped polymers is non-linear when the overall molecular weight is increased, but increases exponentially depending on the arm molecular weights.[195,196]

The viscosity and rheological behaviour of selected star homopolymers and copolymers were studied, varying different parameters such as polymer concentration, temperature and solvent. Firstly, the viscosity of star homopolymers, increasing the concentration from 1 to 10 and 30 weight % in deionised water was measured (**Figure 4-12 – A** and **B**). At all concentrations and different arm lengths, the shear stresses obtained increased linearly when the shear rate was increased which is characteristic of Newtonian solutions. This explained why the viscosity of a given polymer was then linear through the same range of shear rate. As expected, when the polymer concentrations were increased from 1 to 10 and 30 weight %, the viscosity of the solutions gradually increased. For example, when the **Polymer 98** ($DP_{arm} = 50$) was analysed with increasing concentrations from 1, 10 and 30 wt. % of polymers in deionised water the viscosity increased. This behaviour was observed to be the same when the arm length was increased.[221,222] At a given concentration, looking at increased arm length, the viscosities observed were increased.[223] For example, at 30 wt. %, viscosities of the solutions were respectively 180, 390 and 745 mPa.s when the arm length was increased from 50 (**Polymer 98**) to 200 (**Polymer 101**) and finally 400 (**Polymer 104**).

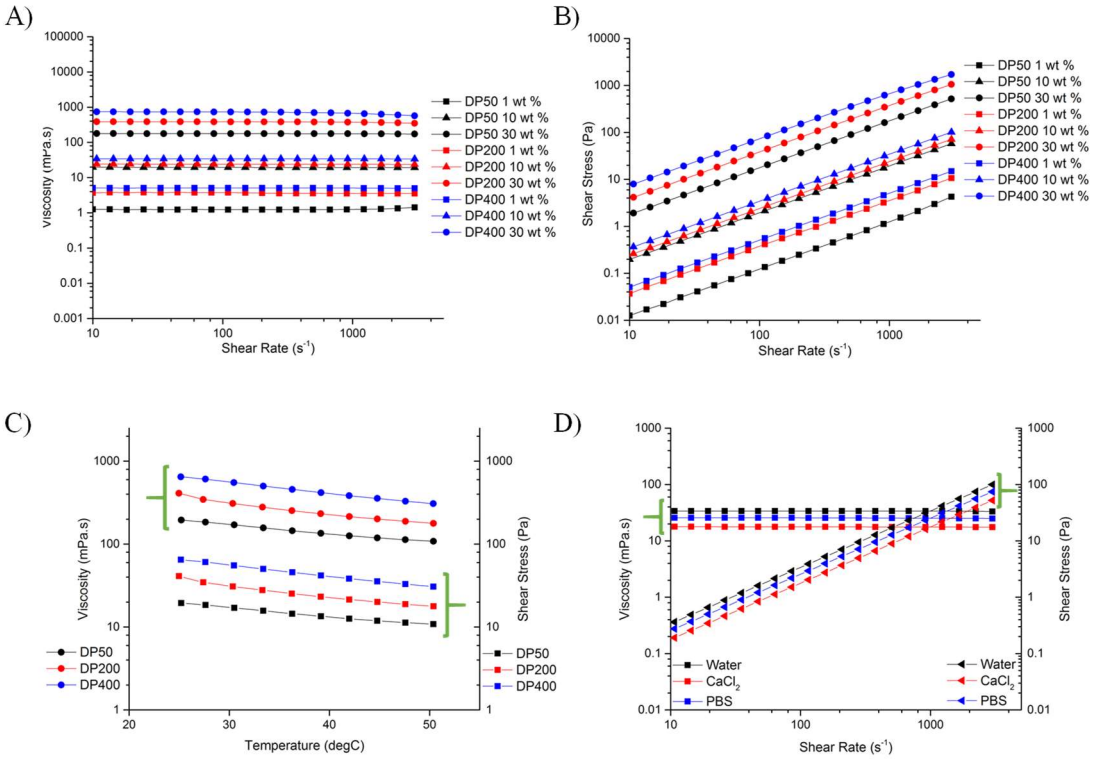

Figure 4-12: Viscosity of star homopolymers with a DP_{arm} = 50, 200 and 400.

A) Viscosity (mPa.s) at 25 °C at 1, 10 and 30 wt. % in water applying a shear rate from 10 to 3,000 s^{-1}; B) Shear stress (Pa) at 25 °C at 1, 10 and 30 wt. % in water applying a shear rate from 10 to 3,000 s^{-1}; C) Viscosity (mPa.s) and shear stress (Pa) at 25 °C at 30 wt. % in water increasing the temperature from 25 to 50 °C (2.5 °C each measurement) at a constant shear rate of 100 s^{-1}; D) Viscosity (mPa.s) and shear stress (Pa) for a DP_{arm} = 400 at 25 °C applying a shear rate from 10 to 3,000 s^{-1} at 10 wt. % either in water, PBS or $CaCl_{2(Aq.)}$ (1M) at a constant shear rate of 100 s^{-1}.

The effect of temperature on the viscosity of polymer solutions at 30 wt. % was then studied. As the temperature increased, the viscosities observed were slowly reduced likely due to a decrease of intramolecular interactions between polymer chains (**Figure 4-12 – C**).[197] Finally, the effect of solvent was determined, by preparing three different solutions of the **Polymer 104** (DP_{arm} = 400) at 10 wt. % in deionised water, phosphate-buffered saline (PBS) and in aqueous $CaCl_2$ (1M). The viscosities and shear stresses are reported in **Figure 4-12 – D**. The viscosities obtained were linear and this is characteristic of a Newtonian fluid. The viscosity obtained in water (34 mPa.s) was higher than the viscosity in aqueous $CaCl_2$ (1 M) (18 mPa.s) and PBS (26 mPa.s). The presence of salts in the solution is likely to exchange with the sodium counter ion of the sulfonate and consequently change the properties of the star polymers.[224]

In a second study the viscosity properties of star copolymers (PAMS-*co*-PHEAm), for which the arm length was kept constant targeting a DP of 80, were analysed. Similar results (**Figure 4-13**) were observed compared to when PAMPS homopolymers were studied: viscosities increased when the polymer concentration was increased, shear stresses increased linearly when the shear rate was increased (Newtonian-fluids), viscosities decreased when the temperature was increased and finally the viscosity obtained in water (21 mPa.s) was higher than the viscosity in aqueous $CaCl_2$ (8 mPa.s) and PBS (13 mPa.s) (**Polymer 110**).

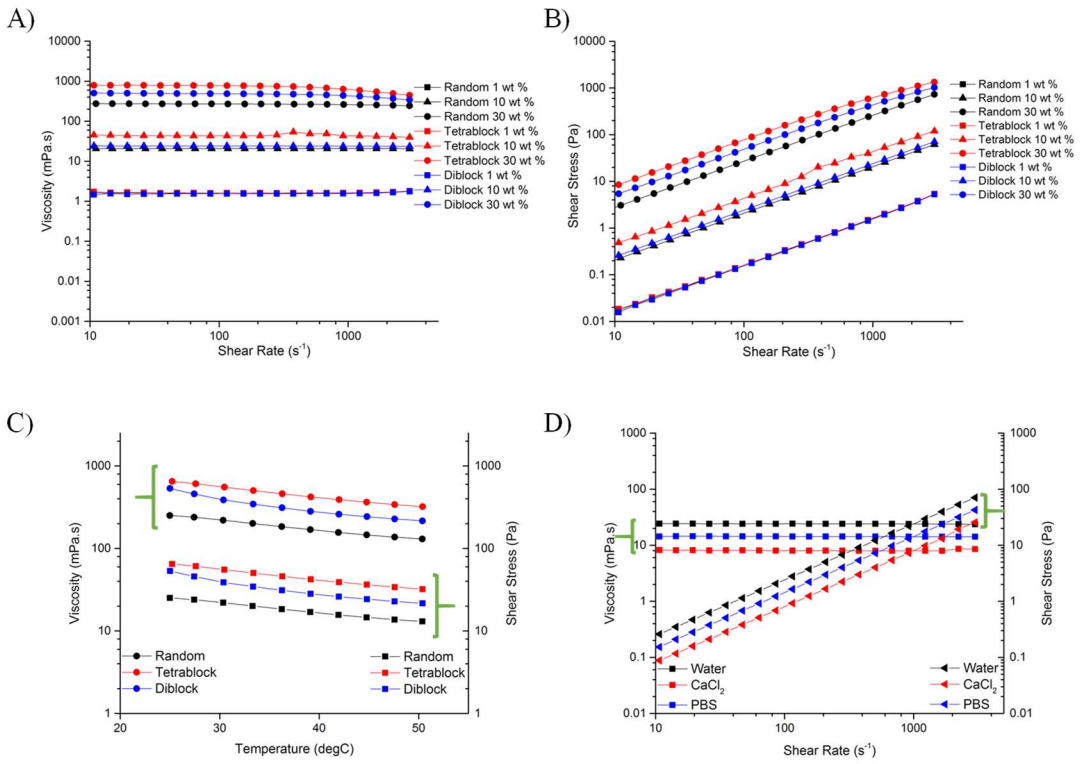

Figure 4-13: Viscosity of star copolymers (diblock, tetrablock, random copolymers).

A) Viscosity (mPa.s) at 25 °C at 1, 10 and 30 wt. % in water applying a shear rate from 10 to 3,000 s^{-1}; B) Shear stress (Pa) at 25 °C at 1, 10 and 30 wt. % in water applying a shear rate from 10 to 3,000 s^{-1}; C) Viscosity (mPa.s) and shear stress (Pa) at 25 °C at 30 wt. % in water increasing the temperature from 25 to 50 °C (2.5 °C each measurement) at a constant shear rate of 100 s^{-1}; D) Viscosity (mPa.s) and shear stress (Pa) of the random star copolymer at 25 °C applying a shear rate from 10 to 3,000 s^{-1} at 10 wt. % either in water, PBS or $CaCl_{2(Aq.)}$ (1M) at a constant shear rate of 100 s^{-1}.

However, microstructures of the arm were shown to affect the overall viscosity properties of the star copolymers solutions. Indeed, the viscosities increased from random (275 mPa.s, **Polymer 110**) to diblock (550 mPa.s, **Polymer 108**) and finally tetrablock (793 mPa.s, **Polymer 112**) star copolymers in water and at 25 °C (**Figure 4-13 – A**). The lower viscosity for the random star polymer can be explained by its lower molecular weight as determined using triple detection SEC (427 kg/mol, f = 36). However, the viscosity of the tetrablock star polymer (793 mPa.s) was almost 3-fold higher than the viscosity of the diblock star polymer (550 mPa.s) and this observation can no longer be explained by a change in molecular weight, both being in the same range (f ~ 55). This can be explained by a change in the arm polarity but also its dynamics (reptation). Indeed, diblock star polymers were more likely to aggregate in solution than tetrablock star polymers, being attributed to longer HEAm segment capable of hydrogen bonding with other diblock copolymer arms.[225,226]

When the viscosity of all-star polymers were analysed in detail at 30 wt. % (**Figure 4-14**), two regions were observed; at shear rates lower than 400 s^{-1} the viscosity was linear, while at higher shear rate a decrease of viscosity was observed. The linear region is so called the Newtonian region while when the viscosity decreases (or increases) at increasing shear rate, the fluid is called non-Newtonian. Newtonian fluid describes a particular flow behaviour of a liquid in which the viscosity is independent to shear rate. The viscosity of non-Newtonian fluid on contrary is shear rate dependant. Here, the decrease of viscosity at increase shear rate is named shear thinning and is explained by the formation of a gel-like liquid collapsing on itself at high shear rates (e.g. tomato sauce).[227] For example the viscosity of the tetrablock copolymer (**Polymer 112**) solution decreased from 793 mPa.s (shear rate = 18 s^{-1}) to 444 mPa.s (shear rate = 2,900 s^{-1}). This decrease of viscosity of about 2-fold needs to be taken in account with respect to the targeted applications.[228,229]

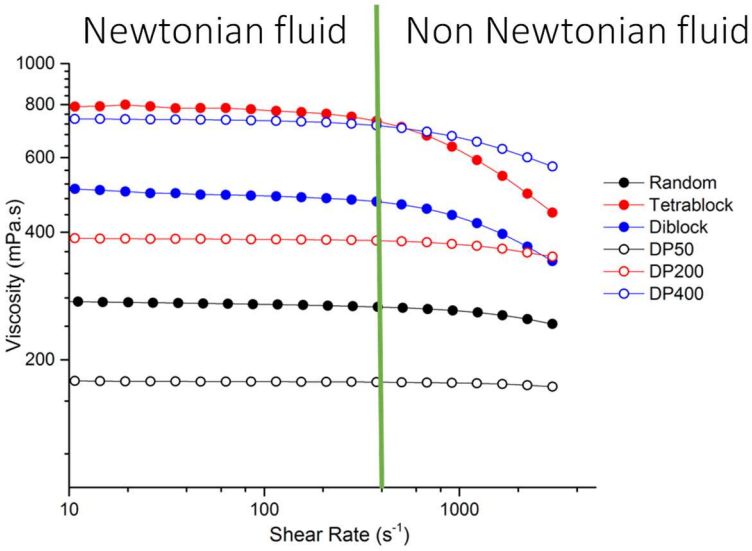

Figure 4-14: Overlaid viscosity (mPa.s) at 25 °C of star homopolymers and copolymers at 30 wt. % in water, applying a shear rate from 10 to 3,000 s^{-1}.

Finally, the rheological properties of such architectures was examined (**Figure S 4-3**). For all polymers, the loss modulus ($1 < G'' < 10$ Pa) was higher than the storage modulus ($4.5x10^{-5} < G' < 4.5x10^{-4}$) which is characteristic of liquid. There was also no frequency dependence on G′ and G″, which is characteristic of a linear viscoelastic region.[230,231] This rheological behaviour was in accordance with the flowing solutions observed. The storage modulus (G′) increased when the arm length was increased (G′ DP50 < G′ DP200 < G′ DP400) and the G′ of the star copolymer series increased from random to diblock and finally tetrablock. These observations were in accordance with the increases in viscosity in both data sets analysed.

4.3.3 Further Characterisations

The viscosity and the rheological properties of the star polymers were compared, not only in terms of molecular weight but also with respect to the microstructure of the arms. Another important parameter to study in order to characterise star polymers is their hydrodynamic size. Here multiple techniques such as DLS, AFM and SEC were used to compare the different sizes obtained and differences were observed whether the analysis was carried out in solution or on a solid surface.

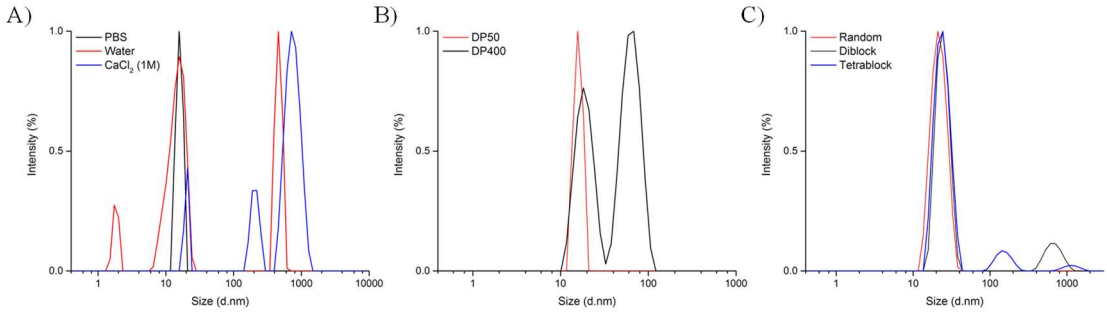

Figure 4-15: DLS size distribution (intensity) of selected star polymers.

A) With a DP_{arm} = 50, either in PBS, water or $CaCl_{2(Aq.)}$ 1M; B) In PBS with either a DP_{arm} = 50 or 400; C) In PBS with different copolymers as arms (random, diblock and tetrablock AMPS-HEAm with DP_{tot} = 80).

Dynamic light scattering provides information on the hydrodynamic radius in a given solvent. For the $PAMPS_{50}$ (**Polymer 98**) star polymer when water or aqueous $CaCl_2$ was used, multiple distributions were observed, especially, with the observation of aggregates with sizes over 100 nm (**Figure 4-15 – A**) while a monodisperse chromatogram was obtained when PBS was used. The aggregates observed with aqueous $CaCl_2$ at 1 M can be explained by a stronger binding of calcium than sodium with the sulfonate, rendering the hydrophobicity of the molecule higher thus inducing flocculation.[232,233] This could also explain the lower viscosity solution in aqueous $CaCl_2$ observed previously (**Figure 4-12 – D** and **Figure 4-13 – D)**. Conversely, the aggregations observed in water could be due a low stabilisation of PAMPS star polymers allowing the aggregation of the hydrophobic core.[234] Additionally, when the star polymers, with either a DP = 50 or 400 as the arm, in PBS, were analysed; a monodisperse distribution was obtained for the $PAMPS_{50}$ star polymers while two peaks were observed for the $PAMPS_{400}$ star polymer. The bimodal peak observed for

the $PAMPS_{400}$ star polymer could be attributed to unreactive chains, which was calculated to be about 50 % (**Table 3-7**) against only 10 % for the $PAMPS_{50}$. The second distribution observed (higher sizes), was then attributed to the star polymer itself. Regarding the star copolymers (**Figure 4-15**), the presence of higher complex structures for the diblock and tetrablock star polymers was observed. Indeed, two peaks are observed: one at 20 - 30 nm, corresponding to the star, and one peak corresponding to a diameter higher than 100 nm, theorised to be due to some aggregation. When analysing the random star polymer only one peak is observed. These results can be correlated to the viscosity of the solution previously obtained. The viscosities of block star polymers (**Figure 4-13**) obtained were higher than the random star copolymers; the HEAm blocks can form hydrogen bonds forming a network-like structure, explaining the shear thinning properties formerly observed, being particularly higher for the diblock and tetrablock copolymers (**Figure 4-14**).[235,236]

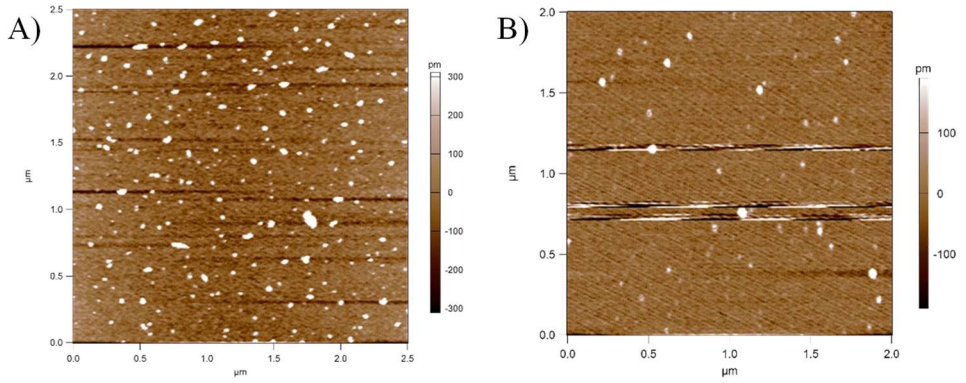

Figure 4-16: AFM topography images of selected star polymers on mica discs.
A) Homopolymer with DP_{arm} = 50; B) Homopolymer with DP_{arm} = 400.

Atomic force microscopy provided information on the morphology of the star homopolymers synthesised (DP_{arm} = 50 and 400) (**Figure 4-16**) where spherical structures were observed. Similar structures have been observed for nanoparticles when characterised by AFM.[237,238] While the star polymers had a radius of 34 nm for the $PAMPS_{50}$ star polymer the depth was only 1.2 nm, demonstrating a flat structure (**Figure S 4-4**).[239]

Finally, the radius determined by the three different techniques, SEC, DLS and AFM, were compared (**Table 4-3**). SEC and DLS gave similar sizes, both providing the hydrodynamic radius. The hydrodynamic radius relates to a hard sphere (core of the star polymer) model and will underestimate the actual size of the star polymers having a softer corona corresponding to the arm.[204] The sizes obtained in solution (DLS and SEC) were 2-fold lower than the size obtained by AFM. This could be explained by de-wetting effects and evaporation, which occur during the casting process causing the aggregation of the star polymers.[240] The type of interaction between the mica surface and polyelectrolytes could also affect the sizes obtained using AFM and has been extensively studied in the literature.[241-243]

Table 4-3: Diameter of selected star homopolymers determined using three different methods: DLS, AFM and SEC with triple detections.

Polymer	Structure	D (SEC) (nm)[a]	D (AFM) (nm)[b]	D (DLS) (nm)[c]	PDI (DLS)[c]
98	$PAMPS_{50}$-star	16.5	34	16.7 ± 0.02	0.166 ± 0.02
104	$PAMPS_{400}$-star	48.6	70	52 ± 13.0	0.540 ± 0.04

[a] Experimental diameter was determined from the R_H values determined by size-exclusion chromatography in 20 % MeOH / 80 % 0.1M $NaNO_3$ in milli-Q water eluent using triple detection (RI, VS and LS); [b] Diameter determined using AFM topography on mica disc; [c] Diameter and PDI determine using DLS in PBS at 25 °C.

In conclusion, it is possible to correlate some properties (viscosity and rheology) of the star polymers with their molecular weights and sizes determined using various techniques. Viscosities were shown to increase when the molecular weights and sizes were increasing. Additionally, the star polymers synthesised have a morphology more similar to nanoparticles than star polymers synthesised using the core first approach (AFM). Both AMPS®2405 and HEAm monomers have pendant group with a functionality (i.e. OH and $SO_3^-Na^+$) responsible either for electrostatic interaction or hydrogen bonding formation. It was then decided to investigate another comonomer, DMA, which has no active pendant group.

4.3.4 PDMA versus PAMPS

In this study the properties of four different star polymers were evaluated, especially with regard to the effect of the charge position either in the core or outside of the star polymer (**Figure 4-17**). Two star homopolymers of AMPS®2405 and DMA and two star block copolymers of AMPS®2405 and DMA were studied (**Table S 4-1** and **Figure S 4-6**, **Table S 4-2** and **Figure S 4-7**). In all cases, an overall DP of 100 was targeted. PAMPS was either the first block synthesised and was positioned outside of the star (outer shell charged), or was the second block synthesised and positioned inside the star (inner shell charged). DMA was chosen as comonomer because it is a non-ionic, water soluble monomer, where the presence of a tertiary amide should stop any intramolecular interaction (i.e. hydrogen bonds) compared to the HEAm previously studied. Hawker *et al.* studied a similar system as nanoscopic imaging agents. They synthesised a core cross-linked star copolymer with a PEG as the outer shell and a copolymer of P(DMA-*co*-NAS) for the inner shell, where the *N*-acryloxysuccinimide allowed for post-polymerisation modifications.[244]

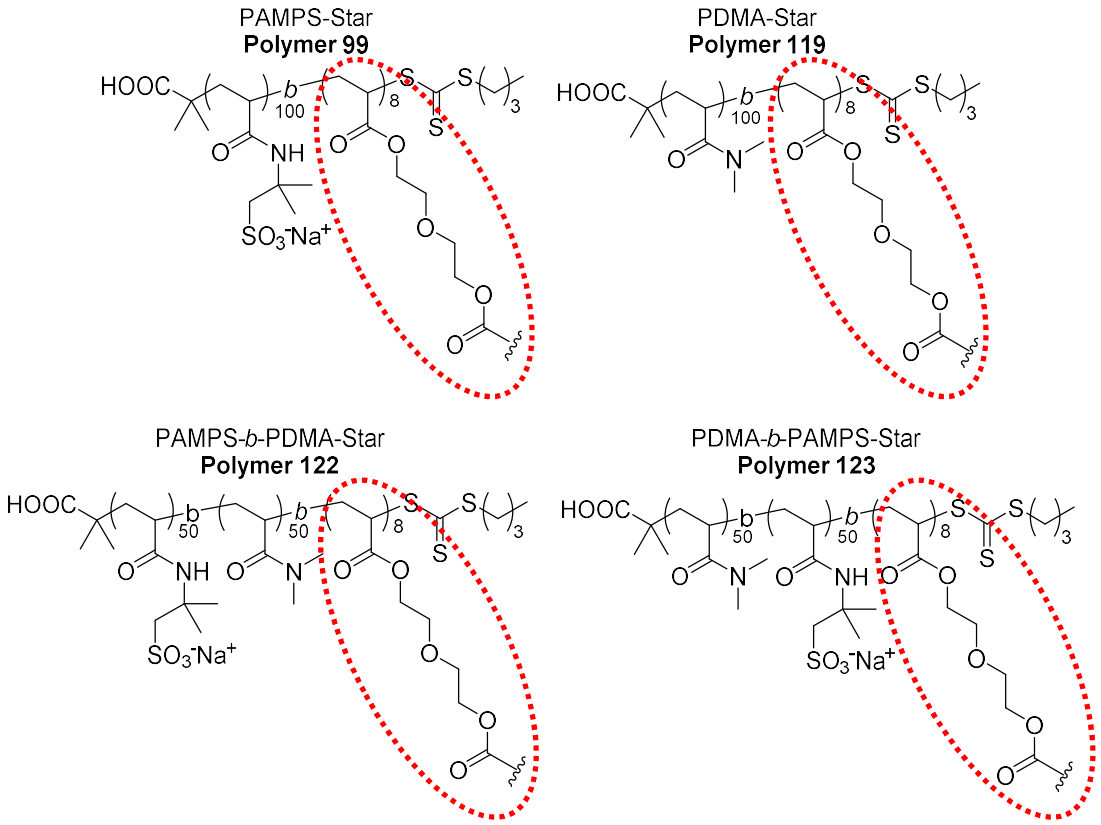

Figure 4-17: The four star polymers used in this section, where the red doted circle denotes the core of the star polymers.

The star polymers synthesised were first analysed using aqueous SEC with triple detection in order to determine their molecular weight, percentage of arms incorporated, and functionality (i.e. number of arms / stars) (**Table 4-4**). The percentage of arms incorporated was measured to be between 70 to 90 %. The functionality (i.e. number of arm per star) of the AMPS®2405 and DMA star homopolymers were 34 and 35 respectively, while the functionalities of the diblock copolymers were higher (f = 86 for $PAMPS_{50}$-*b*-$PDMA_{50}$ star polymer and f = 44 for $PDMA_{50}$-*b*-$PAMPS_{50}$ star polymer). The higher functionality observed when PDMA is the inside block (**Polymer 119** and **122**) can be explained by the synthetic approach (i.e. arm first approach). Indeed, the arm first approach is favoured due to compartmentalisation of the cross-linker, and changes in hydrophobicity allows for the functionality to be tuned.[166] The PDMA block is more hydrophobic than the AMPS®2405 block, and so the compartmentalisation of the cross-linker was reinforced, leading to a higher number of arms. Therefore, the balance between a hydrophobic and hydrophilic block could help control the overall functionality of core cross-linked star polymers. The use of SEC with triple detection not only allowed for determination of the functionality but also confirmed the formation of such structures with alpha values below 0.5. The overlaid Mark-Houwink plot and radius of gyration have shown no particular differences between the four star polymers regarding either their intrinsic viscosities or sizes (**Figure 4-18**).

Table 4-4: Star copolymers prepared by RAFT polymerisation using C4 as cross-linker and either of the following arms: $PAMPS_{100}$, $PDMA_{100}$, $PAMPS_{50}$-*b*-$PDMA_{50}$, $PDMA_{50}$-*b*-$PAMPS_{50}$.

Polymer	Structure	$M_{n,RI}$ (kg/mol)	dn/dc (mL/g)	$M_{n,SEC}$ (kg/mol)	f[c]	Arm (%)[d]	$Đ$	α	K (10^{-5} dL/g)
		RI Detector[a]		RI, MALS, VS Detectors[a]					
99	$PAMPS_{100}$-star[a]	156	0.137	526	34	80	1.01	0.23	1085
119	$PDMA_{100}$-star[a]	83	0.141	327	35	72	1.01	0.24	664
	$PDMA_{100}$-star[b]	156	0.097	349	29	86	1.05	0.19	1600
122	$PAMPS_{50}$-*b*-$PDMA_{50}$-star[a]	200	0.147	1,063	86	87	1.08	0.14	2232
123	$PDMA_{50}$-*b*-$PAMPS_{50}$-star[a]	143	0.137	706	44	82	1.12	0.35	179

[a] Experimental M_n, $Đ$, α, K, f and dn/dc values were determined by size-exclusion chromatography in 20 % MeOH / 80 % 0.1M $NaNO_3$ in milli-Q water eluent using the triple detection options in Agilent GPC/SEC Software which used a combination of a RI, LS and VS detectors. Experimental $M_{n,RI}$ values were determined using a conventional calibration obtained with PEG/PEO standards; [b] Experimental M_n and $Đ$ values were determined by size-exclusion chromatography in DMF with 5 mM NH_4BF_4 using either a combination of Refractive Index (RI), a Multi-Angle Light Scattering (MALS) and a Viscometer (VS) detectors or a conventional calibration obtained with PMMA standards; [c] The star functionality was determined using **Equation 8**; [d] The conversion of the arm into star was determined using **Equation 7**.

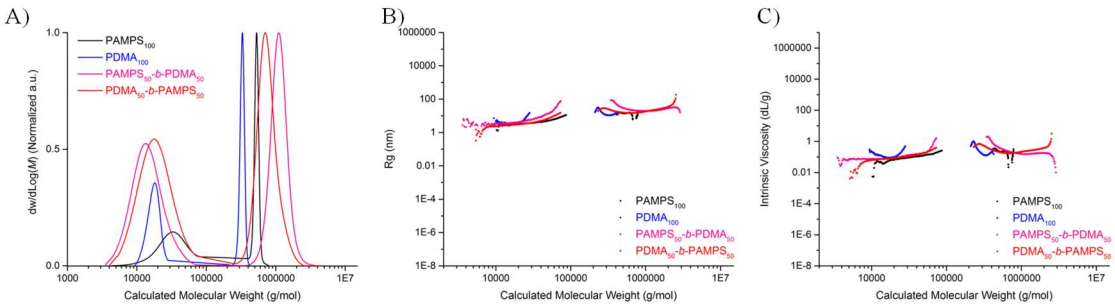

Figure 4-18: SEC in water with triple detection analysis (RI, VS, MALS) of Star homopolymers and copolymers.

A) Molecular weight distributions of the calculated molecular weight; B) Radius of gyration versus calculated molecular weight; C) Intrinsic viscosity versus calculated molecular weight.

Another advantage of studying the $PDMA_{100}$ star polymer (**Polymer 119**) was the possibility for SEC analysis in an organic solvent, such as DMF (**Figure 4-19**). This allowed for comparison of the functionalities and molecular weights obtained using both the aqueous and DMF SEC with triple detection. The molecular weight obtained in DMF SEC (349 kg/mol) was slightly higher than that obtained with the aqueous SEC (327 kg/mol) but in the same molecular weight range.

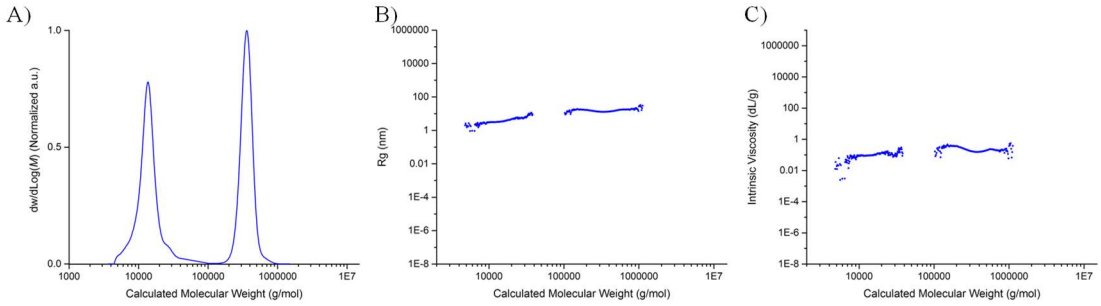

Figure 4-19: SEC in DMF with triple detection analysis (RI, VS, MALS) of $PDMA_{100}$.

A) Molecular weight distributions of the calculated molecular weight; B) Radius of gyration versus calculated molecular weight; C) Intrinsic viscosity versus calculated molecular weight.

Additionally, DLS size distributions (**Figure 4-20**) of these star polymers in PBS were monomodal, suggesting no aggregation due to secondary interaction, as previously observed with HEAm blocks (**Figure 4-15 – C**).

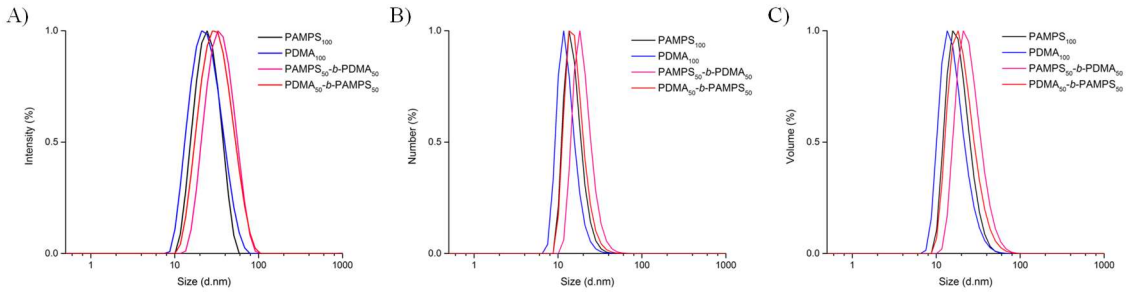

Figure 4-20: DLS size distributions of selected star polymers in PBS at 25 °C.
A) Intensity; B) Number; C) Volume.

Sizes obtained either from DLS or SEC triple detection were comparable, with sizes ranging from 23 to 39 nm (**Table 4-5**). The sizes obtained by DLS were shown to increase from $PDMA_{100}$ star polymer (23 nm, **Polymer 119**) to $PDMA_{50}$-*b*-$PAMPS_{50}$ star polymer (32 nm, **Polymer 123**) to $PAMPS_{100}$ star polymer (33 nm, **Polymer 99**) and finally $PAMPS_{50}$-*b*-$PDMA_{50}$ star polymer (39 nm, **Polymer 122**). The star polymers with the charged block on the outside were bigger as a consequence of electrostatic repulsion and / or steric hindrance, due to the presence of counter ions.

Table 4-5: Diameter of selected star polymers determined using three different methods: DLS, AFM and SEC with triple detection.

Polymer	Structure	D (SEC)[a] nm	D (DLS)[c] nm	PDI (DLS)[c]
99	$PAMPS_{100}$-star	33	23 (± 0.06)	0.091 (± 0.003)
119	$PDMA_{100}$-star	23	23 (± 0.48)	0.221 (± 0.002)
	$PDMA_{100}$-star	27[b]	-	-
122	$PAMPS_{50}$-*b*-$PDMA_{50}$-star	39	32 (± 0.35)	0.124 (± 0.005)
123	$PDMA_{50}$-*b*-$PAMPS_{50}$-star	32	28 (± 0.05)	0.157 (± 0.004)

[a] Experimental diameter was determined from the R_H values itself determined by size-exclusion chromatography in 20 % MeOH / 80 % 0.1M $NaNO_3$ in milli-Q water eluent using triple detection (RI, VS and LS); [b] Experimental diameter was determined from the R_H values itself determined by size-exclusion chromatography in DMF with 5 mM NH_4BF_4 eluent using triple detection (RI, VS and LS); [c] Diameter and PDI determine using DLS in PBS at 25 °C.

The star polymers were further analysed by AFM (**Figure 4-21**) using silicon discs. It could be observed that the AMPS®2405 star homopolymers (**Polymer 99**) were aggregating forming tube like structure. Again, the size obtained using AFM was higher than when determined in solution (DLS or SEC) ($PAMPS_{50}$-*b*-$PDMA_{50}$-star = 67 nm, $PDMA_{100}$-star = 44 nm, $PDMA_{50}$-*b*-$PAMPS_{50}$-star = 55 nm). The diblock star copolymers were larger than the PDMA star homopolymers, which may be attributed to the aggregation phenomenon observed with the AMPS®2405 star homopolymer.

Additionally, when AMPS®2405 was the outside block, an even larger size was observed, which is in accordance with the results obtained by SEC and DLS. AFM analysis demonstrated the possible modulation of star polymer interactions with a solid surface by changing the position of the charged block. This could be further investigated for different applications such as surface modification[245] or drug delivery.[246]

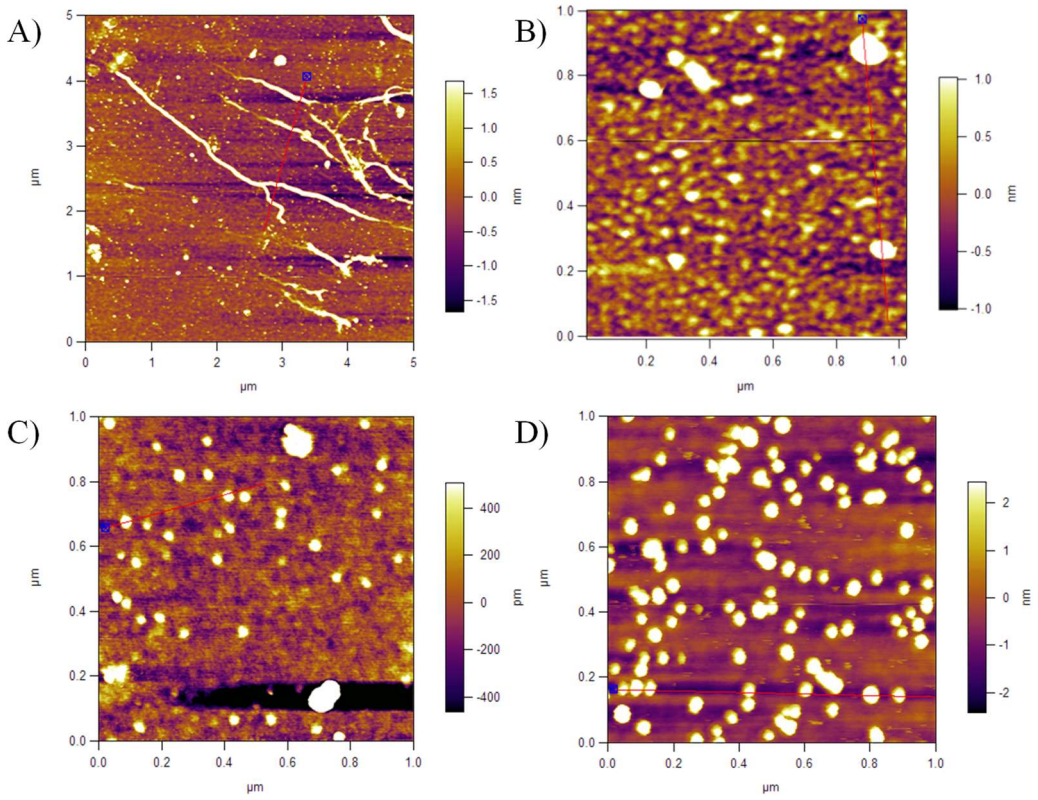

Figure 4-21: AFM topography images of selected star polymers on silicon disc with different arms.

A) $PAMPS_{100}$; B) $PAMPS_{50}$-*b*-$PDMA_{50}$; C) $PDMA_{100}$; D) $PDMA_{50}$-*b*-$PAMPS_{50}$.

The morphology of star polymers formed using the arm first approach was here investigated by determining the alpha values with SEC triple detection (Mark-Houwink plot) and imaging structure using AFM. Neither techniques gave complete information, as SEC yields information on the branching but not the structure itself, while AFM only allows observation of the size and morphology. In order to obtain further orthogonal data, the star polymers were analysed by small-angle X-ray scattering (SAXS) (**Figure 4-22**).

The raw data obtained by SAXS analysis requires fitting to a model to determine the structural information. Firstly, a star model was used, which was unfruitful, however according to the AFM results, a nanoparticle-like structure was obtained, therefore, a sphere model (green) or a core-shell sphere model (yellow) were used instead. The core-shell sphere model fitted much better for the $PDMA_{50}$-b-$PAMPS_{50}$ (**Figure 4-22 – D, Polymer 123**) and $PDMA_{100}$ (**Figure 4-22 – C, Polymer 119**) star polymers, while deviations were observed for the two other materials (**Figure 4-22 – B** and **E, Polymer 122** and **99**). The use of the core-shell structure to define star polymers using the arm first approach has already been described in the literature and can be regarded as complex nanoparticles.[247] Additionally, the intensity observed for $PDMA_{100}$ star polymer (**Polymer 119**) is lower compared to the other three star polymers carrying a negatively charged monomer (AMPS®2405), which was attributed to the charge parameter.[211] Furthermore to improve the fit for $PAMPS_{100}$ (**Figure 4-22 – B, Polymer 99**) and $PAMPS_{50}$-*b*-$PDMA_{50}$ (**Figure 4-22 – E, Polymer 122**) star polymers using a sphere model, a form factor was used in order to take into account the electrostatic interaction between charges between different star polymers and different arms.

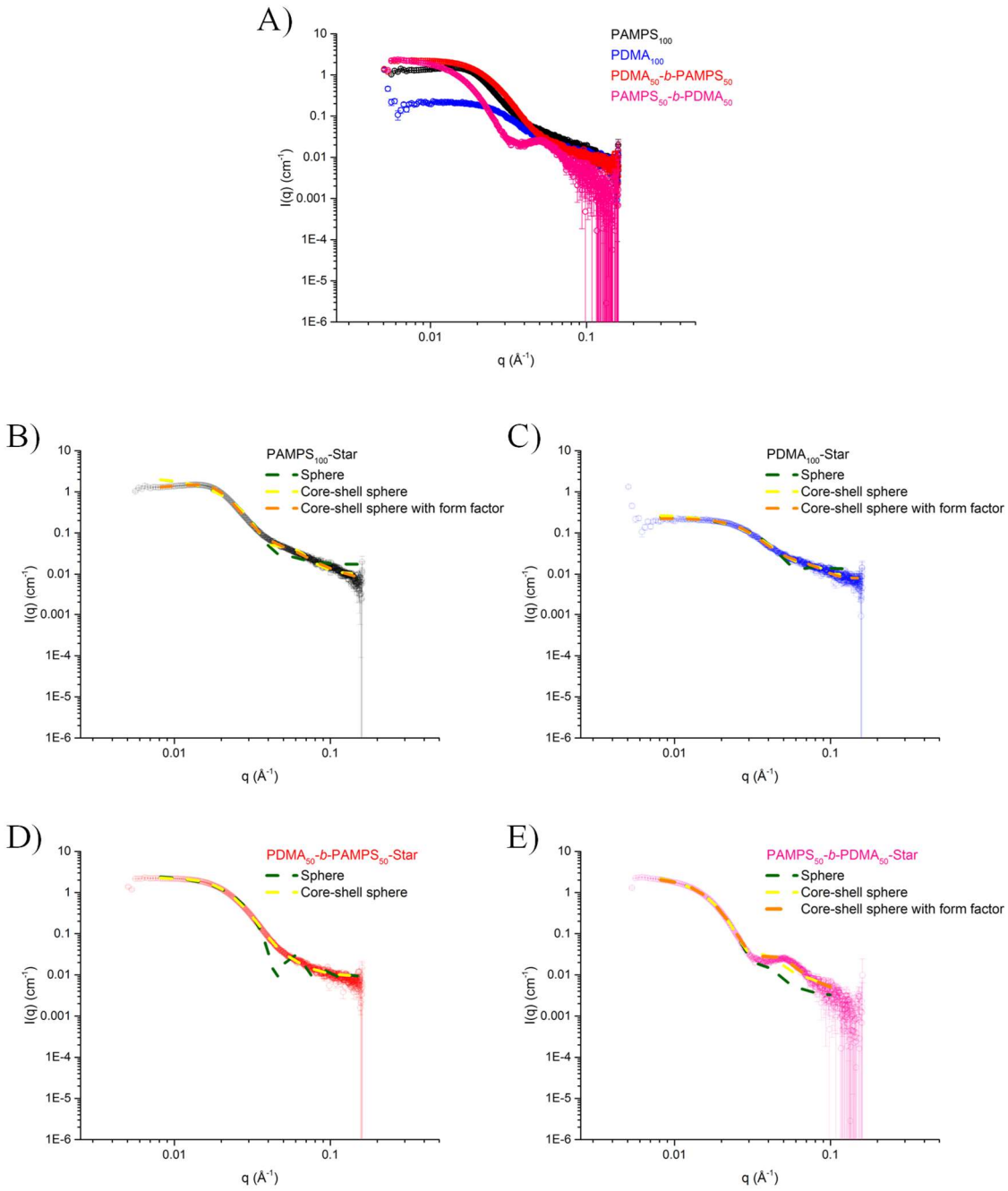

Figure 4-22: SAXS analysis in PBS (25 °C at 5 mg/mL) of star polymers synthesised by RAFT polymerisation with different arms.

A) Overlay of the raw data for $PAMPS_{100}$ arm, $PDMA_{100}$ arm, $PAMPS_{50}$-*b*-$PDMA_{50}$ arm and $PDMA_{50}$-*b*-$PAMPS_{50}$ arm polymers. Raw data and fitting of - B) $PAMPS_{100}$ star polymer; C) $PDMA_{100}$ star polymer; D) $PDMA_{50}$-*b*-$PAMPS_{50}$ star polymer; E) $PAMPS_{50}$-*b*-$PDMA_{50}$ star polymer.

Additionally, when the $PAMPS_{100}$ star polymer (**Polymer 99**) was analysed either in water or PBS (**Figure S 4-5**) by DLS and SAXS, aggregations were observed suggested by the change of intensity in SAXS analysis; similar results were observed by Lund *et al.*.[155] The use of PBS instead of water allowed suppression of the electrostatic interactions / repulsion between AMPS®2405 units. The charge, either inside or outside of the shell of star polymers, had a critical impact on the structure which further supports the previous results obtained by SEC, DLS and AFM. This would dramatically impact any targeted applications.

4.4 Conclusions

In this chapter a wide range of techniques were used to characterise the star polymers synthesised in **CHAPTER 3**. The use of triple detection SEC allowed for determination of the absolute molecular weight of the star polymers, their functionalities and the Mark-Houwink parameters (α and K) of PAMPS (star-) polymers. The viscosity of star homopolymers were investigated and was shown to increase when the arm length was increased. Additionally the viscosities of star copolymer of AMPS®2405 with HEAm can be easily tuned by changing the block length at constant DP and molecular weight (diblock versus tetrablock star polymers). The PHEAm blocks were forming a secondary structure with hydrogen bonding which then allowed shear thinning properties. Finally, the size of the star polymers were determined by DLS, SEC and AFM. The sizes determined by SEC and DLS were in agreement, while the sizes obtained with AFM were higher. This is possibly due to aggregation during the deposition process on mica disc or to surface interactions. PAMPS and PAMPS-*co*-PHEAm star (co-)polymers will be further investigated as heparin-mimicking polymers in **CHAPTER 5**.

Secondly, PAMPS-*co*-PDMA star copolymers were characterised. DMA was chosen due to the lack of hydrogen bonding when compared to HEAm. The effect of the charge position, either outside or inside, in solution was then studied. SAXS analysis of the star polymers fit a core-shell sphere model which was in accordance with the morphologies observed by AFM. It was also demonstrated that the structure of the $PAMPS_{50}$-*b*-$PDMA_{50}$ star polymer was similar to the $PAMPS_{100}$ star polymer, and had to be fitted with an additional form factor structure due to the interactions between the charges. The structure of the $PDMA_{50}$-*b*-$PAMPS_{50}$ star polymer was similar to the $PDMA_{100}$ star polymer and was fitted with a simple core-shell sphere model. These four star polymers are currently being further investigated by Dr Gemma-Louise Davies (UCL) to be used as stabilisers of contrast agents for magnetic resonance imaging.[213] Particularly the effect of the structure (linear versus star polymers) will be studied, but also of charge distribution and conformation on the stabilisation of magnetite Fe_3O_4 nanoparticles.[214,248]

4.5 Experimental

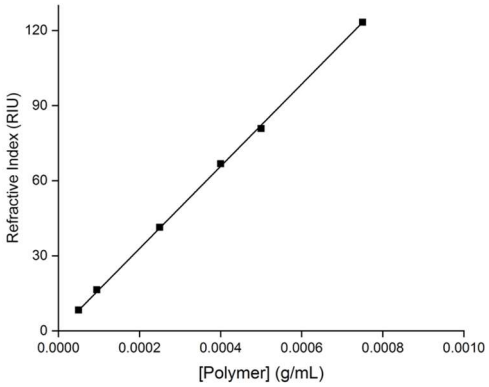

Figure S 4-1: Refractive index *versus* concentration ($PAMPS_{50}$, **Polymer 19**) measured with a refractometer ($y = 1.632x10^{5} + 5.277x10^{-1}$; $r^2 = 0.999$).

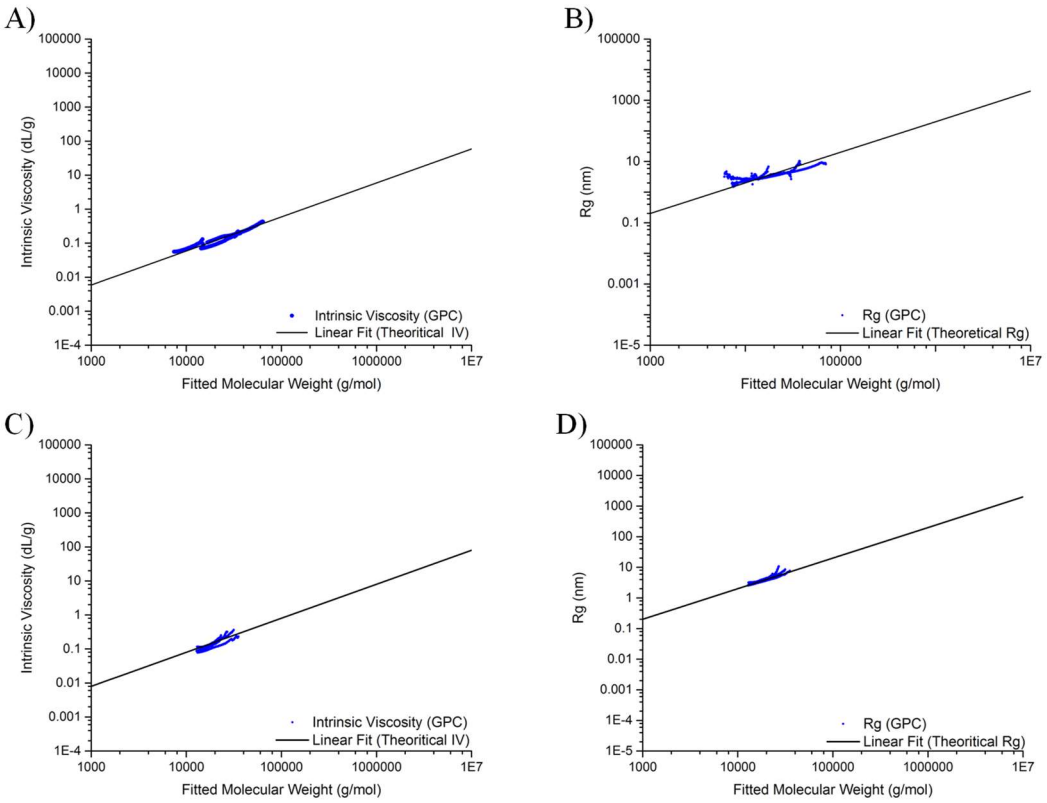

Figure S 4-2: Linear extrapolation of the intrinsic viscosity and the radius of gyration for the linear homopolymers (A and B respectively) and copolymers (C and D respectively).

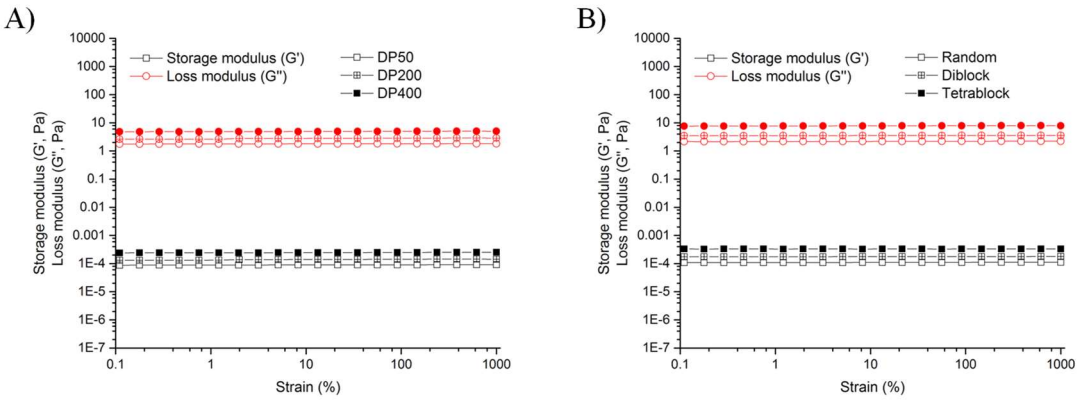

Figure S 4-3: Amplitude sweep of star polymers at 25 °C applying a strain from 0.1 to 1000 % at a constant angular frequency of 10 (s^{-1}).

A) G′ and G″ of star homopolymers; B) G′ and G″ of star copolymers.

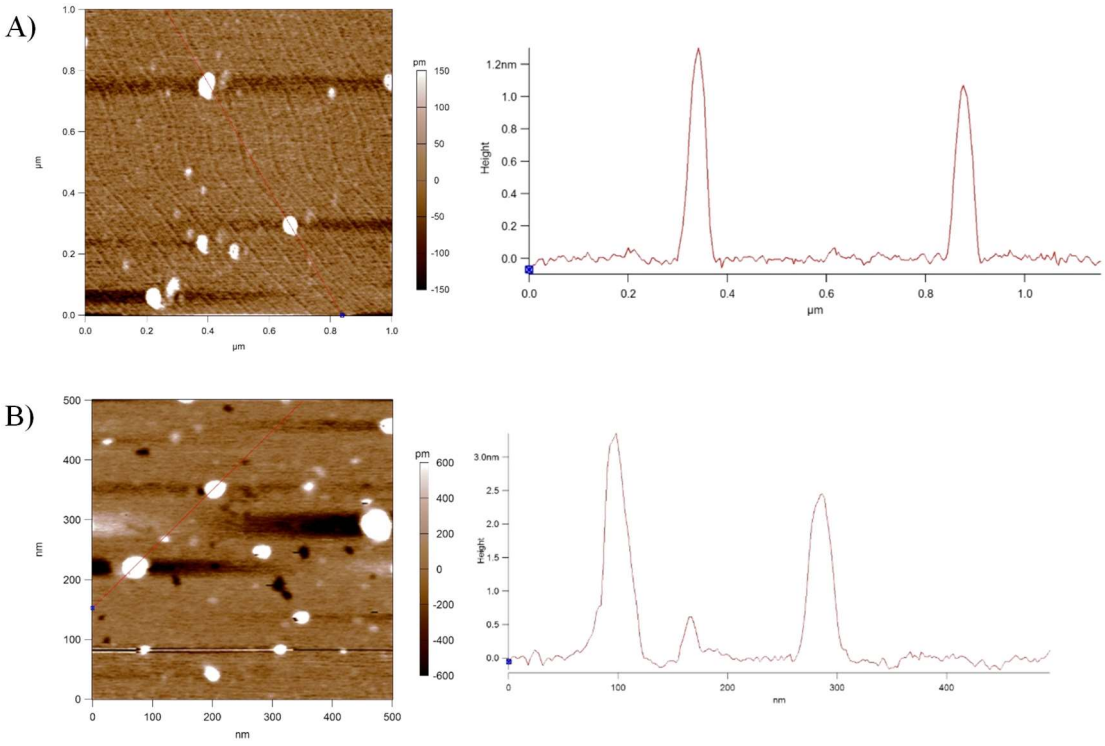

Figure S 4-4: AFM topography images of selected star homopolymers on a mica disc.

A) DP_{arm} = 50, diameter = 34 nm; B) DP_{arm} = 400, diameter = 71 nm.

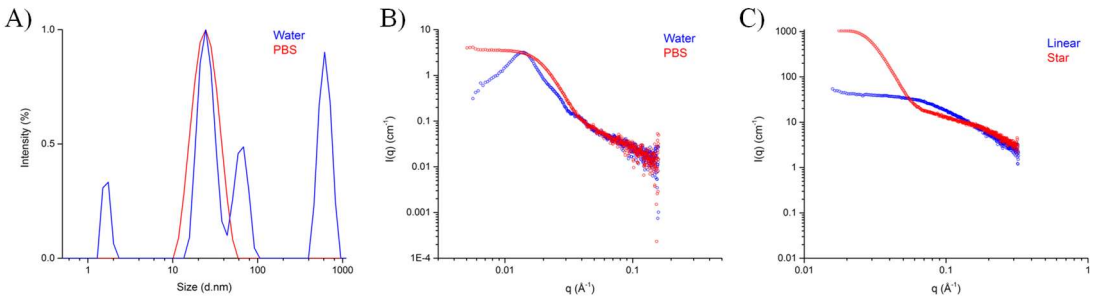

Figure S 4-5: Star homopolymer (DP_{arm} = 100) analysis at 25 °C.

A) DLS of the star polymer; B) SAXS of the star polymer; C) SAXS in PBS of the star polymer (red) and the corresponding arm used (blue).

Polymer Synthesis

For the synthesis of the materials used, see experimental sections from the following chapters: **CHAPTER 2** and **CHAPTER 3**, **Section Star Polymer Synthesis – General Procedure**.

Table S 4-1: Conditions used for the preparation of linear PAMPS and PDMA (DP50 or 100).

Compound	**5**	**124**	**19**	**20**
Monomer	DMA	DMA	AMPS®2405	AMPS®2405
$DP_{targeted}$	50	100	50	100
$m_{monomer}$ (mg)	1000	1000	1000	1000
m_{CTA} (mg)	51	25.5	12.8	6.4
m_{VA-086} (mg)	4.8	4.8	1.2	1.2
m_{NaOH} (mg)	-	-	1	0.5
m_{H2O} (mg)	5685	5685	850	855
$[CTA]_t/[VA\text{-}086]_0$	12	6	12	6
L (%)[a]	98.4	96.8	98.4	96.8
Conv (%)[b]	> 99	> 99	> 99	> 99
$M_{n,\,th}$[c]	5,200	10,200	11,700	23,200
$M_{n,\,SEC}$[d]	1,700	5,500	11,400	24,000
$Đ$[d]	1.26	1.22	1.19	1.25

[a] Theoretical estimation of the fraction of living chains per block; [b] Conversions were determined by ^{1}H NMR spectroscopy, using **Equation 1**; [c] Theoretical M_n values were calculated using **Equation 2**; [d] Experimental M_n and $Đ$ values were determined by size-exclusion chromatography in 20 % MeOH / 80 % 0.1M $NaNO_3$ in milli-Q water eluent using a conventional calibration obtained with PEG/PEO standards.

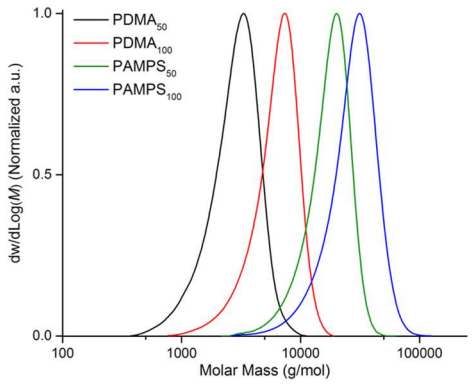

Figure S 4-6: Aqueous SEC molecular weight distributions of AMPS®2405 and DMA homopolymers targeting either a DP 50 or 100.

Table S 4-2: Conditions used for the preparation of the diblock copolymers $PAMPS_{50}$-*b*-$PDMA_{50}$ and $PDMA_{50}$-*b*-$PAMPS_{50}$.

Compound	**125**	**126**
Structure	$PAMPS_{50}$-*b*-$PDMA_{50}$	$PDMA_{50}$-*b*-$PAMPS_{50}$
MacroCTA	**19**	**5**
Monomer	DMA	AMPS®2405
$DP_{targeted}$	50	50
$m_{monomer}$ (mg)	251	4000
m_{VA-086} (mg)	0.43	3.4
Cumulative L (%)[a]	97.5	97.6
Conv (%)[b]	> 99	> 99
$M_{n,\,th}$[c]	16,700	16,700
$M_{n,\,SEC}$[d]	11,500	14,000
$Đ$[d]	1.18	1.14

[a] Theoretical estimation of the cumulated fraction of living chains; [b] Conversions were determined by ^{1}H NMR spectroscopy, using **Equation 1**; [c] Theoretical M_n values were calculated using **Equation 2**; [d] Experimental M_n and $Đ$ values were determined by size-exclusion chromatography in 20 % MeOH / 80 % 0.1M $NaNO_3$ in milli-Q water eluent using a conventional calibration obtained with PEG/PEO standards.

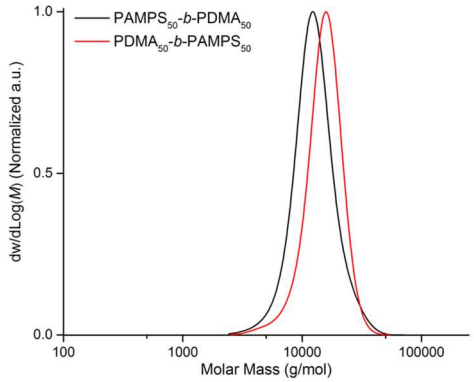

Figure S 4-7: Aqueous SEC molecular weight distributions of the following diblock copolymers synthesised: $PAMPS_{50}$-*b*-$PDMA_{50}$ and $PDMA_{50}$-*b*-$PAMPS_{50}$.

4.6 References

(152) N. H. Aloorkar, A. S. K., R. A. Patil, D. J. Ingale *IJPSN* **2012**, *5*, 1675.

(155) Bekhradnia, S.; Diget, J. S.; Zinn, T.; Zhu, K.; Sande, S. A.et al *Macromolecules* **2015**, *48*, 2637.

(166) Chen, Q.; Xu, Y.; Cao, X.; Qin, L.; An, Z. *Polym. Chem.* **2014**, *5*, 175.

(177) McKenzie, T. G.; Ren, J. M.; Dunstan, D. E.; Wong, E. H. H.; Qiao, G. G. *J. Polym. Sci., Part A: Polym. Chem.* **2016**, *54*, 135.

(185) Duro-Castano, A.; Movellan, J.; Vicent, M. J. *Biomater. Sci.* **2015**, *3*, 1321.

(186) Wu, W.; Wang, W.; Li, J. *Prog. Polym. Sci.* **2015**, *46*, 55.

(187) Viswanathan, K.; Long, T. E.; Ward, T. C. *J. Polym. Sci., Part A: Polym. Chem.* **2005**, *43*, 3655.

(188) Knox, J. H.; Scott, H. P. *J. Chromatogr.* **1984**, *316*, 311.

(189) Kostanski, L. K.; Keller, D. M.; Hamielec, A. E. *J. Biochem. Biophys. Methods* **2004**, *58*, 159.

(190) Striegel, A. M.; Yau, W. W.; Kirkland, J. J.; Bly, D. D. In *Modern Size-Exclusion Liquid Chromatography*; John Wiley & Sons, Inc.: 2009, p 18.

(191) Gaborieau, M.; Castignolles, P. *Anal. Bioanal. Chem.* **2011**, *399*, 1413.

(192) Kasaai, M. R. *Carbohydr. Polym.* **2007**, *68*, 477.

(193) Lesec, J.; Millequant, M. *Int. J. Polym. Anal. Charact.* **1996**, *2*, 305.

(194) Wiltshire, J. T.; Qiao, G. G. *Macromolecules* **2008**, *41*, 623.

(195) Pearson, D. S.; Helfand, E. *Macromolecules* **1984**, *17*, 888.

(196) Fetters, L. J.; Kiss, A. D.; Pearson, D. S.; Quack, G. F.; Vitus, F. J. *Macromolecules* **1993**, *26*, 647.

(197) Alfrey, T.; Bartovics, A.; Mark, H. *J. Am. Chem. Soc.* **1942**, *64*, 1557.

(198) Cullen, P. J.; Duffy, A. P.; O'Donnell, C. P.; O'Callaghan, D. J. *Trends Food Sci. Technol.* **2000**, *11*, 451.

(199) Korosi, A.; Fabuss, B. M. *Anal. Chem.* **1968**, *40*, 157.

(200) Sutterby, J. L. *Journal of Physics E: Scientific Instruments* **1973**, *6*, 1001.

(201) Yabuno, H.; Higashino, K.; Kuroda, M.; Yamamoto, Y. *J. Appl. Phys.* **2014**, *116*, 124305.

(202) Servais, C.; Ranc, H.; Roberts, I. D. *Journal of Texture Studies* **2003**, *34*, 467.

(203) Barnes, H. A.; Nguyen, Q. D. *Journal of Non-Newtonian Fluid Mechanics* **2001**, *98*, 1.

(204) Bhattacharjee, S. *J. Controlled Release* **2016**, *235*, 337.

(205) Yoshizaki, T.; Kanazawa, A.; Kanaoka, S.; Aoshima, S. *Macromolecules* **2016**, *49*, 71.

(206) Kikhney, A. G.; Svergun, D. I. *FEBS Lett.* **2015**, *589*, 2570.

(207) Lyngsø, J.; Al-Manasir, N.; Behrens, M. A.; Zhu, K.; Kjøniksen, A.-L.et al *Macromolecules* **2015**, *48*, 2235.

(208) Prosa, T. J.; Bauer, B. J.; Amis, E. J. *Macromolecules* **2001**, *34*, 4897.

(209) Felberg, L. E.; Doshi, A.; Hura, G. L.; Sly, J.; Piunova, V. A.et al *Mol. Phys.* **2016**, *114*, 3221.

(210) Narumi, A.; Ohashi, Y.; Togashi, D.; Saito, Y.; Jinbo, Y.et al *J. Polym. Sci., Part A: Polym. Chem.* **2012**, *50*, 3546.

(211) Moinard, D.; Taton, D.; Gnanou, Y.; Rochas, C.; Borsali, R. *Macromol. Chem. Phys.* **2003**, *204*, 89.

(212) Bray, C.; Peltier, R.; Kim, H.; Mastrangelo, A.; Perrier, S. *Polym. Chem.* **2017**, *8*, 5513.

(213) Davies, G.-L.; Kramberger, I.; Davis, J. J. *Chem. Commun.* **2013**, *49*, 9704.

(214) Ternent, L.; Mayoh, D. A.; Lees, M. R.; Davies, G.-L. *J. Mater. Chem. B* **2016**, *4*, 3065.

(215) Drott, E. E.; Mendelson, R. A. *Journal of Polymer Science Part B: Polymer Letters* **1964**, *2*, 187.

(216) Striegel, A. M. *Chromatographia* **2017**, *80*, 989.

(217) Tumolo, T.; Angnes, L.; Baptista, M. S. *Anal. Biochem.* **2004**, *333*, 273.

(218) Bello, A.; Guzman, G. M. *Eur. Polym. J.* **1966**, *2*, 85.

(219) Huglin, M. B. *J. Appl. Polym. Sci.* **1965**, *9*, 3963.

(220) Pawcenis, D.; Syrek, M.; Aksamit-Koperska, M. A.; Lojewski, T.; Lojewska, J. *RSC Adv.* **2016**, *6*, 38071.

(221) Pezzin, G.; Gligo, N. *J. Appl. Polym. Sci.* **1966**, *10*, 1.

(222) Al-Shammari, B.; Al-Fariss, T.; Al-Sewailm, F.; Elleithy, R. *Journal of King Saud University - Engineering Sciences* **2011**, *23*, 9.

(223) Hayahara, T.; Takao, S. *Kolloid-Zeitschrift und Zeitschrift für Polymere* **1968**, *225*, 106.

(224) Nap, R. J.; Park, S. H.; Szleifer, I. *Soft Matter* **2018**.

(225) Cosimbescu, L.; Robinson, J. W.; Zhou, Y.; Qu, J. *RSC Adv.* **2016**, *6*, 86259.

(226) Asthana, S.; Kennedy, J. P. *J. Polym. Sci., Part A: Polym. Chem.* **1999**, *37*, 2235.

(227) Porter, R. S.; Johnson, J. F. *J. Appl. Phys.* **1961**, *32*, 2326.

(228) Sotiropoulou, M.; Bokias, G.; Staikos, G. *Macromolecules* **2003**, *36*, 1349.

(229) Duan, F.; Chen, C.; Zhao, X.; Yang, Y.; Liu, X.et al *Environmental Science: Nano* **2016**, *3*, 213.

(230) Raju, V. R.; Menezes, E. V.; Marin, G.; Graessley, W. W.; Fetters, L. J. *Macromolecules* **1981**, *14*, 1668.

(231) Wood-Adams, P. M.; Dealy, J. M.; deGroot, A. W.; Redwine, O. D. *Macromolecules* **2000**, *33*, 7489.

(232) Rublova, Y. D.; Velichko, O. V.; Danilov, F. I. *Protection of Metals and Physical Chemistry of Surfaces* **2017**, *53*, 916.

(233) Urist, M. R.; Speer, D. P.; Ibsen, K. J.; Strates, B. S. *Calcified Tissue Research* **1968**, *2*, 253.

(234) Crupi, V.; Majolino, D.; Migliardo, P.; Venuti, V.; Micali, N.et al *J. Mol. Struct.* **2003**, *651-653*, 675.

(235) Hendricks, S. B.; Wulf, O. R.; Hilbert, G. E.; Liddel, U. *J. Am. Chem. Soc.* **1936**, *58*, 1991.

(236) Zhao, C.; Zheng, J. *Biomacromolecules* **2011**, *12*, 4071.

(237) Zhang, J.; Tanaka, J.; Gurnani, P.; Wilson, P.; Hartlieb, M.et al *Polym. Chem.* **2017**, *8*, 4079.

(238) Tanaka, J.; Tani, S.; Peltier, R.; Pilkington, E. H.; Kerr, A.et al *Polym. Chem.* **2018**.

(239) Pang, X.; Feng, C.; Xu, H.; Han, W.; Xin, X.et al *Polym. Chem.* **2014**, *5*, 2747.

(240) Zhang, J.; Gody, G.; Hartlieb, M.; Catrouillet, S.; Moffat, J.et al *Macromolecules* **2016**, *49*, 8933.

(241) Maslova, M. V.; Gerasimova, L. G.; Forsling, W. *Colloid J.* **2004**, *66*, 322.

(242) Gliemann, H.; Mei, Y.; Ballauff, M.; Schimmel, T. *Langmuir* **2006**, *22*, 7254.

(243) Christenson, H. K.; Thomson, N. H. *Surf. Sci. Rep.* **2016**, *71*, 367.

(244) Fukukawa, K.-i.; Rossin, R.; Hagooly, A.; Pressly, E. D.; Hunt, J. N.et al *Biomacromolecules* **2008**, *9*, 1329.

(245) Gernandt, R.; Wågberg, L.; Gärdlund, L.; Dautzenberg, H. *Colloids Surf. Physicochem. Eng. Aspects* **2003**, *213*, 15.

(246) Lankalapalli, S.; Kolapalli, V. R. M. *Indian Journal of Pharmaceutical Sciences* **2009**, *71*, 481.

(247) Gao, H.; Matyjaszewski, K. *Prog. Polym. Sci.* **2009**, *34*, 317.

(248) Kurzhals, S.; Schroffenegger, M.; Gal, N.; Zirbs, R.; Reimhult, E. *Biomacromolecules* **2017**.

CHAPTER 5:
HEPARIN-MIMICKING POLYMERS

5.1 Abstract

Heparin is a natural macromolecule involved in a wide range of biological processes, such as protein stabilisation, anticoagulation and tissue regeneration; but also in diverse biomedical applications such as medical device coating, therapeutics and wound healing. These applications are often associated with the presence of the highly negatively charged sulfate groups along the polysaccharide chains. Unfortunately, heparin possesses undesirable side effects, particularly virus contamination and heterogeneity. Furthermore, heparin is difficult to extract in large quantities, and therefore a synthetic alternative would be of commercial interest. Here, the effect of sulfonated synthetic polymeric architectures (PAMPS) was studied as an alternative to heparin. As a model application, the potential stabilisation of fibroblast growth factor (FGF) by synthetic sulfonated polymers was studied, and compared with natural stabilisation and activation of FGF by heparin. The proliferation of BaF3-FR1c, was used as a model assay to investigate the structure-activity relationship for the stabilisation of bFGF by our newly synthesised polymers. A library of different polymeric architectures was synthesised to investigate at the effect of molecular weight, comonomer type and polymer architecture on protein stabilisation. Among other parameters, the architectural size was shown to be a critical parameter in this stabilisation.

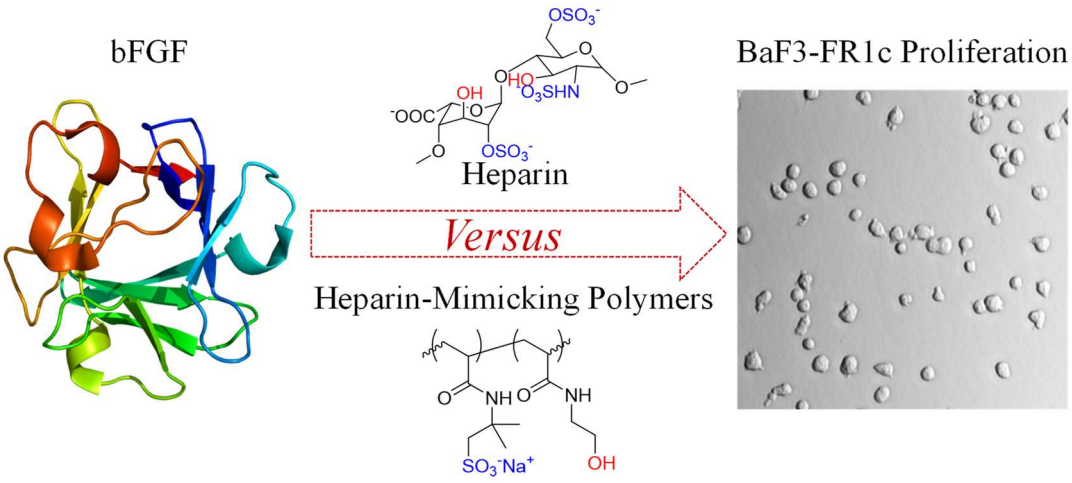

5.2 Introduction

5.2.1 Heparin Overview

Heparin is natural biomacromolecule produced by mast cells, which was first observed by McLean in 1916, but was formally extracted and characterised by Howell in 1925.[249,250] The extraction of heparin on an industrial scale was initially performed using cattle lungs, however, due to the long extraction process and financial competition in the food industry, pig intestinal mucosa was then utilised as the source.[251]

Heparin is a well-known and widely used medicinal and therapeutic molecule, facilitating a wide-range of biological applications, in addition to being approved by the Federal Drug Administration (FDA) for clinical use. It plays a major role in antithrombotic therapy as an anticoagulant, in protein binding and activation, as well as in biological processes such as cell differentiation, adhesion and interaction.[252-256] Heparin is also utilised in several new biomedicinal applications such as the heparinisation of medical devices, which has recently been shown to increase their hemocompatibility.[257,258] Other examples include the change of the transfection efficiency of DNA and trehalose (Tr4) polyplexes (by decreasing the toxicity of Tr4), [259] as an antigenic agent in cancer treatments,[260] and its use as a colloidal stabiliser for contrast agents used in magnetic resonance imaging (MRI).[214]

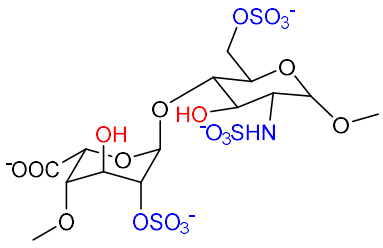

Figure 5-1: Structure of heparin.[261]

The structure of heparin consists mostly of unbranched polysaccharide chains, belonging to the family of glycosaminoglycans (GAGs). GAGs are composed of repeating disaccharide units, which in the case for heparin are mostly sulfated. The disaccharides for heparin are uronic acid and glucosamine, bound via a 1→4 linkage,

averaging 2.7 sulfate groups per disaccharide as part of the ~ 15,000 g/mol molecule.[261] These functional groups render heparin very negatively charged as a consequence of both the carboxylic and sulfate groups (**Figure 5-1**).[262-264] In aqueous solution, heparin exhibits a helical structure which allows for binding to other positively charged biomolecules such as proteins (e.g. chemokines and growth factors).[265,266] Heparin binds to proteins through electrostatic interactions with the positively charged amino acids (arginine and lysine). The interactions between heparin and growth factors are further supported through hydrogen bonding with asparagine and glutamine residues surrounding the heparin binding domain present in growth factors.[267] The heparin binding growth factor proteins include, but are not limited to, acidic fibroblast growth factor (aFGF, FGF1), basic fibroblast growth factor (bFGF, FGF2), vascular endothelial growth factor (VEGF), and transforming growth factor (TGF).[261,268-273]

5.2.2 Heparin Binding Protein – Fibroblast Growth Factor

The stabilisation of FGFs is a widely studied phenomenon due to its importance for a wide range of biological applications. For example, FGF can be utilised for wound healing due to its capacity for repairing tissue through the promotion of proliferating fibroblast cells. When environmental stressors (e.g. enzymatic inactivation or thermal and acid degradation) from the wound are applied to FGFs, the protein degrades and becomes biologically inactive, an area where heparin has been shown to help with their stabilisation in such conditions.[274,275] Fibroblast growth factors exist under two forms: the basic growth factor named bFGF (or FGF2) (pI9.6), and the acidic growth factor aFGF (or FGF1) (pI5.6-6.0), with the pH regulating the overall charge density of each protein. Both growth factors are involved in the proliferation and differentiation of a variety of cells by binding to their fibroblast growth factor receptors (FGFRs) (e.g. mesoderm cells).[276,277] Basic and acidic fibroblast growth factors are composed of a single-chain polypeptide with 55 % of the peptide sequence being identical to each other, both having a molecular weight of about 16 kDa and carrying two heparin binding domains rich in positively charged amino acids. Basic growth factor (bFGF) exists either with 146 or 131 amino acids, depending on truncation, while the acidic growth factor (aFGF) exists either with 140 or 134 residues. Both of these forms, truncated or not, are biologically active.[278,279]

Heparin or heparan sulfate, both glycosaminoglycans displaying different disaccharide composition, have both been shown to be co-factors of FGF which interact with the heparin binding domains of the proteins. These interactions not only activate FGFRs but also promote the dimerization of the receptors, inducing phosphorylation that is responsible for a variety of cellular responses.[280-283] Ornitz *et al.* widely studied the mechanism of FGF activation by heparin, through the formation of a trimolecular complexes with FGFRs.[269] They have shown that upon binding to FGF, heparin induces a change in the FGF spatial conformation, allowing it to dimerise with another FGF through self-association.[284] This dimer can then bind to two FGFRs, inducing its dimerization and phosphorylation, with heparin then being linked to both the FGF and the FGFR (heparin:FGF:FGFR 1:2:2). [285,286]

Despite heparin being naturally produced by biological processes, it can have extensive adverse side effects. Similarly, the bioactivity is batch-to-batch and also patient dependent.[261,287]

Some of the constraints of using heparin are summarised below:

- Naturally occurring heparin has a high molecular weight distribution with sizes ranging from 5 to 40 kDa. As a result, heparin needs to be fractionated to produce ultralow molecular weight heparin, which increases its production costs.[288]
- Its extraction from animal tissues (cattle or pork) can generate a high risk of virus contamination, which can be deadly.[288,289]
- Its heterogeneity in structure, which contains different binding motifs and degrees of sulfation associated with diverse degradation rate can be problematic in certain biological applications.[290]

With consideration to the importance of heparin in several biological applications and the aforementioned drawbacks, researchers have been extensively investigating replacing heparin with other synthetic (macro)-molecules.

5.2.3 Heparin-Mimicking Polymers

Polymers have been widely studied as heparin-mimics in order to overcome the constraints associated with the use of heparin.[261,270] In particular, the use of synthetic sulfonated polymers allows control over the molecular weight by targeting specific degrees of polymerisation (DPs). The use of synthetic alternatives also facilitates industrial production, rendering scale-up of the reaction possible. In addition, the possibility to modify the structure, for example by incorporating a selection of functional groups, greatly increases the ability to target specific applications. A popular route to replace heparin is to chemically modify chitosan to synthesise heparin-like chitosan polymers or hydrogels. Such compounds have been previously tested for their antithrombic activity or as drug and protein-loading vectors.[258,291,292] Sulfated synthetic glycopolymers, which can be synthesised using a wide range of polymerisation methods such as free radical polymerisation (FRP)[293,294] or even using control radical polymerisation techniques such as reversible addition-fragmentation chain transfer polymerisation (RAFT), have also been studied.[295] While these polymerisation processes allow for good control over the molecular weights of the resulting sulfated glycomonomers, they tend to be prone to desulfation, and consequently a loss in biological activity could be observed.

More recently, synthetic polysulfonated polymers have been studied. Garcia-Fernandez *et al.* synthesised two copolymers using 2-acrylamido-2-methylpropane sulfonic acid (AMPS®) and either 1-vinyl-2-pyrrolidinone (VP), a hydrophilic monomer, or butyl acrylate (BA), a hydrophobic monomer, using free radical polymerisation (**Figure 5-2**).[296] They have shown that by controlling the monomers distribution along the polymer backbones, they could control the bioactivity of acidic fibroblast growth factor (aFGF) using either of these polymers as additives. When BA was used as a comonomer, a diblock like polymer was obtained, while an alternating polymer was obtained with VP. The interaction with aFGF was further favoured when BA was used as the co-monomer, inducing a more extended antiproliferative activity towards Balb/c 3T3 fibroblast cells. The antiproliferative activity was then modulated by varying either the polymer concentrations in the cell media or by varying the copolymer composition. The AMPS® rich polymer (BA:AMPS® 25:75) displayed

higher antiproliferative effects than the BA rich polymer (BA:AMPS® 75:25), due to a lower affinity of binding to aFGF. PAMPS-*co*-PBA copolymers have demonstrated some potential to be used as antitumoral polymer drugs in the presence of aFGF.[296,297]

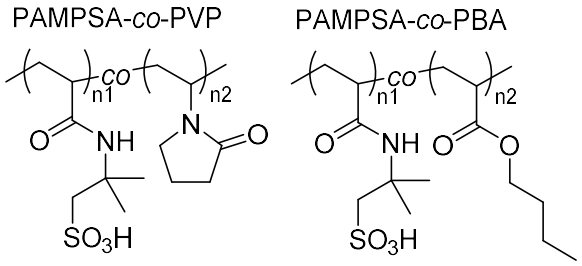

Figure 5-2: Polymers used by Garcia-Fernandez *et al.* to investigate the bioactivity of polymers containing AMPS®.[296]

The use of controlled radical polymerisation, such as RAFT polymerisation, allows control over molecular weight, unlike natural heparin, but also modification of the microstructure using different non-sulfonated monomers.[256,296-300] More recently, Maynard *et al.* studied a range of synthetic sulfonated polymers for use as heparin-mimicking polymers to stabilise bFGF, inducing cell proliferation of IL-3 dependant murine pro B cell line (BaF3-FR1c), which had been modified to over-express FGFR, whilst lacking extracellular heparan sulfates.[298-301] In 2013, they first studied the stabilisation of bFGF against various environmental stressors (thermal, pH and enzymatic) by covalently attaching a polystyrene sulfonate copolymer onto the bFGF protein, by post-polymerisation modifications via disulfide bond formation.[301] The copolymer was synthesised by RAFT polymerisation and was composed of styrene sulfonate and poly(ethylene glycol) methacrylate monomers (P(SS-*co*-PEGMA)). Their polymer bFGF complexes induced similar proliferative activity to heparin-bFGF mixtures at equivalent concentrations. Additionally, they have shown that by conjugating the polymer onto the bFGF protein increased the stabilisation when stressors were applied.[301] In a second study, they investigated the effect of polymer length and microstructure on bFGF dimerization and activation, and the effect of sulfonation percentage on bFGF protein stabilisation.[299] They found that a degree of sulfonation of 81 % was most effective, while the binding of bFGF proteins onto FGFR appeared to be independent of polymer size.

In 2015, the same group investigated the influence of the polymer structure and studied five different homopolymers carrying a sulfonated pendant group (**Figure 5-3**).[298] They found that PVS(Na) and PAHPS(Na) (poly(sodium 1-allyloxy-2 hydroxypropyl sulfonate)) stimulate BaF3-FR1c cell proliferation similarly to heparin by binding to two bFGF proteins and then easing the receptor dimerization. They also compared polymers synthesised using different approaches (i.e. free radical polymerisation versus RAFT polymerisation). RAFT polymerisation was used to explore the size dependence of poly(vinyl sulfonate) (PVS(Na)) to the activation of bFGF towards FGFR binding. When the degree of polymerisation was varied to target molecular weights from 6.6 to 80.3 kDa, the cell proliferation was independent of the size of the polymers (i.e. polymer length). They also showed that PAMPS(Na) acted like an inhibitor (antiproliferative) at high concentrations (100 µg/mL) while showing little to no activity at lower concentrations.[298]

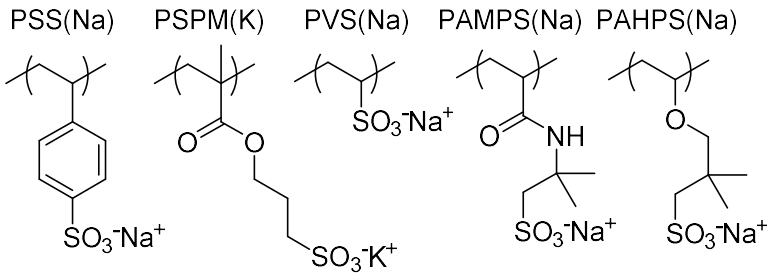

Figure 5-3: Polymers used by Maynard *et al.* in their study of proliferative activity of sulfonated-polymers.[298]

5.2.4 Project Approach

In this chapter, the use of AMPS®2405 homopolymers and copolymers as replacement for heparin for bFGF stabilisation was explored. The synthesis and characterisation of these polymers are reported in **CHAPTER 2**, **CHAPTER 3** and **CHAPTER 4**.[212] The potential activation of bFGF was evaluated by quantifying the proliferation of BaF3-FR1c.[269] The more proliferation exhibited by the synthesised polymers, the higher the attributed heparin-mimicking properties of the polymer. It has been previously shown that PAMPS does not act as an activator of FGF, instead behaving more like an inhibitor of BaF3-FR1c proliferation (antiproliferative) at higher concentrations (up to 100 µg/mL). However, this example used a 403 kDa polymer (i.e. DP ~ 1,800) which was synthesised by free radical polymerisation. Here, RAFT polymerisation was used to investigate the structure-activity relationship of PAMPS.

- The effect of molecular weight was first investigated using AMPS®2405 homopolymers with DPs ranging from 10 (M_n = 2,500 g/mol) to 400 (M_n = 91,000 g/mol) in order to cover the range of molecular weights of heparin (5,000 to 40,000 g/mol).

- While it has been shown that the interaction of heparin with FGF is mainly through electrostatic interactions, hydrogen bonding is thought to support the process. Bearing in mind that heparin has two main functional groups alongside its sulfonated group (**Figure 5-1**), a homopolymer bearing a hydroxyl group only (PHEAm) was also synthesised and was used as a hydrogen-bonding only control.

- The effect of microstructure was also investigated by introducing a comonomer with an OH functionality along the polymer backbone. A library of PAMPS-*co*-PHEAm was synthesised to study as activators of bFGF, and explore the effect of monomer distribution for different ratios of AMPS®2405 to HEAm, whilst always targeting an overall DP of 80 (**Scheme 5-1**, **Table S 5-1, Table S 5-2, Figure S 5-1** and **Figure S 5-2**).

- Finally, star polymers were tested as an alternative to heparin mimicking polymers, which provide a different conformation compared to linear polymers.

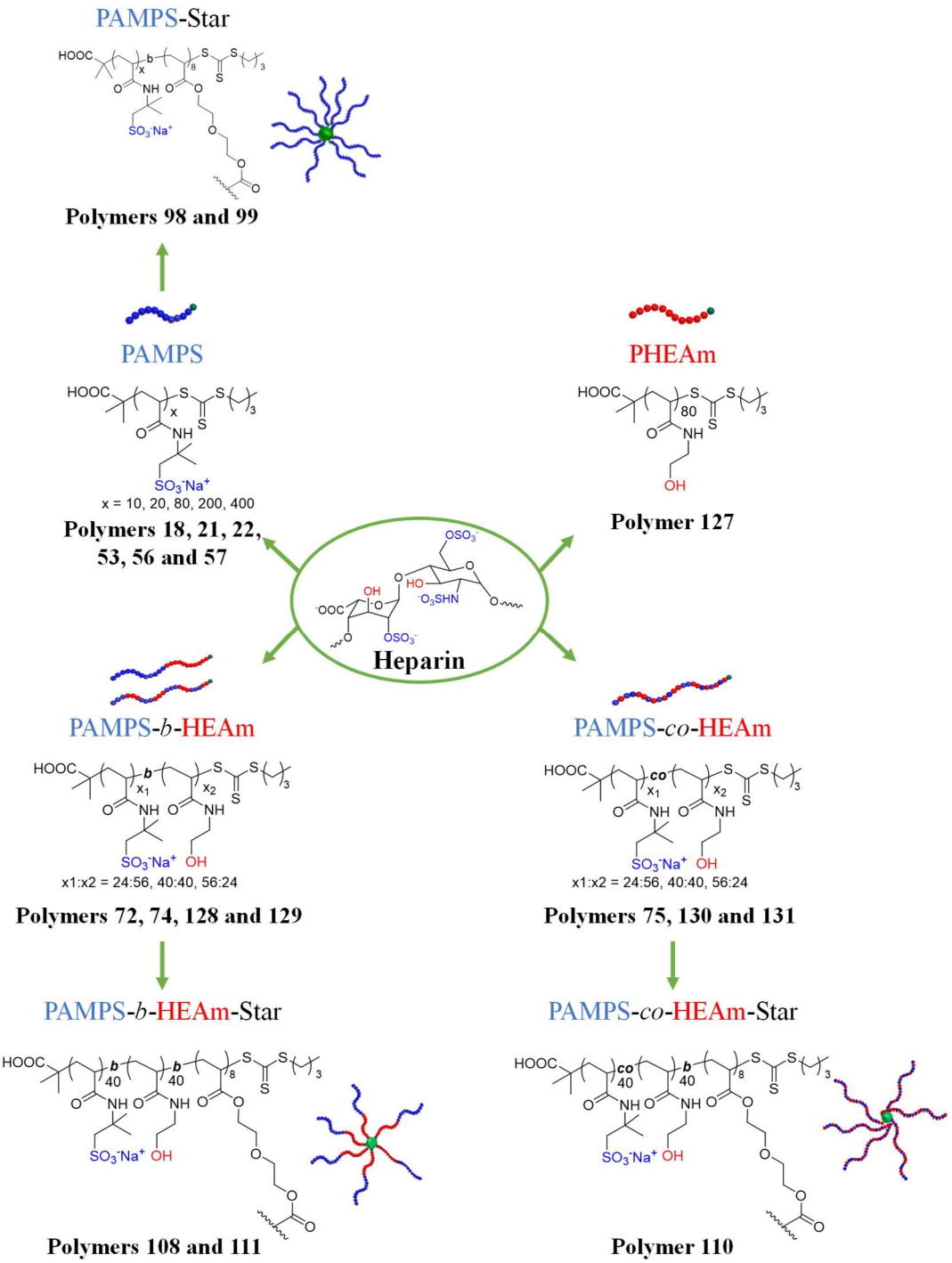

Scheme 5-1: Polymers used in this chapter as heparin mimicking polymers (**Table 5-1**).

5.3 Results and Discussions

5.3.1 Toxicity of Polymers

Firstly, the cytotoxicity of all polymers were evaluated against murine embryonic fibroblast cells (NIH-3T3) as a model of healthy fibroblast cells. Various concentrations of each polymer were incubated with NIH-3T3 cells in the absence of bFGF for 48 hours. A typical protocol for the XTT assay was then performed to determine their cell viability.[238] Results show that none of the polymers induce cytotoxicity at concentrations up to 1 mg/mL (**Figure 5-4**).

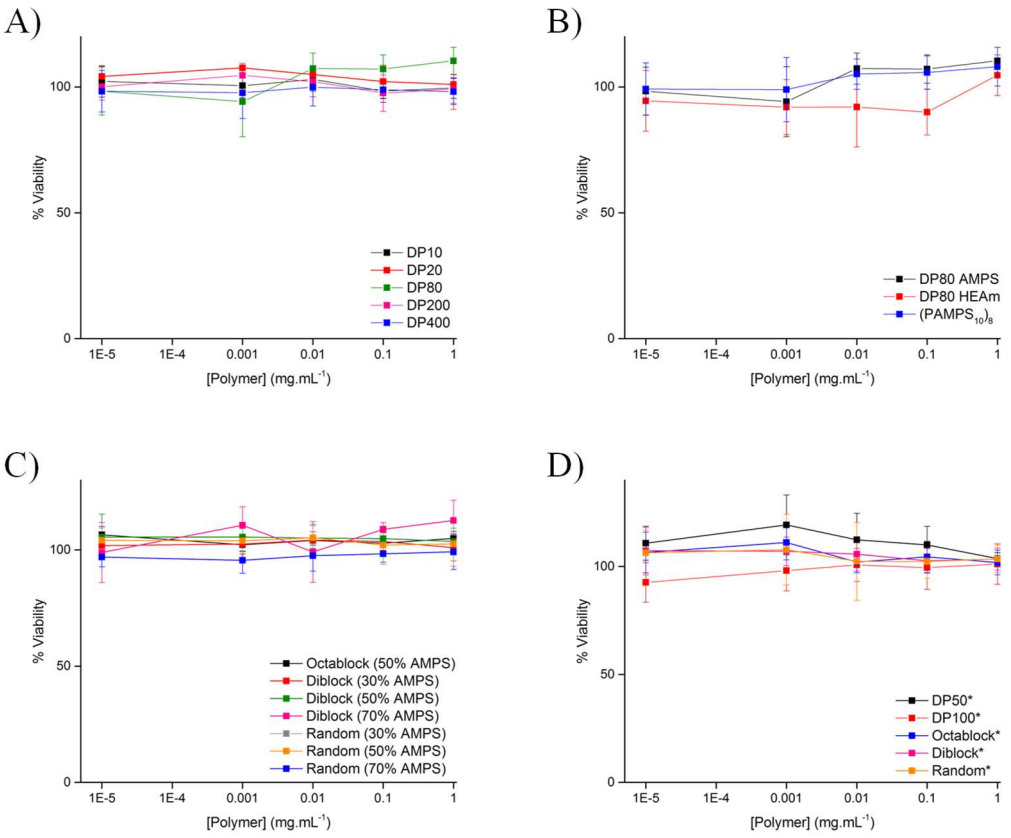

Figure 5-4: Cytotoxicity studies on NIH-3T3 cells incubated for 48 hours in the presence of varying concentrations of polymers.

A) PAMPS with various DPs; B) PAMPS and PHEAm; C) copolymers with varying percentages of charges; D) star-shaped (co-)polymers. Cell viability was determined using typical protocol for XTT assay. Each data point represents the means of triplicates from two independent experiments (N = 6). The error bars represent the standard deviation of the mean.

Table 5-1: Heparin mimicking polymers studied in this chapter and their associated haemolysis results.

Polymer	Structure	10 µg/mL [a]	100 µg/mL [a]	200 µg/mL [a]
Heparin	Heparin	-0.5 ± 0.1	0.0 ± 0.4	0.1 ± 0.1
53	$PAMPS_{10}$	0.1 ± 0.6	0.7 ± 0.7	1.7 ± 0.8
18	$PAMPS_{20}$	0.9 ± 0.7	-0.3 ± 0.3	0.3 ± 0.3
57	$PAMPS_{80}$	0.3 ± 0.6	0.0 ± 0.6	0.7 ± 1.1
21	$PAMPS_{200}$	-0.2 ± 0.5	-0.3 ± 0.3	-0.3 ± 0.3
22	$PAMPS_{400}$	0.0 ± 0.3	-0.2 ± 0.9	0.0 ± 0.8
127	$PHEAm_{80}$	1.1 ± 0.4	-0.3 ± 0.6	1.8 ± 0.5
56	$(PAMPS_{10})_8$	0.1 ± 0.6	0.5 ± 0.3	0.7 ± 0.6
72	$(PAMPS_{10}$-*b*-$PHEAm_{10})_4$	1.1 ± 0.2	0.6 ± 0.4	0.4 ± 1.0
128	$PAMPS_{24}$-*b*-$PHEAm_{56}$	0.6 ± 0.5	0.5 ± 0.4	1.2 ± 0.3
74	$PAMPS_{40}$-*b*-$PHEAm_{40}$	0.5 ± 0.2	0.8 ± 0.1	1.3 ± 0.4
129	$PAMPS_{56}$-*b*-$PHEAm_{24}$	0.5 ± 0.5	0.8 ± 0.7	1.4 ± 0.3
130	$PAMPS_{24}$-*co*-$PHEAm_{56}$	1.1 ± 0.7	1.6 ± 0.1	2.1 ± 0.2
75	$PAMPS_{40}$-*co*-$PHEAm_{40}$	0.8 ± 0.5	0.8 ± 0.2	1.1 ± 0.9
131	$PAMPS_{56}$-*co*-$PHEAm_{24}$	0.5 ± 0.4	0.8 ± 0.2	1.9 ± 0.7
98	$PAMPS_{50}$-star	-0.1 ± 0.4	0.5 ± 0.5	0.6 ± 0.6
99	$PAMPS_{100}$-star	-0.1 ± 0.2	0.0 ± 0.3	-0.2 ± 0.7
111	$(PAMPS_{10}$-*b*-$PHEAm_{10})_4$-star	1.4 ± 0.6	1.7 ± 0.5	2.0 ± 0.6
108	$PAMPS_{40}$-*b*-$PHEAm_{40}$-star	1.4 ± 0.2	2.1 ± 0.3	1.7 ± 0.9
110	$PAMPS_{40}$-*co*-$PHEAm_{40}$-star	1.6 ± 0.3	1.6 ± 1.2	0.2 ± 0.1

[a] Haemolysis of heparin mimicking polymers against defibrinated sheep blood red cells at 37 °C for 2 hours, triton X was used as positive control (100 %) while PBS was used as negative control.

As one of the main biological applications of bFGF is wound healing formulation, the cytotoxicity of such polymers against red blood cells was also investigated. The polymers were incubated with red blood cells from defibrinated sheep red blood cells for 2 hours at 37 °C at three different concentrations (10, 100 and 200 µg/mL). The results, summarised in **Table 5-1**, show that none of the polymers display haemolytic activity (< 2.5 %) when taking triton-X as positive control (100 % haemolysis) and PBS as a negative control (haemolysis 6.5 %).

5.3.2 Proliferation Study

Next, the propensity of PAMPS synthetic polymers to promote proliferation of BaF3-FR1c cells in the presence of bFGF was evaluated and compared to that of heparin. This particular cell line was kindly provided by Professor Jerry Turnbull (Liverpool University, UK). This cell line was engineered to over express the FGFR1 receptor, which is the receptor of FGFs, but also with the lack of heparan sulfate proteoglycan usually present on the proximity of cell surfaces. The absence of HS proteoglycans is needed in order to avoid any competition with our synthetic sulfonated polymers. Consequently, the extended proliferation of such cells is expected to be due to the presence of the synthetic polymers only, rather than any other sulfated molecules which reside in the extracellular matrix. In order to evaluate the ability of the synthetic polymers to help the proliferation of BaF3-FR1c cells, cells were incubated with bFGF (5 ng/mL), with or without heparin or the synthetic polymers, at increasing concentration from 0.1 to 1 and finally 100 µg/mL. Cell proliferation was then quantified using a proliferation assay (CellTiter-Blue®). The results were normalised to the proliferation of cells incubated with medium only (100 %). Despite none of the polymers exhibiting significantly higher cell proliferation rates than heparin at equivalent concentrations, differences in activities were observed between the various analysed polymers (**Figure 5-5**).

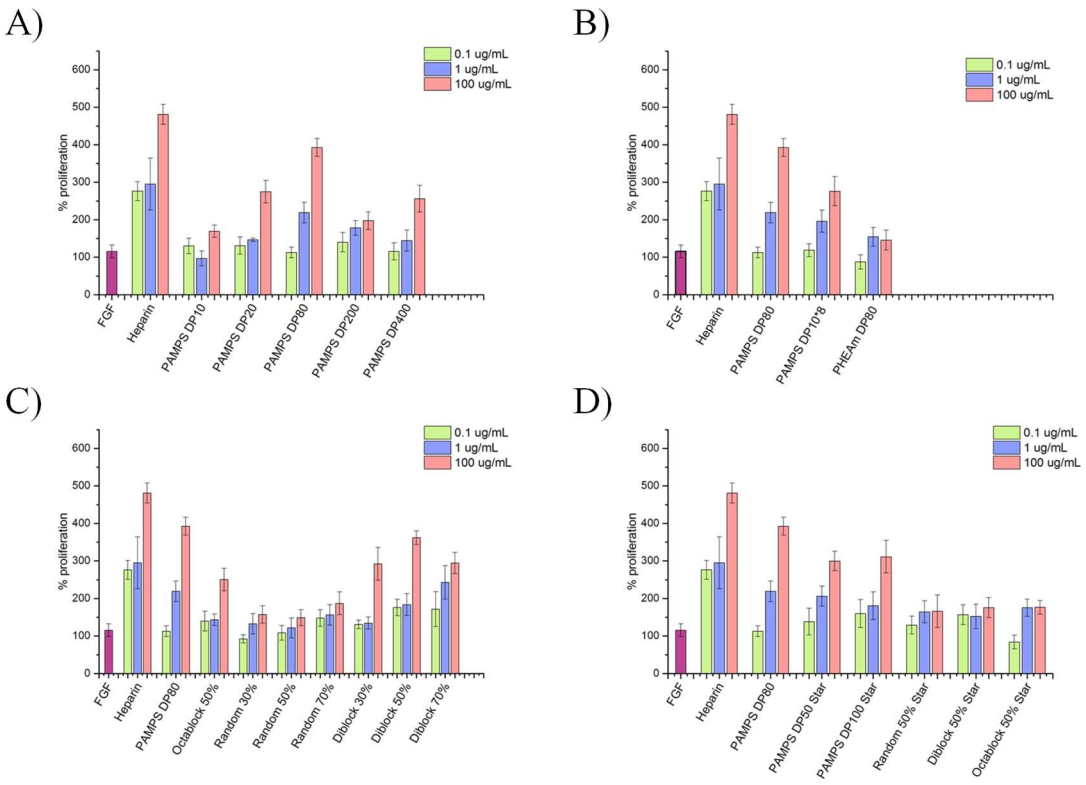

Figure 5-5: Proliferation of BaF3-FR1c cells incubated for 48 hours at 37 °C in the presence of 5 ng/mL of bFGF and various concentrations of polymers.

A) PAMPS homopolymers with increasing DPs from 10 to 400; B) PAMPS and PHEAm homopolymers targeting an overall DP of 80; C) Octablock, diblock and random copolymers of AMPS and HEAm targeting an overall DP of 80 with varying the percentage of charges from 30 to 50 and 70 %; D) Different star-shaped (co-)polymers architecture (homopolymer with DP_{arm} = 50 and 100; random, diblock and octablock copolymers of AMPS and HEAm with DP_{arm} = 80 and 50 % of charge). Cell growth was determined using a typical protocol for the CellTiter-Blue® assay. Data were normalised to the blank medium containing cells and was set at 100 %. Each data point represents four replicates of four independent experiment (N = 16). The error bars represent the standard deviation from the mean.

Effect of Molecular Weight

The effect of molecular weight was first studied by increasing the degree of polymerisation of AMPS®2405 homopolymers from 10 to 400. **Figure 5-5 – A** shows that there is no significant cell proliferation when incubated with bFGF alone (115 ± 17 %). The proliferation increases from 170 ± 16 % to 275 ± 30 % and finally reached the highest proliferation to 392 ± 24 % upon co-incubating with PAMPS, with increasing DPs of 10, 20 and 80, respectively. The maximum proliferation value reached for $PAMPS_{80}$ (**Polymer 57**) remains slightly lower than the proliferation obtained for heparin at 100 µg/mL (481 ± 27 %). The optimum results obtained with PAMPS having a DP of 80 matches heparin nature's optimum length (i.e. overall negative charge of 75 units).[261] When the degree of polymerisation was further increased to 200 and finally 400, the proliferation extent slightly decreased to 197 ± 24 % and 256 ± 35 % respectively. Finally, **Figure 5-6** – **A** shows an overlay of the experimental average molecular weight and intrinsic viscosity obtained using triple detection SEC of heparin and the various AMPS®2405 homopolymers synthesised, while **Figure 5-6 – B** shows the overlaid molecular weight distributions of heparin and $PAMPS_{80}$. From **Figure 5-6** – **A** and **B** it can be observed that heparin has a slightly higher intrinsic viscosity than $PAMPS_{80}$ but has a similar experimental molecular weight (~ 15,000 g/mol). Both are denoted by the green circle in **Figure 5-6** – **A**. These results may explain why both heparin and $PAMPS_{80}$ show similar proliferation effect, suggesting that the size is a critical parameter affecting cell proliferation by binding to FGF. This observation was attributed to differences in the propensity of polymers with different lengths to induce dimerization of the growth factor.[269,302] Chains smaller than the optimal length are less likely to bind to both the FGF and FGFR and, further, they are less likely to bind to two FGF to provoke their dimerization due to steric hindrance. In contrast, while longer polymeric chains can bind to multiple copies of bFGF, they do not constrain the proteins into spatial proximity which then does not allow simultaneously the dimerization of bFGF and its binding to FGFR. Finally, the optimum results being obtained with PAMPS having a DP of 80 matches heparin nature's optimum length.

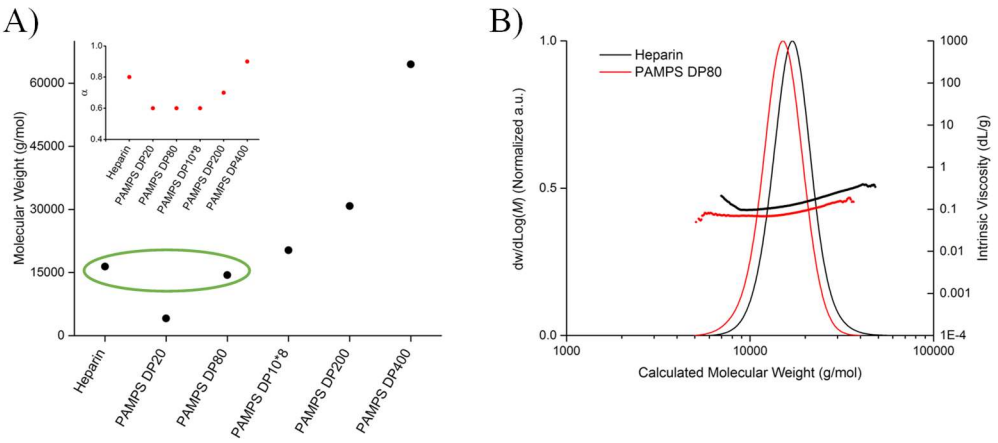

Figure 5-6: A) Molecular weight and alpha-value (insert graph) of selected linear PAMPS and heparin as determined using size-exclusion chromatography with triple detection. B) Molecular weight distributions *versus* chain fraction (left axis) and intrinsic viscosity (right axis) of heparin sample used in this study and $PAMPS_{80}$ using size-exclusion chromatography with triple detection.

The influence of the polymerisation route (homopolymer DP 80 versus Homopolymer 8 times DP10) on cell proliferation was then investigated. The polymer showing the best increase in cell proliferation, $PAMPS_{80}$ (**Polymer 57**) was compared to a newly synthesised octablock homopolymer of AMPS®2405 targeting a DP 10 for each block $[PAMPS_{10}]_8$ (**Polymer 56**). The same theoretical DP of 80 was targeted but the experimental molecular weight of the octablock homopolymer was determined to be higher (**Figure 5-6** – **A,** PAMPS DP10*8), $M_{n,SEC}$ = 19,000 g/mol compared to $M_{n,SEC}$ = 15,000 g/mol for the $PAMPS_{80}$, however both displayed dispersities of around 1.2. A lower proliferation was observed when the $[PAMPS_{10}]_8$ (276 ± 39 %) was used as the additive in the cell medium compared to the $PAMPS_{80}$ (392 ± 24 %) (**Figure 5-5** – **B**). This is in agreement with the above-mentioned conclusion regarding the impact of higher molecular weight on FGF-based cell proliferation.

Taken together, these results determined that the chain length is a critical parameter to reach a similar cell proliferation to heparin. This is in contrast to the results of Maynard *et al.* who argue that the molecular weight did not affect the extend of the cell proliferation in the case of P(SS-*co*-PEGMA), which is likely due to the PEGMA macromonomer having a high molecular weight and higher steric hindrance.[299]

Effect of Monomer Distribution

The effect of introducing hydroxyl groups, another functionality present on heparin molecules which allow further interaction by hydrogen bonding with the heparin binding domain of FGFs, into our synthetic sulfonated polymers was investigated next. PHEAm homopolymer targeting a final DP of 80 in order to keep the number of active groups constant (**Polymer 127**), when compared to $PAMPS_{80}$, was synthesised. It is important to note that the theoretical molecular weight of such polymer is 9,500 g/mol compared to 18,600 g/mol for the $PAMPS_{80}$. No increase, nor inhibition of BaF3-FR1c cells proliferation was observed compared to using $PAMPS_{80}$ (**Figure 5-5 – B**). While a small increase in BaF3-FR1c proliferation was observed when incubating bFGF with 10 or 100 µg/mL of $PHEAm_{80}$ (145 ± 27 % compared to 115 ± 17 % when no polymer was added), the increase can be considered as negligible when compared with the proliferation increase observed in the presence of heparin or PAMPS at similar concentrations. This result is in accordance with the accepted mechanism of interaction between heparin and bFGF, which rely mostly on electrostatic interactions between the sulfated groups from heparin and the positively charged amino acid residue from the FGF protein (i.e. arginine and lysine).[268]

Copolymers of AMPS®2405 and HEAm were then studied by synthesising a library of copolymers (octablock, diblock and random copolymers) with an overall DP target of 80, but with varying percentage of AMPS®2405 to HEAm, from 30 to 50 and finally 70 %. SEC molecular weight distribution for each polymer suggests that differences in the solution conformation exists between each copolymer (**Figure 5-7**). These differences are expected to affect affinity to bFGF, which would in turn affect the mechanism of dimerization and therefore change the potential proliferation of BaF3-FR1c cells.

The influence of copolymer segmentation on bFGF-based proliferation of BaF3-FR1c cells is discussed first for octablock **(Polymer 72**), diblock (**Polymer 74**) and random (**Polymer 75**) copolymers with 50 % of AMPS®2405 and HEAm (**Figure 5-5 – C**). At 100 µg/mL, an increase in cell proliferation with segmentation from random (149 ± 21 %) to octablock (250 ± 30 %) and finally diblock (362 ± 18 %) copolymers were observed. The overall proliferation is still lower than heparin (481 ± 27 %) but similar

to $PAMPS_{80}$ (392 ± 24 %) for the diblock copolymers, with only half the number of sulfonate groups. Condensing the density of anionic charge in a particular section of the polymer for the diblock compared to the octablock or random copolymers increases the diblock copolymer affinity for the positively charged FGF and FGF, thus accounting for the observed increase in proliferation , as previously suggested by Garcia-Fernandez *et al*.[296]

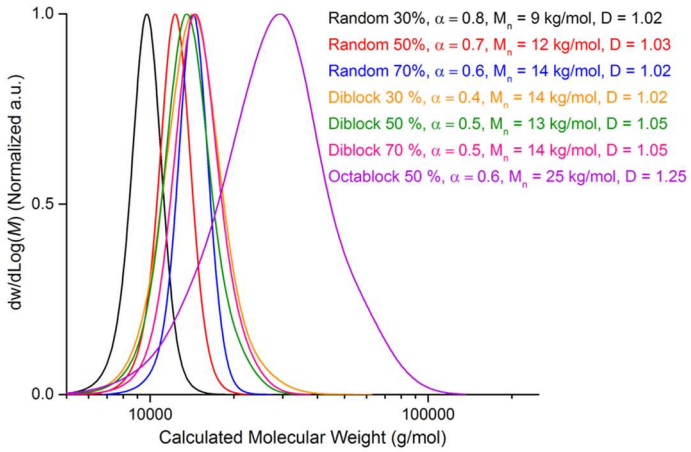

Figure 5-7: SEC molecular weight distributions of AMPS®2405 and HEAm copolymers (random, diblock and octablock) (targeted DP = 80) with different ratio of AMPS®2405 to HEAm.

Data obtained using triple detections (RI, VS, MALS) in 20 % methanol and 80 % 0.1 M $NaNO_3$ in milli-Q water. Percentages listed represent the percentage of AMPS®2405 (i.e. random 30 % = 30 % of AMPS®2405 and 70 % of HEAm).

When the percentage of AMPS®2405 compared to HEAm was increased from 30 to up to 70 % in the random copolymers, the cell proliferation did not appear to improve and was reduced to 200 %. In order to understand why, the apparent reactivity ratio of AMPS®2405 and HEAm was determined. Proton NMR was first used, however, the relevant peaks of each monomer and polymer were overlapping (**Figure S 5-3**).[303,304] Therefore, HPLC was used to determine the apparent reactivity ratio. Each monomer was able to be separated and the peak associated to it quantified (area under the curve) (**Figure 5-8 – B**) where a calibration curve was created from AMPS®2405 monomer at different concentrations (**Figure 5-8 – A**).[305] The consumption of AMPS®2405 and HEAm during the synthesis of a random copolymer $PAMPS_{40}$-*co*-$PEAHm_{40}$ was monitored by HPLC by withdrawing a sample every 5 minutes (**Figure 5-8 – C**). It should be noted that, there is a linear decrease of each monomer peak intensity, which

is depicted by a similar slope of the linear regression $4.2x10^4$ for AMPS®2405 and $3.1x10^4$ for HEAm, suggesting that the copolymer is mostly composed of alternating AMPS®2405 and HEAm monomers. Hence, the lower cell proliferation observed for non-segregated copolymers can be explained by a decrease of the affinity of polymers with bFGF, further supporting that hydrogen bonding does not play an important role in the interaction process.[306,307]

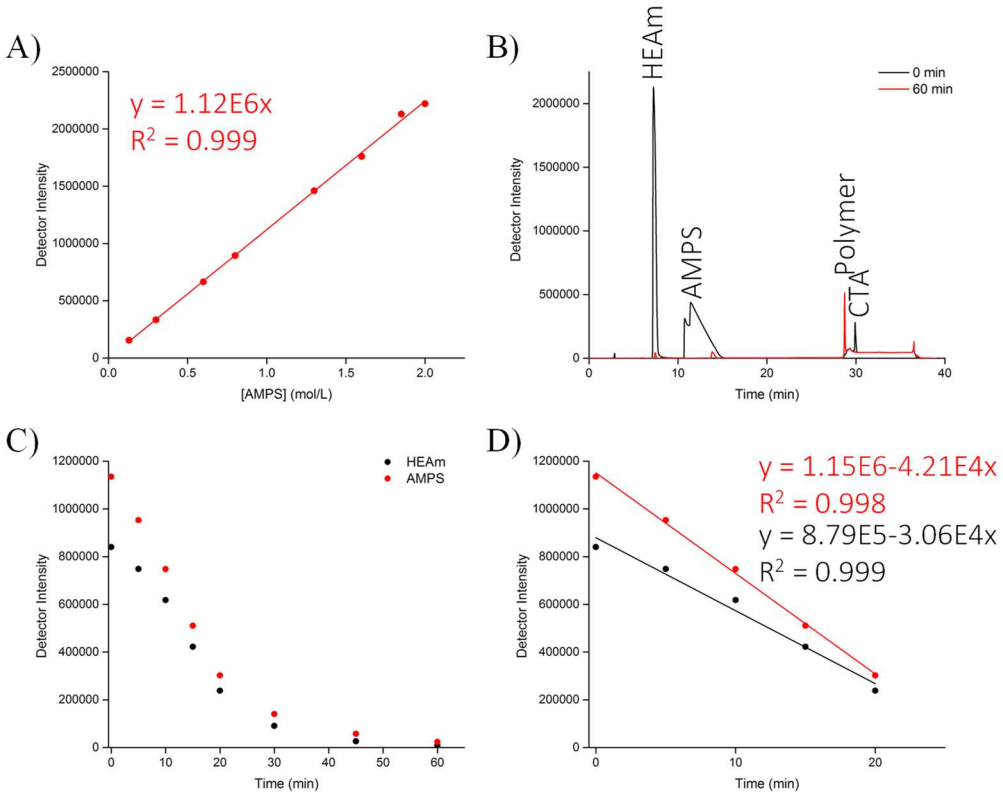

Figure 5-8: Study of the different reactivity ratios during $PAMPS_{40}$-*co*-$PHEAm_{40}$ synthesis.

A) Calibration curve for AMPS®2405 monomer using HPLC (λ = 260 nm); B) HPLC chromatograms of reaction media at t = 0 min (black line) and t = 60 min (red line); C) Consumption of AMPS®2405 (red line) and HEAm (black line) over time as determined using HPLC (λ = 260 nm); D) Zoom of the consumption curve over the linear region between 0 to 20 minutes. Solvent: water:MeOH. Gradient: 1 to 15 % MeOH in 25 minutes at 37 °C. Column: C18 (4.6 mm x 250 mm).

Effect of Polymer Architectures

Finally, the influence of the polymer architectures on bFGF stabilisation was studied by breaking away from the linear structure of the heparin-mimicking polymers studied above, and testing more complex structures instead, namely star polymer (**Figure 5-5 – D**). Star architectures are expected to induce differences in conformation and differences in availability of the charges linked to the low mobility of the arms linked into the core.

Star homopolymers were showing only a slight improvement of cell proliferation compared to bFGF alone, where the proliferation was observed to be about 300 ± 26 % for $PAMPS_{50}$ star polymer and 311 ± 43 % for $PAMPS_{100}$ star polymer compared to 392 ± 24 % for $PAMPS_{80}$. Direct comparison between star and linear polymers is not possible due to the dramatic difference in molecular weight. However, the low proliferation observed is likely due to the difference of overall molecular weights between star polymers and heparin but also to the fact that the arms have a lower mobility than a linear homopolymer. Consequently, bFGF can only bind onto the surface of the polymer which is likely to pose problem for the bFGF dimerization. Overall, unlike their linear counterparts, none of the star copolymers (random *versus* diblock *versus* octablock star copolymers) showed improvement compared to heparin (**Figure 5-5– D**). Again the lack of extend proliferation can be explained by the low mobility of the arm of the star polymers which can affect not only the binding but also the dimerization of bFGF. Moreover, the surface is not only covered of AMPS but also of HEAm which was shown to not affect the BaF3-FR1c cell proliferation in the presence of bFGF.

5.3.3 Effect of Temperature

Finally, the stability of bFGF in solution was studied in the presence or absence of either heparin or heparin mimicking polymers, at both room temperature (~ 20 °C) and 37 °C for 12 hours (**Figure 5-9**). FGFs are known to be subject to degradation when environmental stressors are applied.[301,308] Heparin is then known to act as its natural stabiliser.[309] Here, the potential use of selected heparin-mimicking polymers were used instead as a stabiliser for bFGF for enhanced storage capacity. Different temperature stressors were applied to a solution containing bFGF at 5 ng/mL, with or without polymer or heparin at either 50 or 100 µg/mL in media. Solutions were prepared at double the desired final concentration and stored at two different temperatures over 12 hours either at room temperature (~ 20 °C) or at 37 °C. This is expected to mimic conditions faced by bFGF during transport and storage. The solutions were then diluted and added to BaF3-FR1c cells. Following 48 hours incubation at 37 °C, 5 % CO_2, the extended proliferation was measured using a CellTiter-Blue® assay.

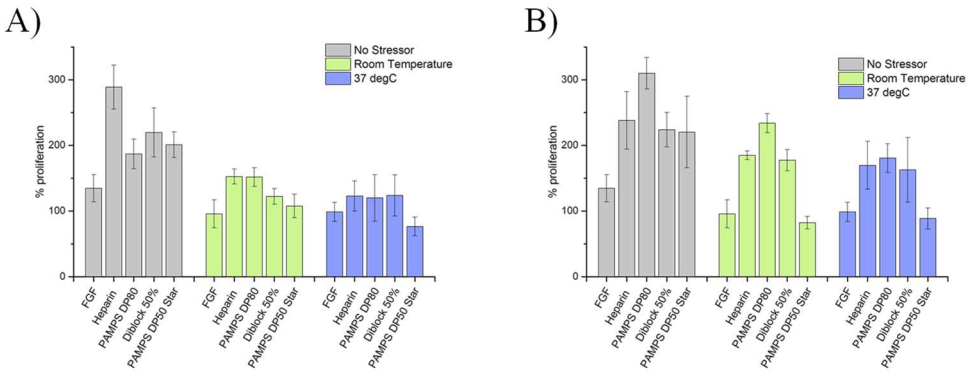

Figure 5-9: Proliferation of BaF3-FR1c cells incubated for 48 hours at 37 °C in the presence of FGF (5 ng/mL). FGF was pre-incubated at the indicated temperatures for 12 hours in the presence of polymers.

A) Polymers at 50 µg/mL; B) Polymers at 100 µg/mL. Cell growth was determined using typical protocol for CellTiter-Blue® assay. Data were normalised to the blank medium containing cells and was set at 100 %. Each data point represents four replicates of two independent experiment (N = 8). The error bar represents the standard deviation from the mean.

When bFGF alone was stored at either room temperature or 37 °C, a slight decrease in its cell proliferation activity was observed, from 135 ± 21 % (no stressors) to 99 ± 14 % (37 °C for 12 hours) (**Figure 5-9** – **A** and **B**). As expected, better proliferation of the cells was obtained using bFGF that was stored in the presence of a higher concentration of polymer/heparin. When FGF was pre-mixed with heparin (50 µg/mL) and stored for 12 hours at increasing temperatures (up to 37 °C), a decrease in bioactivity was observed from 289 ± 34 % to 153 ± 11 % and finally 123 ± 23 %. A similar trend was observed at 100 µg/mL. For example, when $PAMPS_{80}$ was stored with bFGF (5 ng/mL) at 37 °C over 12 hours, an extended cell proliferation of 120 ± 36 % was measured at 50 µg/mL compared to181 ± 22 % at 100 µg/mL. When the diblock copolymer was stored either at room temperature or at 37 °C, an increase in the proliferation was observed by 150 – 200 % at both polymer concentrations. Overall, $PAMPS_{80}$ gave the best results with only a slight decrease of proliferation during storage, which is dependent on temperature. The diblock provided the second best result, with a decrease of activity during storage, which was not shown to be temperature dependent. Finally no improvement of stability was observed with the star polymers during storage at any temperatures.

5.4 Conclusions

In this chapter it has been shown that PAMPS can be used as a heparin-mimicking polymer. Overall, the best proliferation results were generally obtained at 100 µg/mL while heparin has shown improvement to cell proliferation with concentrations as low as 0.1 µg/mL. While in the past PAMPS has been shown to have an antiproliferative effect towards BaF3-FR1c cells, a proliferation effect was observed as high as heparin itself. The influence of a variety of physical parameters were investigated, such as molecular weight, number of charges, charge distribution and charge density (**Figure 5-10**).

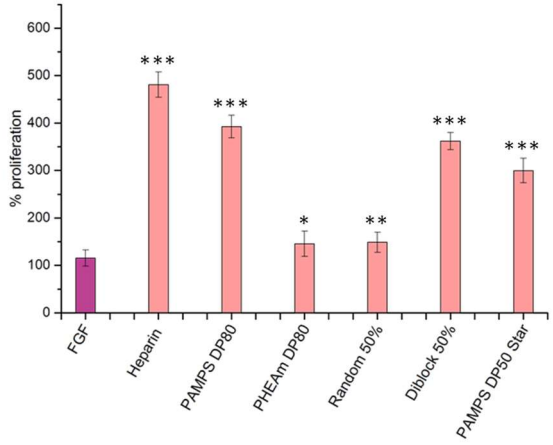

Figure 5-10: Proliferation of BaF3-FR1c cells in the presence of selected compounds. Cells were incubated for 48 hours at 37 °C in the presence of 5 ng/mL of bFGF and 100 µg/mL of selected polymers.

Data were normalised to the blank medium containing cells and was set at 100 %. Each data point represents four replicates of four independent experiment (n = 16). The error bar represents the standard deviation. Statistical analysis was performed using Student's t test to compare samples to the control group incubated with "FGF" only, with * $p < 0.05$, ** $p < 0.01$, *** $p < 0.001$.

It has been demonstrated that AMPS®2405 homopolymers could be used as a replacement for heparin, but only, at higher concentration, and that the polymer length but also the charge density were critical parameters to obtain the highest cell proliferations. PHEAm demonstrated that interaction between bFGF and heparin is mainly through electrostatic interaction as no improvement of the proliferation was observed when used. When using copolymers of AMPS®2405 and HEAm, the charge distribution was shown to have a significant influence, with the highest charge density showing the best proliferation of BaF3-FR1c cells (i.e. diblock > octablock > random

copolymer). Finally, when branched polymers were used there was no improvement of the proliferation. These observations would be attributed to a limitation of the arm mobility which could affect both the binding of two copies of bFGF and consequently the dimerization. Finally, when thermal stressors were applied to the protein, $PAMPS_{80}$ was shown to be the best synthetic candidate to replace heparin.

5.5 Experimental

Polymer Synthesis

For the synthesis of the materials used, see experimental sections from the following chapters: **CHAPTER 2** and **CHAPTER 3**. All polymers were dialysed with water for 48 hours, changing the water three times. Float-A-Lyzer® with a molecular weight cut off range between 0.5-1 kDa from Spectrum were used to remove any undesirable reactants such as monomers and initiator leftover.

Table S 5-1: Conditions used for the preparation of PAMPS-*b*-PHEAm diblock copolymers targeting an overall DP of 80 with different ratio of AMPS® to HEAm (30, 50 and 70 %).[a]

Compound	**128**		**74**		**129**	
Structure	$PAMPS_{24}$-*b*-$PHEAm_{56}$		$PAMPS_{40}$-*b*-$PHEAm_{40}$		$PAMPS_{56}$-*b*-$PHEAm_{24}$	
	Block 1	Block 2	Block 1	Block 2	Block 1	Block 2
$m_{AMPS®2405}$ (mg)	500	-	500		500	-
m_{HEAm} (mg)	-	340	-	146	-	62
m_{BDMAT} (mg)	13	-	8	-	6	-
m_{NaOH} (mg)	1	-	0.6	-	0.45	-
m_{VA-086} (mg)	0.6	0.3	0.6	0.2	0.6	0.2
m_{H2O} (mg)	427	-	427	-	427	-
Conv (%)[b]	> 99		> 99		> 99	
$M_{n,th}$ (g/mol)[c]	12,200		14,000		15,800	
$M_{n,SEC}$ (g/mol)[d]	9,200		10,000		12,100	
$Đ$[d]	1.18		1.21		1.23	

[a] Polymerisations were conducted at 90 °C in phosphate buffer solution during 120 minutes for each block ($[CTA]_0$:$[I]_0$ = 1:0.13, $[AMPS®2405]_0$ = 1.5 M) with VA-086 as the initiator; [b] Conversions were determined by ^{1}H NMR spectroscopy, using **Equation 1**; [c] Theoretical M_n values were calculated using **Equation 2**; [d] Experimental M_n and $Đ$ values were determined by size-exclusion chromatography using 20:80 MeOH / 0.1M $NaNO_3$ in milli-Q water as eluent, using a conventional calibration obtained with PEG/PEO standards.

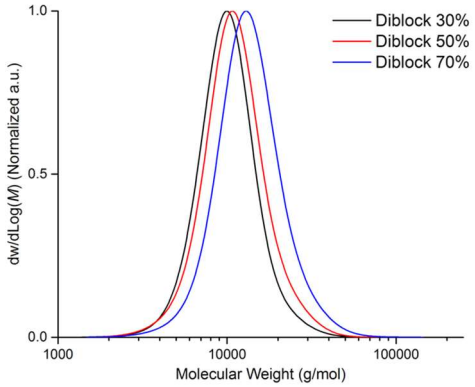

Figure S 5-1: Molecular weight distributions (Aqueous SEC) of diblock copolymers AMPS®2405 / HEAm increasing the percentage of AMPS®2405 from 30 to 50 and then 70 % while targeting an overall DP of 80.

Table S 5-2: Conditions used for the preparation of PAMPS-*co*-PHEAm random copolymers targeting an overall DP of 80 but different ratio of AMPS®2405 to HEAm (30, 50 and 70 %).[a]

Compound	**130**	**75**	**131**
Structure	$PAMPS_{24}$-*co*-$PHEAm_{56}$	$PAMPS_{40}$-*co*-$PHEAm_{40}$	$PAMPS_{56}$-*co*-$PHEAm_{24}$
$m_{AMPS®2405}$ (mg)	533	890	1250
m_{HEAm} (mg)	363	260	155
m_{BDMAT} (mg)	14	14	14
m_{NaOH} (mg)	1.1	1.1	1.1
m_{VA-086} (mg)	2.2	2.2	2.2
m_{H2O} (mg)	2230	2030	1820
Conv (%)[b]	> 99	> 99	> 99
$M_{n,th}$ (g/mol)[c]	12,200	14,000	15,800
$M_{n,SEC}$ (g/mol)[d]	10,500	12,400	14,100
$Đ$[d]	1.15	1.15	1.16

[a] Polymerisations were conducted at 90 °C in phosphate buffer solution during 60 minutes ($[CTA]_0$:$[I]_0$ = 1:0.13, $[Monomer]_0$ = 1.5 M) with VA-086 as the initiator; [b] Conversions were determined by ^{1}H NMR spectroscopy, using **Equation 1**; [c] Theoretical M_n values were calculated using **Equation 2**; [d] Experimental M_n and $Đ$ values were determined by size-exclusion chromatography using 20:80 MeOH / 0.1 M $NaNO_3$ in milli-Q water as eluent, using a conventional calibration obtained with PEG/PEO standards.

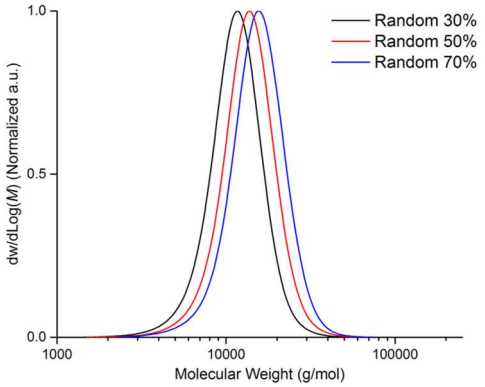

Figure S 5-2: Molecular weight distributions (Aqueous SEC) of random copolymers AMPS®2405 / HEAm increasing the percentage of AMPS®2405 from 30 to 50 and then 70 % while targeting an overall DP of 80.

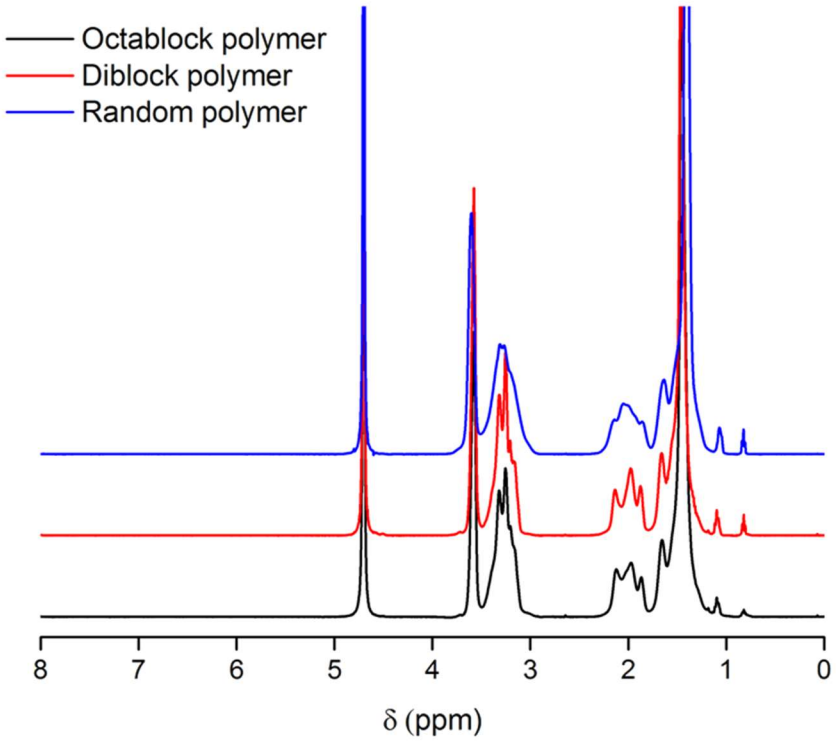

Figure S 5-3: ^{1}H NMR spectra of the diblock (red, **74**), octablock (black, **72**) and random (blue, **75**) copolymers PAMPS-*co*-PHEAm, targeting an overall DP of 80.

Student's T-Test

Table S 5-3: Results of statistical analysis performed using a student's t-test for results from **Section 5.3.2**.

Polymer	Structure	100 µg/mL[a]	1 µg/mL[a]	0.1 µg/mL[a]	100 µg/mL[b]	1 µg/mL[b]	0.1 µg/mL[b]
bFGF	bFGF	-	-	-	$1.9x10^{-9}$	0.0011	$1.7x10^{-8}$
Heparin	Heparin	$2.0x10^{-9}$	0.0011	$3.7x10^{-8}$	-	-	-
53	$PAMPS_{10}$	$1.5x10^{-5}$	0.065	0.14	$9.7x10^{-9}$	0.00064	$2.2x10^{-8}$
18	$PAMPS_{20}$	$4.2x10^{-8}$	0.0011	0.15	$1.9x10^{-8}$	0.0032	$2.4x10^{-8}$
57	$PAMPS_{80}$	$2.8x10^{-9}$	$1.2x10^{-6}$	0.72	0.00013	0.042	$4.5x10^{-8}$
21	$PAMPS_{200}$	$7.3x10^{-7}$	$1.9x10^{-6}$	0.043	$1.4x10^{-9}$	0.0082	$6.8x10^{-8}$
22	$PAMPS_{400}$	$2.2x10^{-7}$	0.010	0.99	$4.3x10^{-9}$	0.0023	$4.1x10^{-9}$
132	$PHEAm_{80}$	0.014	0.0034	0.005	$9.7x10^{-11}$	0.0031	$2.4x10^{-9}$
56	$(PAMPS_{10})_8$	$1.2x10^{-6}$	$4.0x10^{-7}$	0.67	$7.0x10^{-8}$	0.015	$4.5x10^{-8}$
72	$(PAMPS_{10}$-*b*-$PHEAm_{10})_4$	$2.7x10^{-7}$	0.0037	0.050	$5.5x10^{-9}$	0.0026	$7.9x10^{-8}$
133	$PAMPS_{24}$-*b*-$PHEAm_{56}$	$1.8x10^{-6}$	0.028	0.054	$4.4x10^{-7}$	0.0020	$3.6x10^{-7}$
74	$PAMPS_{40}$-*b*-$PHEAm_{40}$	$8.4x10^{-11}$	$4.7x10^{-5}$	$1.3x10^{-5}$	$9.6x10^{-6}$	0.0091	$6.4x10^{-7}$
134	$PAMPS_{56}$-*b*-$PHEAm_{24}$	$5.0x10^{-9}$	$1.8x10^{-7}$	0.0017	$5.5x10^{-8}$	0.13	$2.8x10^{-6}$
135	$PAMPS_{24}$-*co*-$PHEAm_{56}$	0.00073	0.15	0.0099	$4.5x10^{-10}$	0.0014	$5.8x10^{-8}$
75	$PAMPS_{40}$-*co*-$PHEAm_{40}$	0.0026	0.53	0.43	$8.7x10^{-10}$	0.0012	$9.1x10^{-9}$
136	$PAMPS_{56}$-*co*-$PHEAm_{24}$	0.00011	0.002	0.0017	$3.7x10^{-10}$	0.0033	$4.7x10^{-8}$
98	$PAMPS_{50}$-star	$5.9x10^{-6}$	$8.3x10^{-5}$	0.13	$1.5x10^{-6}$	0.024	$8.7x10^{-7}$
99	$PAMPS_{100}$-star	$3.6x10^{-5}$	0.0011	0.013	$3.0x10^{-5}$	0.0076	$6.8x10^{-6}$
111	$(PAMPS_{10}$-*b*-$PHEAm_{10})_4$-star	$7.7x10^{-5}$	0.0065	0.015	$3.0x10^{-9}$	0.0066	$4.0x10^{-8}$
108	$PAMPS_{40}$-*b*-$PHEAm_{40}$-star	0.0013	0.015	0.0028	$2.3x10^{-9}$	0.0026	$2.9x10^{-7}$
110	$PAMPS_{40}$-*co*-$PHEAm_{40}$-star	0.0022	0.0016	0.21	$6.6x10^{-12}$	0.0043	$2.2x10^{-8}$

Statistical analysis performed using a student's t test to compare samples to a control group incubated either with: FGF only (a) or bFGF with heparin (b).

Table S 5-4: Results of statistical analysis performed using a student's t-test for results from **Section 5.3.3** using cells incubated with bFGF only as reference.

Polymer	Structure	100 µg/mL[a]	50 µg/mL[a]	100 µg/mL[b]	50 µg/mL[b]	100 µg/mL[c]	50 µg/mL[c]
bFGF	bFGF	-	-	-	-	-	-
Heparin	Heparin	0.013	0.0074	$1.2x10^{-6}$	$3.4x10^{-5}$	0.0089	0.073
57	$PAMPS_{80}$	$1.2x10^{-6}$	0.0032	$4.9x10^{-9}$	$3.8x10^{-5}$	0.00028	0.27
74	$PAMPS_{40}$-*b*-$PHEAm_{40}$	$6.8x10^{-5}$	0.0041	$1.8x10^{-6}$	0.0065	0.076	0.22
98	$PAMPS_{50}$-star	0.10	0.0013	0.33	0.16	0.34	0.051

Statistical analysis performed using a student's t test to compare samples to a control group incubated with FGF only: (a) no stressors, (b) stored at room temperature for 12 hours, (c) stored at 37 °C for 12 hours.

Table S 5-5: Results of statistical analysis performed using a student's t-test for results from **Section 5.3.3** with cells incubated with bFGF pre-mixed with heparin as reference.

Polymer	Structure	100 µg/mL[a]	50 µg/mL[a]	100 µg/mL[b]	50 µg/mL[b]	100 µg/mL[c]	50 µg/mL[c]
bFGF	bFGF	0.013	0.007	$1.3x10^{-6}$	$7.3x10^{-5}$	0.0089	0.073
Heparin	Heparin	-	-	-	-	-	-
57	$PAMPS_{80}$	0.038	0.017	0.0001	0.92	0.58	0.88
74	$PAMPS_{40}$-*b*-$PHEAm_{40}$	0.59	0.045	0.33	0.002	0.83	0.97
98	$PAMPS_{50}$-star	0.67	0.027	$1.7x10^{-7}$	0.002	0.005	0.0026

Statistical analysis performed using a student's t test to compare samples to a control group incubated with bFGF pre-mixed with heparin: (a) no stressors, (b) stored at room temperature for 12 hours, (c) stored at 37 °C for 12 hours.

Cell Lines and Cell Culture

NIH-3T3 cells were cultivated in Dulbecco's modified eagle medium (DMEM) supplemented with 10 % bovine calf serum (BCS) and 1 % L-glutamine, at 37 °C and 5 % CO_2 atmosphere. Cells were passaged every 3 days when reaching approximately 80 % confluency. BaF3-FR1c cells were cultivated in RPMI1640 GlutaMAX media supplemented with 10 % foetal bovine serum (FBS), 2 ng/mL of recombinant mouse IL-3, 600 µg/mL of G418, at 37 °C and 5 % CO_2 atmosphere. Cell media was replaced every 2-3 days by centrifuging at 1000 rpm for 5 minutes and kept at a density between 500,000 to 1,000,000 cells/mL and were used up to a month.

Cytotoxicity Assays on NIH-3T3 Cells

NIH-3T3 cells were washed with 10 mL of PBS, trypsinized and re-suspended in media. The cells were plated at a concentration of 2,000 cells/well in a 96-well plate and allowed to attach for 12 hours. The medium was replaced with 100 µL of fresh medium containing a series of polymer dilutions ranging from 10 ng/mL to 1 mg/mL (10 ng/mL, 1, 10 and 100 µg/mL and 1 mg/mL). After an incubation of 48 hours at 37 °C and 5 % CO_2, the cells were washed and the medium replaced with fresh culture medium containing 25 µL of XTT (1 mg/mL) and PMS (25 µmol/L). Cells were further incubated for 12 hours at 37 °C, 5 % CO_2. Absorbance of each wells was measured using a Synergy HTX plate reader at 475 nm and 650 nm (background) with $A = A_{475nm} - A_{475nm(blank)} - A_{650nm}$. The viability of cells was normalised to samples in which cells were incubated with medium only (positive control = 100 %). Each sample had three replicates and the experiment was repeated two times (N = 6).

Haemolysis Study

Defibrinated sheep red blood cells were prepared by washing the blood (2 mL) three times with PBS (750 µL) by ultracentrifugation (4,500 g for 1 minute) and removing the plasma each time. The blood was then diluted with PBS at 1:150. Polymers were dissolved in PBS and a three serial dilutions were prepared, 10, 100 and 200 µg/mL. 380 µL of blood was mixed with 20 µL of polymer samples and incubated at 37 °C for 2 hours. The samples were then centrifuged at 1,000 g for 10 minutes and then 200 µL of the supernatant was transferred into a 96-well plate and the absorbance was read at 414 nm and normalised against a positive and negative control. A solution of 2 % of triton X-100 in PBS was used as a positive control and set at 100 % of haemolysis of red blood cells.

Cell Proliferation

BaF3-FR1c cell line was kindly provided by Professor Jerry Turnbull (Liverpool University, UK). BaF3-FR1c cells were collected (1,000 rpm for 5 minutes) and washed twice (1,000 rpm for 5 minutes) with medium to remove traces of IL-3 and G418. Cells were plated at a concentration of 20,000 cells/well/50 µL in the internal wells of a 96-well plate in the presence of medium without IL-3 and G418. Further 50 µL of medium containing polymers or heparin and bFGF at double the final desired concentration ($[polymers]_{final}$ = 100, 1 and 0.1 µg/mL and $[bFGF]_{final}$ = 5 ng/mL) were added to the wells. Controls with cells only and with cells in the presence of 5 ng/mL of bFGF were used as references. External wells were filled with 100 µL of PBS and a gas permeable moisture barrier seal (4titude) was used to decrease the evaporation into the plate. After incubation for 48 hours at 37 °C, 5 % CO_2, 20 µL of the CellTiter-Blue® assay was added into each wells and further incubated for 6 hours at 37 °C, 5 % CO_2. Fluorescence of each well was measured using a Synergy HTX plate reader with the excitation set to 560 nm and the emission at 590 nm. The extension of cell proliferation was calculated by using the wells containing cells in medium only as positive controls (100 %). Each sample had four replicates and the experiment was repeated four times (N = 16).

Cell Proliferation Applying Thermal Stressors

Solutions of bFGF alone, bFGF with polymers or bFGF with heparin were prepared in medium at double the final desired concentration ($[polymers]_{final}$ = 100, and 50 µg/mL and $[bFGF]_{final}$ = 5 ng/mL). Solutions were then stored for 12 hours at the desired temperature either at approximately 20 °C (room temperature) or 37 °C. BaF3-FR1c cells were collected (1,000 rpm for 5 minutes) and washed twice (1,000 rpm for 5 minutes) with medium to remove traces of IL-3 and G418. Cells were plated at a concentration of 20,000 cells/well/50 µL in the internal wells of a 96-well plate in the presence of medium without IL-3 and G418. A further 50 µL of polymers or heparin solution at double the final desired concentration were added to the wells. Controls with cells only and with cells in presence of 5 ng/mL of bFGF with applied thermal stressors were used as references. External wells were filled with 100 µL of PBS and a gas permeable moisture barrier seal (4titude) was used to decrease the evaporation into the plate. After incubation for 48 hours at 37 °C, 5 % CO_2, 20 µL of the CellTiter-Blue assay was added into each wells and further incubated for 6 hours at 37 °C, 5 % CO_2. Fluorescence of each wells was measured using a Synergy HTX plate reader at set up at $560_{Ex}/590_{Em}$. The extension of cells proliferation was calculated by using the wells with cells with medium only as positive control (100 %). Each sample had four replicates and the experiment was repeated two times (N = 8).

5.6 References

(212) Bray, C.; Peltier, R.; Kim, H.; Mastrangelo, A.; Perrier, S. *Polym. Chem.* **2017**, *8*, 5513.

(214) Ternent, L.; Mayoh, D. A.; Lees, M. R.; Davies, G.-L. *J. Mater. Chem. B* **2016**, *4*, 3065.

(238) Tanaka, J.; Tani, S.; Peltier, R.; Pilkington, E. H.; Kerr, A.et al *Polym. Chem.* **2018**.

(249) Marcum, J. A. *Perspect. Biol. Med.* **1990**, *33*, 214.

(250) Hemker, H. C. *JTH* **2016**, *14*, 2329.

(251) Barrowcliffe, T. W. In *Handb. Exp. Pharmacol.*; Lever, R., Mulloy, B., Page, C. P., Eds.; Springer Berlin Heidelberg: 2012; Vol. 207, p 3.

(252) Quaranta, M.; Erez, O.; Mastrolia, S. A.; Koifman, A.; Leron, E.et al *PeerJ* **2015**, *3*, e691.

(253) Olczyk, P.; Mencner, L.; Komosinska-Vassev, K. *BioMed Res. Int.* **2015**, *2015*, 549417.

(254) Wadajkar, A. S.; Santimano, S.; Rahimi, M.; Yuan, B.; Banerjee, S.et al *Biotechnol. Adv.* **2013**, *31*, 504.

(255) Wardrop, D.; Keeling, D. *Br. J. Haematol.* **2008**, *141*, 757.

(256) Wang, M.; Lyu, Z.; Chen, G.; Wang, H.; Yuan, Y.et al *Chem. Commun.* **2015**, *51*, 15434.

(257) Ji, H.-f.; Xiong, L.; Shi, Z.-q.; He, M.; Zhao, W.-f.et al *Biomater. Sci.* **2017**, *5*, 1112.

(258) Huang, X.; Wang, R.; Lu, T.; Zhou, D.; Zhao, W.et al *Biomacromolecules* **2016**, *17*, 4011.

(259) Boyle, W. S.; Senger, K.; Tolar, J.; Reineke, T. M. *Biomacromolecules* **2017**, *18*, 56.

(260) Rak, J.; Weitz, J. I. *Atertio. Thromb. Vasc. Biol.* **2003**, *23*, 1954.

(261) Paluck, S. J.; Nguyen, T. H.; Maynard, H. D. *Biomacromolecules* **2016**, *17*, 3417.

(262) Jorpes, E. *Biochem. J.* **1935**, *29*, 1817.

(263) Casu, B. *Ann. N. Y. Acad. Sci.* **1989**, *556*, 1.

(264) Holme, K. R.; Perlin, A. S. *Carbohydr. Res.* **1989**, *186*, 301.

(265) Mulloy, B.; Forster, M. J.; Jones, C.; Davies, D. B. *Biochem. J.* **1993**, *293*, 849.

(266) Pellegrini, L.; Burke, D. F.; Von Delft, F.; Mulloy, B.; Blundell, T. L. *Nature* **2000**, *407*, 1029.

(267) Stauber, D. J.; DiGabriele, A. D.; Hendrickson, W. A. *Proceedings of the National Academy of Sciences of the United States of America* **2000**, *97*, 49.

(268) Cross, M. J.; Claesson-Welsh, L. *Trends Pharmacol. Sci.* **2001**, *22*, 201.

(269) Ornitz, D. M.; Yayon, A.; Flanagan, J. G.; Svahn, C. M.; Levi, E.et al *Mol. Cell. Biol.* **1992**, *12*, 240.

(270) Cheng, C.; Sun, S.; Zhao, C. *J. Mater. Chem. B* **2014**, *2*, 7649.

(271) Canalis, E.; Centrella, M.; McCarthy, T. *J. Clin. Invest.* **1988**, *81*, 1572.

(272) Capila, I.; Linhardt, R. J. *Angew. Chem. Int. Ed.* **2002**, *41*, 390.

(273) Cardin, A. D.; Weintraub, H. J. *Atertio. Thromb. Vasc. Biol.* **1989**, *9*, 21.

(274) Thomas, A. *FASEB* **1987**, *1*, 434.

(275) Baird, A.; Schubert, D.; Ling, N.; Guillemin, R. *Proc. Natl. Acad. Sci. USA* **1988**, *85*, 2324.

(276) Baird, A.; Bohlen, P. *Sptinger-Verlag,.Berlin.* **1990**, *1*, 369.

(277) Ornitz, D. M.; Itoh, N. *Wiley Interdiscip. Rev. Dev. Biol.* **2015**, *4*, 215.

(278) Gospodarowicz, D.; Neufeld, G.; Schweigerer, L. *J. Cell. Physiol.* **1987**, *Suppl 5*, 15.

(279) Gospodarowicz, D.; Cheng, J. *J. Cell. Physiol.* **1986**, *128*, 475.

(280) Yun, Y.-R.; Won, J. E.; Jeon, E.; Lee, S.; Kang, W.et al *J. Tissue Eng.* **2010**, *1*, 218142.

(281) Eswarakumar, V. P.; Lax, I.; Schlessinger, J. *Cytokine Growth Factor Rev.* **2005**, *16*, 139.

(282) Ishihara, M. *Glycobiology* **1994**, *4*, 817.

(283) Loo, B.-M.; Kreuger, J.; Jalkanen, M.; Lindahl, U.; Salmivirta, M. *J. Biol. Chem.* **2001**, *276*, 16868.

(284) Venkataraman, G.; Sasisekharan, V.; Herr, A. B.; Ornitz, D. M.; Waksman, G.et al *Proceedings of the National Academy of Sciences* **1996**, *93*, 845.

(285) Schlessinger, J.; Plotnikov, A. N.; Ibrahimi, O. A.; Eliseenkova, A. V.; Yeh, B. K.et al *Mol. Cell* **2000**, *6*, 743.

(286) Waksman, G.; Herr, A. B. *Nat. Struct. Biol.* **1998**, *5*, 527.

(287) Alban, S. In *Handb. Exp. Pharmacol.*; Lever, R., Mulloy, B., Page, C. P., Eds.; Springer Berlin Heidelberg: Berlin, Heidelberg, 2012; Vol. 207, p 211.

(288) Kishimoto, T. K.; Viswanathan, K.; Ganguly, T.; Elankumaran, S.; Smith, S.et al *New Engl. J. Med.* **2008**, *358*, 2457.

(289) Blossom, D. B.; Kallen, A. J.; Patel, P. R.; Elward, A.; Robinson, L.et al *New Engl. J. Med.* **2008**, *359*, 2674.

(290) Guerrini, M.; Beccati, D.; Shriver, Z.; Naggi, A.; Viswanathan, K.et al *Nat. Biotechnol.* **2008**, *26*, 669.

(291) Mauzac, M.; Aubert, N.; Jozefonvicz, J. *Biomaterials* **1982**, *3*, 221.

(292) Mauzac, M.; Jozefonvicz, J. *Biomaterials* **1984**, *5*, 301.

(293) Akashi, M.; Sakamoto, N.; Suzuki, K.; Kishida, A. *Bioconjugate Chem.* **1996**, *7*, 393.

(294) Huang, Y.; Shaw, M. A.; Mullins, E. S.; Kirley, T. L.; Ayres, N. *Biomacromolecules* **2014**, *15*, 4455.

(295) Miura, Y.; Fukuda, T.; Seto, H.; Hoshino, Y. *Polym. J.* **2016**, *48*, 229.

(296) García-Fernández, L.; Aguilar, M. R.; Fernández, M. M.; Lozano, R. M.; Giménez, G.et al *Biomacromolecules* **2010**, *11*, 626.

(297) García-Fernández, L.; Halstenberg, S.; Unger, R. E.; Aguilar, M. R.; Kirkpatrick, C. J.et al *Biomaterials* **2010**, *31*, 7863.

(298) Nguyen, T. H.; Paluck, S. J.; McGahran, A. J.; Maynard, H. D. *Biomacromolecules* **2015**, *16*, 2684.

(299) Paluck, S. J.; Maynard, H. D. *Polym. Chem.* **2017**, *8*, 4548.

(300) Paluck, S. J.; Nguyen, T. H.; Lee, J. P.; Maynard, H. D. *Biomacromolecules* **2016**, *17*, 3386.

(301) Nguyen, T. H.; Kim, S. H.; Decker, C. G.; Wong, D. Y.; Loo, J. A.et al *Nat. Chem.* **2013**, *5*, 221.

(302) Peysselon, F.; Ricard-Blum, S. *Matrix Biol.* **2014**, *35*, 73.

(303) Kruft, M.-A. B.; Koole, L. H. *Macromolecules* **1996**, *29*, 5513.

(304) Aguilar, M. R.; Gallardo, A.; Del Mar Fernández, M.; Román, J. S. *Macromolecules* **2002**, *35*, 2036.

(305) Rainaldi, I.; Cristallini, C.; Ciardelli, G.; Giusti, P. *Macromol. Chem. Phys.* **2000**, *201*, 2424.

(306) Paschek, D.; Golub, B.; Ludwig, R. *Phys. Chem. Chem. Phys.* **2015**, *17*, 8431.

(307) Zhang, Q.-G.; Wang, N.-N.; Yu, Z.-W. *J. Phys. Chem. B* **2010**, *114*, 4747.

(308) Chen, G.; Gulbranson, D. R.; Yu, P.; Hou, Z.; Thomson, J. A. *Stem Cells* **2012**, *30*, 623.

(309) Xu, R.; Ori, A.; Rudd, T. R.; Uniewicz, K. A.; Ahmed, Y. A.et al *J. Biol. Chem.* **2012**, *287*, 40061.

CHAPTER 6:
CONCLUSIONS

6.1 Conclusions

The aim of this thesis was not only to synthesise a linear homopolymer with AMPS®2405, but also to target more complex architectures (multiblock copolymers and star polymers) using reversible addition-fragmentation chain-transfer (RAFT) polymerisation in aqueous solution.

In **CHAPTER 2** it has been shown that even though BDMAT and DDMAT have a similar structure (i.e. same R-group and slightly different Z-groups), different controls over the polymerisation was obtained. While homopolymers with low dispersities and good control over molecular weights (i.e. linear increase of molecular weights with time and increasing DPs) were obtained with BDMAT, little control was obtained with DDMAT ($Đ$ >> 1.5) in deionised water. The lower control was attributed to the formation of aggregates with DDMAT which were broken down by performing the reaction in a mixture of water and a miscible organic solvent.[113] Consequently, better control over polymerisation of AMPS®2405 was obtained using DDMAT in a mixture of 20 % methanol and 80 % water. Finally, the homopolymerisation of DMA and NAM using either DDMAT or BDMAT allowed well-defined materials with dispersities lower than 1.3. However, when HEAm was used similar results to when AMPS®2405 was polymerised were obtained (i.e. $Đ_{HEAm,BDMAT}$ = 1.31 versus $Đ_{HEAm,DDMAT}$ = 1.57). While theoretical livingness was calculated, further characterisation / quantification of the chain end fidelity would be required.

In **CHAPTER 3**, the synthesis of different copolymers using $PAMPS_{50}$-BDMAT macroCTA was explored. The effect of pH was first investigated (i.e. pH 2, 6 and 10) by the chain extension of $PAMPS_{50}$ by AMPS®2405 itself. The pH was shown to be a crucial parameter on polymerisation control obtaining bimodal SEC chromatograms at pH 10. This was attributed to chain-end loss at pH 10 linked to CTA hydrolysis. The efficiency of the $PAMPS_{50}$ reinitiation with other monomers (NAM, HEAm, AA,

DMA, AM) was secondly evaluated. While full monomer conversion was obtained for any of the monomers utilised, no shift to higher molecular weight was observed by SEC when conventional calibration was used. This was attributed to the difference of hydrodynamic volume between the AMPS®2405 hompolymer (highly charged) and the diblock (2nd block neutral) copolymer synthesised. SEC with triple detection was used to overcome this problem, where a clear shift towards higher molecular weights was observed. The SEC distributions obtained with triple detection were monomodal and narrow ($Đ$ < 1.3), indicative of a good reinitiation. Finally, star polymers were successfully synthesised using the arm first approach. A few parameters such as the cross-linker type, the cross-linker to CTA ratio, the cross-linker concentration and the arm length were evaluated. Star shaped polymers were obtained within 40 minutes using di(ethylene glycol) diacrylate cross-linker (% arm incorporated = 89 %, $Đ$ = 1.15, $M_{n,SEC}$ = 67 kg/mol). The higher the compartmentalisation of the cross-linker due to its lower solubility, the higher the efficiency was found to be. The formation of a star polymer was confirmed by the appearance of a peak at higher molecular weight in SEC chromatograms. Lastly, the first octablock star copolymer synthesised by RAFT polymerisation in a one-pot process in aqueous solution was reported (% arm incorporated = 67 %, $Đ$ = 1.27, $M_{n,SEC}$ = 230 kg/mol), however, the molecular weights calculated were underestimated when conventional calibration was used due to the nature of the standards used (Linear PEG).

In **CHAPTER 4**, a wide range of analytical techniques was used to fully characterise the highly charged star polymers which have been synthesised so far. SEC with triple detection was shown to be a powerful analytical tool for branched polymers. Indeed, while linear hompolymer molecular weights were only slightly underestimated with conventional calibration, the gap was not as negligible for star polymers. The number of arms of the $PAMPS_{50}$-BDMAT star polymer was calculated to be 37 when triple detection was used compared to only 8 with conventional calibration. Atomic force microscopy gave further insight on the structure, with observed globular structures. Additionally, this globular structure found was further confirmed by the analysis of the star polymer by small angle X-ray scattering. While a star shaped model could not be used to fit the raw data for the system, a core-shell sphere model could perfectly fit the system. This is attributed to the compartmentalisation of the cross-linker during

the star polymer synthesis, also called core-shell star nanoparticles or core cross-linked micelles.[153]

Finally, in **CHAPTER 5** the use of synthetic AMPS®2405 homopolymers and copolymers were evaluated to replace naturally occurring heparin. So far in literature AMPS®2405 polymers have been shown to have an antiproliferative effect towards BaF3-FR1c cells, however, only PAMPS obtained by conventional radical polymerisation were studied.[298] In this thesis the targeted molecular weight of the homopolymer was shown to be essential to induce any proliferation. The best proliferation results were obtained with PAMPS with a DP of 80 (molecular weight comparable to heparin) while the proliferation was drastically decreased when the targeted DP was increased. This also helps to explain the antiproliferative effect observed with polymers obtained by conventional radical polymerisation (i.e. no control over molecular weight and polymers with very high molecular weight being obtained). Finally, a high charge density was required to achieve high enough proliferation. Indeed, while diblock copolymers were shown to have good heparin-like properties, the random copolymers were not active.

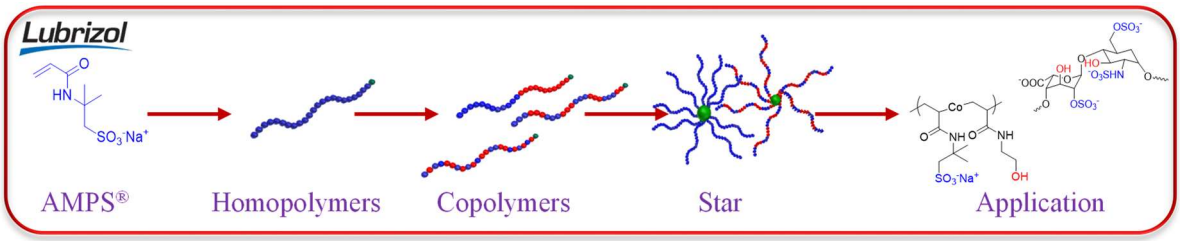

6.2 Future Work

The ability for DDMAT to aggregate in water was demonstrated in this thesis (**CHAPTER 1**) and it would be an opportunity to develop emulsion polymerisation for industrial purpose using RAFT polymerisation (e.g. food industry, drug delivery, crude oil).[310,311] Nanoparticles are interesting for industrial purpose as the process allows the synthesis of high molecular weight polymers with low viscosities. This DDMAT CTA could, for example, be used for the reverse emulsion polymerisation of AMPS®2405. Additionally, other structures (e.g. brush polymers, network, cyclic) with the same molecular weights as the star polymers synthesised in this thesis could be synthesised in order to compare their properties and consequently their potential applications.[312] Finally, other comonomers could be used to synthesis complex architectures to increase the scope of applications using such structures (i.e. multiblock copolymers or star polymers). Thermo- or pH- responsive polymers would be of great interest for several biological applications such as drug encapsulation and delivery.[313]

Additionally, heparin like properties of AMPS®2405 Copolymers (NAM, DMA, AM, AA) synthesised in **Section 3.3.2** could be evaluated. Even though no effect was observed when HEAm was used, other comonomers, such as AM or AA could drastically affect these properties. Additionally, a PAMPS-*co*-PPEGMA could be synthesised and tested as heparin mimicking-polymers, indeed, Maynard *et al.* have shown the importance of the PEGMA segment in their heparin-mimicking polymers.[301] Lastly, the potential use of these polyelectrolyte copolymers could be investigated for a wider range of applications. For example, they have the potential to be used as contrast agent stabilisers for magnetic resonance imaging.[214] Additionally, these polyelectrolytes, and especially the star polymers, could be used in lithium polymer batteries due to their high mechanical and thermal resistance.[314] Similarly these polymers could be tested for ion and metal extraction in water treatment with the ion conduction of the $-SO_3H$.[315,316]

6.3 References

(113) Stoffelbach, F.; Tibiletti, L.; Rieger, J.; Charleux, B. *Macromolecules* **2008**, *41*, 7850.

(153) Ren, J. M.; McKenzie, T. G.; Fu, Q.; Wong, E. H. H.; Xu, J.et al *Chem. Rev.* **2016**, *116*, 6743.

(214) Ternent, L.; Mayoh, D. A.; Lees, M. R.; Davies, G.-L. *J. Mater. Chem. B* **2016**, *4*, 3065.

(298) Nguyen, T. H.; Paluck, S. J.; McGahran, A. J.; Maynard, H. D. *Biomacromolecules* **2015**, *16*, 2684.

(301) Nguyen, T. H.; Kim, S. H.; Decker, C. G.; Wong, D. Y.; Loo, J. A.et al *Nat. Chem.* **2013**, *5*, 221.

(310) Nakashima, T.; Shimizu, M.; Kukizaki, M. *Adv. Drug Del. Rev.* **2000**, *45*, 47.

(311) Lu, Y.; Kang, W.; Jiang, J.; Chen, J.; Xu, D.et al *RSC Adv.* **2017**, *7*, 8156.

(312) Kerr, A.; Hartlieb, M.; Sanchis, J.; Smith, T.; Perrier, S. *Chem. Commun.* **2017**, *53*, 11901.

(313) Wei, M.; Gao, Y.; Li, X.; Serpe, M. J. *Polym. Chem.* **2017**, *8*, 127.

(314) Lee, W.-J.; Jung, H.-R.; Lee, M. S.; Kim, J.-H.; Yang, K. S. *Solid State Ionics* **2003**, *164*, 65.

(315) Hickner, M. A. *Mater. Today* **2010**, *13*, 34.

(316) Dąbrowski, A.; Hubicki, Z.; Podkościelny, P.; Robens, E. *Chemosphere* **2004**, *56*, 91.

APPENDIX

A.Equations for all Chapters

Equation 1 - *Determination of Monomer Conversion*. Monomer conversion (p) was calculated from ^{1}H NMR spectroscopy data using the following equation:

$$p = \frac{[M]_0 - [M]_t}{[M]_0} = 1 - \frac{[M]_t}{[M]_0} = 1 - \frac{\frac{\int I_{5.5-6.75\ ppm}}{\int I_a}}{DP_{targeted}}$$

Where $[M]_0$ and $[M]_t$ are the monomer concentrations at time 0 and time t, respectively; $(\int I_{5.5-6.75\ ppm} / \int I_a)$ is the corrected integration of the signal for the vinyl protons of the monomer; $DP_{targeted}$ is the number average degree of polymerisation targeted; $\int I_a$ is the integration of the signal for the three methyl protons belonging to the Z-group of the RAFT agent (-CH_2-C$\underline{H_3}$) used as an internal reference.

Equation 2 - *Calculation of the theoretical number-average molar mass ($M_{n,th}$)*. The theoretical number-average molar mass ($M_{n,th}$) was calculated using the following equation:

$$M_{n,th} = \frac{[M]_0 p M_M}{[\mathrm{CTA}]_0} + M_{CTA}$$

Where $[M]_0$ and $[\mathrm{CTA}]_0$ are the initial concentrations of monomer and chain transfer agent, respectively; p is the monomer conversion as determined using equation 1; M_M and M_{CTA} are the molecular mass (g/mol) of the monomer and chain transfer agent, respectively.

Equation 3 - *Calculation of the Number-Average Molar Mass by ^{1}H NMR spectroscopy ($M_{n,NMR}$).* the NMR average molar mass ($M_{n,NMR}$) was calculated using the following equation:

$$M_{n,NMR} = \int I_{1.95-2.55\,ppm}\, M_M + M_{CTA}$$

M_M and M_{CTA} are, respectively, the molar mass (g/mol) of the monomer and chain transfer agent. $\int I_{1.95-2.55\,ppm}$ is the corrected integration of the signal for the vinyl protons of the backbone polymer CH2=C*H* normalised by the internal reference $\int I_{0.90\,ppm}$ (three methyl protons belonging to the Z-group of the RAFT agent, -CH_2-C*H*$_3$).

Equation 4 - *Calculation of the Theoretical Number Fraction of Living Chains (L)*. The number of living chains (L) was calculated using the following equation:

$$L = \frac{[\mathrm{CTA}]_0}{[\mathrm{CTA}]_0 + 2f[I]_0(1 - e^{-k_d t})}$$

Where $[I]_0$ and $[CTA]_0$ are the initial concentrations of initiator and chain transfer agent, respectively; k_d is the decomposition rate constant (in s^{-1}) of the azoinitiator at a given temperature; t is the polymerisation time (s); f is the efficiency of the initiator and is equal to 0.5.

Equation 5 - *Determination of Chain Agent Transfer Consumption*. Consumption of the chain transfer agent was followed by ^{1}H NMR spectroscopy (**Figure 23**). CTA consumption was followed by the appearance of a peak at approximately 1.10 ppm corresponding to the C(C*H*$_3$)$_2$ of the R-group of the CTA as the polymer chains form. The CH_2-C*H*$_3$ (C_4H_9 alkyl chain) of the Z-group (~ 0.90 ppm, triplet) was taken as the internal reference due to the chemical shift remaining unchanged for consumed and non-consumed CTA.

$$\mathrm{x} = \frac{\int I_{1.1\,ppm}}{6}$$

Equation 6 - *Determination of the Chain Transfer Constant*. The apparent chain transfer constant (C_{tr}^{app}) of AMPS®2405 monomer (salt form) in phosphate buffer solution at 90 °C was determined experimentally by plotting Ln([CTA]$_{consumed}$) in function of Ln([AMPS®2405]$_{consumed}$) using the following equation:

$$C_{tr}^{app} = \frac{dLn[CTA]}{dLn[M]}$$

Consumption of the chain transfer agent and monomer were followed by ^{1}H NMR spectroscopy. CTA consumption was followed by the appearance of a peak at approximately 1.10 ppm corresponding to the $C(C\underline{H}_3)_2$ of the R-group of the CTA as the polymer chains were formed. Monomer consumption was followed by the disappearance of the vinylic proton between 5.50 and 6.50 ppm. The CH_2-$C\underline{H}_3$ (C_4H_9 or $C_{12}H_{25}$ alkyl chain) of the Z-group (~ 0.90 ppm, triplet) was taken as the internal reference due to the chemical shift remaining unchanged for incorporated and non-incorporated monomer units.

Equation 7 – *Calculation of the Percentage of Arm Incorporated into the Star.* The percentage of arm incorporated into each star was determined by deconvolution of multimodal SEC traces using the following equation.

$$Conversion\ to\ Star\ = \frac{\int Air_{Star}}{\int Air_{Star} + \int Air_{Arm}}$$

Where $\int Air_{Star}$ is the integration of the SEC signal corresponding to the star polymer and $\int Air_{Arm}$ is the integration of the SEC signal corresponding to the arm only.
The $\int Air$ can be determined using either OriginPro 2016 (**Figure Appendix 1**) or Agilent GPC/SEC Software (**Figure Appendix 2**).

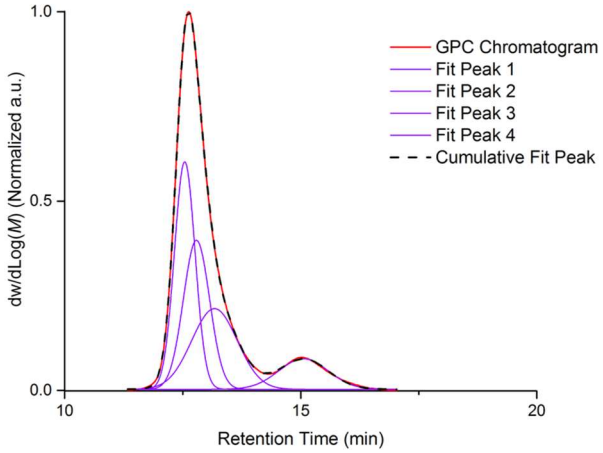

Figure Appendix 1: Core cross-linked star polymer ($PAMPS_{50}$,C4) chromatogram obtained by aqueous SEC (red), deconvolution using a Gaussian fitting curve (purple) and its cumulative fit peak (black dotted line) using OriginPro 2016.

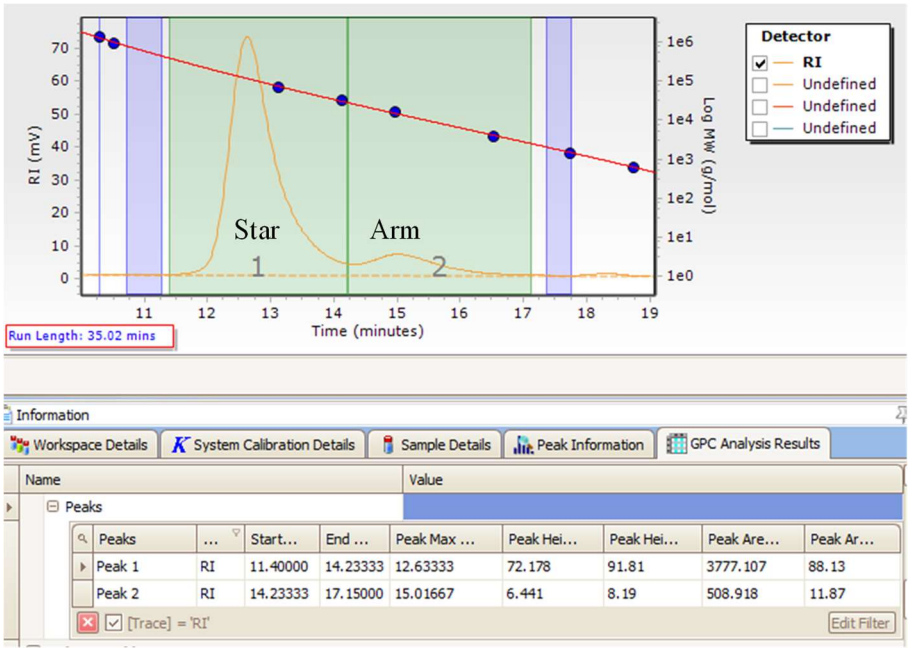

Figure Appendix 2: Core cross-linked star polymers ($PAMPS_{50}$,C4) - deconvolution of the chromatogram obtained by aqueous SEC using the Agilent GPC/SEC Software.

When OriginPro 2016 is used the raw data obtained with the SEC software were plotted and each peaks was deconvoluted using a Gaussian fitting curve to obtain the closest cumulative fit peak shape possible to the peak obtained experimentally by SEC. When the Agilent GPC/SEC Software was used we simply integrated each peak separately (arm and star) and processed it to measure each peak area. The Origin software gave a percentage of 90 % compared to 88 % of arm incorporated into the star when the SEC software was used.

Equation 8 – *Determination of Star Polymers Functionality (f).* The functionality of each star polymers was determined using the following equation.

$$f = \frac{M_{\mathrm{w,star}}}{M_{\mathrm{w,arm}}} \times \frac{Conv_{arm} X_{arm} m_{arm}}{Conv_{arm} X_{arm} m_{arm} + Conv_{CL} m_{CL}}$$

Where f is the functionality, M_w is the molecular weight respectively of the star and the linear polymer (g/mol), Conv is the conversion respectively of the arm and the cross-linker (CL), X is the weight fraction respectively of the arm and the cross-linker, m is the mass (g) respectively of the arm and the cross-linker. As the mass of the cross-linker is negligible compared to the mass of the arm the equation can be simplified by:

$$f = \frac{M_{\mathrm{w,star}}}{M_{\mathrm{w,arm}}}$$

Equation 9 – O*ff-line dn/dc Determination.* dn/dc was determined by preparing six solutions of increasing polymer concentrations from 0.05 to 0.75 mg/mL. The solutions were prepared in the SEC eluent (80:20 0.1 M $NaNO_{3(aq)}$:methanol) and were run at 35 °C to obtain comparable results to the on-line dn/dc determination; using the aqueous SEC. The dn/dc was determined by plotting the RI against the polymer concentrations and using the following equation:

$$RI = \mathrm{B}\frac{dn}{\mathrm{dc}}C$$

Where RI is the refractive index, B is the refractometer constant and is equal to 1398000, C is the concentration of polymer in the sample in g/mL, dn/dc is the change in the refractive index of a solution as a function of the concentration in mL/g. The dn/dc was determined using the slope.

B. Materials for all Chapters

CHAPTER 2. Sodium hydroxide (NaOH; Fischer Scientific, 97 %, pellets), 1-butanethiol (Sigma-Aldrich, 99 %), carbon disulfide (CS2; Sigma-Aldrich, 99 %), 2-bromo-2-methylpropionic acid (Sigma-Aldrich, 98 %), hydrochloric acid solution (HCl, VWR chemical, 35 %), acetone (Sigma-Aldrich, 99 %), n-hexane (VWR chemical, 99 %), chloroform (Sigma-Aldrich, 99 %), distilled water, toluene (Sigma-Aldrich, > 99.5 %), *N*,*N*-dimethylformamide (DMF, Sigma-Aldrich, 99.8 %), dimethyl sulfoxide (DMSO, Fisher Scientific, > 99.7 %), 1,4-dioxane (Fisher Scientific, 99.8 %), Acetonitrile (ACN, Fisher Scientific, 99.9 %), *tert*-butanol (Sigma-Aldrich, > 99 %), butan-1-ol (Fisher Scientific, 99.5 %), methanol (MeOH, Sigma-Aldrich, 99.8 %), formic acid (Acros Organics, > 98 %), acetic acid (Merck, 96%), Buffer Tablets pH 7 phosphate (Fisher Scientific), *N*,*N*-dimethylacrylamide (DMA, Sigma-Aldrich, 99 %), 4-acryloylmorpholine (NAM, Sigma-Aldrich, 97 %), *N*-hydroxyethyl acrylamide (HEAm, Sigma-Aldrich, 97 %), sodium 2-acrylamido-2-methylpropane sulfonate (AMPS®2405, Lubrizol, 50 % in water), 2-(((butylthio)-carbonothioyl)thio)-2-methylpropanoic acid (BDMAT, synthesised using method from literature[118]), 2-(((dodecylthio)-carbonothioyl)thio)-2-methylpropanoic acid (DDMAT, Lubrizol, purified by recrystallization in hexane), 1,1′-azobis(cyclohexanecarbonitrile) (V-40, Wako Chemical, 95 %), 4,4′-azobis(4-cyanopentanoic acid), 2,2′-azobis[2-methyl-*N*-((2-hydroxyethyl)propionamide] (VA-086, Wako Chemical, 98 %), 2,2′-azobis[*N*-(2-carboxyethyl)-2-methylpropionamidine]tetrahydrate (VA-057, Wako Chemical), deuterium oxide (D_2O, Sigma-Aldrich, 99.9 % D atom), methanol-d_4 (MeOD; Sigma-Aldrich, 99.8 % D atom), acetone-d_6 ($(CD_3)_2CO$, Sigma-Aldrich, 99.9 % D atom), N,N-dimethylformamide-d_7 ($DCON(CD_3)_2$, Sigma Aldrich, ≥ 99.5 % D atom). Chemicals were used as received with no further purification unless specified.

CHAPTER 3. Sodium hydroxide (NaOH; Fischer Scientific, 97 %, pellets), hydrochloric acid solution (HCl, VWR chemical, 35 %), distilled water, methanol (MeOH, Sigma-Aldrich, 99.8 %), dimethyl sulfoxide (DMSO, Fisher Scientific, > 99.7 %), buffer tablets pH 7 phosphate (Fisher Scientific), *N*,*N*-dimethylacrylamide (DMA, Sigma-Aldrich, 99 %), 4-acryloylmorpholine (NAM, Sigma-Aldrich, 97 %), *N*-hydroxyethyl acrylamide (HEAm, Sigma-Aldrich, 97 %), sodium 2-acrylamido-2-methylpropane sulfonate (AMPS®2405, Lubrizol, 50 % in water), acrylic acid (AA, Merck, 99 %), acrylamide (AM, Sigma-Aldrich, 98 %), *N*,*N*′-methylenebisacrylamide (Sigma-Aldrich, 99 %), di(ethylene glycol) diacrylate (Sigma-Aldrich, 75 %), divinylbenzene (Sigma-Aldrich, 80 %), *N*,*N*′-(1,2-dihydroxyethylene) bisacrylamide (Alfa Aesar, 97 %), 1,6-hexanediol diacrylate (Alfa Aesar, 99 %), pentaerythritol tetraacrylate (Sigma-Aldrich, 10-40 % triester), pentaerythritol triacrylate (Sigma-Aldrich, technical grade), 2-(((butylthio)-carbonothioyl)thio)-2-methylpropanoic acid (BDMAT, synthesised using method from literature[118]), 2-(((dodecylthio)-carbonothioyl)thio)-2-methylpropanoic acid (DDMAT, Lubrizol, purified by recrystallisation in hexane), 4,4′-azobis(4-cyanopentanoic acid), 2,2′-azobis[2-methyl-N-((2-hydroxyethyl)propionamide] (VA-086, Wako Chemical, 98 %), deuterium oxide (D_2O, Sigma-Aldrich, 99.9 % D atom), methanol-d_4 (MeOD; Sigma-Aldrich, 99.8 % D atom). Chemicals were used as received with no further purification unless specified.

CHAPTER 4. SEC solvents: milli-Q water, methanol (MeOH, Fisher Scientific, HPLC grade), sodium nitrate ($NaNO_3$, Scientific Laboratory Supplies, > 99 %), PEG/PEO calibration kits EasiVial (Agilent Technologies). Rheology and viscosity solvents: milli-Q water, posphate-buffered saline (PBS, media preparation service), calcium chloride ($CaCl_2$, ACROS Organic, Fisher Scientific, 96 %). Chemicals were used as received with no further purification unless specified.

CHAPTER 5. BaF3-FR1c cells expressing FGFR1c were kindly provided by Professor Jerry Turnbull (Liverpool University, United Kingdom), NIH/3T3 (Mouse Swiss NIH embryo, Fisher Scientific). RPMI1640 medium with GlutaMAX supplement (Invitrogen, Fisher Scientific, Sterile), IL-3 mouse recombinant expressed in E. coli (Sigma-Aldrich, > 98 %, Sterile), geneticin selective antibiotic (G418 Sulfate, Invitrogen, Fisher Scientific, 50 mg/mL in water, Sterile), CellTiter-Blue® cell viability assay (Promega), heparin sodium salt from porcine intestinal mucosa (Sigma-Aldrich, ≥180 USP units/mg); basic Fibroblast Growth Factor human recombinant (bFGF, Corning, Fischer Scientific, Sterile-Filtered-Lyophilised, > 95 %), 2,3-bis(2-methoxy-4-nitro-5-sulfophenyl)-2H-tetrazolium-5-carboxanilide inner salt (XTT sodium salt, Sigma-Aldrich, > 90 %), phenazine methosulfate (PMS, Sigma-Aldrich, > 90 %), defibrinated sheep blood (Thermo Scientific Oxoid, Fisher Scientific), Triton X-100 (Sigma-Aldrich), Dulbecco's Modified Eagle Medium (DMEM), foetal bovine serum (FBS, Sigma-Aldrich), calf bovine serum (CBS, Sigma-Aldrich, Sterile-Filtered), posphate-buffered saline (PBS), L-glutamine and sterile water were prepared under sterile condition by the media preparation service at the School of Life Science at the University of Warwick. RP-HPLC solvents: water (H_2O, Fisher Scientific, HPLC gradient grade), methanol (MeOH, Fisher Scientific, HPLC grade), trifluoroacetic acid (CF_3CO_2H; Sigma-Aldrich, 99 %). SEC solvents: milli-Q water, methanol (MeOH, Fisher Scientific, HPLC grade), sodium nitrate ($NaNO_3$, Scientific Laboratory Supplies, > 99 %), PEG/PEO calibration kits EasiVial (Agilent Technologies). Chemicals were used as received with no further purification unless specified.

C.Instrumentation for all Chapters

PL50 Aqueous SEC. Agilent PL50 instrument equipped with differential refractive index (DRI) detector. The system was equipped with 2 x Agilent PL Aquagel OH Mixed M columns (30 cm x 7.5 mm ID) with 8 μm pore size and an Agilent Aquagel 8 μm guard column. The mobile phase used was 80:20 0.1 M $NaNO_{3(aq)}$:methanol. Samples were run at 1mL/min at 35 °C regulated with a column oven. Poly(ethylene oxide) standards (Agilent EasyVials) were used for calibration between 1,368,000 – 106 g/mol. Analyte samples were prepared at a final concentration of 1 mg/mL and filtered through a membrane with 0.22 μm pore size before injection. Respectively, experimental molar mass ($M_{n,SEC}$) and dispersity ($Đ$) values of synthesised polymers were determined by conventional calibration using Agilent GPC/SEC software.

Infinity Aqueous SEC. Agilent Technologies Infinity 1260 MDS instrument equipped with light scattering (LS), differential refractive index (DRI), viscometer (VS) and ultra-violet (UV) detectors in series. The system was equipped with 2 x Tosoh TSKGel GMPWXL columns (30 cm x 7.8 mm ID) with 13 μm pore size. The mobile phase used was 80:20 0.1 M $NaNO_{3(aq)}$:methanol. Samples were run at 1mL/min at 35 °C regulated with a column oven. Poly(ethylene oxide) standards (Agilent EasyVials) were used for calibration between 1,368,000 – 106 g/mol. Analyte samples were prepared at a final concentration of 7 mg/mL for linear polymers and 2.5 mg/mL for star polymers and filtered through a membrane with 0.22 μm pore size before injection. Respectively, experimental molar mass ($M_{n,SEC}$) and dispersity ($Đ$) values of synthesised polymers were determined either by conventional calibration or triple detection using Agilent GPC/SEC software.

PL50 DMF SEC. Agilent PL50 instrument equipped with differential refractive index (DRI) and ultra-violet (UV) detectors. The system was equipped with 2 x Agilent PolarGel M columns (30 cm x 7.5 mm ID) and an Agilent PolarGel 5 μm guard column. The mobile phase used was DMF with 0.1 wt / v % LiBr additive. Samples were run at 1 mL/min at 50 °C regulated with a column oven. Poly(methyl methacrylate) standards (Agilent EasyVials) were used for calibration between 955,000 – 550 g/mol. Analyte samples were prepared at a final concentration of 1 mg/mL and filtered through a nylon membrane with 0.22 μm pore size before injection Respectively, experimental molar mass ($M_{n,SEC}$) and dispersity ($Đ$) values of synthesised polymers were determined by conventional calibration using Agilent GPC/SEC software.

DMF SEC. Agilent 390-LC MDS instrument equipped with dual angle light scatter (LS), differential refractive index (DRI), viscometer (VS) and ultra-violet (UV) detectors in series. The system was equipped with 2 x Agilent PLgel Mixed D columns (30 cm x 7.5 mm ID) and an Agilent PLgel 5 μm guard column. The mobile phase used was DMF with 5 mmol NH_4BF_4 additive. Samples were run at 1 mL/min at 50 °C regulated with a column oven. Poly(methyl methacrylate) standards (Agilent EasyVials) were used for calibration between 955,000 – 550 g/mol. Analyte samples were prepared at a final concentration of 1 mg/mL unless using triple detection then the solution of linear polymers was 5 mg/mL and 2.5 mg/mL for the star polymers, and filtered through a nylon membrane with 0.22 μm pore size before injection Respectively, experimental molar mass ($M_{n,SEC}$) and dispersity ($Đ$) values of synthesised polymers were determined by conventional calibration using Agilent GPC/SEC software.

Proton and carbon NMR Measurement. ^{1}H and ^{13}C Nuclear Magnetic Resonance (NMR) spectra were recorded on either a Bruker Avance 300 MHz (AV300), a Bruker Avance III HD 300 MHz (HD300) or a Bruker Avance III HD 500 MHz (HD500) spectrometer using either deuterium oxide (D_2O) or deuterated methanol (MeOD) at 27 °C. All measurement were done at 25 mg/mL. Chemical shift values (δ) are reported in ppm. Data were analysed using MestReNova.

DLS Measurement. Dynamic Light Scattering (DLS) measurements were carried out on a Malvern Zetasizer at 25 °C with 4 mM He-Ne 633 nm laser at a scattering angle of 173° (back scattering). Measurements were made either in water, PBS or $CaCl_{2(Aq.)}$ (1 M) using disposable cuvette at a polymer concentration of 10 mg/mL and filtered through a membrane with 0.22 μm pore size. Each sample were measured three times with 13 runs. Hydrodynamic diameters (D_h) and size distributions were analysed using Zetasizer Software 7.11.

TEM Imaging. Transmission Electron Microscopy (TEM) images were obtained in a JEOL 2100 transmission electron microscope using an accelerating voltage of 200 kV. Star polymers were diluted at 1 in 500 fold in deionised water. 10 μL of sample was cast on a hydrophobic petri-dish surface and a graphene oxide coated lacey carbon grid (EM Resolutions) was placed coated side down on the droplet, left for 30 seconds, and left until dry.

AFM Imaging (4.6.4). Atomic Force Microscopy (AFM) images were acquired in AC mode on a Cypher S system (Oxford Instruments Asylum Research). The probes used were the AC160TS from Olympus probes with a nominal resonant frequency of 300 kHz and a spring constant of approximately 40 N/m on a multimode AFM (Oxford Instruments Asylum Research). Images were acquired at a pixel resolution of 512 and a scan rate of 1 Hz. Samples were diluted to 1 μg/mL in water and 10 μL of the solution was drop-deposited onto freshly cleaved mica disc. The data were analysed using the Asylum Research software.

AFM Imaging (4.6.6). Atomic Force Microscopy (AFM) images were acquired out using an Asylum MFP-3D AFM equipped with AC240-TS probes with a spring constant of 0.67 to 3.52 N/m in intermittent contact (tapping) mode. Sample were diluted at 1 μg/mL in water and drop cast onto a substrate, covered and allowed to dry under ambient conditions. The substrate was a silicon wafer which was clean prior to sample deposition by sonication in acetone and then in IPA

MALDI Experiment. Matrix-Assist Laser Desorption / Ionisation (MALDI) was performed on a Bruker UltraFlextreme MALDI-ToF, in linear positive ion mode using a 19kV accelerating voltage. 500 shots were taken at each measurement of the spot, with ten measurements being taken and accumulated into the final spectra (5000 shots taken overall). Sample was dissolve in water at a concentration of 10 mg/ml, with a NaI concentration of 0.1 mg/ml. This was then mixed with a matrix sample of 15 mg/ml super dihydroxybenzoic acid, 0.1mg/ml NaI, and 0.2 M Chloroacetic acid in THF. The sample was then spotted and crystallised upon an anchorchip 328 stainless steel target plate.

HPLC Experiment. Reversed-Phase High-Performance Liquid Chromatography (RP-HPLC) of polymers were recorded on a Shimadzu Prominence HPLC equipped with photodiode array (PDA) detector. HPLC systems were equipped with a Phenomenex Luna C18 column, (250 x 4.6mm, 5 μm diameter particle size, 10 nm pore size). Water was used as solvent A and methanol was used as solvent B. All solvents were complemented with 0.04 % of trifluoroacetic acid (TFA). Solution were prepared from the reaction media (15 μL) further diluted in water (985 μL). Injection volume were 100 μL for all samples. Flow rate was fixed at 1.0 mL/min, temperature was set at 37 ºC. Signal was recorded by UV lamp within the range of the wavelength between 200 nm and 600 nm. Chromatograms are reported at 260 nm, which corresponds to the absorbance of the double bond of monomers. AMPS®2405 monomer was used to create a UV calibration curve, a mother solution of AMPS®2405 at 2 M was used to make a series of dilution from 2 to 0.13 M (8 dilutions), 15 μL of this solution was further diluted with 985 μL of water before injection. Data were extracted and subsequently plotted and analysed using OriginPro 9.1®.

Rheological Measurement. Rheological testing were carried out using an Anton Paar MCR 302 rheometer equipped with parallel plate configuration with a diameter of 8 mm and measuring gap of 1 mm. A Peltier system was used to maintain the temperature at 25 °C throughout the study. The amplitude sweep applied a constant frequency of 10 rad/s and the strain was ramped logarithmically from 0.01 % to 1000 %. The normal force was kept constant at 0 N and 25 points were recorded. All measurements were repeated in triplicate and the average storage and loss moduli were calculated at increasing amounts of strain. Data was analysed using RheoCompass software.

Viscosity Measurement. Viscosity testing were carried out using an Anton Paar MCR 302 rheometer equipped with parallel cone and plate configuration with a diameter of 60 mm. A Peltier system was used to maintain the desired temperature throughout the study.

i. At constant temperature (25 °C) a pre shear at 1000 s^{-1} was applied for 12 seconds, the viscosity was then measured at decreasing shear rate from 3000 to 10 s^{-1}.
ii. At increasing temperature from 25 to 50 °C, a pre shear at 100 s^{-1} and 25 °C was applied for 12 seconds, the viscosity was then measure at a constant shear rate of 100 s^{-1} while increasing the temperature at a rate of 5 °C per minutes leaving the sample to stabilize for 0.5 min before each measurements.

All measurements were repeated in triplicate. Data was analysed using RheoCompass software.

SAXS Measurement. Small-angle X-ray scattering (SAXS) measurements were made using a Xenocs Xeuss 2.0 equipped with a micro-focus Cu Kα source collimated with Scatterless slits. The scattering was measured using a Pilatus 300k detector with a pixel size of 0.172 μm x 0.172 μm. The distance between the detector and the sample was calibrated using silver behenate ($AgC_{22}H_{43}O_2$), giving a value of 2.495(5) m. The magnitude of the scattering vector (q) is given by $q = 4\pi \sin\theta/\lambda$, where 2θ is the angle between the incident and scattered X-rays and λ is the wavelength of the incident X-rays. This gave a q range for the detector of 0.006 $Å^{-1}$ and 0.16 $Å^{-1}$. The samples were mounted in 1 mm borosilicate capillaries and measured for 6 hours. A radial integration of the 2D scattering profile was performed and the resulting data corrected for the absorption, sample thickness and solvent background. Finally, the scattering intensity was then rescaled to absolute intensity using glassy carbon as a standard.[317]

D.References

(118) Lai, J. T.; Filla, D.; Shea, R. *Macromolecules* **2002**, *43*, 122.

(317) Zhang, F.; Ilavsky, J.; Long, G. G.; Quintana, J. P. G.; Allen, A. J.et al *Metall. Mater. Trans. A* **2010**, *41*, 1151.